I. A Crossover Mechanistic Investigation of the Wolff vs. photo-Favorskii Rearrangement of Diazo-*p*-Hydroxyacetophenone: Methoxy Substituent Effects on *p*-Hydroxyphenacyl Cage

II. Exploratory Studies of Hydroxyquinoline-Based Phototriggers

By

Sanjeewa N. Senadheera
2010

Submitted to the Department of Chemistry and the Faculty of the graduate School of the University of Kansas in partial fulfillment of the requirements for the degree of Doctor of Philosophy

Richard S. Givens, Committee Chair

Robert G. Carlson

Paul R. Hanson

Jane V. Aldrich

Michael A. Johnson

Date Defended: ……

The Dissertation Committee for Sanjeewa N. Senadheera certifies
That this is the approved version of the following dissertation:

I. A Crossover Mechanistic Investigation of the Wolff vs. photo-Favorskii Rearrangement of Diazo-*p*-Hydroxyacetophenone: Methoxy Substituent Effects on *p*-Hydroxyphenacyl Cage

II. Exploratory Studies of Hydroxyquinoline-Based Phototriggers

Richard S. Givens, Committee Chair

Robert G. Carlson

Paul R. Hanson

Jane V. Aldrich

Michael A. Johnson

Date Defended: ……

Abstract

α-Diazo-*p*-hydroxyacetophenone (**1.165**), both a model compound and a synthetic precursor to other *p*-hydroxyphenacyl (*p*HP) derivatives, has been synthesized and its photochemistry explored. α-Diazo-*p*-hydroxyacetophenone (**1.165**) itself is a unique structure for investigating the influence of a substituent effect on the known rearrangement of α-diazoacetophenones which could follow a photo-Wolff or photo-Favorskii rearrangement pathway. Photochemical and photophysical studies on diazo *p*HP **1.165** in aqueous acetonitrile provided insight into the mechanism of nitrogen (N_2) release and its rearrangement to the major product, 4-hydroxyphenylacetic acid (PAA). X-ray crystallographic data and ^{1}H NMR spectroscopy of diazo *p*HP **1.165** reveal that the *syn* (s-Z) form is the dominant conformation both in the crystalline state and in solution. These observations are in strong agreement with the reported data for similar α-diazoketones by Kaplan et al. and also by others. The triplet sensitized photolysis of diazo *p*HP **1.165** was unsuccessful with mangiferin (a xanthone derivative) and 4,4'-dicarboxylic benzophenone. However, quenching studies with molecular oxygen reduced the efficiency of the reaction by 50%, revealing the involvement of the triplet excited state in the photo-decomposition of diazo *p*HP **1.165.** The Stern-Volmer quenching studies with oxygen produced a triplet life time of 15 ns and a rate of 6.6×10^7 s^{-1} for the photoreaction in aqueous acetonitrile (1:1). Additional studies in collaboration with Tuscano et al. using time-resolved IR spectroscopy revealed a ketene intermediate, defining this as a Wolff rearrangement pathway. Photorelease of N_2 from diazo *p*HP **1.165** was not sensitized with either mangiferin or benzophenone, and the observed ketene intermediate from time-resolved IR studies, suggesting that the N_2 release occurs predominantly through the singlet manifold. However, the role of the

quenchable triplet excited state by oxygen is not clear at this point. Thus, the major pathway of N_2 photorelease from diazo *p*HP **1.165** is the Wolff rearrangement, whereas the Favorskii rearrangement might be less likely pathway.

Convenient, high yield, one pot syntheses of other *p*HP based chromophores were developed by expanding the α-diazo-*p*-hydroxyacetophenone (**1.165**) chemistry to include additional leaving groups and substituents on the hydroxyacetophenone. Strategies were developed for the synthesis of *p*HP caged carboxylates, sulfonates, phosphates, phenolates and amino acids and the "diazo approach" was extended to include the synthesis of *ortho* and *meta* substituted *p*HP caged diethyl phosphates. The light induced release of diethyl phosphoric acid and N_2 in aqueous acetonitrile was studied. UV/vis spectroscopy studies on solvent effects, pH effects, substituent effects and the effects of the leaving group were examined. The effects caused by *ortho* vs. *meta* substitution on the *p*HP chromophore were altered the quantum yields for release, e.g., *ortho* methoxy substituted *p*HP derivatives were 50% higher in quantum yields than *meta* methoxy derivatives. The neighboring methoxy group participation in N_2 release from the *ortho* and *meta* methoxy substituted derivatives 4-(2-diazoacetyl)-3-methoxyphenyl acetate **1.204** and 4-(2-diazoacetyl)-2-methoxyphenyl acetate **1.198a** demonstrated neighboring methoxy participation. *Ortho* methoxy **1.204** led to cyclization to 6-acetoxy-3-coumaranone along with the rearranged acid, whereas *meta* methoxy **1.198a** only produced the rearranged acid.

In another study, a series of 8-hydroxyquinoline based photoremovable protecting groups were designed, synthesized, and their photochemistry explored. UV/vis spectroscopic studies, solvent effects, pH effects, and effects of the leaving group were examined. From these, it was demonstrated that the photochemistry of 1,5-substituted 8-hydroxyquinolines is

dependent on the nature of the leaving group and the presence or absence of oxygen. The photorelease of diethyl phosphate from 2-(8-(benzyloxy)quinolin-5-yl)-2-oxoethyl diethyl phosphate (**2.44**) was observed. However, 8-hydroxyquinoline benzoates, i.e., 2-(8-hydroxyquinolin-5-yl)-2-oxoethyl benzoate **2.37** and 2-(8-benzyloxy)quinolin-5-yl)-2-oxoethyl benzoate **2.39** instead formed 2-(benzoyloxy)acetic acid **2.46** and quinoline-5,8-dione **2.47**. Singlet oxygen, generated by 8-hydroxyl-5-acetylquinoline photosensitization of the oxygen present in non-degassed studies, oxidized the caged benzoates. Interestingly, the photolysis of benzyl protected diethyl 2-(8-hydroxyquinoline-5-yl)-2-oxoethyl phosphate, **2.44**, with or without degassing with argon, gave diethyl phosphoric acid as the major photoproduct. This behavior can be rationalized by the fact that the phosphate group is a better leaving group and can compete favorably with oxidation by singlet oxygen generated by 8-hydroxyl-5-acetylquinoline photosensitization. For the benzoate derivatives, the singlet oxygen reaction with quinoline is more rapid than loss of the poorer leaving group (benzoate). Furthermore, no reaction occurs in the absence of oxygen. Finally, zinc chelated benzoate ester **2.40** was found to be photochemically inert.

Affectionately dedicated to my beloved father, my ever loving mother, my family,

and son, Thenuja Akain Senadheera

Acknowledgements

I would like to express my utmost thanks and appreciation to Professor Richard S. Givens, my research advisor for the last five years. I have not only learned so much from you both as a teacher and as a research advisor but also received remarkable encouragement and guidance throughout my Ph D career. I am also very appreciative for the wonderful opportunity I had in his research group when I had a hard time to choose a research advisor in the second year of the graduate school. I would really appreciate your continuous support, kindness and helpfulness that you have given in my entire graduate career, especially when I was suffering from a terrible back pain for six months. Again I really appreciate for everything that you have done during my hard times both in academics and in my personal life. My sincere thanks for you to being a role model, an excellent teacher and an advisor: The way you have shown will guide the rest of my career. I believe that it has been an honor and a privilege to work for you. I would also like to express my utmost gratitude to Ms. Sue Givens for her continuous motherly care throughout these years extended to my family.

I would also like to thank the former group members in the Givens' group and all the collaborators at other universities, both in the USA and abroad. My sincere thanks go to Professor John P. Toscano and Anthony Evans in Johns Hopkins University for their time-resolved IR spectroscopy studies on α-diazo-*p*-hydroxyacetophenone. Much of the mechanistic work with α-diazo-*p*-hydroxyacetophenone would not have been possible without their collaborative research work. My thanks are also due to Dr. David VanderVelde, Sarah Neuenswander, and Justin Douglas of NMR Laboratory; Dr. Todd D. Williams, Bob Drake and Lawrence Seib of Mass Spectrometry Laboratory; and Dr. Victor Day of X-ray Crystallography Laboratory. Also thanks go out to my Ph D committee members, namely

Prof. Robert G. Carlson, Prof. Paul R. Hanson, Prof. Michael Johnson, Prof. Elizabeth M. Topp, and Prof. Jane V. Aldrich. My special thanks go to Dr. Marina Rubina for helping me when I was having trouble with synthesis at the research lab, for proofreading my thesis, and providing me valuable suggestions. I would also take this opportunity to thank the University of Kansas and NIH for support.

My heartfelt and sincere thanks go to my wife for her patience and for her supportive encouragements to finish my graduate studies. I am really grateful and honored for having my son, Thenuja Akain Senadheera, before the schedule date of my Ph D defense and I would also like to take this opportunity to express my heartfelt love and best wishes for him. At last but not least, I would like to express my deepest gratitude to my family members, relatives and neighbors, especially my beloved father, mother, sisters, brothers, brothers-in-law, sisters-in-law, nephews, nieces, and Mr. B. K. K. Jayamewan for their endless support and encouragement throughout my academic carrier. Finally, I would like to thank my present and past friends for their help and encouragement at different stages of my life so far.

Table of Contents

List of Tables

List of Figures

List of Schemes

List of Equations

List of Abbreviations

A	= Acceptor
Ala-Ala	= Alanine-Alanine
AMP	= Adenosine Monophosphate
ATP	= Adenosine Triphosphate
BHQ	= 8-Bromo-7-Hydroxyquinolyl Group
°C	= Centigrade (Celsius)
cAMP	= Cyclic Adenosine Monophosphate
D	= Donor
Diazo *p*HP	= α-Diazo-*p*-Hydroxyacetophenone
DBU	= 1,8-Diazabicycloundec-7-ene
DEA	= Diethylamine
DMNPE	= 1-(4,5-Dimethoxy-2-nitrophenyl)diazoethane
DNA	= Deoxyribonucleic Acid
ESIPT	= Excited State Intramolecular Proton Transfer
ESPT	= Excited State Proton Transfer
FTIR	= Fourier Transform Infrared Spectroscopy
fs	= femtoseconds
GABA	= γ-Aminobutyric Acid
GC/MS	= Gas Liquid Chromatography coupled with Mass Spectroscopy
Glu	= Glutamate
GTP	= Guanosine Triphosphate
HAQ	= 5-Acetyl-8-Hhydroxyquinoline Group

HOMO = Highest Occupied Molecular Orbital

HQ = 8-Hydroxyquinoline

ISC = Inter System Crossing

k_{diff} = Diffusion rate conasatnt

k_q = Quenching rate constant

k_r = Rate of Release of a Substrate

K_{SV} = Stern-Volmer Quenching Constant

KMOPS = Pottasium salt of 3-(N-Morpholino)-Propanesulfonic Acid

LFP = Laser Flash Photolysis

LUMO = Lowest Unoccupied Molecular Orbital

NAD = Nicotinamide Adenine Dinnucleotide

$NAADP^+$ = Nicotinic Acid Adenine Dinucleotide Phosphate

$NADP^+$ = Nicotinamide Adenine Dinnucleotide Phosphate

NADPH = Nicotinamide Adenine Dinnucleotide Phosphate (Reduced form)

NMR = Nuclear Magnetic Resonance Spectroscopy

ns = nanoseconds

*o*NB = *o*-Nitrobenzyl group

PAA = *p*-Hydroxyphenylacetic acid

*p*HP = *p*-Hydroxyphenacyl group

PPGs = Photoremovable Protecting Groups

ps = picoseconds

Q = Quencher

RNA = Ribonucleic Acid

RP-HPLC = Reverse Phase High Performance Liquid Chromatography

S = Sensitizer

SKIE = Solvent Kinetic Isotope Effect

TBDPS = Tert-Butyldiphenylsilane

TD-DFT = Time-dependent Density Functional Theory

TES = N-Tris(hydroxymethyl)methyl-2-Aminomethanesulfonic Acid

TFA = Trifluoroacetic Acid

TPP = *meso*-Tetraphenyl Porphine

TRIR = Time-resolved Infrared Spectroscopy

TRIS = Tris(hydroxymethyl) Aminomethane

UV/vis = Ultraviolet-visible Spectroscopy

Φ = Quantum Efficiency

Φdis = Quantum Yield for the Disappearance of a Starting Material

Φapp = Quantum Yield for the Appearance of a Product

(*) = Excited State

Part I

A Crossover Mechanistic Investigation of the Wolff vs. photo-Favorskii Rearrangement of Diazo-*p*-Hydroxyacetophenone: Methoxy Substituent Effects on *p*-Hydroxyphenacyl Cage

Introduction

Protecting groups play a vital role in multiple group transformations in organic syntheses.[1] They are usually covalently attached to functional groups to suspend the reactivity of the functional group under given conditions. Upon exposure to appropriate conditions for their removal at the completion of a reaction, the protecting group can be removed to restore the original activity of the functionality.[1,2] The deprotection normally requires additional reagents, oftentimes acids or bases, which may be deleterious to physiological conditions or applications in living tissues. In addition, conventional protecting groups that have proven to be efficient in the synthesis of organic molecules may not be released or react fast enough for applications in studies of very rapid biological processes.[3] Accordingly, photoremovable protecting groups (PPG), or phototriggers, have emerged to address these concerns and the growing needs for initiators or triggers in biological research. Photoremovable protecting groups are removed very rapidly under physiological conditions, without applying any deleterious reagents or temperatures, by using light, a "traceless" reagent.[4-9]

Over four decades ago Barltrop et al.[10] were among the first to report a photochemical deprotection of a biological substrate; glycine (**1.3**) was released from N-benzyloxycarbonyl glycine (**1.1)** as illustrated in Equation 1.1.

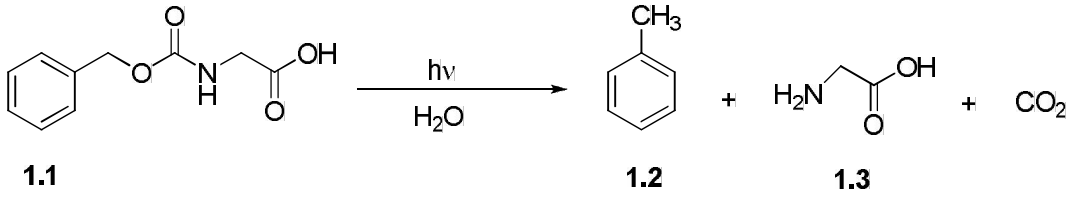

1.1 **1.2** **1.3**

Eq. 1.1

Later, Kaplan et al.[11] demonstrated that the *o*-nitrobenzyl phosphate ester of ATP can efficiently release ATP **1.8**, thus setting a hallmark in the development of novel photoremovable protecting groups of biological relevance (Equation 1.2).

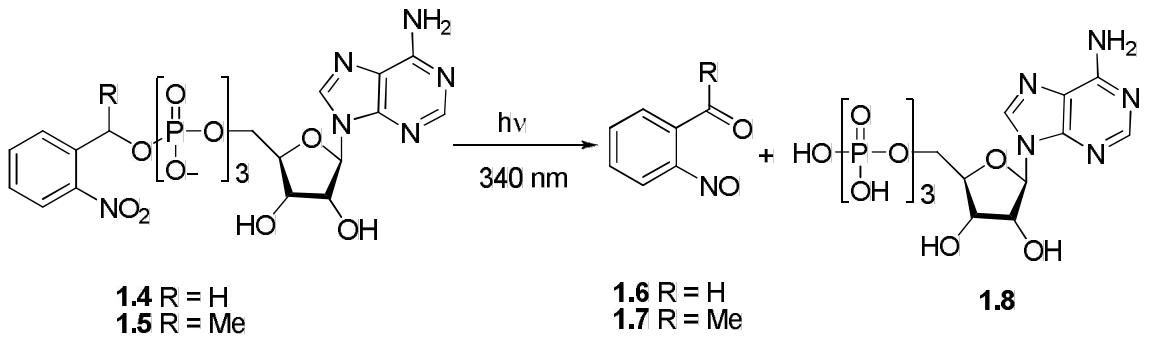

1.4 R = H
1.5 R = Me

1.6 R = H
1.7 R = Me

1.8

Eq. 1.2

Kaplan was the first to describe photoremovable protecting groups as "caged" compounds because of their ability to block the bioactivity of substrates by a covalent bond attachment to the chromophore.[12-15] Beyond the ability to release the substrate by the action of light, a cage compound must satisfy several other conditions to be successful in the biological arena. These criteria were initially proposed by Sheehan[3] and Lester,[16] and were further elaborated by several other researchers.[4-9] Among these criteria are hydrophilicity, reasonably high absorptivity (a), ease of synthesis, fast release of the substrate through a primary photochemical process, good quantum yields, robustness or at least being benign with respect to the media, and quantitative separation of caged and uncaged derivatives.

From the extensive studies by several researchers during the 1960s several other photoremovable protecting groups have emerged such as the *o*-nitrobenzyl esters and their analogs, benzoins, α-substituted acetophenones, cinnamate esters, coumarin derivatives, quinolines, etc.[4-9] However, the *o*-nitrobenzyl esters and their analogs remain the most extensively studied and widely used photoremovable protecting groups to date.

Barltrop[17] and coworkers first used the *o*-nitrobenzyl group to release benzoic acid (**1.10**) in 17% yield from *o*-nitrobenzyl benzoate (**1.9**).

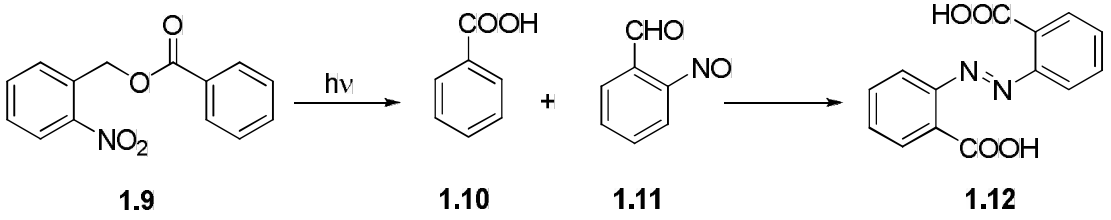

1.9 **1.10** **1.11** **1.12**

Eq. 1.3

A secondary photoproduct, azobenzene-2,2-dicarboxylic acid (**1.12**) that was produced from subsequent reaction of nitroso aldehyde **1.11**, was also observed. It was later found that the poor deprotection yield was due to the competition between the cage compound **1.9** and dicarboxylic acid **1.12** for light absorption.[18] This problem was overcome by using α-substituted nitrobenzyl esters resulting higher yields (75-95%) of deprotection as seen in Equation 1.4.

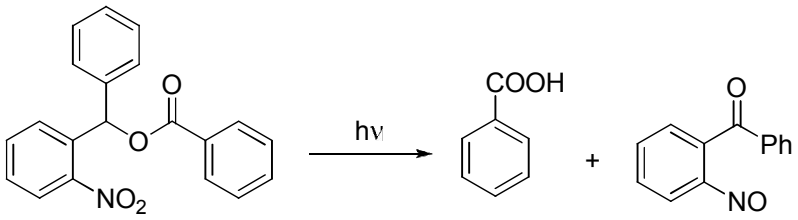

1.13 **1.10** **1.14**

Eq. 1.4

After these initial studies, *o*-nitrobenzyl and its analogs were extensively used by other researches to cage amino acids, amino sugars, glycosides, nucleotides and peptides.[4,5,9] Another historical landmark of ATP synthesis and photorelease was reported by Trentham and co-workers[19] in the late 1980s, modeled after the pioneering work by Kaplan and co-workers (Scheme 1.1). The synthesis began with *o*-nitroacetophenone (**1.15**) which was

converted to the corresponding hydrazone **1.16** with hydrazine, followed by oxidation with MnO_2 providing the aryldiazoethane precursor **1.17** used to alkylate ATP quantitatively in a $CHCl_3/H_2O$ biphasic system (Scheme 1.1).

Scheme 1.1 Trentham's Synthesis of Caged ATP

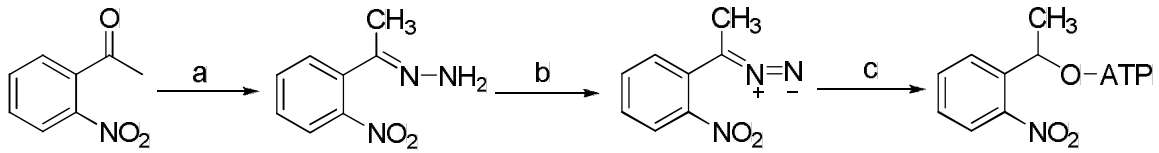

1.15 **1.16** **1.17** **1.5**

Reagents and conditions: (a) $NH_2NH_2.H_2O$, AcOH, EtOH, reflux, 3 h, 95%; (b) MnO_2, $CHCl_3$, rt, 5 min in dark, > 95%; (c) ATP, $H_2O/CHCl_3$, rt, 20 h, 80-100%.

The photolysis of the caged ATP **1.5** in TES buffer at pH of 7.1 furnished ATP **1.8** with a quantum yield of 0.63. The rate of release of ATP was determined to be dependent on the relative concentration of Mg^{2+} in solution and the pH of the medium (Equation 1.5).[19]

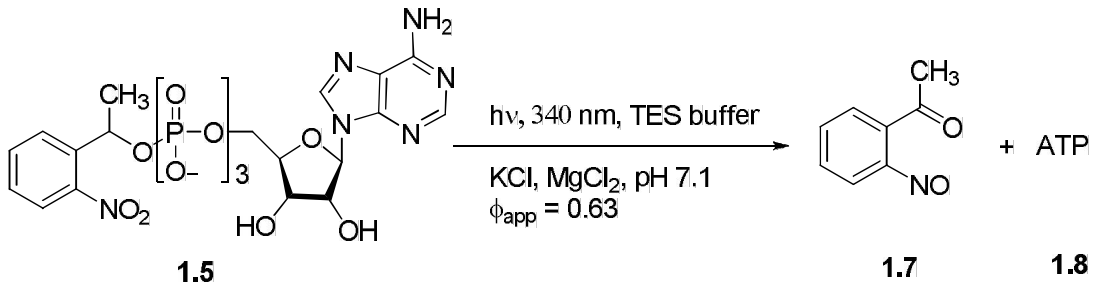

1.5 **1.7** **1.8**

Eq. 1.5

Recently, the *o*-nitrobenzyl group and its analogs have been used by several researchers to cage NAADP and NAD in order to explore the biochemical reactions which involve these oxidative cofactors.[21-25] The synthesis of these caged molecules has been achieved through either the aryldiazoethane precursor **1.17** or substituted analogs. Churchill and co-workers[20] generated caged NADP **1.20** using 4,5-dimethoxyaryldiazoethane **1.19** as outlined in Equation 1.6.

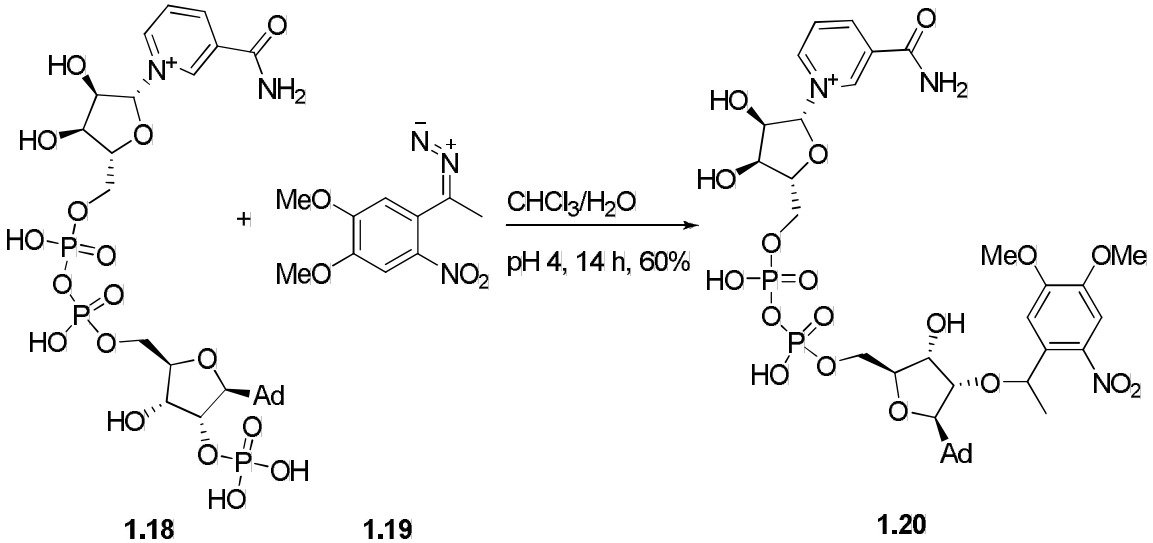

1.18 **1.19** **1.20**

Eq.1.6

The 4,5-dimethoxy-*o*-nitrobenzyl caged nicotinic acid adenine dinuclotide phosphate (DMNPE-NAADP$^+$, **1.21**) was generated by a chemo-enzymatic synthesis with ADP-ribosyl cyclase and caged NADP$^+$ **1.20** in the presence of excess nicotinic acid. The photolysis of DMNPE-NAADP$^+$ **1.21** furnished NAADP$^+$ **1.23** with an efficiency of 0.20, as illustrated in Equation 1.7.

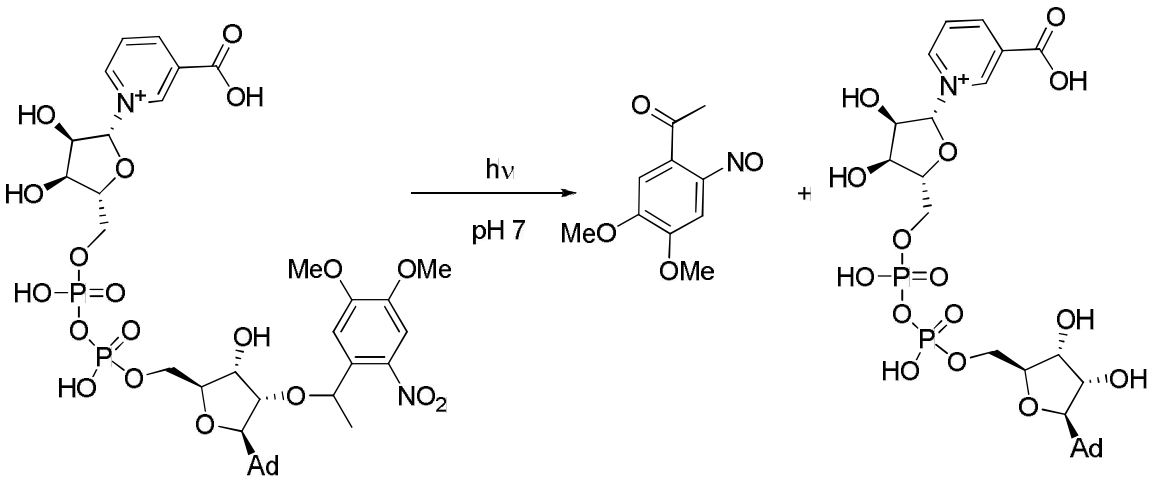

1.21 **1.22** **1.23**

Eq.1.7

The reaction mechanism for the substrate release from *o*-nitrobenzyl esters proceeds via an intramolecular redox reaction.[4,5,26] Upon irradiation, the chromophore is excited to its

excited state followed by intramolecular hydrogen atom abstraction leading to the formation of an aci-nitro intermediate **1.24**. This aci-nitro intermediate deprotonates and then cyclizes to form the isoxazole intermediate **1.25**. The isoxazole intermediate forms the hemiacetal **1.26** followed by a collapse of the hemiacetal to release the substrate. The rate determining step (rds) of the mechanism is the collapse of intermediate **1.26** which is the final step (Scheme 1.2). Wirz and co-workers have shown that the rds is the decay of the hemiacetal (or hemiketal) intermediate **1.26** by using laser flash studies with the help of time resolved infrared spectroscopy (TRIR).[26,27]

Scheme 1.2 *o*-Nitrobenzyl Photorelease Mechanism[26]

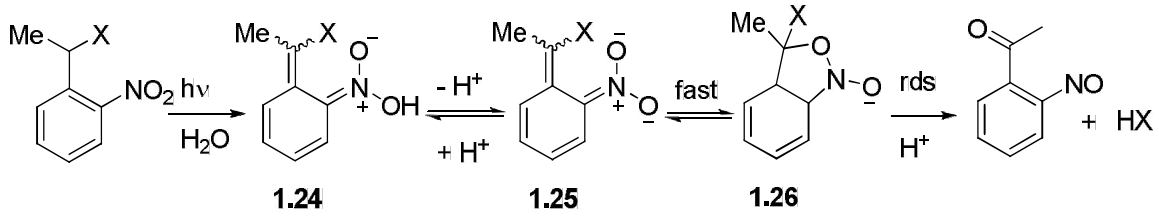

Although the *o*-nitrobenzyl group and its analogs have been widely used in diverse areas of chemistry and biology, they suffer from a number of disadvantages. The major photoproduct, a nitrosoaldehyde or nitrosoketone, is a highly absorbing chromophore in the excitation region of the caged substrate. Therefore, lower quantum yields and lower conversions can be seen for the release process. This is due to the competition between caged substrate and the nitrosoaldehyde or nitrosoketone for incident radiation. In addition, these nitroso compounds are highly reactive and toxic. They can react with the nucleophiles in the surrounding media making the *o*-nitrobenzyl protecting group problematic for use in biochemical reactions because proteins and other nucleophilic substrates can complicate the analyses.

The rds of the substrate release of *o*-nitrobenzyl esters is the hydrolysis of the hemiacetal (or hemiketal) intermediate in the ground state[19,26,27] which results in rate of release of ca. $< 10^3\ s^{-1}$. This rate of release is too slow for studying fast biochemical processes like studies on neurotransmitters at synapses. Another disadvantage is that some *o*-nitrobenzyl esters are not stable in biological media which can cause premature release of the substrate. It also has been reported that the aci-nitro intermediate **1.24** can be trapped by buffer solutions like acetate that would further delay the release of the substrate.

The *o*-nitrobenzyl protecting group is widely used in diverse areas of chemistry and biology in spite of its major limitations.[4,5] However, there is an increased demand for novel photoprotecting groups with faster release rates and a wider range of excitation wavelengths. These trends prompted researchers to design and develop other photoremovable protecting groups.

The photosolvolysis studies of benzyl acetates in 50 % aqueous dioxane by Zimmerman[28] were an encouragement to others to employ *m*,*m*′-dimethoxybenzyl as a photoremovable protecting group in the early 1960s (Equation 1.8)

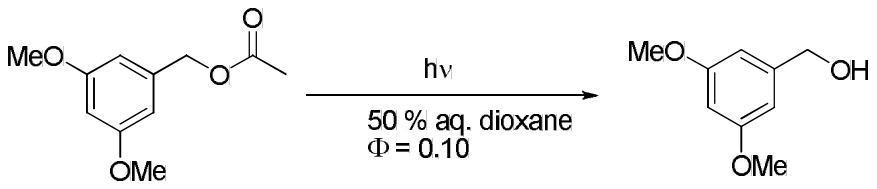

1.27 **1.28**, 79 %

Eq. 1.8

Generally, photofragmentation reactions of benzyl acetates are singlet excited state processes and relatively rapid with rate constants of $10^8\ s^{-1}$. The *meta* activation of the excited singlet state of benzyl acetate **1.27** occurs through the approach of the excited and the ground state energy surfaces funneling the excited state toward heterolysis of the benzyl-ester bond.

Homolytic fission and radical derived products could be seen when the electron donating substituents were located at the *para* position.

In the 1990s both Zimmerman[29,30] and Pincock[31,32] extensively studied the nature of the *meta* effect to identify whether heterolytic or homolytic cleavage was the primary photochemical process. According to Pincock's point of view, the *meta* substituted arylmethyl analogs undergo homolysis of the C-O ester bond to the substrate followed by a competition between electron transfer to an ion pair or typical ground state radical reaction (Scheme 1.3).[32]

Scheme 1.3 Pincock's Mechanistic Scheme for Arylmethyl Ester **1.29** Photolysis in Methanol[32]

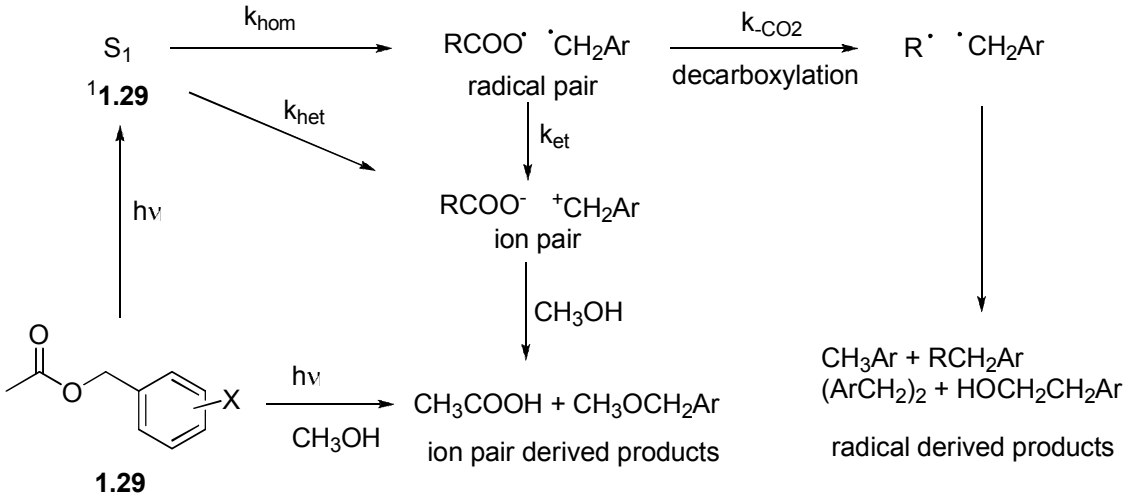

For the *meta* methoxy substituted arylmethyl derivatives, the electron transfer occurs more rapidly than competing radical processes due to favorable redox properties of the radical pair. The decarbonylation of the initially generated carboxy radicals from the carboxylate esters **1.29** such as C-protected amino acids, peptides, and protein derivatives can compete with the electron transfer to the ion pair. This process can become destructive for the released substrate. The product-determining process for the *meta* methoxy substituted

derivative leads mainly to an ion pair or an intermediate arylmethylcarbocation by either of these mechanisms (Scheme 1.3).[32]

The coumaryl chromaphore, another arylmethyl derivative that also has a high yield of fluorescence emission, has become an attractive photoremovable protecting group in biological studies since its discovery in the early 1980s. In 1983, Givens and co-workers[33] reported the release of diethyl phosphoric acid (**1.31**) from coumarylmethyl diethyl phosphate **1.30.**

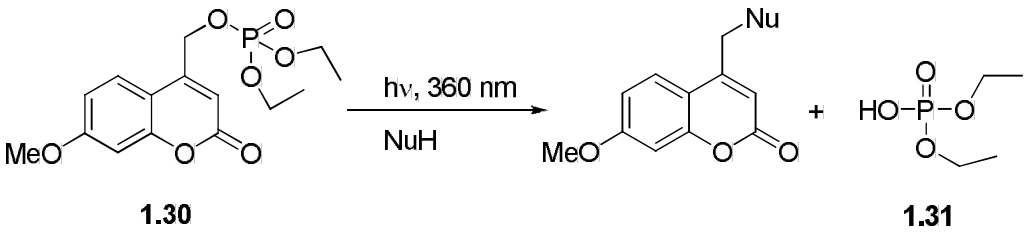

1.30 **1.31**

NuH = CH_3OH, cysteine, tyrosine, α-chymotrypsin

Eq. 1.9

A wide variety of nucleophilic reagents (NuH) can react with the coumarylmethyl cation that is formed during the photolysis reaction. Several investigators have successfully employed the coumaryl group to cage several other substrates such as alcohols,[34] ketones and aldehydes,[35] cyclic nucleotide monophosphates,[36] diols,[37] neurotransmitters,[38,39] and DNA and RNA.[40] Recently, Hagen and co-workers[41] have shown the photocleavage of several cAMP and cGMP derivatives occurs within a few nanoseconds. They have modified the chromophore as illustrated in Equation 1.10 not only to increase the water solubility but also to extend the effective wavelength range into the visible region. Upon photolysis, coumaryl derivative **1.32** in aqueous buffer released the corresponding cyclic nucleotides along with the hydrolyzed chromophore **1.33** as illustrated in Table 1.1. The most red-shifted coumaryl

derivative within the series, **1.32a**, was the least water soluble derivative but gave the highest quantum yield.

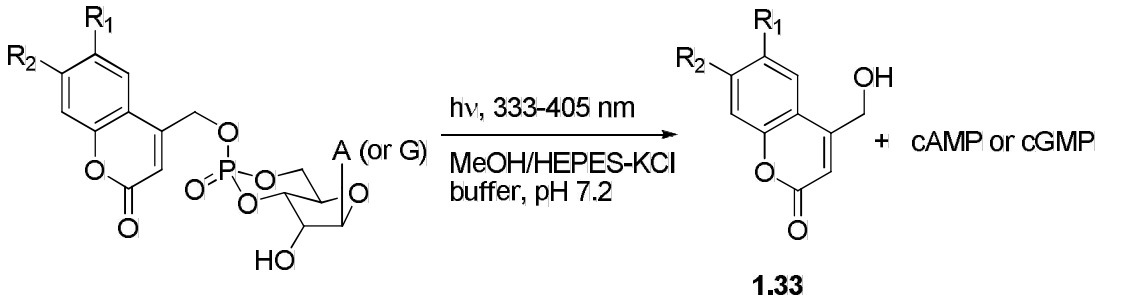

1.33

1.32a. R_1 = H, R_2 = Et_2N
1.32b. R_1 = H, R_2 = OCH_2COOH
1.32c. R_1 = R_2 = OCH_2COOH

Eq. 1.10

Table 1.1 Excitation Wavelengths and Quantum Yields for cAMP and cGMP Coumaryl Esters

Coumaryl derivative	Solvent	Φ_{dis}[a]	λ_{max} /nm
1.32a	80:20 HEPES-KCl buffer/MeOH	0.21 (0.25)	402
b	HEPES-KCl buffer, pH 7.2	0.12 (0.16)	326
c	HEPES-KCl buffer, pH 7.4	0.10 (0.14)	346

[a] For the disappearance of the cAMP derivative; quantum yields for the disappearance of cGMP analogs are in parentheses.

Sheehan and Wilson discovered benzoins as a photoremovable protecting group by doing studies on acetates **1.34a-b** (Equation 1.11).[42,43] They reported that photolysis of methoxy substituted and unsubstituted benzoin acetates **1.34a-b** rearranged to the corresponding phenylbenzofurans **1.35a-b** along with concomitant release of groups α to the carbonyl group.

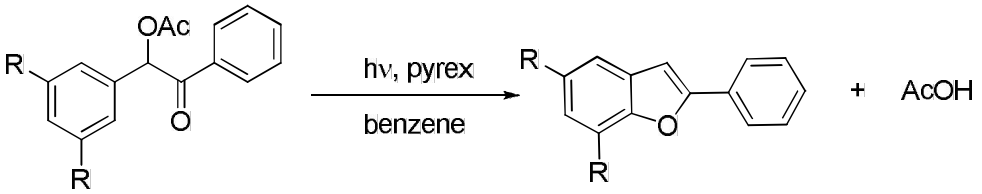

1.34a R = H
1.34b R = OMe

1.35a R = H 15 %
1.35b R = OMe 94 %

Eq. 1.11

The quantitative release of phosphates from the unsubstituted benzoin was described by Givens and co-workers[33] in the early 1990s as illustrated in Equation 1.12.

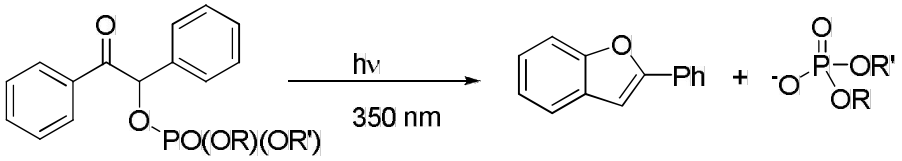

1.36a R = R' = Et
1.36b R = ^{i}Pr, R' = $^{+}$Na, or $^{+}$H
1.36c R = R' = $^{+}$Na, or $^{+}$H

1.37a R = R' = Et
1.37b R = ^{i}Pr, R' = $^{+}$Na, or $^{+}$H
1.37c R = R' = $^{+}$Na, or $^{+}$H

Eq. 1.12

Table 1.2 Quantum Yields for Benzoin Phosphate Esters **1.36a-c**[43,44]

Phosphate ester	Solvent	pH	Φ_{dis}	Φ_{furan}	$\Phi_{phosphate}$
1.36a	C_6H_6	Nd	0.28	0.26	nd
b	H_2O/CH_3CN	2	0.37	0.2	0.12
b	H_2O/CH_3CN	7	nd	0.07	0.013
c	H_2O/CH_3CN	2	0.38	0.14	0.15
c	H_2O/CH_3CN	7	nd	0.08	0.01

Except **1.36a** as indicated, all the other reactions were run in 60% aqueous acetonitrile. Phosphate esters were irradiated at 350 nm and monitored with ^{31}P NMR.

The short-lived ($^{3}\tau$ = 3-14 ns) triplet excited state was established for benzoin by performing quenching studies with triplet quenchers such as naphthalene, piperylene, and sodium 2-naphthylenesulfonate for aqueous studies. The rate of release of phosphates was

found to be > 10^8 s^{-1} by Stern-Volmer quenching studies, and good quantum yield values were also observed as illustrated in Table 1.2.[44-46]

The higher efficiency for release of phosphate at low pH suggests that the protonated phosphate is a better leaving group than its conjugate base. The applicability of benzoin group in biological studies was accomplished by caging cAMP as illustrated in Equation 1.13.[44] The quantum yields for the disappearance of **1.38** (Φ_{dis} = 0.37-0.40) and formation of the exclusive products **1.35a** (Φ_{furan} = 0.16-0.19) and cAMP (Φ_{cAMP} = 0.34-0.36) were found to be the same order of magnitude. There was no pH dependence as seen with **1.36**.

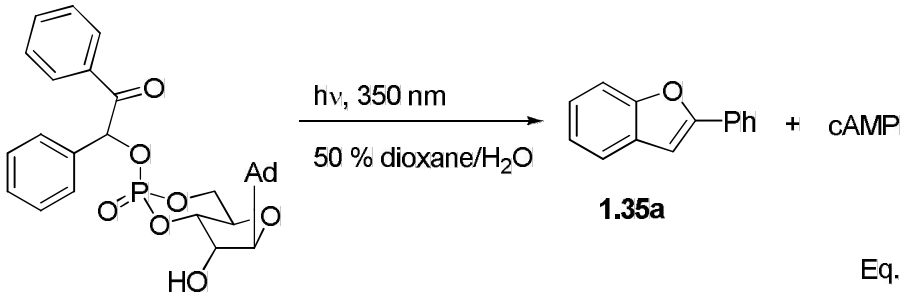

1.38 **1.35a** Eq. 1.13

The benzoin photorelease mechanism was believed to happen through an n,π* singlet state because of the observation that electron donating groups at *meta* positions of the benzyl ring enhanced the efficiency. Sheehan's proposed mechanism[43] would run through a biradical intermediate followed by ground state oxetane ring formation of **1.39** which would then open with the help of the electron donating methoxy groups along with concurrent release of the carboxylate. Rearomatization via loss of a proton would generate the benzofuran **1.40** (Scheme 1.4).

Scheme 1.4 Sheehan's Benzoin Photorelease Mechanism[43]

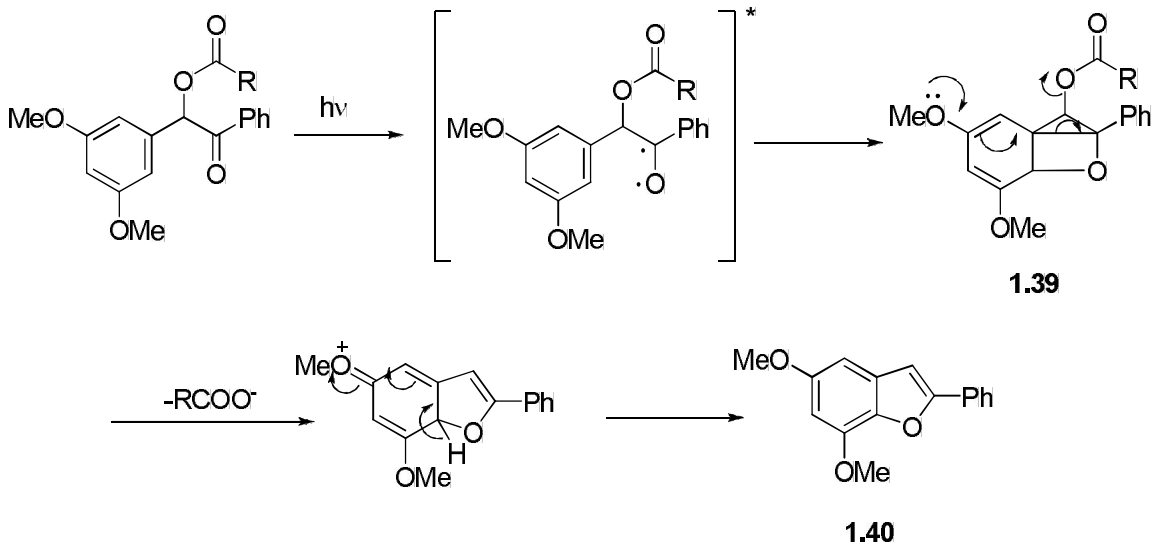

These benzoin derivatives suffer from a number of disadvantages despite their fast rate and high quantum yields of release (ca. k_r 10^5 s^{-1}, Φ_{app} 0.78, respectively; Trentham et al.[47]) making them better candidates for biological studies. However, the photoproducts are generally not soluble in aqueous media. The benzofuran byproduct **1.35a** is a highly absorbing chromophore which competes with incident light and to highly fluorescent. Therefore, the benzoin protection group is difficult to use when a fluorescent indicator is used in the analysis process. The photoproducts can also form photodimers upon further irradiation, thereby further complicating the photorelease chemistry. An added complication is the synthetic procedure or required separation of diasteeomers due to the presence of a chiral center in the chomophore.

The *p*-methoxyphenacyl group was introduced by Sheehan and Umezawa[3] as a photoremovable protecting group after studying its ability to release several substrates in ethanol or dioxane (Equation 1.14).

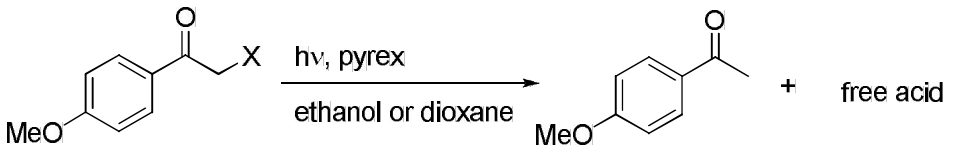

1.41 **1.42**

X = benzoic acid, amino acids, peptides Eq. 1.14

They proposed a simple homolysis mechanism for the formation of the photoproduct, *p*-methoxyacetophenone **1.42** which was a reduction product (Scheme 1.5). It was found that triplet quenchers like naphthalene or benzophenone completely quenched the reaction indicating a triplet reaction pathway.

Scheme 1.5 Sheehan and Umezawa's Homolysis Mechanism[3]

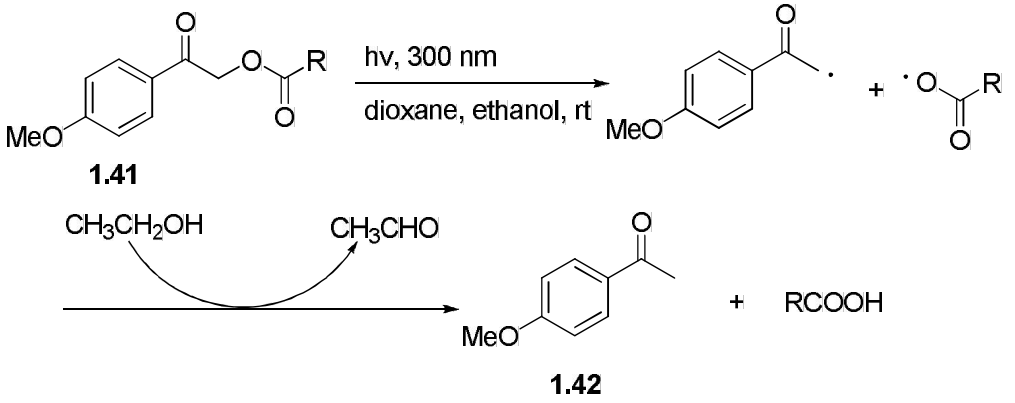

In a separate study by Epstein and Garrossian,[48] diethyl and diphenyl phosphate esters were released from the corresponding *p*-methoxyphenacyl phosphates in 1,4-dioxane. The reduced product **1.42** was recovered in high yields (84 - 91%) along with released phosphates (Et: 86%; Ph; 74%).

In the early 1990s, the photorelease of phosphate esters from the corresponding *p*-methoxyphenacyl phosphates **1.43** were extensively studied by Givens and co-workers[45] (Equation 1.15). The product distribution in *t*-butyl alcohol and methanol was dependent on the nature of the solvent. It was found that the rearranged ester **1.44** was the major product

whereas the photoreduction product **1.42** was the minor product in *t*-butyl alcohol and methanol. This controversy between results of Epstein et al. and Givens et al. may be due to the solvent polarity and the ease of hydrogen atom abstraction. *t*-Butyl alcohol and methanol both are much more polar solvents than 1,4-dioxane. In addition, 1,4-dioxane and methanol are better hydrogen atom sources compared to *t*-butyl alcohol. Thus, more radical derived products are possible from solvents which are good H-atom sources.

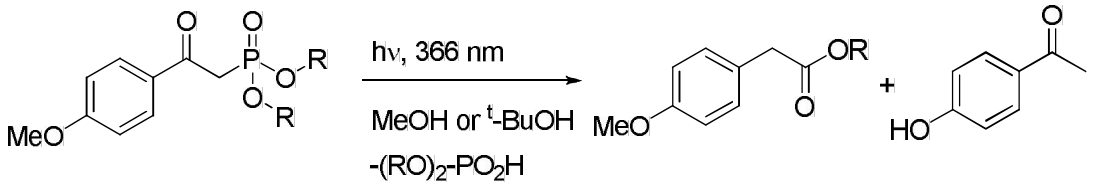

1.43a R = Et
1.43b R = Ph
1.43c R = H

1.44a R = Me
1.44b R = ^{t}Bu

1.42

Eq. 1.15

Solvent isotope studies were performed on the release of phosphates from the caged phosphates **1.43** to determine the solvent dependency on the product distribution. These studies suggested that a rate-determining hydrogen abstraction occurs in the photoreduction process which was first proposed by Sheehan as described earlier.

Solvent dependency on product distribution (rearrangement vs. reduction) of α-chloroacetophenones was studied by Dhavale et al.[49] They found that the ratio of rearrangement to reduction increased with the electron donating power of the substituent for a given solvent. It was also found that the photolysis of α-chloro ketone **1.45** produced more reduction product **1.46** in methanol, whereas rearranged analogs **1.47** and **1.48** are the major products in aqueous acetonitrile (Equation 1.16). In methanol the reduction product **1.46** was the major product, because methanol is a better hydrogen atom donating source than acetonitrile.

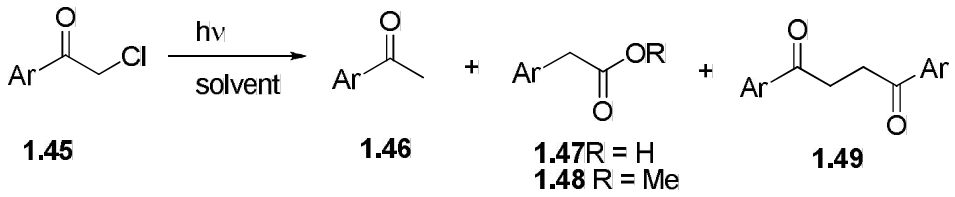

Eq. 1.16

The authors proposed a mechanism to explain the product distribution as illustrated in Scheme 1.6. Upon irradiation the initial loss of chloride from **1.45** is by bond homolysis followed by single electron transfer (SET) to generate an ion pair **1.50**.

Scheme 1.6 Suggested Mechanism by Dhavale et al.[49]

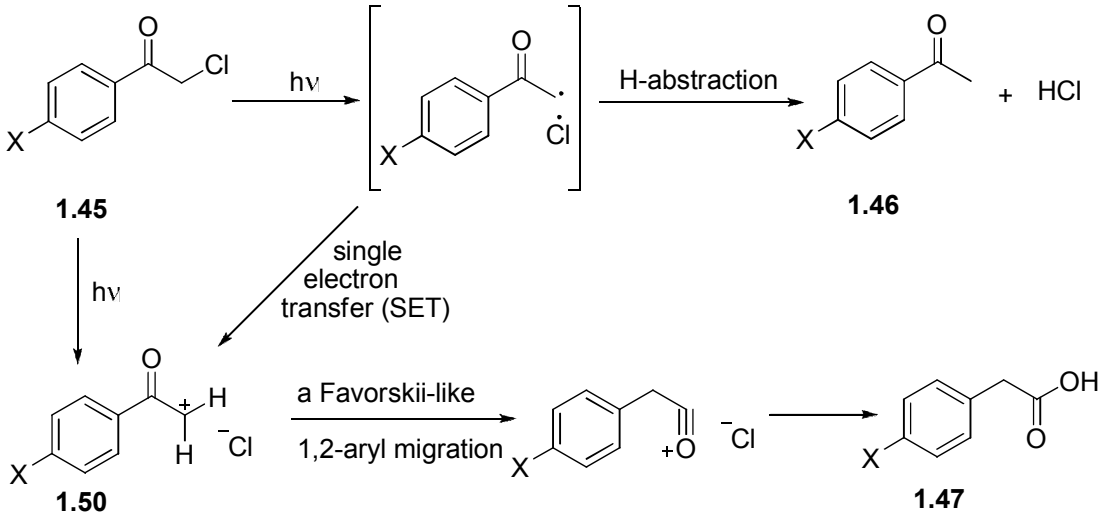

In polar aprotic solvents, the ion pair **1.50** rearranges to the acid through a Favorskki-like intermediate whereas in hydrogen atom donating solvents H-abstraction generates the reduction product **1.46** from the initial radical pair.

The initial earlier studies by Anderson and Reese[50] in the early 1960s opened the door for the *p*-hydroxyphenacyl group to revolutionize the photoremovable protecting group landscape. The photochemistry of a series of substituted phenacyl chlorides in an alcoholic solution was reported as depicted in Equation 1.17 and in Table 1.3.

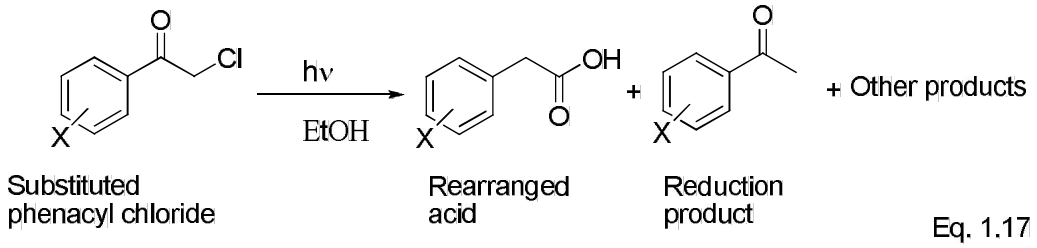

Eq. 1.17

Table 1.3 Photoproducts Distribution from the Photolysis of Substituted Phenacyl Chlorides[a]

Aryl substituent, X	% yield of rearranged ester	% yield of reduction product	% yield of other products
p-OH	32	26	2[b]
p-OMe	32	30	16[c]
o-OH	-	3	40[d]
o-OMe	32	16	11[e]
p-Me	4	58	nd
H	-	53	nd
p-CO_2Me	-	48	nd
p-Cl	-	55	nd
o-Cl	-	45	nd
m-OMe	-	15	50[f]

[a]IR spectroscopy was used to follow the course of the reaction; the yields were estimated either by vapor phase chromatography, by isolation, or by derivatization; [b]*p*-chlorophenol; [c]*p*-chloroanisole; [d]coumaran-3-one; [e]*o*-chloroanisole; [f]2-chloro-5-methoxy acetophenone; nd = Not determined.

In their studies on *p*-hydroxyphenacyl chloride both the rearranged acid **1.53** through a Favorskii like rearrangement and the reduction product **1.52** (Equation 1.18) were formed. It was also reported that electron donating groups at *ortho* and *para* positions favor the rearrangement (Table 1.4). A spirodienedione intermediate **1.54** was proposed by the authors to explain the major Favorskii-like product formation.

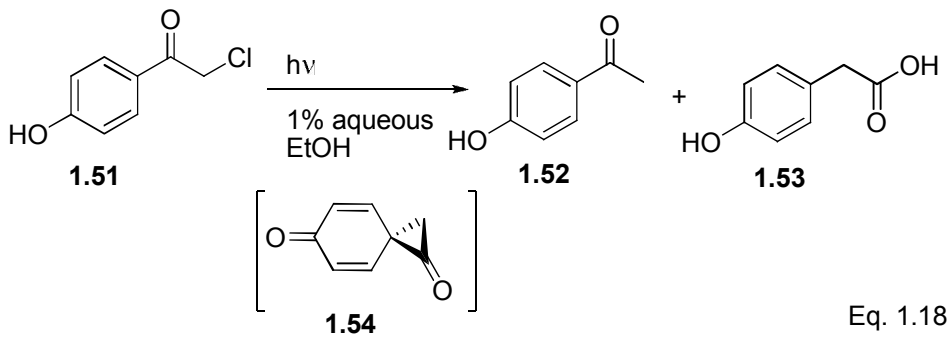

Eq. 1.18

p-Hydroxyphenylacetic acid **1.53** was the major product from the *o*-OMe substituted derivative (Table 1.3, entry 4), whereas substantial amounts of acetophenone and *o*-chloroanisole were also formed. The authors also found neighboring group participation in 2-hydroxyphenacyl chloride (**1.55**), which upon irradiation generated 3-coumaranone **1.56** as the major product and *p*-hydroxyacetophenone **1.52** as the minor product (Equation 1.19).[50]

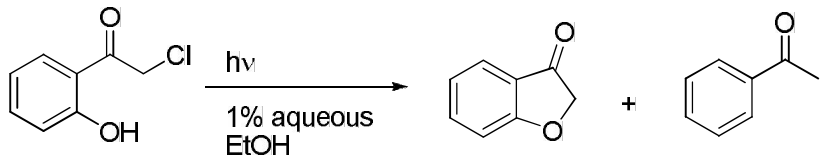

Eq. 1.19

Anderson and Reese's results and other studies on benzoin derivatives by Sheehan and by Givens prompted the Givens group to develop the *p*-hydroxyphenacyl group (*p*HP) as a photoremovable protecting group. In the mid 1990s, they performed a series of studies on *para* substituted phenacyl phosphates (Equation 1.20).[51,52] It was also found that *p*-amino, *p*-acetamido, and methyl *p*-carbamoyl substituted derivatives produced mixtures of products upon irradiation in TRIS buffer. All released the phosphate leaving group, but few gave the rearrangement of the chromophore.

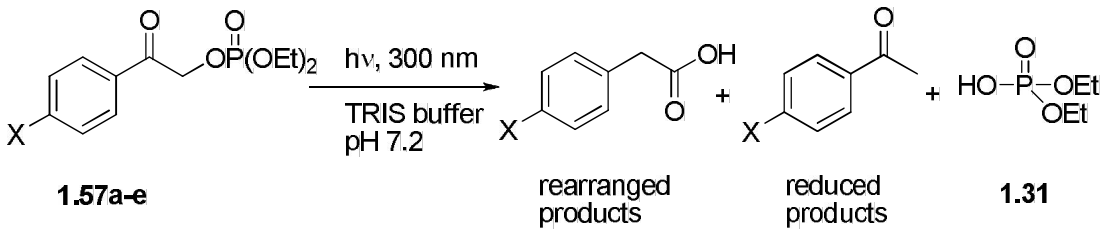

Eq. 1.20

Among these derivatives the methoxy substituted derivative **1.57d** produced only two products compared to phosphates **1.57a-c**. Interestingly, the hydroxyl substituted **1.57e** gave only the rearranged acid when photolyzed in aqueous buffer. This rapid and clean reaction further encouraged them to explore the potential of the *p*HP chromophore as a photoremovable protecting group.

Table 1.4 Disappearance and Product Quantum Yields for *para*-Substituted Phenacyl Phosphates **1.57a-e** in TRIS Buffer at 300 nm

Aryl substituent (X)	Φ_{dis}	Φ_{rear}	Φ_{red}
1.57a *p*-NH_2	< 0.05	0.00	< 0.05
b *p*-$NHCOCH_3$	0.38	0.00	0.11
c *p*-$NHOCOCH_3$	0.34	0.00	nd
d *p*-OMe[a]	0.42	0.20	0.07
e *p*-OH[b]	0.38	0.12	0.00

[a]Solvent was MeOH and diethyl phosphate was the leaving group; [b]The diammonium salt of the monoester; 10% CH_3CN was added to the solvent; dis = disappearance; rear = rearrangement; red = reduction

The *p*-hydroxyphenacyl group has several attractive features suggesting its development into a successful phototrigger. The hydroxyl group at the *para* position enhances the water solubility, making it is a better photoremovable protecting group than the previous candidates for the study of biological processes. This chromophore eliminates the stereogenic center problem found with the benzoin derivatives. In addition, the photo-

Favorskii rearranged acid **1.53** does not compete for incident radiation for absorption because of the significant hypsochromic shift in the rearranged chromophore.

After these initial studies, Givens and Park[51,52] suggested its potential applicability for biological studies by caging ATP (Equation 1.21). The caged ATP **1.58** releases ATP **1.8** and *p*-hydroxyphenylacetic acid with a quantum yield of 0.37 ± 0.01 and a rate of 6.9 ± 1.2 10^8 s^{-1}. This observed very fast rate constant suggests its potential for the study of rapid biochemical processes.

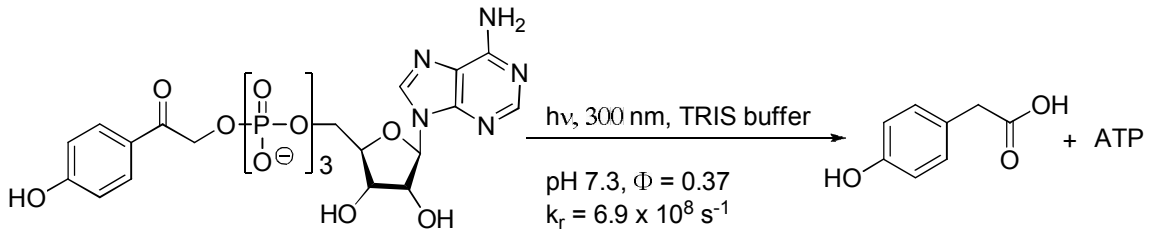

1.58 **1.53** **1.8**

Eq. 1.21

Photorelease of biologically important neurotransmitters L-glutamate (Glu) and γ-amino butric acid (GABA)[53,54] from *p*HP caged analogs was also rapid and gave comparable rate constants to those of caged ATP. In addition, the *p*-hydroxyphenacyl group (*p*HP) was successfully employed to cage peptides, e.g., Ala-Ala and bradykinin.[53]

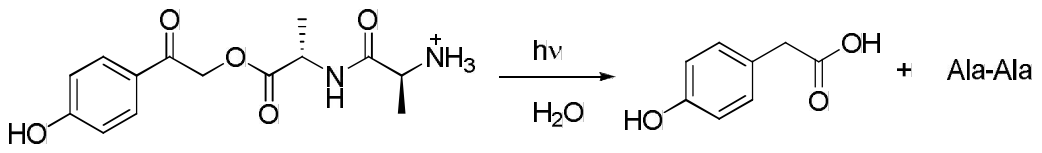

1.59 **1.53**

Eq. 1.22

The phosphorescence emission studies and quenching studies on *p*HP carboxylate **1.57b**, *p*HP-Ala-Ala **1.59**, *p*HP-acetate **1.63**, *p*HP-phenylacetate and phosphates **1.56e** and *p*-hydroxyacetophenone **1.52** and 2,4'-dihydroxyacetophenone revealed that the photorelease occurs via a triplet excited state.[5,55,56] The phosphorescence emission studies exhibited triplet

energies of 68.9-70.6 kcal/mol and the excited triplets were quenchable by triplet quenchers. The well known triplet quenchers like 2-naphthalenesulfonate and potassium sorbate have triplet energies that are ca. < 3.0 kcal/mol than that of above mentioned *p*HP esters. A short-lived triplet excited state ($^3\tau$ = 5 ns) was identified by performing Stern-Volmer quenching studies on the photorelease of Ala-Ala from *p*HP-Ala-Ala using sodium 2-naphthalnesulfonate as the triplet quencher. The rate of release was found to be k_{rel} = 1.82 x 10^8 s^{-1}.

The initial mechanism for the photorelease of the substrate from the *p*HP group in aqueous media is illustrated in Scheme 1.7. Upon irradiation, caged *p*HP **1.60** is excited to its singlet excited state followed by rapid singlet-triplet intersystem crossing (k_{ST} = 2.7 x 10^{11} s^{-1}) to produce the triplet state ^{3}**1.60**. The triplet phenoxide anion **1.61** is formed by a solvent assisted adiabatic proton transfer from the triplet phenolic group. The triplet phenoxide anion could be the precursor for the rate determining release of the substrate. The other possibility is that the concerted proton transfer can couple with concomitant release of the substrate.

Scheme 1.7 Givens' *p*HP Photorelease Mechanism

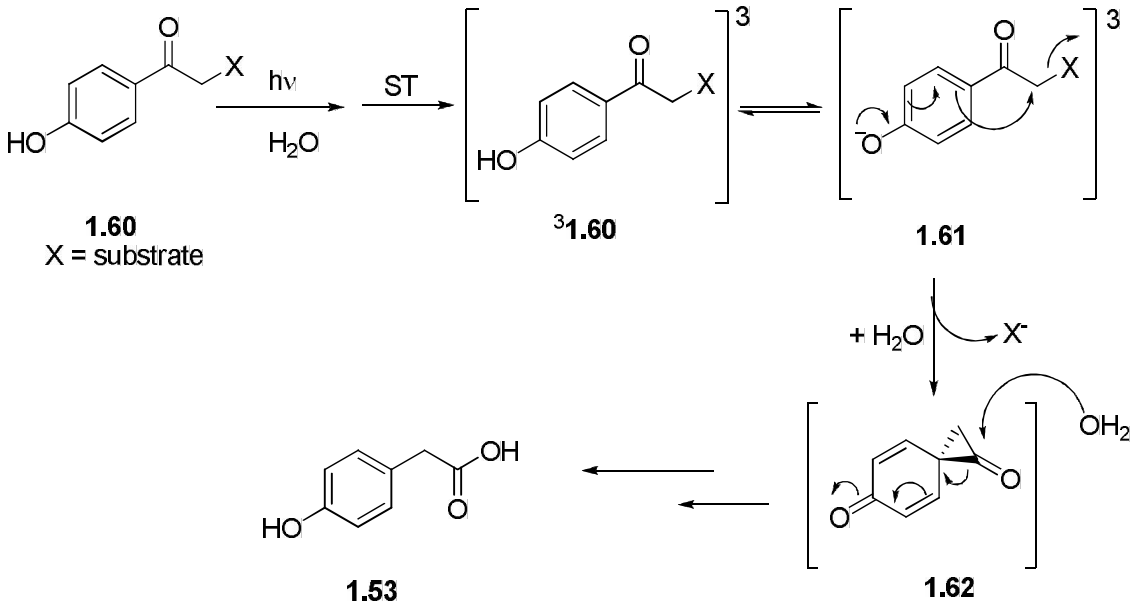

The putative ground state spirodienedione **1.62** is formed by the decay of the triplet biradical intermediate produced initially from the loss of the leaving group and the proton. The hydrolysis of spirodienedione **1.62** then yields *p*-hydroxyphenylacetic acid **1.53** as the major product. Phillips and co-workers[57-62] performed several studies on *p*HP phosphates using time-resolved Raman spectroscopy which confirmed the importance of water in the mechanism and the triplet nature of the photorelaese process.

Earlier studies on the mechanism of *p*HP photorelease suggested the direct heterolytic bond cleavage (*p*HP substrate) from the triplet phenol, or homolytic cleavage followed by rapid electron transfer to the putative intermediate **1.62**.[4,5,55] These earlier versions of the mechanism did not consider the seminal role of the phenolic group and the role of water which appears to be necessary for this triplet rearrangement. In some cases, a minor product which was identified as 2,4'-dihydroxyacetophenone is formed (ca. < 10 %) via photohydrolysis of starting material.

The laser flash studies (LFP) on *p*-hydroxyacetophenone **1.52** in aqueous acetonitrile[63] are strongly in agreement with the idea of the substrate release from the triplet excited state of the *p*HP chromophore ^{3}**1.60** which was originally proposed by Givens and co-workers.[4,5,55] According to these studies, the acidity of the substrate is increased from the ground state to triplet excited state (ca. 60-fold).[5]

Wan and co-workers[64] reported a photosolvolitic mechanism for the rearrangement of *p*HP acetate in aqueous medium based on results from nanosecond LFP studies. The authors proposed a much different mechanism than that of Givens and co-workers (Scheme 1.8). According to the authors, the reaction precedes through a singlet excited state pathway involving an excited state intramolecular proton transfer (ESIPT) to generate intermediate

enolate/phenolate **1.65**. The intermediate **1.65** either can return to the starting material **1.63** by proton tautomerization or can produce the rearranged acid **1.53** through a ground state Favorskii rearrangement. Some ambiguity regarding the nature of the electronic state of the rearranging tautomer was not addressed in the article, suggesting that it might still be an excited singlet (*).

Scheme 1.8 Corrie and Wan *p*HP Photorelease Mechanism[64]

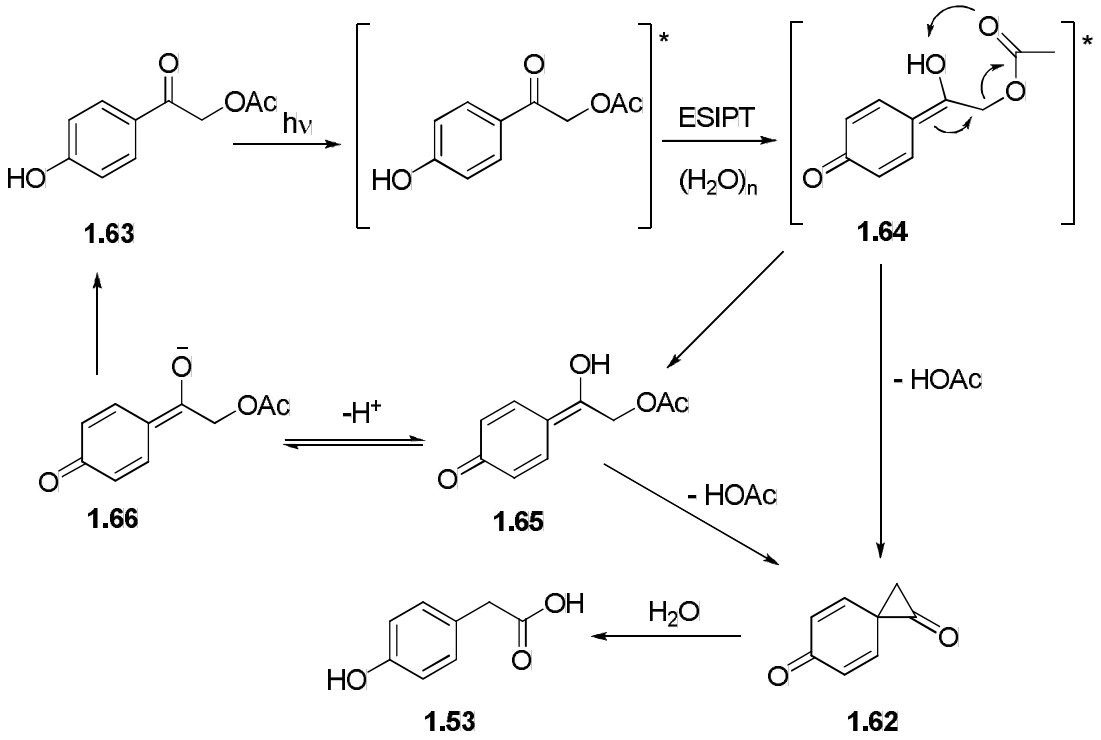

In 2000, Givens and co-workers[65] found that *meta* methoxy *p*HP-GABA and -Glu derivatives **1.67** and **1.68** have longer wavelength π-π* absorption bands than the parent *p*HP analogs, but their efficacy to release the substrate was diminished by an order of magnitude (Equation 1.23 and Table 1.5).

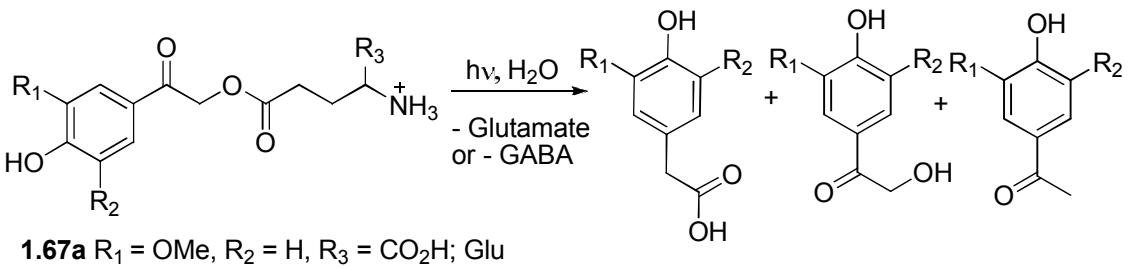

1.67a R_1 = OMe, R_2 = H, R_3 = CO_2H; Glu
1.67b R_1, R_2 = OMe, R_3 = CO_2H; Glu
1.68a R_1 = OMe, R_2 = H, R_3 = H; GABA
1.68b R_1, R_2 = OMe, R_3 = H; GABA

Eq. 1.23

The effects of electron withdrawing groups ($CONH_2$ and CO_2Me)[5] and electron donating groups (OMe)[5,65] on *p*HP photochemistry for releasing GABA were studied through comparison of rates determined by quenching experiments and pK_a measurements (Table 1.5).

Table 1.5 Substituent Effects on Photorelease of GABA from *p*HP Esters[5]

*p*HP derivative	Φ_{dis}[a]	Φ_{GABA}[a,b]	K_{SV} (M^{-1})[c]	τ^3 (ns)[c]	k_{rel} (10^7 s^{-1})[c,d]	^3pK_a[e]
3-$CONH_2$	0.48	0.38	106	14.3	3.4	3.75
3-CO_2Me	0.31	0.31	5.7	0.77	40	4.28
H	0.22	0.21	38	5.1	4.3	5.15
3-OMe	0.04	0.04	3.2	0.43	9.3	6.14
3,5-2OMe	0.03	0.03	343	46.3	0.065	6.46

[a]Quantum efficiencies for *p*HP ester disappearance and GABA appearance were measured for 0.01 M aerated (not degassed) aqueous solutions of caged GABA at 300 nm. Error limits are ± 10%. [b]GABA appearance. [c]k_{diff} = 7.4 x 10^9 $M^{-1}s^{-1}$ (H_2O) was used for the rate of diffusion in the quenching experiments (k_q, K^+ sorbate quencher) for calculation of τ^3 and K_{SV} = (k_q) (τ^3). [d]The rate constants were calculated by the equation $k_{rel} = \Phi_{GABA}/\tau^3$. [e]The ^3pK_a was determined from ionization and tautomerization equilibria of the corresponding *p*-hydroxyacetophenones by LFP.[5,56]

These results suggested that the substrate release occurs from the phenoxide anion **1.61** on the triplet excited state energy surface via adiabatic ionization of the phenol. It was found that the phenolic proton acidity was increased by 4-fold in the triplet state whereas the carbonyl group becomes more basic.[56] Interestingly, a nice correlation was observed in the

plot of quantum yield for release of GABA as a function of the ^3pK_a of substituted *p*HP GABA derivatives (Figure 1.1).

Figure 1.1 The Plot of Φ_{dis} vs ^3pK_a

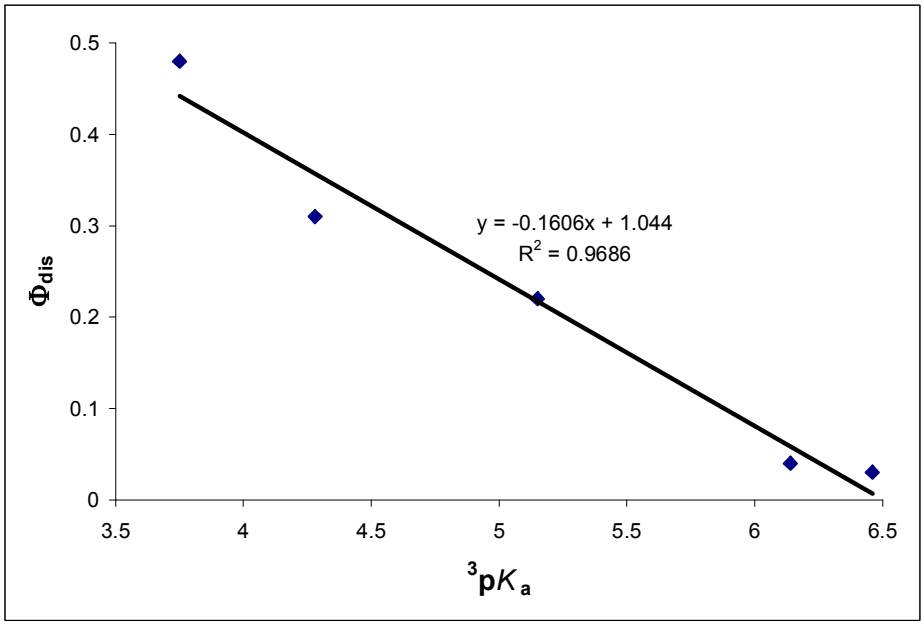

It is clearly seen from the graph that electron donating groups (OMe) have much less of an effect due to their lower acidity than that of electron withdrawing groups ($CONH_2$ and CO_2Me).

Photo-Favorskii rearrangement

In 2008, Givens and co-workers further explored the photo-Favorskii rearrangement of *p*HP diethyl phosphate **1.57e** in 10% aqueous acetonitrile using solvent kinetic isotope effect (SKIE) studies with the help of nanosecond LFP.[66] The overall SKIE was found to be large, $k_H/k_D = 2.17 \pm 0.03$, and the proton inventory method was used to calculate number of protons transferred in the excited state in the rate determining step. The curved nature of the resulted proton inventory plot indicates the involvement of at least two weakly bonded

protons in the transition state. Phillips and co-workers[57-62] quantified the importance of water in the photo-Favorskii rearrangement of *p*HP diethyl phosphate **1.57e** in aqueous acetonitrile by varying the H_2O concentrattion. He proposed that both solvent protonation of the triplet *p*HP carbonyl and leaving phosphate might be possible. Wan and co-workers[64] also showed the importance of solvent protonation of the *p*HP carbonyl. Therefore, the triplet transition state of *p*HP diethyl phosphate **1.57e** may involve the dynamic removal of phenolic hydrogen by water and at the same time solvent protonation of *p*HP carbonyl and the leaving phosphate group (Equation 1.24). This process generates the triplet biradical **1.69** detected through ns-laser flash studies ((λ_{max} = 445, 420, and 330 nm; $^3\tau$ ~ 0.6 ns) and diethyl phosphoric acid **1.31**.

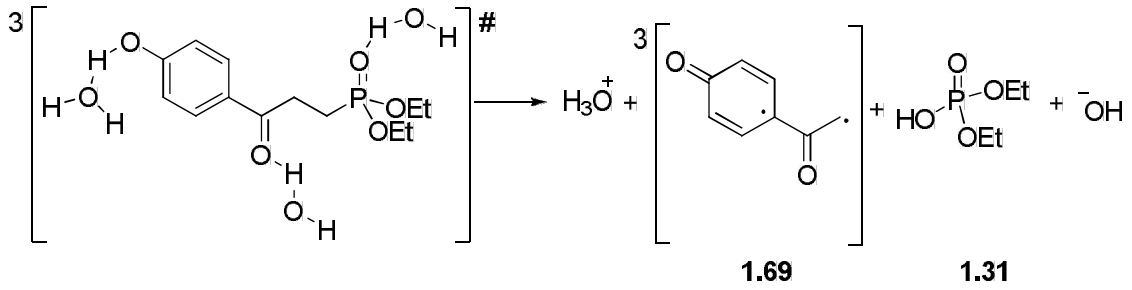

1.69 **1.31**

Eq. 1.24

The triplet biradical **1.69** then must intersystem cross to its singlet and cyclize to form the putative spirodienedione intermediate **1.62** (Scheme 1.9). As an additional mechanistic feature, the authors also observed a *p*-quinone methide transient intermediate **1.70** at 1647 cm^{-1} (λ_{max} = 276 nm) by time-resolved IR absorption which they speculated was formed by decarbonylation of **1.62** (Scheme 1.9). The *p*-quinone methide **1.70** leads to the formation of benzyl alcohol **1.71**, a minor product in *p*HP photorelease chemistry. The spirodienedione **1.62** is hydrolyzed by water to form phenylacetic acid **1.53** as the major product (Scheme 1.9).

Scheme 1.9 Revised Mechanism of the photo-Favorskii Rearrangement

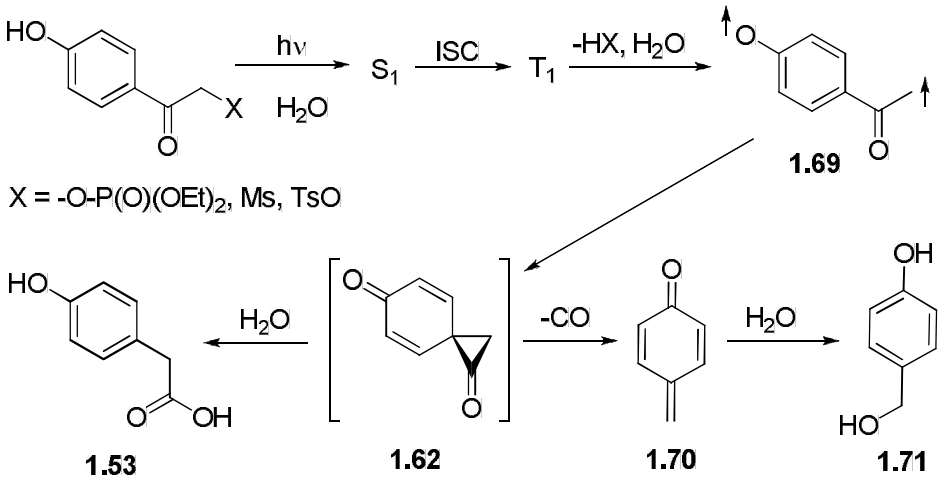

Attempts to detect the putative Favorskii intermediate **1.62** have failed under all conditions including step-scan FTIR. No transient signal was observed within the region of the C=O stretching frequency of the cyclopropanone moiety of the spirodienedione intermediate **1.62** (266 nm with 4 ns, 5-mJ pulses from a Nd/YAG laser).

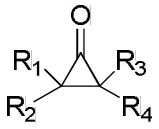

1.72a $R_1, R_2, R_3, R_4 = H$
b $R_1 = CH_3, R_2, R_3, R_4 = H$
c $R_1, R_2 = CH_3, R_3, R_4 = H$
d $R_1, R_2, R_3, R_4 = CH_3$

Table 1.6 Spectral Properties of Cyclopropanones **1.72a-d** in Methylene Chloride[53]

cyclopropanone	R_1	R_2	R_3	R_4	IR (C=O)/cm^{-1}	UV-vis/ Å
1.72a	H	H	H	H	1813	3100, 3300
b	CH_3	H	H	H	1822, 1850	3300
c	CH_3	CH_3	H	H	1815	3400
d	CH_3	CH_3	CH_3	CH_3	1843, 1823	3400

In accordance with extensive studies on cyclopropanones by Turro, the C=O stretching frequency of cyclopropanone **1.72** lies in the 1800 cm^{-1} to 1850 cm^{-1} range (Table 1.6).[67,68]

However, DFT calculations predict 1880 cm^{-1} for the C=O stretching of spirodienedione **1.62**.[66]

Recently, Givens and co-workers extensively studied the effect of fluorine substituents on the *p*HP photochemistry.[69] A series of *ortho* and *meta* fluorinated *p*HP GABA derivatives **1.73a-h** have been utilized to explore the influence of fluoro substituents on the photo-Favorskii rearrangement in water (Equation 1.25). It was found that *ortho* and *meta* fluoro substituted *p*HP caged derivatives **1.73a-h** exhibited modest changes in the quantum yields of release (Φ_{dis} = 0.09-0.28), but maintained rapid release rates ($k_r = 10^7$-10^8 s^{-1}) and short triplet lifetime of 0.4-6.0 ns when compared with the parent *p*HP GABA derivative **1.73a-h** (Φ_{dis} = 0.21, $k_r = 10^8$ s^{-1}). The differences in photochemical and photophysical properties of these compounds derived from the ground state pK_a of the phenolic groups (Table 1.7).

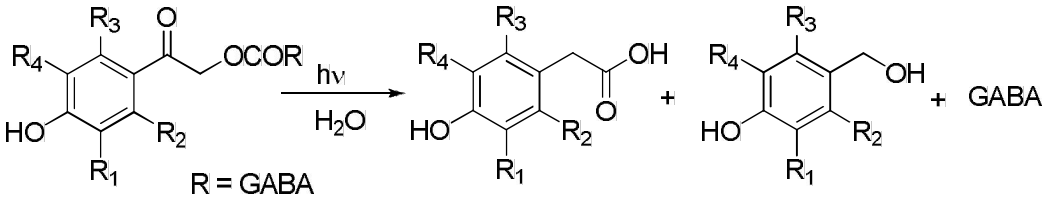

1.73a R_1 = F, R_2, R_3, R_4 = H
b R_1, R_3, R_4 = H, R_2 = F
c R_1, R_2 = F, R_3, R_4 = H
d R_1, R_3 = F, R_2, R_4 = H
e R_1, R_4 = F, R_2, R_3 = H
f R_1, R_4 = H, R_2, R_3 = F
g R_1, R_2, R_4 = F, R_3 = H
h R_1, R_2, R_3, R_4 = F

1.74a-h **1.75a-h**

Eq. 1.25

The most recent studies by Givens and co-workers[70] on *meta* trifluoromethoxy substituted caged *p*HP GABA and *p*HP Glu derivatives **1.67**, **1.68**, and **1.76a-d** revealed a competing pathway in the photo-Favorskii rearrangement (Equation 1.26 and Scheme 1.10).

Table 1.7 Quantum Yields (Φ_{dis} and Φ_{app}), pK_a, and λ_{max} for Fluoro *p*HP GABA Derivatives in Water[69]

Fluoro *p*HP GABA analogs	λ_{max}/nm (log ε/$M^{-1}cm^{-1}$)[a]	Φ_{dis}[b]	Φ_{app}[c]	pK_a
1.73a	274 (4.00), 335 (2.97)	0.16 ± 0.02	0.15 ± 0.01	6.5
b	271 (3.97)	0.28 ± 0.03	0.26 ± 0.03	7.2
c	272 (4.09), 328 (3.04)	0.24 ± 0.02	0.22 ± 0.02	5.9
d	278 (3.26), 326 (3.92)	0.22 ± 0.02	0.20 ± 0.02	5.7
e	331 (4.14)	0.11 ± 0.01	0.10 ± 0.01	5.3
f	274 (4.00)	0.16 ± 0.02	0.15 ± 0.01	6.8
g	324 (4.05)	0.08 ± 0.01	0.06 ± 0.01	4.5
h	316 (3.95)	0.11 ± 0.01	0.10 ± 0.01	3.9
1.76b	274 (4.20), 331 (3.54)	0.09 ± 0.01	0.07 ± 0.01	6.7
c	328 (4.11)	0.17 ± 0.02	0.18 ± 0.02	5.5

[a]Determined in 18 MΩ ultrapure water; [b]Quantum yields for the disappearance of fluoro *p*HP GABA derivatives; [c]Quantum yields for the appearance of *p*-hydroxyphenylacetic acids.

An "energy wasting" or a chemically unproductive triplet pathway, which is the deprotonation of the phenol group that competes with the rearrangement, has been observed. The resulting *p*HP conjugate bases **1.79a-c** reprotonate to yield the starting esters **1.76a-c** (Scheme 1.10).

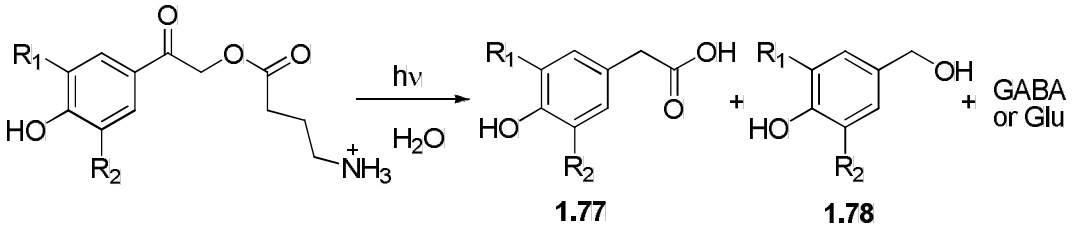

1.68a $R_1 = OCH_3$, $R_2 = H$
b $R_1, R_2 = OCH_3$
1.76a. $R_1, R_2 = H$; GABA
b. $R_1 = OCF_3$, $R_2 = H$; GABA
c. $R_1 = CF_3$, $R_2 = H$; GABA
d. $R_1 = CF_3$, $R_2 = H$; Glu

1.77 rearranged phenylacetic acid

1.78 decarbonylation product < 5 %

Eq. 1.26

Scheme 1.10 Competing Photo-Favorskii and Deprotonation of *p*HP Esters[70]

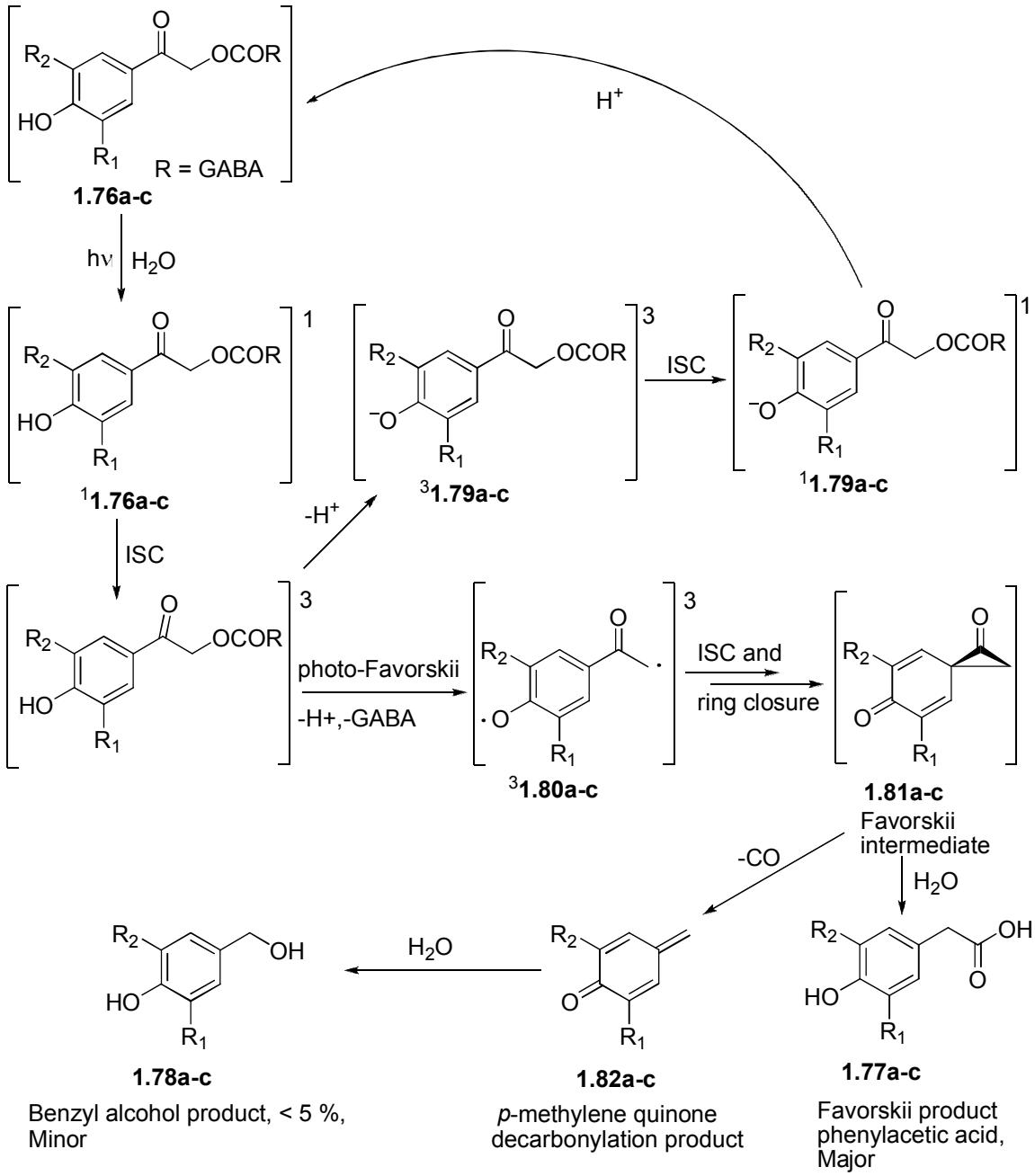

The rest of the photochemistry is the same as portrayed above in Scheme 1.9. In conclusion, we can argue that the efficiency of *p*HP substrate release depends on several factors. The most important one is the nucleofugacity of the caged substrate and p*K*a of the phenolic

group on the chromophore.[70] For example, *p*HP phosphates have higher quantum yields (ca. 0.30-0.63) than the *p*HP carboxylates such as GABA derivatives (ca. 0.04-0.20).

As an example of the latter, it was found that conjugate bases of meta trifluoromethoxy substitituted *p*HP GABA and Glu, **1.76c,d**, are much less efficient at pH 9, well above the pK_a's of the *p*HP derivatives, where only the conjugate base absorbs. Therefore, substituents on the *p*HP ring can alter the pK_a of the *p*-hydroxy group resulting in changes in the effective *p*H range and the wavelength region for photorelease. Other factors that may affect the partitioning of the pathways include the water content of the solvent, pH, and media effects. The photochemical and photophysical properties which are altered by substituents on the *p*HP chromophore, including effects that influence the partitioning of the dominant triplet pathways, have to be addressed more thoroughly.

The reviews of chemical and biological applications with other known photoremovable protecting groups (PPGs) are a useful source of information about this broad topic.[4,5,7,71,72] There is tremendous desire to design and develop better PPGs both from existing as well as novel PPG chromophores to satisfy more of the demands to meet criteria that a PPG should possess (e.g., Sheehan[3] and Lester's[16] criteria). As far as known PPGs are concerned, *p*-hydroxyphenacyl group (*p*HP) enjoys several advantages over the other PPGs including its improved water solubility, relatively high quantum yields, fast release rates, relative ease of installation, photostability (robustness), and quantitative conversion to products.

α-Diazocarbonyl compounds

The synthesis of α-diazocarbonyl compounds was first reported by Curtius[73] more than 125 years ago; even before the discovery of the Wolff rearrangement. In 1883 Curtius reported the synthesis of an α-diazocarbonyl compound by diazotization of natural α-amino acids; glycine was used to synthesize ethyl diazoacetate.[73,74] In 1902, Wolff[75] discovered a specific 1,2 rearrangement of a diazocarbonyl compound, initiated by loss of nitrogen, to a ketene that may react with nucleophiles (HX) such as water, alcohols, and amines to give carboxylic acids, or may undergo [2+2] addition with unsaturated systems (a=b) [(Scheme 1.11)].[74]

Scheme 1.11 Wolff Rearrangement

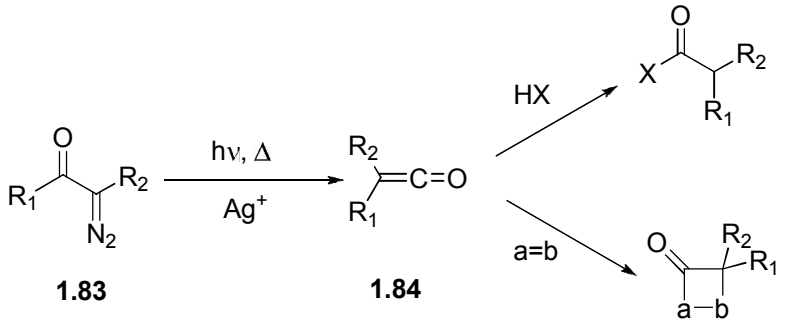

1.83 **1.84**

Wolff[75-77] obtained ethane-1,1-dicarboxylic acid (**1.87**) by heating 2-diazo-3-oxo-butyrate (**1.85**) with water via the ethyl ester (**1.86**) whereas 1-phenylpropan-2-one (**1.90**) was obtained from 2-diazo-1-phenylbutane-1,3-dione (**1.88**) under the same reaction conditions (Scheme 1.12). However, it was not clear how water was incorporated in the formation of carboxylic acids until the chemistry of ketenes was developed by Staudinger[78] and a few years later by also Schröter.[79] Schröter demonstrated that diphenylketene (R_1, R_2 = Ph) can be obtained by heating 2-diazo-1,2-diphenylethanone.[79]

Scheme 1.12 Wolff rearrangement; First Examples[75-77]

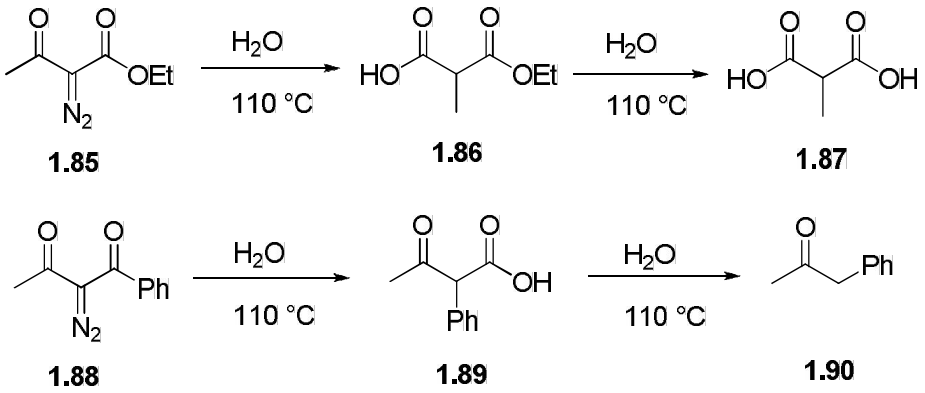

These results prompted Wolff to publish his results indicating that formation of carboxylic acids in aqueous media proceeds by way of ketenes, a process that also describes silver-ion catalyzed rearrangements of α-diazoketones.[80] After this seminal discovery and for over the next twenty years, the Wolff rearrangement was regarded to have little potential in synthesis until efficient methods were developed to generate α-diazoketones. In the 1920s, Arndt and Eistert developed a simple method to generate diazoketones by addition of an acyl chloride to ether solutions of diazomethane.[81,82] After this pioneering work and also work by Bradley and Robinson,[83] the simpler diazocarbonyl compounds became more readily available in the late 1930s. Ring contraction by light-induced Wolff rearrangement became a hallmark for the generation of strained molecules in the 1940s.[84,85] Thus, photolysis was found to be an efficient methodology for initiating Wolff rearrangement of α-diazoketones (acyclic and alicyclic).[86] In the 1950s, ketenes derived from Wolff rearrangements were used extensively in [2+2] cycloaddition reactions.[87] In the 1960s, researchers began to study the mechanism of the Wolff rearrangement more thoroughly and further explored the synthetic applications of the Wolff rearrangement. Since then, α-diazocarbonyl compounds have become the subject of many mechanistic studies as well as more widely applied in organic synthesis including a wide array of insertion reactions.[74]

Transitions metal catalysts[88-90] [$Cu(acac)_2$] and $Rh(OAc)_4$), light,[91] and Lewis acids[92] ($BF_3.OEt_2$) have been extensively employed for carbine X-H insertion reactions using diazocarbonyl compounds.[74] Generally, polar X-H bond insertions, such as the X-H bonds in sulfonic acids and strong carboxylic acids, lead to acceleration in the rate of the reaction without any catalyst present. Weak carboxylic acids, water, alcohols, and phenols require copper (II) or rhodium (II) salts as catalysts. However, there are reported examples where catalysts were not required to effect the X-H insertion. The proposed mechanisms for the decomposition of diazo ketones **1.91** along with O-H insertion are depicted in Scheme 1.13. The photochemical mechanism for reactions with alcohols proceeds through carbene **1.95** formation followed by addition of R_2OH to generate an oxonium ylide **1.96** which then rearranges by 1,2-rearrangement to form the O-H insertion product **1.97**. On the other hand, the transition metal catalyzed reaction mechanism proceeds via the electrophilic metal carbene **1.92** formation followed by the nucleophilic attack by R_2OH to form an oxonium ylide **1.94**. The ylide **1.94** then undergoes a 1,2-rearrangement by transferring a proton from oxygen to carbon with regeneration of the catalyst producing the target **1.97**.

The Lewis acid catalyzed mechanism starts with coordination of the carbonyl group to the Lewis acid (e.g., boron trifluoride etherate) followed by the nucleophilic attack on the diazocarbonyl substrate **1.98** by R_2OH which then rearranges to the O-H insertion product **1.97** with regeneration of the catalyst. However, the photochemical pathway is the least productive among those outlined above because α-diazo carbonyl compounds undergo photo-Wolff rearrangement via ketene intermediates to give rearranged products instead of generating O-H insertion products.[74]

Scheme 1.13 Mechanisms for O-H Insertion of Diazocarbonyl Compounds in the Presence of Light, Transition Metals, and Lewis Acids[74]

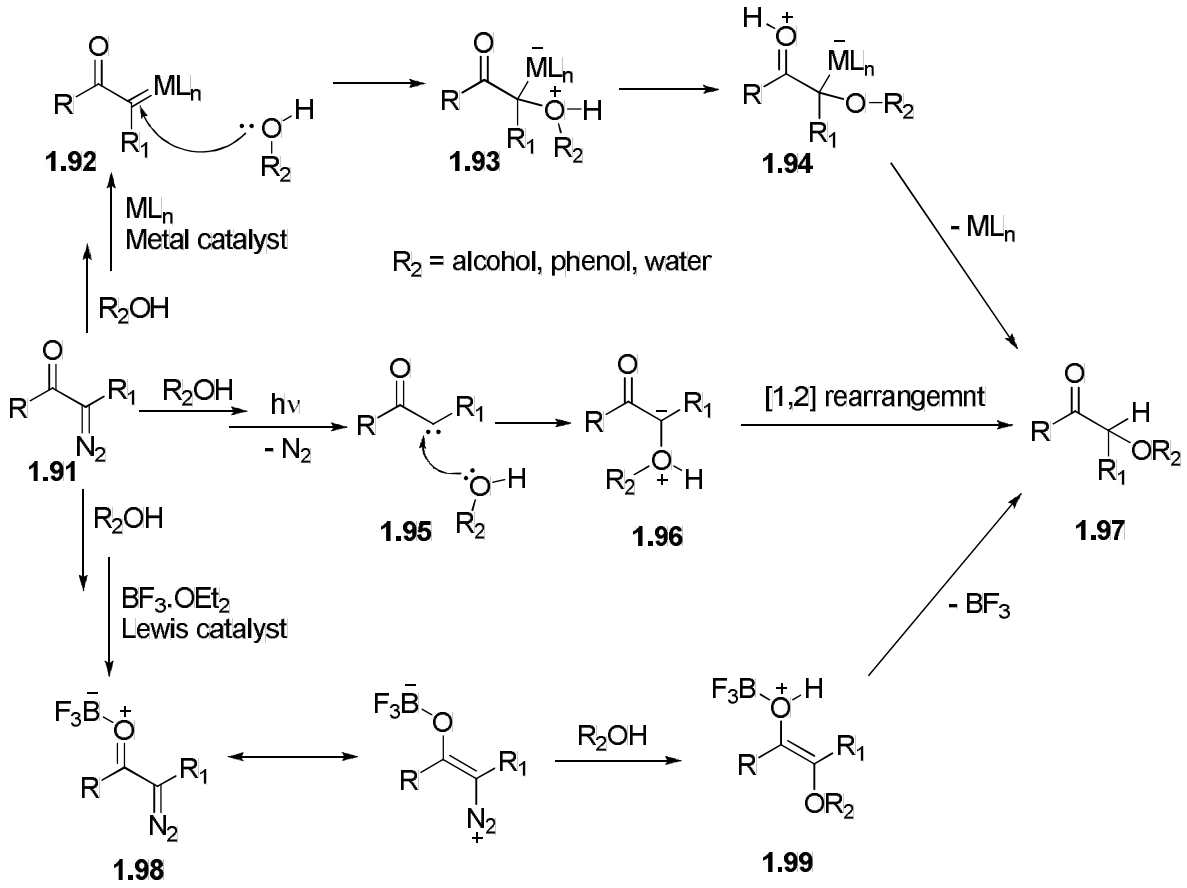

α-Diazo-*p*-hydroxyacetophenone [93] analogs are intriguing model compounds to explore potential competing pathways of photo-Wolff rearrangement and photo-Favorskii rearrangement to the identical rearranged acid **1.53**. In addition, diazo *p*HP derivatives can also have the potential to be used as synthetic precursors for the generation of *p*HP analogues. As explained earlier, α-diazocarbonyl compounds **1.100** undergo an array of X-H insertion reactions generating a wide variety of compounds **1.101** where X can be a nitrogen, oxygen, sulfur, phosphorus, or a halogen atom (Equation 1.27).[74]

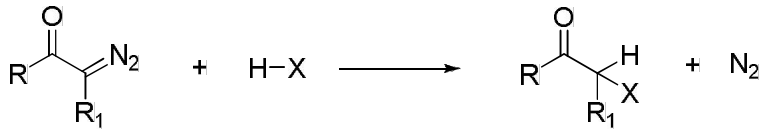

1.100 **1.101**

Eq. 1.27

A similar approach may be employed to produce a wide variety of *p*HP protected esters in a one-pot synthesis. Previously, during the development of the *p*-hydoxyphenacyl (*p*HP) group as a photoremovable protecting group in 1996 by Givens and co-workers,[51,52] a number of synthetic routes had been developed for the preparation of various *p*HP protected functionalities such as carboxylates, phosphates, sulfonates, phenolates, and amino acids. Some of the more familiar approaches,[46,51,52,94,95] particularly those used to access *p*HP phosphates, are laborious, time consuming, and result in low yields. For example, simple S_N2 displacement of α-haloketones may require either organic or inorganic bases or protecting groups to complete the reaction. When strong acids and bases are required, the phosphate functionality may not be compatible with the lprocess. Therefore, a general synthetic precursor that would allow facile installation of the *p*HP protection on phosphates under mild reaction conditions, potentially via a one-pot approach, would be greatly desired. It was rationalized that α-diazo-*p*-hydroxyacetophenone[93] may play that role and might serve as a universal precursor through the known acid catalyzed insertion chemistry of diazoketones **1.102**. This relatively simple approach has been used previously to generate ketophosphates **1.103**, a process that has been widely used in enzymatic studies (Equation 1.28).[96-98]

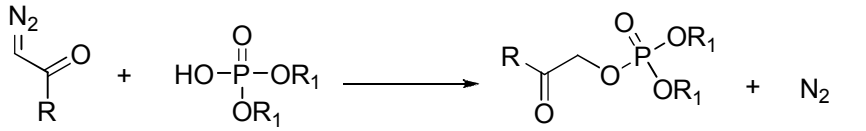

1.102

R = *p*-NO_2-C_6H_4-$O(CH_2)_2C(O)CH_2$-

R_1 = PO_4^{2-}

1.103

Eq. 1.28

Photo-Wolff Rearrangement

Since its discovery in 1902, the ground state (thermal/catalytic) and the excited state photo-Wolff rearrangements have been employed in a variety of areas such as synthetic chemistry, photolithography, and in drug delivery. [74,75,99,100] The Wolff rearrangement of α-diazo ketones follows either a concerted or stepwise mechanism or both via a ketene intermediate to a variety of products depending on the nature of the nucleophile (Scheme 1.14).[74,101,102]

Scheme 1.14 The Wolff Rearrangement Reaction Pathway Followed by Nucleophile Addition (i.e. alcohol) Generating an Ester. Carbene Trapping Product also Shown

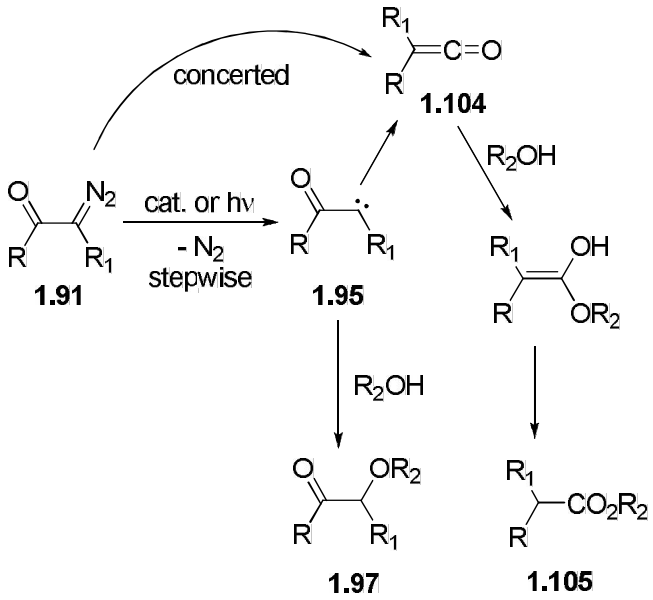

The concerted pathway, which can be envisaged as proceding through an abridged interemediate similar to that proposed in the photo-Favorskii rearrrantement, generates the ketene **1.104** directly from the starting material **1.91** which is subsequently trapped by a nucleophile (i.e. alcohol, amines, etc.) to form the ester (or amide) **1.105**. On the other hand, the stepwise mechanism produces the carbene **1.95** by extrusion of nitrogen followed by rearrangement to the ketene **1.104**. The carbene **1.95** can also be trapped by the nucleophile

to form **1.97**. However, these two plausible mechanisms shown in Scheme 1.13 fail to explain the discrete excited state pathway.

The reactivity of diazocarbonyls has been extensively studied both experimentally and theoretically.[99-105] Diazocarbonyls are typically planar with regard to the O=C-C=N_2 group. It was found that α-diazocarbonyl compounds exist as an equilibrium mixture of two isomers, s-Z and s-E, because of restricted rotation around the C-C single bond (Scheme 1.15). The s-Z conformer **1.91 s-Z'** is sometimes favored due to an interaction between partially positively charged nitrogen's attraction to the partially negatively charged oxygen atom. Another factor which supports this assumption is the partial double bond character of the C-C bond.[99,100] If R_1 is H, bulky R groups would favor the s-Z conformation since the bulky R group has less interaction with the methine hydrogen whereas sterically bulky R groups would destabilize the s-E conformation due to strong interference with the dizo group.[99-105]

Scheme 1.15 Conformers of the Acyclic α-Diazoketones

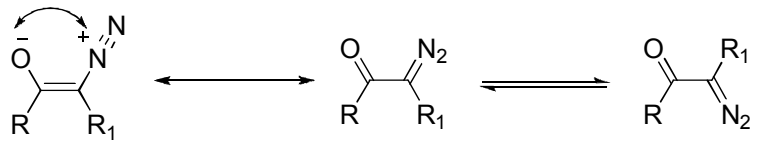

1.91 s-Z' **1.91 s-Z** **1.91 s-E**

If R_1 is not H, the equilibrium between s-Z and s-E can be shifted towards the s-E conformer using sterically bulky R groups. The opposing alignment of dipoles may also favor the s-E conformer. Empirical data have shown that ketene formation is preferred when the α-diazoketone is in its s-Z conformer, whereas trappable carbene formation is dominant when the diazo ketone is in its s-E conformation.

In 1960s Kaplan and Meloy[106,107] reported hindered internal rotation about the carbon-carbon bond in diazoketones using low-temperature, high-resolution ^{1}H NMR spectroscopy. It was observed that the methine proton appears as two separated signals for aliphatic diazoketones **1.105a-e** at lower temperatures in the -40 °C to -50 °C range (Figure 1.2).

Figure 1.2 Aliphatic Diazoketones and *p*-Substituted Diazoacetophenones

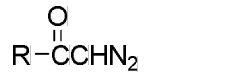

1.105a R = H
b R = CH_3
c R = C_2H_5
d R = CH_3O
e R = C_2H_5O

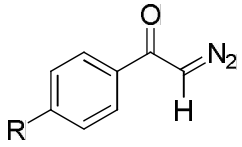

1.106a R = H
b R = Me
c R = Cl
d R = Br
e R = OMe
f R = NO_2

This observation reveals that aliphatic diazoketones **1.105a-e** exist as an equilibrium mixture of s-*cis* and s-*trans* forms in solution (in this case the solvent was $CDCl_3$). However, *para*-substituted diazoacetophenones **1.106a,e-f** gave only one peak for the methine proton in ^{1}H NMR even at -40 °C (Figure 1.2). The authors suggested that *para*-substituted diazo derivatives strongly prefer the s-*cis* conformation because of stability from cross-conjugation. Later Sorriso et al.[108,109] reported that the *syn* and *anti* equilibrium of *para*-substituted diazoacetophenones **1.106a-f** is almost entirely shifted to the *syn* conformer (s-Z, > 98%) in accordance with the dipole moment calculations. The authors did not observe any rapid interconversion between s-Z and s-E conformers of *para*-substituted diazoacetophenones **1.106a-f**. The X-ray crystal structure of **1.106a** confirms the s-Z conformation for the CO-CHN_2 groups.[110] Computational calculations both at the semiemperical level (AM1) and the *ab initio* level calculations [HF/6-31G(d)] on the diazoketones **1.106a-f** in the gas phase prefer the twisted synperiplanar (syn, s-Z) rather than antiperiplanar (anti, s-E) conformation

of the CO-CHN_2 group.[111,112] The angle between the plane of the benzene ring and the plane of the $COCHN_2$ group is < 2° for the unsubstituted diazoketone **1.106a** in the crystalline state. However, the computational calculations indicate 1.6-2.9° distortion for the gas phase (unsolvated) **1.106a** and for other diazo ketones **1.106b-c,e-f**.[99,111,112]

Scheme 1.16 Key Intermediates in the Wolff Rearrangement[113]

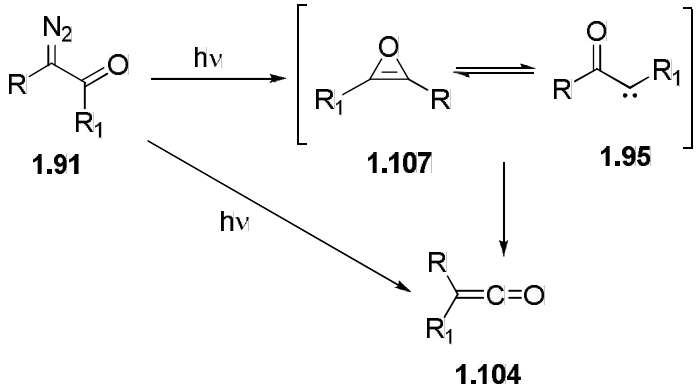

Extensive mechanistic studies have been performed on α-diazoketones because of their wide applicability.[113] Several key intermediates such as carbenes **1.95**, oxirenes **1.107**, and excited-state species play crucial roles in the proposed mechanism of the Wolff rearrangement (Scheme 1.16).

Ketene derived products from the Wolff rearrangement have been by far the most thoroughly studied.[114] Carbene[99,100] and oxirene[115,116] intermediates have been detected both directly and indirectly with the help of spectroscopic methodologies such as time-resolved UV-vis, time-resolved IR, FTIR and low-temperature ESR spectroscopy.[113] Isotope labeling experiments provide a wealth of indirect evidence for the formation of an oxirene intermediate in the course of the reaction.[117,118] For example, a diazoketone **1.108** labeled at the carbonyl carbon rearranges via an oxirene intermediate **1.110** to yield ketenes **1.112** and **1.113** which possess labels at both carbon atoms (Scheme 1.17).

Scheme 1.17 Indirect Evidences for the Formation of Oxirene Intermediate

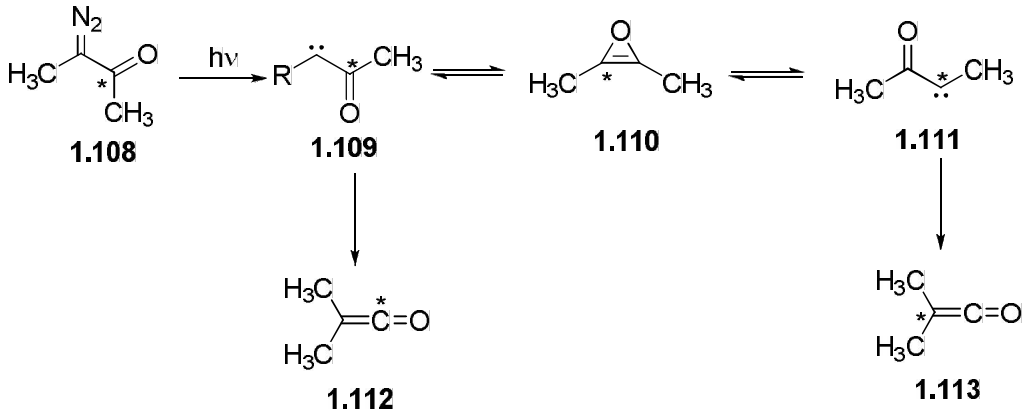

Unsymmetrically substituted diazoketones also gave similar results indicating the involvement of the oxirene intermediate in the Wolff rearrangement.[119] The direct observation of the dimethyloxirene intermediate and its deuterated analogue was reported by Bodot and co-workers by low-temperature FTIR methods.[120] Recently, Platz and co-workers reported the direct observation of the oxirene intermediate in their ultrafast carbene-carbene isomerization studies by fs UV-vis transient absorption spectroscopy.[121] Previous studies have shown that the Wolff rearrangement occurs in the singlet rather than triplet manifold.[113,122] Nonetheless, triplet sensitized photolysis of diazoketone **1.114** gave carbene adducts **1.116**, indicating that either the diazo precursor or the carbene is involved in the rearrangement (Scheme 1.18).

Scheme 1.18 Carbene Adduct Formation in the Triplet Sensitized Photolysis[122]

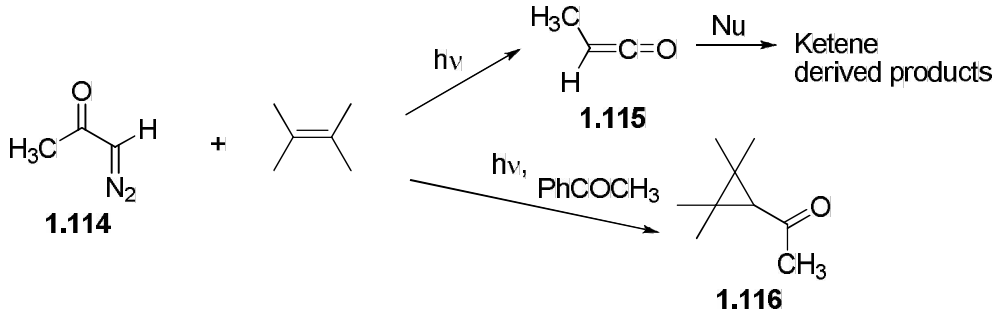

The extensive study on the photochemistry of methyl diazoacetate **1.117**, including direct and triplet sensitized photolysis along with quenching studies, by Tomioka and co-workers[123,124] gave further insight into the multiplicity of species involved in the Wolff rearrangement (Scheme 1.19).

Shcheme 1.19 Photochemistry of Methyl Diazoacetate **1.117** in Neat Alcohol[123]

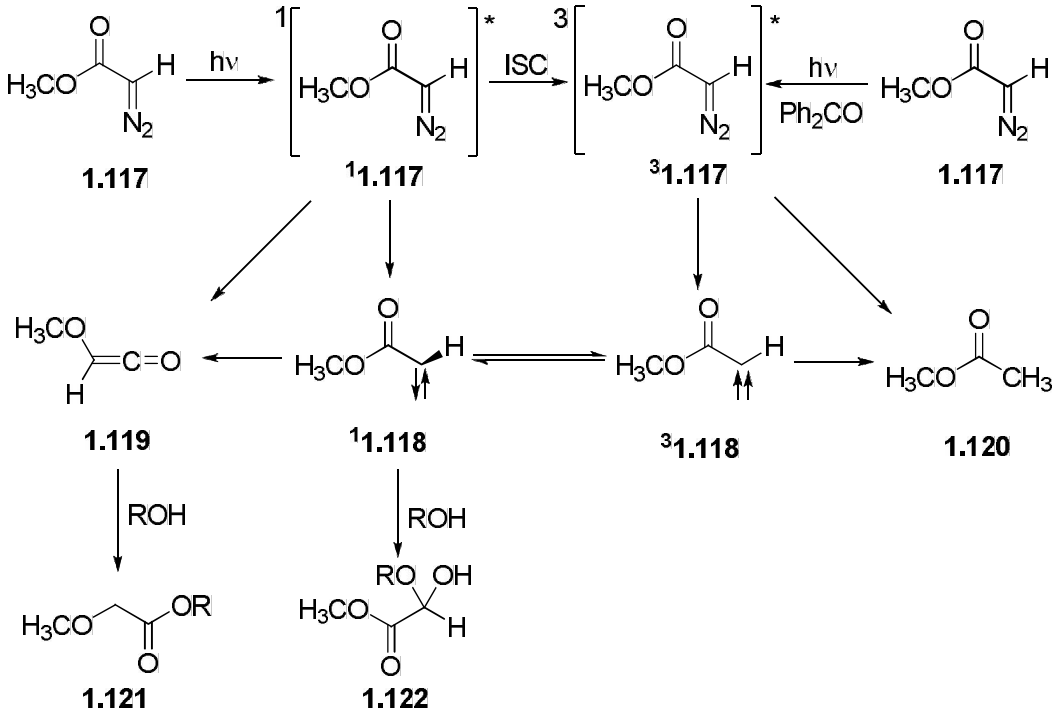

The direct photolysis of methyl diazoacetate **1.117** generates the singlet excited diazoacetate ^{1}**1.117** which can follow three different pathways; it either can undergo Wolff rearrangement concurrent with nitrogen extrusion to yield ketene **1.119** or can intersystem cross to produce triplet excited diazoacetate ^{3}**1.117** or can lose nitrogen to give the singlet carbene ^{1}**1.118**. The ketene **1.119** and singlet carbene ^{1}**1.118** can be trapped by alcohol (ROH) yielding the Wolff rearranged product **1.121** and an alcohol addition product **1.122**, respectively. Methyl acetate (**1.120**), a reduction product, has also been observed which is clearly derived from triplet excited species ^{3}**1.117** and ^{3}**1.118**.

Authors further demonstrated that triplet sensitized photolysis with benzophenone enhanced the yield of the reduction product **1.120**, whereas quenching studies with piperylene diminished the yield of the reduction product **1.120**. Nonetheless, the alcohol insertion product **1.122** has been observed with the triplet sensitized photolysis indicating an interconversion between the triplet carbene ^{3}**1.118** and the singlet carbene ^{1}**1.118**. Previous studies by Hutton and Roth[125] showed that the triplet carbene ^{3}**1.118** is the ground state of the carbene derived from methyl diazoacetate **1.117** by low-temperature ESR spectroscopy. Therefore, Tomioka and co-workers' results clearly indicate that the more reactive singlet excited carbene ^{1}**1.118** is close in energy with the triplet carbene ^{3}**1.118**. In the case of triplet sensitized photolysis of methyl diazoacetate **1.117**, any singlet carbene ^{1}**1.118** formed should react faster with alcohol to produce an insertion product than the Wolff rearrangement to produce ketene **1.119**, because triplet sensitized photolysis suppressed the formation of the ketene **1.119**.

In the 1960s Kaplan and co-workers[106,107] demonstrated that the conformation of the diazo precursor plays a crucial role in the Wolff rearrangement. They found that aliphatic diazocarbonyl compounds exist as an equilibrium mixture of *syn* and *anti* form, whereas aryl diazocarbonyl compounds exist predominantly in the *syn* conformation. The facile concerted rearrangement is possible from the *syn* conformation, but less likely from the *anti* conformation (Scheme 1.20).

They also found that the *syn* conformation locked doazocarbonyl compound **1.123** produces almost exclusively Wolff rearranged product **1.124**, whereas the *anti* conformation preferred diazocarbonyl compound **1.125** does not generate the ketene. Instead, carbene derived products were observed; mainly carbene adducts **1.126** and **1.127** (Scheme 1.20).

Scheme 1.20 Kaplan's Initial Studies on Diazocarbonyl Compounds

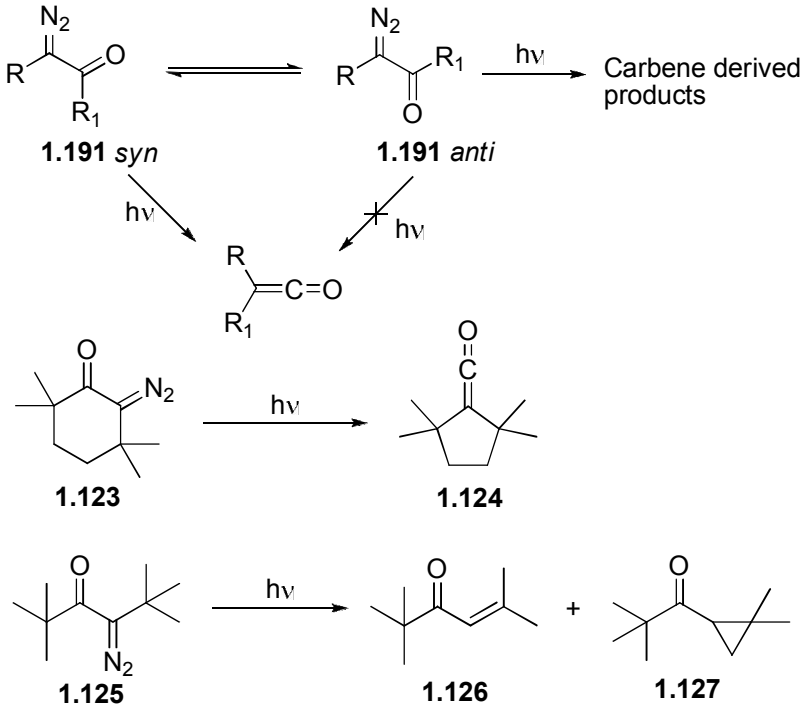

Later, Tomioka and co-workers[124] expanded on Kaplan's initial work using a series of diazoketones including aryldiazoketones. They found that aryl diazoketones which predominantly exist in the *syn* conformation lead to Wolff rearrangement-derived products in methanol. Nonetheless, triplet sensitized photolysis generates a significant decrease of Wolff rearrangement-derived products and produces carbene-derived products. These results are in strong agreement with Kaplan's hypothesis[106,107] which states that diazocarbonyl conformation is preserved in the singlet excited state and the Wolff rearrangement occurs in concerted manner with nitrogen loss from the *syn* conformer.

Recently, Platz and co-workers [126] reexamined the Kaplan's hypothesis on aryl diazocarbonyl compounds using diazo Meldrum's acid which predominantly exists in the *syn* conformation with ps time-resolved transient IR absorption spectroscopy (with 300 fs time resolution). In contrast to Kaplan's hypothesis, the authors found that both concerted and

stepwise mechanisms contribute to the Wolff rearrangement process. They have observed a singlet carbene species with a lifetime of 2.3 ps using UV-vis transient spectroscopy which is in agreement with the TD-DFT calculations.[126]

The pioneering work on α-diazoketones performed by Platz and co-workers to determine how the photo-Wolff rearrangement differs from that of the thermal Wolff rearrangement.[101,126-129] Furthermore, in contrast to Kaplan's original hypothesis, the authors argue based on extensive spectroscopic and computational studies that both concerted and stepwise mechanisms contribute to the Wolff rearrangement in α-diazoketones. Their studies on *p*-biphenyl diazoketone and ester (R = -CH_3) **1.128** discovered three plausible pathways to the ketene **1.131** intermediate in the excited state (Scheme 1.21).

Scheme 1.21 Plausible Mechanistic Pathways for the Conversion of Diazoketone to Ketene[101,127]

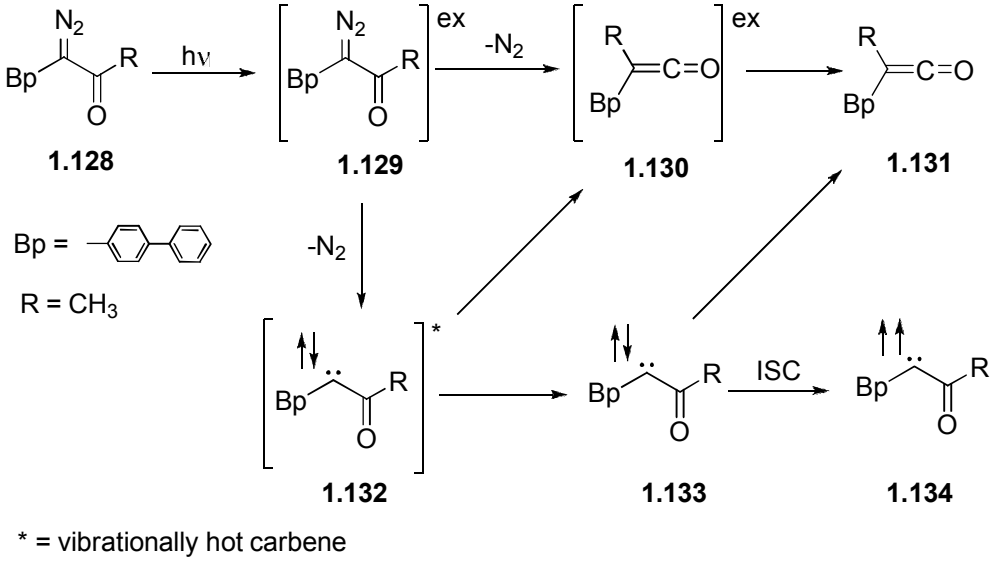

Upon irradiation *p*-biphenylyl diazo ketone **1.128** is excited into its excited (singlet) state **1.129**. At that point, the singlet excited diazoketone **1.129** can either follow the concerted pathway, thereby losing molecular nitrogen and forming an excited state ketene

1.130, or expel molecular nitrogen forming a hot (vibrationally excited) carbene **1.132**. The vibrationally hot carbene **1.132** then either rearranges to the excited ketene **1.130** or it relaxes to a lower energy carbene **1.133**. The relaxed carbene **1.133** may intersystem cross (ISC) to a triplet carbene **1.134**. The species **1.130** and **1.133** eventually rearrange to a ground state ketene **1.131**. Under a given set of conditions, a diazocarbonyl compound may take one or more of these different pathways to the ground state ketene **1.131**.

Platz and co-workers further studied the diazo analog **1.128** using femtosecond UV-vis and time-resolved IR studies to determine the optimal pathway of ketene formation by calculating the reaction rates for each step (Scheme 1.22).

Scheme 1.22 Reaction Kinetics for Each Transition[127]

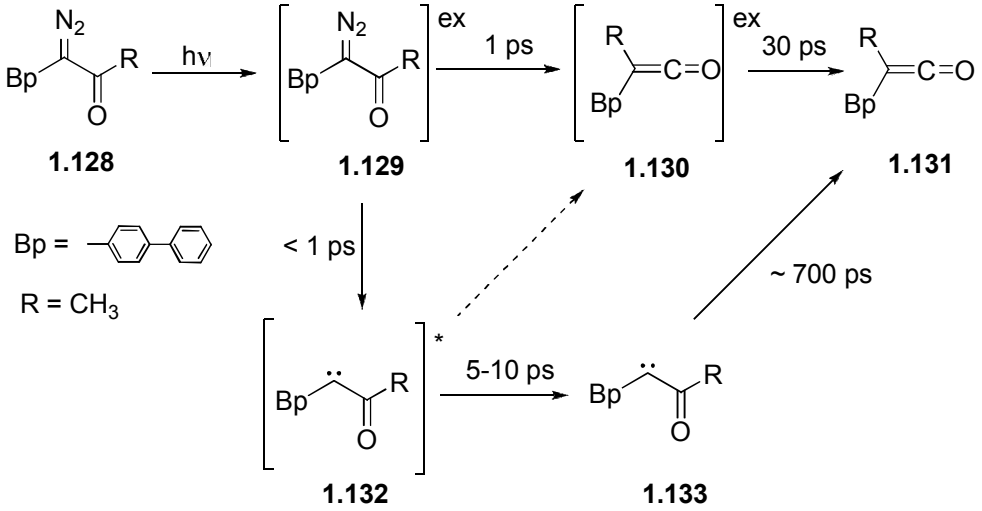

According to their findings, the singlet diazo excited state **1.129** decays either to the rearranged ketene **1.130** or to the vibrationally hot carbene in less than 1 ps. The hot carbene **1.132** then undergoes a Wolff rearrangement in 5-10 ps to form either the relaxed carbene **1.133** or the excited state ketene **1.130**. The relaxed carbene then undergoes the

rearrangement to form the ketene **1.131** in 700 ps, making it to the rate determining step in the photo-Wolff rearrangement. The data were inconclusive with respect to delineating the pathway from **1.132** to **1.130**. By excluding this step, the formation of the ground state ketene can follow two pathways (Scheme 1.22).

The photolysis of the anti (s-E) conformer of **1.128** released molecular nitrogen first; hot carbene relaxation was followed by rearrangement to the ground state ketene, whereas the syn (s-Z) conformer of **1.128** followed the rapid formation of a hot ketene by a concerted pathway.

Further research in the Platz lab suggested an ultrafast carbene-crbene isomerization via an oxirene intermediate, even at 77 K, when two isomeric α-diazoketones were photolyzed. The two isomers gave the same ketene upon both direct and triplet sensitized photolysis according to ultrafast LFP (Scheme 1.23).[101,121] Ultrafast laser flash photolysis of **1.135** and **1.136** excited into their corresponding singlet excited states **1.137** and **1.138**. The singlet excited state diazo analog **1.138** decays into carbene **1.141** which is unstable due to excess vibrational energy. Therefore, **1.138** isomerizes into a more stable carbene **1.140** due to carbene delocalization onto the aromatic ring; **1.140** is also formed from the excited species of the other isomer, **1.137**. Alternatively, the excited species **1.138** can decay to the more stable carbene **1.140** bypassing the vibrationally hot unstable carbene **1.141**. Both carbenes eventually relax into the ground state ketene **1.139**. The migration of oxygen and loss of molecular nitrogen by a concerted pathway produce the relaxed ketene **1.139** bypassing formation of carbenes **1.140** and **1.141**. The formation of an oxirene intermediate was supported by TD-DFT studies.

Scheme 1.23 Three Possible Pathways to the Ketene **1.139**[101,121]

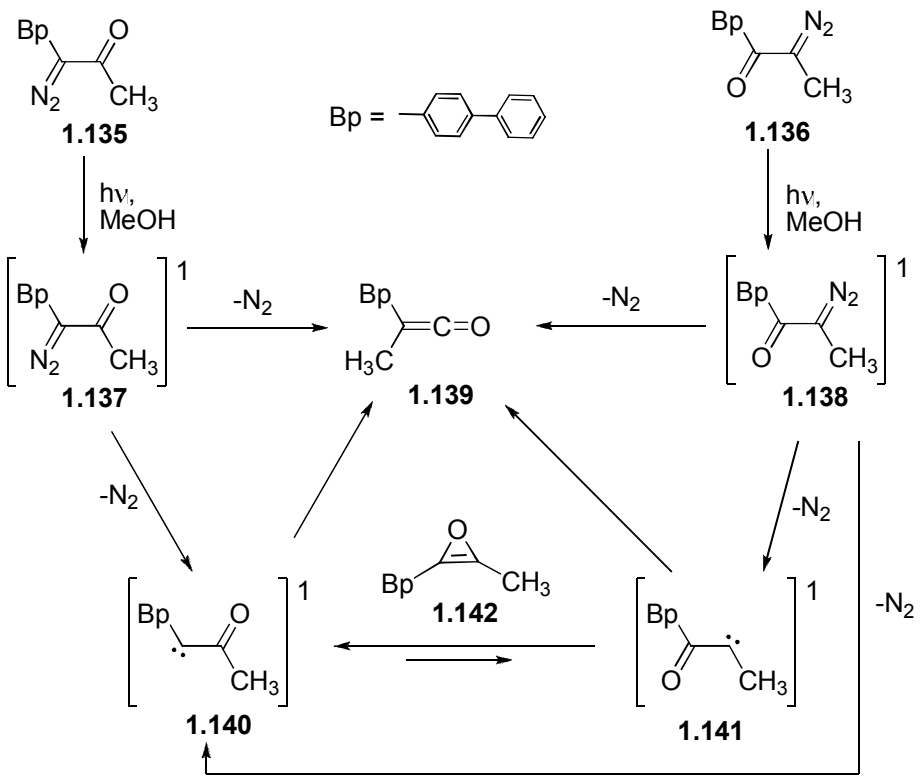

Confirmation of the transient absorption assignable to oxirene intermediate **1.142** failed due to overlap of the absorption with that of the carbene (at 380 nm). The oxirene intermediate either may be an unstable transition state or a short-lived intermediate with negligible detectability.The activation barrier for the carbene-carbene isomerization was found to be 0.70 kcal/mol by gas phase studies (DFT calculations) on two carbens **1.140** and **1.141** (Equation 1.29).

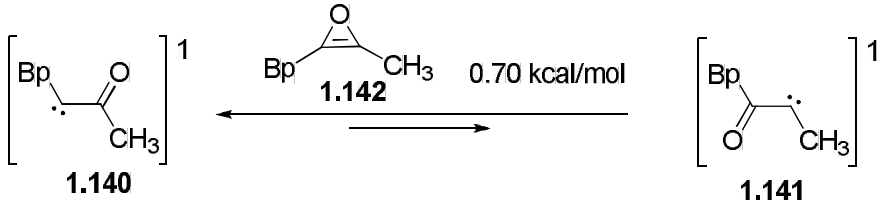

Eq. 1.29

According to the Gibbs free energy calculations, the anti (s-E) conformer is the more stable, resulting in the stepwise mechanism being favored over the concerted mechanism, whereas the *syn* (s-Z) conformer favors the concerted over the stepwise mechanism.

Stabilities of carbene singlet and triplet states

The ketocarbenes favor the singlet ground state due to an electronic effect.[101,102] Extensive theoretical studies have been performed on carbonyl-substituted carbenes in both singlet and triplet states. A carbene ground state can exist as either a singlet or triplet state as illustrated in Figure 1.3.

Figure 1.3 Orbital Overlap between Carbene and Carbonyl π System[101]

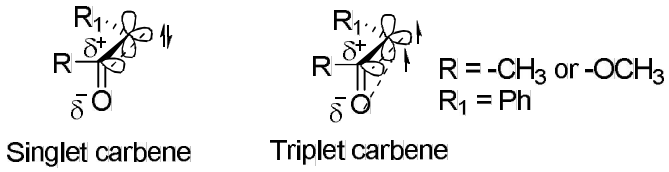

In the ground state the carbonyl group of the singlet carbene lies nearly orthogonal to the plane defined by the carbene carbon atom and its two substituents (the two atoms bonded to the carbene).[101,130,131] This arrangement allows better interaction between the π* system of the carbonyl and the filled hybrid orbital of the carbene which is coming out of the plane of the page. As a result, enolate anion type stabilization is accomplished by the singlet carbene (Figure 1.4). In addition, the in-plane oxygen lone pair of the carbonyl group can be donated to the empty p orbital of the singlet carbene because of its orthogonal orientation.

Figure 1.4 Stabilization in the Singlet Carbene[126]

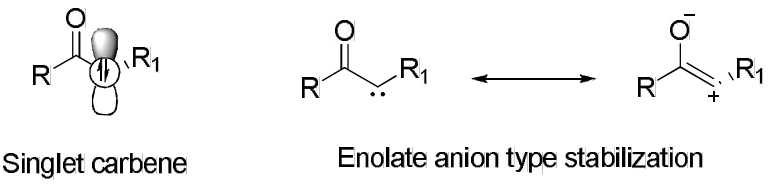

On the other hand, in triplet carbonyl carbenes one unpaired electron is orthogonal to the carbonyl while the other electron is nearly in the same plane as the carbonyl (Figure 1.3). The overlap between the π system of the carbonyl with the carbene orbital occupied by only one of the carbene unpaired electrons is still possible in the triplet state. In addition, there is a destabilizing effect from the carbene electron which is in the same plane as carbonyl. Thus, ketocarbenes generally favor a singlet state.

Ketene trapping by diethylamine

The kinetics of ketene trapping experiments has been extensively studied by Wagner and co-workers[132] on a variety of α-diazoacetophenones. Some of the ketenes which have been used in Wagner's studies and their characteristic IR frequencies are depicted in Equation 1.30and Table 1.8.

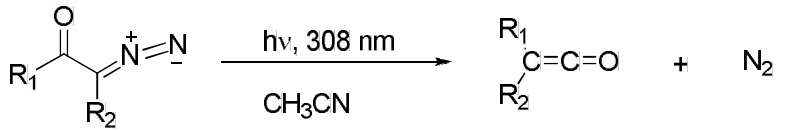

1.143a R_1 = Ph, R_2 = H
b R_1 = *p*-MeOPh, R_2 = H
c R_1 = *p*-CNPh, R_2 = H
d R_1 = *p*-NO_2Ph, R_2 = H
e R_1 = Ph, R_2 = Ph
f R_1 = Ph(CO), R_2 = Ph

1.144a-f

Eq. 1.30

Table 1.8 Stretching Frequencies of Ketene Intermediates in Acetonitrile Reported by Wagner[132]

Ketene	R_1	R_2	ν/cm^{-1}
1.144a	Ph	H	2118
b	*p*-MeOPh	H	2115
c	*p*-CNPh	H	2120
d	*p*-NO_2Ph	H	2122
e	Ph	Ph	2100
f	Ph(CO)	Ph	2119

The authors[132] studied the decay of the ketene as a function of diethylamine concentration to determine the order of the ketene quenching process. It was found that lifetimes of all ketenes (> 500 μs) were shortened upon addition of diethylamine, and the decay of ketenes followed first-order kinetics. In the case of phenyl ketene **1.144a**, the second-order rate constant was found to be 4.8×10^8 M^{-1} s^{-1} from the plot of the observed pseudo first-order decay rate constants vs diethylamine concentrations. The photolysis of the α-diazoacetophenone **1.143a** in CH_3CN in the presence of diethylamine produced a transient species at 1680 cm^{-1} which grows with a kinetic order identical to the decay of the phenyl ketene **1.144a** intermediate (band at 2116 cm^{-1}). The plot of the observed pseudo first-order rate constant of the growth of this transient species vs. diethylamine concentration gave a second order rate constant of 4.5×10^8 M^{-1} s^{-1}. The identical rate constants reveal that this new transient species is the first intermediate from the reaction between phenyl ketene and diethylamine. This unstable new species decays to a more stable species and the formation of the new transient appeared at 1640 cm^{-1}. The species which decays at 1680 cm^{-1} and the new species at 1640 cm^{-1} gave identical kinetics. The second order rate constants were calculated for decay of the species at 1680 cm^{-1} and the growth of the species at 1640 cm^{-1} using plots of the observed first-order decay or growth rate constants vs diethylamine concentration. The values were 2.1×10^7 M^{-1} s^{-1} for the first unstable species at 1680 cm^{-1} and 2.0×10^7 M^{-1} s^{-1} for the second stable species at 1640 cm^{-1}. The stable species was identified as *N,N*-diethylphenylacetamide [**1.147a** (Scheme 1.24)].

Scheme 1.24 Wagner Mechanism for the Decay of Phenyl Ketene **1.144a** with Diethylamine[132]

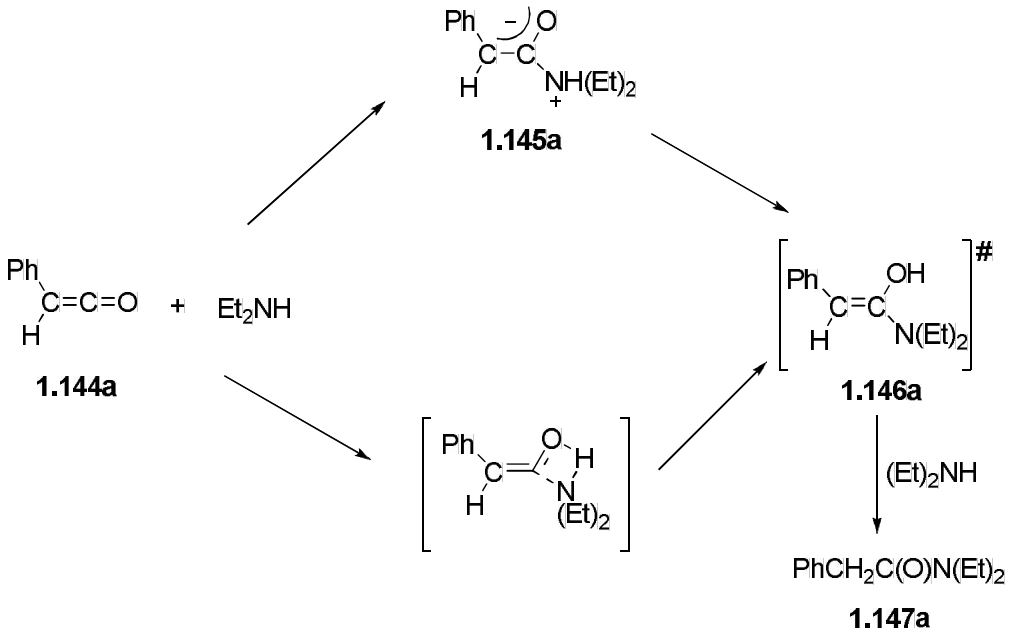

The first unstable species was assigned to a zwitterionic ylide **1.145a** which results from attack of the amine at C_α position of the ketene. These kinds of species were described previously using time-resolved UV-vis spectroscopy [133, 134] and IR in matrix-isolation studies[135,136] of this reaction with the corresponding bands assigned in the 1650 – 1730 cm^{-1} region. In addition, C=C stretching frequencies of amide enols (for example ketene *O,N*-acetals[137]) in the IR spectrum also should appear in the 1640-1680 cm^{-1} region.[138] According to these observations the transient species at 1680 cm^{-1} can be either the zwitterionic ylide **1.145a** or the amide enol **1.146a**. Therefore, the first observable intermediate, the amide enol **1.146a**, can be generated via either a four-membered-ring transition state or a short lived zwitterionic intermediate (Scheme 1.24). Bimolecular rate constants were measured for ketenes **1.144a-f** with diethylamine in acetonitrile, and the results are depicted in Table 1.9.

Table 1.9 Observed Rate Constants for Quenching Kinetics of Ketenes **1.144a-f** with Diethylamine[132]

Ketene	R_1	R_2	ν/cm^{-1}	k_q / 10^7 M^{-1} s^{-1}
1.144a	Ph	H	2118	48
b	*p*-MeOPh	H	2115	33
c	*p*-CNPh	H	2120	95
b	*p*-NO_2Ph	H	2122	95
e	Ph	Ph	2100	1.2
f	Ph(CO)	Ph	2119	2.1

In the early 1990s, a very similar reactivity pattern for amine addition reactions to diphenyl ketene and ketenes derived from diazonaphthoquinones was reported by Andraos and Kresge[139,140] using LFP studies in aqueous solutions. The recorded rate constant values in their mechanistic studies were two orders of magnitude lower (ca. 10^5 M^{-1} s^{-1}) than those observed in Wagner's studies. Similar behavior was also reported by McClelland et al.[141] in the reactions of amines with diarylmethyl cations. The authors have found two orders of magnitude lower reactivity in water than in acetonitrile for the second order rate constants for quenching of diarylmethyl cations by n-propylamine. The explanation for this behavior was that an equilibrium desolvation must precede the quenching reaction because of unreactive hydrated amine complex, $RNH_2 \cdot H_2O$, in the mechanism.

Effects of solvents on carbene formation

The solvent effects on α-diazoketones **1.128** and α-diazoesters **1.148** have been studied in a variety of polar and non-polar solvents such as cyclohexane, acetonitrile, and methanol.[101] It was found that in cyclohexane the triplet carbene is the favored ground state carbene and only the stepwise mechanism occurred because, if the concerted mechanism occurs, the ester product **1.151** would have been formed (Scheme 1.25). The triplet state was

confirmed by oxygen quenching experiments. The major product **1.149** was the triplet carbene derived product. Cyclohexane also acts as a triplet carbene trapping agent. However, the diazoketone **1.128** follows the Wolff rearrangement via the singlet carbene intermediate in cyclohenxane producing ester **1.152** as the major product.

Scheme 1.25 Cyclohexane Solvent Effect on Diazo Ester and Ketone[101]

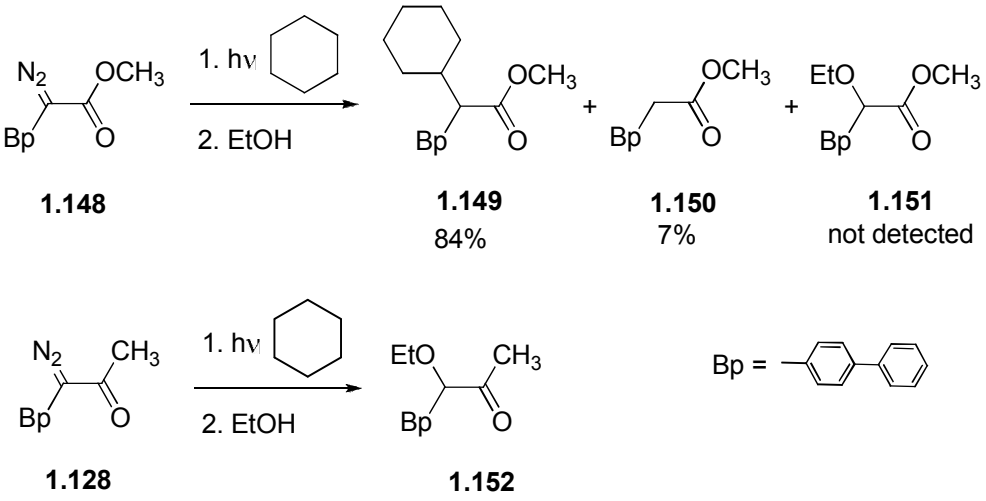

In acetonitrile the lifetime of the carbene does not change under oxygen saturated conditions or argon saturated conditions, confirming the singlet state reaction. The diazoester **1.148** forms the solvent ylide **1.153** without generating a triplet carbene (Scheme 1.26).

Scheme 1.26 Acetonitrile Solvent Effects on Diazo Ester and Ketone[101]

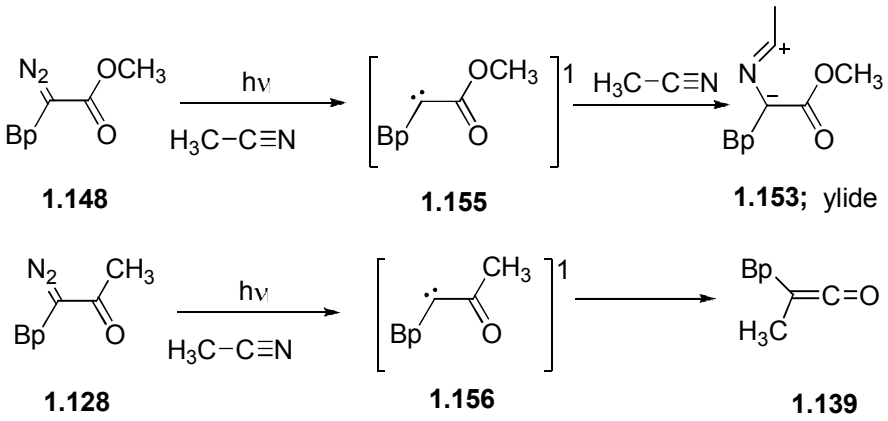

However, diazoketone **1.128** in acetonitrile follows the Wolff rearrangement generating the ketene intermediate **1.139**.

Solvent effects on diazoketones **1.154** and **1.159** were determined in methanol using ultrafast LFP. Even in methanol, an excellent singlet carbene trapping agent, the Wolff rearrangement product was not able to be suppressed. According to the product distribution of the methanol trapped product **1.157** and the Wolff rearrangement product **1.158**, the diazoester **1.154** follows the stepwise mechanism via the singlet excited state (Scheme 1.27).

Scheme 1.27 Methanol Solvent Effects on Diazo Ester and Ketone[101]

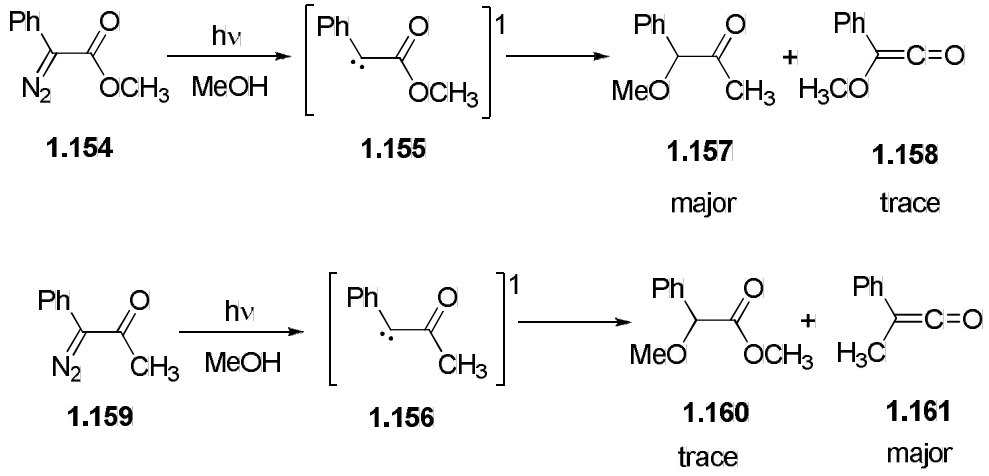

The resonance stability of the ester carbene has a longer lifetime, thereby making the carbene insertion faster than the photo-Wolff rearrangement. On the other hand, the Wolff rearrangement is thought to be a slightly faster process than reaction with the solvent (methanol) with diazoketone **1.159** generating ketene **1.161** as the major product and the carbene insertion product **1.160** as the minor product.

From these solvent studies two conclusions were gained. The photo-Wolff rearrangement is faster for diazoketones in non-polar solvents than polar solvents because singlet carbenes are more polar than the transition state of the Wolff rearrangement. The second factor is that photo-Wolff rearrangement is slower for ester carbenes than keto

carbenes due to a loss of resonance energy in ester carbenes upon rearrangement. Therefore, it is possible to predict the effect that solvent and the type of diazo carbonyl has on which mechanistic pathway of a photo-excited diazo compound would take from these solvent studies on diazoketone **1.128** and diazoester **1.154**.

Through the years α-diazocarbonyl compounds have found wide applications in diverse areas of research and technology including long-standing use in organic synthesis,[74, 142] recent use in surface science,[143] and in the lithographic production of integrated circuits used by the computer industry.[144] It is well known that α-diazocarbonyl compounds undergo an array of insertion reactions generating a wide variety of compounds.[74] Epstein and Garrossian[48] demonstrated that α-diazo-*p*-methoxyacetophenone can be successfully employed to cage diethyl phosphoric acid in high yields. This result sparked interest into whether or not the same type of chemistry could be observed in α-diazo-*p*-hydroxyacetophenone (diazo *p*HP) and in the synthesis of other *p*HP derivatives such as phosphates, carboxylates, sulfonates, and phenolates. Thus, synthetic methodologies have been designed and developed to generate cage *p*HP derivatives from diazo *p*HP. In addition, α-diazo-*p*-hydroxyacetophenone is itself a well-suited model compound to study the photo-Favorskii rearrangement, although it is known that the chemistry of α-diazocarbonyl compounds is closely associated with the Wolff rearrangement.[99,100,101,102] This mechanistic dilemma prompted us to explore the mechanism of nitrogen release from the diazo *p*HP to provide insight into the actual mechanism. Time-resolved IR spectroscopic studies, sensitization, and quenching studies have provided quantitative mechanistic information on this reaction. The effects of methoxy substituents on the *p*HP photochemistry to release phosphates have also been determined.

Statement of Problem

Over the past three decades photoremovable protecting groups have been applied in biology and related areas to study biochemical reactions; some studies were even conducted in living tissue. It is well understood that several of these biochemical reactions are driven by the released energy stored in the phosphate bonds of biologically active substrates such as ATP and GTP. These biochemical processes, some of which are very fast, can be studied by using photoremovable protecting groups, known as caged compounds, to temporally and spatially control the release of substrates (e.g., phosphates). Thus, there is a growing trend to apply this fascinating chemistry to other biological important phosphates such as cAMP, inositol phosphates, adenophostin, afuranophostin, and ribophostin which play crucial roles in rapid biochemical reactions. *p*-Hydroxyphenacyl (*p*HP) is an emerging photoremovable protecting group with the potential to be applied to these challenging derivatives mainly due to its properties of good water solubility, its clean photochemistry, and its rapid release of substrates. The current synthetic approaches to generate *p*HP caged phosphates are generally laborious and limited. If one were able to develop a universal synthetic route to cage these substrates with *p*HP, especially by a one step reaction, a whole new arena of *p*HP chemistry would be available to researchers who explore biochemical processes. A universal synthetic precursor could be α-diazo-*p*-hydroxyacetophenone, based on the well documented use of α-diazoketones in successful reactions for alkylation in synthetic organic chemistry. Therefore, a feasible synthetic protocol for the synthesis and esterification chemistry of α-diazo-*p*-hydroxyacetophenone is targeted. This approach was also envisaged for the synthesis of other *p*HP esters such as carboxylates, sulfonates, and amino acids and phenolate ethers. Interestingly, α-diazo-*p*-hydroxyacetophenone serves as a model for the mechanistically

challenging study of the photo-Favorskii rearrangement. α-Diazoketones follow a photo-Wolff rearrangement pathway upon irradiation. Photolysis of α-diazo-*p*-hydroxyacetophenone could follow either the Wolff or the photo-Favorskii pathways or both. This dilemma prompted us to study the mechanism of nitrogen release from α-diazo-*p*-hydroxyacetophenone providing insight into the actual mechanism.

Using this new synthetic entry to *p*HP derivatives, the effect of ortho substituents on the *p*HP chromophore will be explored. It is worthwhile to study the effects of methoxy and acetyl groups on the *p*HP chromphore with regard to releasing phosphates, and these derivatives may be accessible through the one-pot synthesis outlined above with substituted α-diazo-*p*-hydroxyacetophenones. These studies may provide not only better chromophores but also additional probes for the controversial photo-Favorskii/Wolff dichotomy.

Results and Discussion

A. Synthetic Methodologies

Synthesis of the *p*HP protected diphenylphosphate via the PO-H insertion in phosphoric acids.

The proposed synthetic approach to *p*HP protected phosphates is depicted in Scheme 1.28. The *p*-hydroxyphenacyl diphenyl phosphate triester can be generated by reacting a OH-protected or unprotected diazoketone **1.165** with biphenyl phosphoric acid[145] Diazoketones **1.164** could, in turn, be obtained via reacting with diazomethane of the corresponding acid chlorides of *p*-acetoxybenzoic acid or *p*-benzyloxybenzoic acid **1.162**.[145]

Scheme 1.28 Proposed Synthetic Route to the *p*HP Diphenylphosphate via Protected or Unprotected Diazo *p*HP

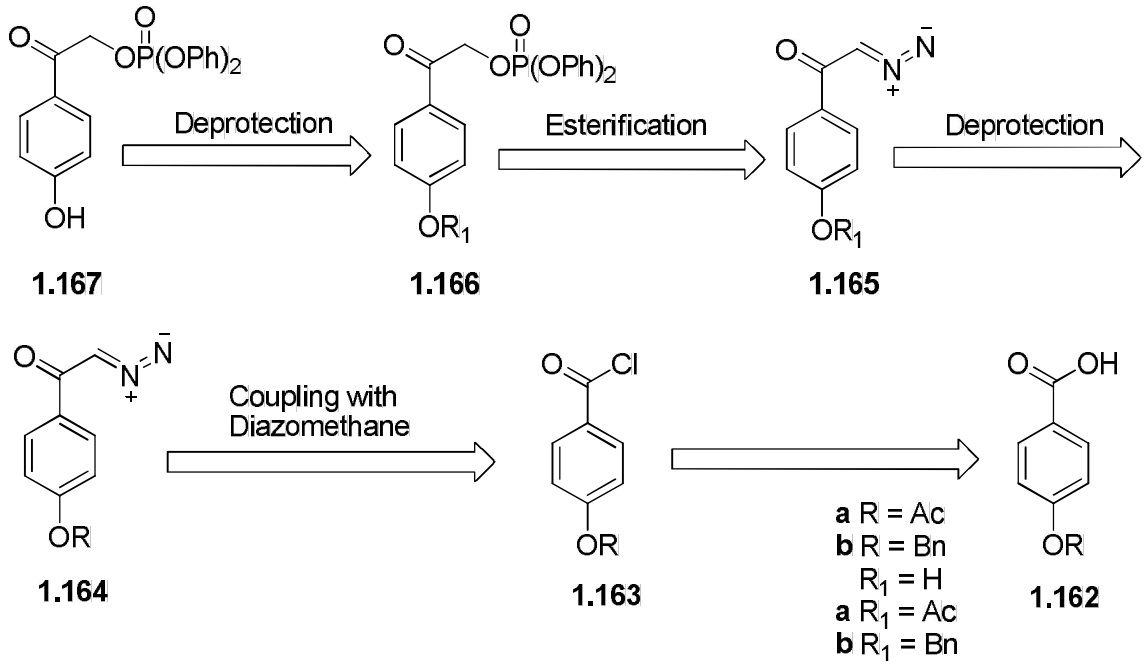

Synthesis of phosphate esters via α-diazo-*p*-hydroxyacetophenone.

The correct choice of a protecting group for the phenol was key to the success in this synthesis. The deprotection of the phenol group could potentially be performed either after generation of the caged phosphate ester **1.166** or prior to reacting diphenylphosphoric acid with the diazo *p*HP **1.165**. It was found that the standard conditions used for removal of benzyl protection were incompatible with the phosphate or diazo functionality. The acetate protection was found to be the best suited approach because it could be efficiently cleaved under mild conditions (NH_4OAc in aqueous methanol) without disturbing either the diazo or diethyl phosphate functionalities. *p*-Acetoxybenzoic acid (**1.162a**), a readily available starting material, was used to generate α-diazo-*p*-hydroxyacetophenone (**1.165**), as illustrated in Scheme 1.29.

Scheme 1.29 Synthesis of α-Diazo-*p*-Hydroxyacetophenone (**1.165**)

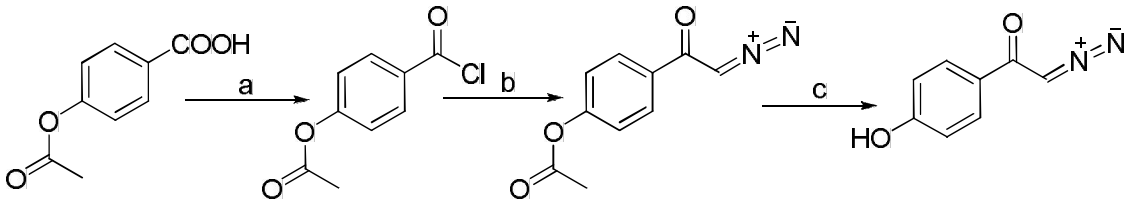

Reagents and conditions: (a) $SOCl_2$, reflux, 8 h, 99%; (b) CH_2N_2, Et_2O, - 5 °C – rt, 54%; (c) NH_4OAc, H_2O/ MeOH, (1:4), 50 °C, 8 h, 98%.

Treatment of the *p*-acetoxybenzoic acid **1.162a** with $SOCl_2$ at reflux produced the acid chloride **1.163a**, which was then reacted with excess diazomethane to give *p*-acetoxy-α-diazoacetophenone (**1.164a**) in moderate yield. The deprotection of **1.164** proceeded uneventfully to produce diazo *p*HP **1.165**, which was used in the subsequent syntheses of phosphate esters **1.167** and **1.168.** (Equation 1.30) Thus, the synthesis of 4-acetoxyphenacyl diphenyl phosphate was achieved by reacting *p*-acetoxy-α-diazoacetophenone (**1.164a**) with

diphenyl phosphoric acid in dry benzene. However, the removal of the acetate protecting group from **1.166** was unsuccessful with either NH_4OAc or $NaHCO_3/Na_2CO_3$ without disturbing the diphenyl phosphate group. Therefore, the same synthesis was performed with **1.165** to generate 2-(4-hydroxyphenyl)-2-oxoethyl diphenyl phosphate (**1.167**) to avoid difficulties of removing the acetate protecting group without affecting diphenyl phosphate group. The applicability of this method was further explored by synthesizing 2-(4-hydroxyphenyl)-2-oxoethyl diethyl phosphate (**1.168**) following the same procedure (Equation 1.31).

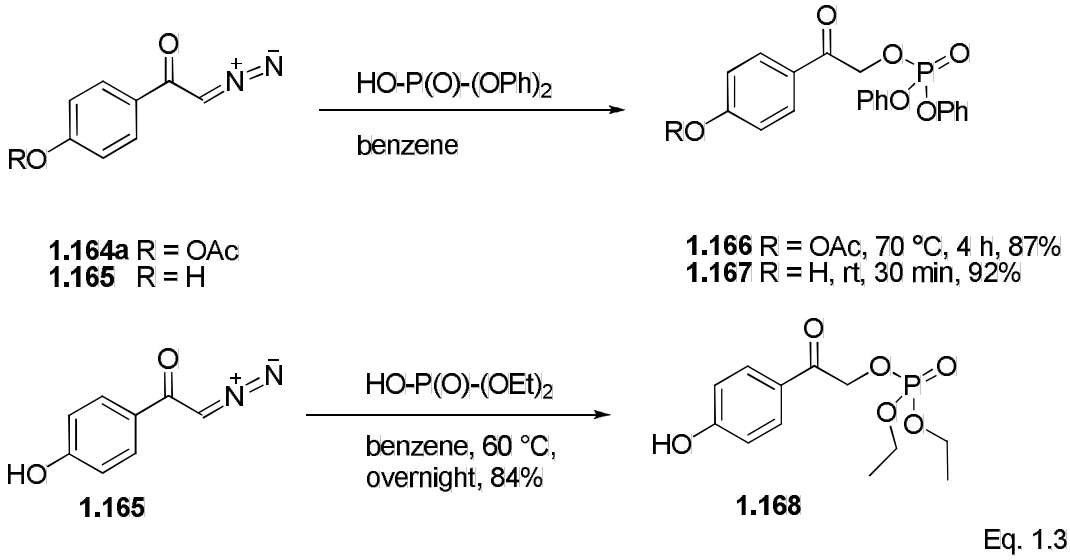

Eq. 1.31

Reaction of diazo *p*HP **1.165** with diphenyl phosphate proceeded smoothly at room temperature, while that with diethyl phosphate required heating at 60 °C overnight to achieve complete conversion. The reason for the decreased reactivity may be the higher pK_a value of diethyl phosphoric acid (ca. 1.42 ± 0.50) as compared to diphenyl phosphoric acid (ca. 1.12 ± 0.50).[146]

Synthesis of carboxylate and sulfonate esters using α-diazo-*p*-hydroxyacetophenone

The same protocol was applied to the synthesis of the *p*HP caged carboxylates (benzoate and acetate) and sulfonates (mesylate and tosylate) **1.169-1.174** (Scheme 1.30). The rate of the acid catalyzed decomposition of α-diazoketones increased with decreasing pK_a of the acids.[74] To suppress the unwanted decomposition of the starting material, the reactions were carried out at 0 °C with the strong acids such as methanesulfonic acid, triflic acid, *p*-toluenesulfonic acid, and trifluoroacetic acid.[147,148]

Scheme 1.30 Synthesis of the *p*HP Caged Carboxylates and Sulfonates

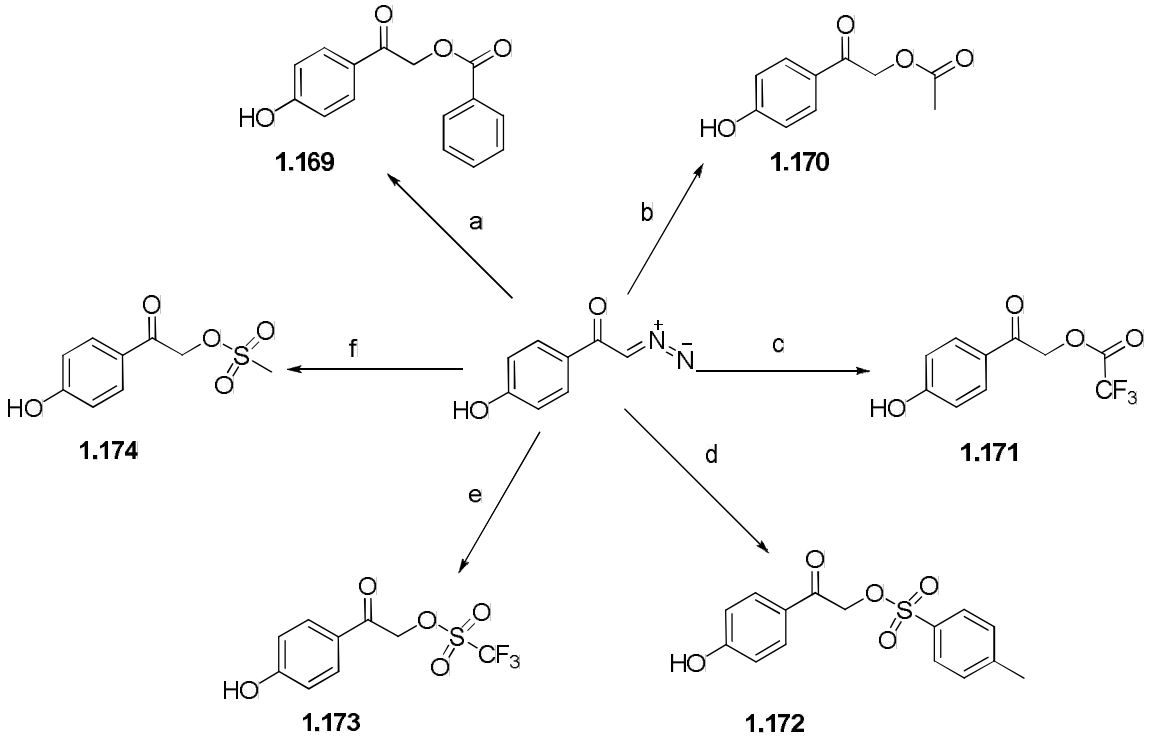

Reagents and conditions: (a) PhCOOH, benzene, 70 °C, 42 h, 97%; (b) CH_3COOH, H_2O/CH_3CN, 1:1, 16 h, rt, 98%; (c) CF_3COOH, benzene, 0 °C - rt, 1 h, 94%; (d) *p*-$TsOH.H_2O$, CH_3CN, 0 °C – rt, 1 h, 71%; (e) CF_3SO_3H, benzene, 0 °C – rt, 30 min, 91% (crude); (f) MsOH, benzene, 0 ^{0}C – rt, 1.5 h, 98%.

Synthesis of the *p*HP caged amino acids via α-diazo-*p*-hydroxyacetophenone

The synthesis of *p*HP caged amino acids, such as 4-hydroxyphenacyl GABA and D-glutamate, required the use of copper (II) acetylacetonate catalyst to achieve good product yields, increasing from 5-10% in its absence to 75-80% in the presence of Cu (II) (Equation 1.32). The water soluble copper salts could be easily removed during post reaction aqueous work up. The Boc-protected amino functionality was subsequently treated with TFA to obtain the *p*HP GABA or D-Glu derivative as its trifluoroacetate salt.

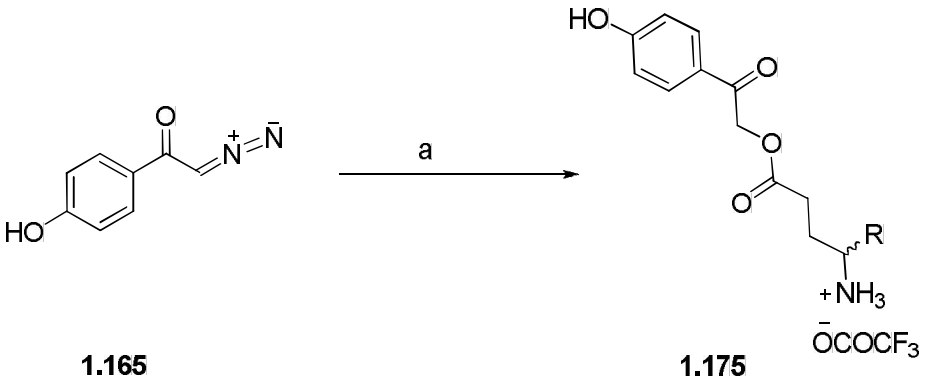

1.165 **1.175**

a. R = H
b. R = COOH

Eq. 1.32

Reagents and conditions: (a) Boc-GABA, cat. $Cu(acac)_2$, toluene, 60 °C, 2 h followed by TFA/CH_2Cl_2, 1:1, 15 min, rt, 75% overall yield of **1.175a**; (a) Boc-D-Glu(O^tBu)-OH, cat. $Cu(acac)_2$, toluene, 60 °C, 2 h, followed by TFA/CH_2Cl_2, 1:1, 15 min, rt, 71% overall yield of **1.175b**.

Synthesis of the *p*HP caged phenolates via α-diazo-*p*-acetoxyacetophenone

The acidity of phenols under ambient conditions was insufficient for nitrogen extrusion from α-diazo-*p*-acetoxyacetophenone (**1.164a**). Accordingly, rhodium tetraacetate [$(Rh(OAc)_4$] or copper(II) acetylacetonate [$Cu(acac)_2$] catalyst was employed to generate caged phenolates. Deprotection of crude caged phenolates **1.176a** and **1.176b** was accomplished quantitatively with NH_4OAc in aqueous methanol to generate the desired *p*HP phenolates **1.177a** and **1.177b** in 56 – 68% overall yields (Scheme 1.31).

Scheme 1.31 Synthesis of 4-Hydroxyphenacyl Phenolates

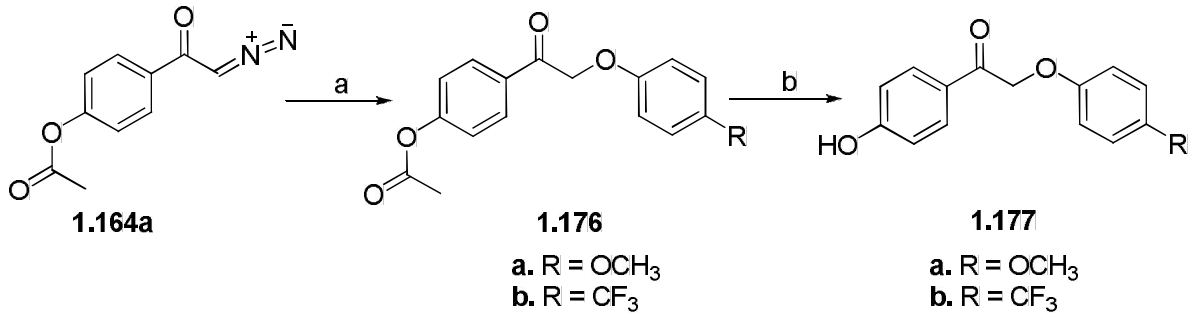

Reagents and conditions: (a) *p*-HO-Ph-OMe/CF_3, 50 °C, 8 h; (b) NH_4OAc, H_2O/ MeOH, (1:4), 50 °C, 8 h, 56-68% overall yield.

Synthesis of the *p*HP caged biologically active phosphates

The applicability of diazo *p*HP **1.165** for caging of biologically active phosphates, such as AMP, cAMP, ATP, NADPH, and D-glucose-6-phosphate, was also tested. As explained in the Introduction, Trentham et al.[19] have shown that the use of $CHCl_3/H_2O$ as the solvent was successful for generating *o*-nitrobenzyl caged ATP from 1-(2-nitrophenyl)diazoethane (NPE), and Churchill et al.[20] have used the same synthetic strategy to synthesize 4,5-dimethoxy-2-nitroacetophenone (DMNPE) caged $NADP^+$ from 1-(4,5-dimethoxy-2-nitrophenyl)diazoethane. Unfortunately, all of our attempts at a parallel approach with **1.165** resulted in the formation of α,*p*-dihydroxyacetophenone (**1.168**) as the only reaction product (Equation 1.33) along with recovered unreacted phosphates.

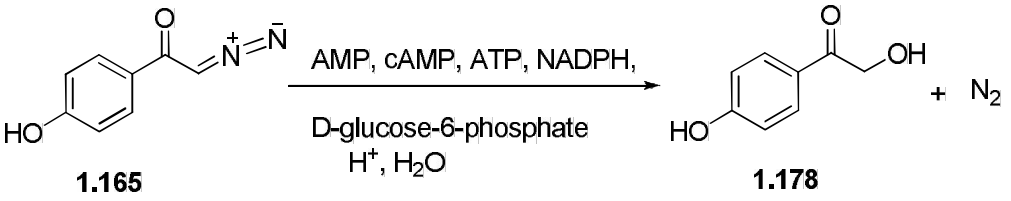

Eq. 1.33

It has been reported that phosphates can be caged with *p*HP or coumarylmethyl groups using α-bromo-*p*-hydroxyacetophenone (**1.181a**)[44,45,52] or 4-(bromomethyl)coumarin derivatives, [34-37,40,41] respectively. Accordingly, we attempted the synthesis of phosphate esters using α-bromo-*p*-hydroxyacetophenone (**1.181a**). To this end, the nucleosides were converted to the corresponding ammonium salts by passing them as aqueous solutions through a Dowex column saturated with tertabutylammonium hydroxide.[41, 149 , 150] The tetrabutylammonium salt of cAMP **1.180** was reacted with α-bromo-*p*-hydroxyacetophenone in CH_3CN at reflux for 5 h (Scheme 1.32).

Scheme 1.32 Synthesis of Protected and Unprotected *p*HP Caged cAMP

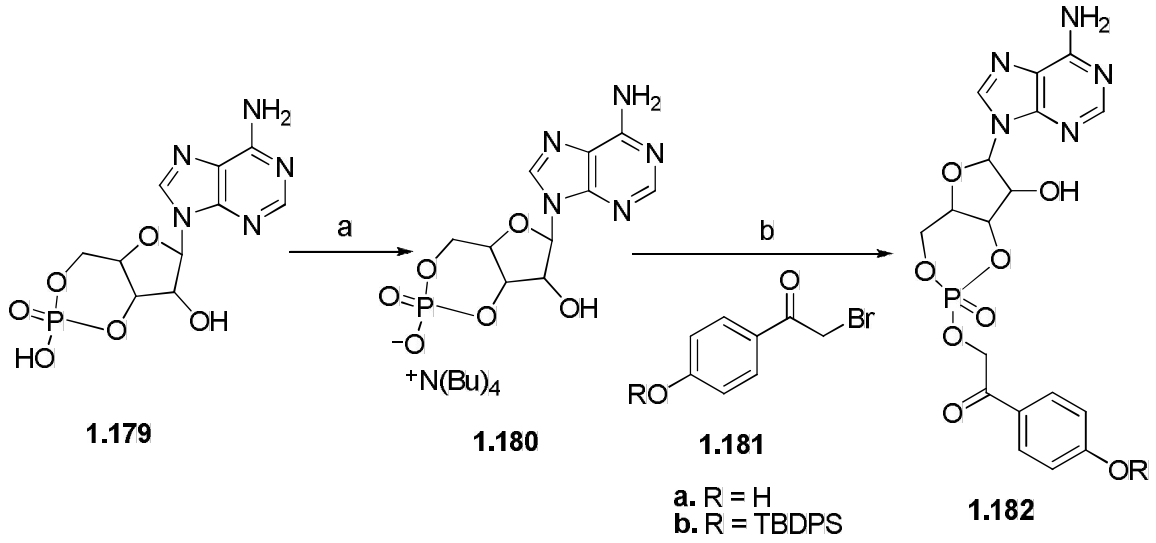

Reagents and conditions: (a) $^{+}N(Bu)_4^{-}OH$, H_2O, Dowex column, 100%; (b) CH_3CN, 85 °C, 5 h, not isolated.

According to ^{31}P NMR analysis of crude reaction mixtures, two major peaks appeared at -5.20 ppm and -3.31 ppm in the ratio of 3:1, which were putatively assigned to the axial and equatorial isomers of the *p*HP caged cAMP **1.182**. The analogous reaction with AMP produced phosphate esters with ^{31}P NMR chemical shifts of -0.79 ppm and 0.01 ppm,

respectively. It should be mentioned, however, that the conversion in both reactions did not exceed 20-25%. Attempts to isolate products by column chromatography,[41,149,150] RP-HPLC, and preparative TLC were unsuccessful. The major problem in isolation with the individual compounds from the crude mixtures was their poor solubility in organic solvents. To overcome this problem, the TBDPS protected *p*HP bromide[122] **1.181b** was used to synthesize caged cAMP. However, the TBDPS protection resulted in no significant improvement in the solubility of the crude products in DMF and MeOH/$CHCl_3$[41,149,150] and therefore no improvement in the chromatographic isolation of products.

Crystal structure analysis of α-diazo ketone 1.165

The X-ray crystal structure of diazo *p*HP **1.165** was obtained to establish the conformation of the molecule in its crystalline ground state (Figure 1.5, Experimental). The obtained data show that the chromophore is planar in its crystalline ground state and that hydrogen bonding between neighboring molecules form an array of planar sheets which allow for efficient π-stacking (Figure 1.6).

Figure 1.5 X-ray Crystal Structure of Diazo *p*HP **1.165**

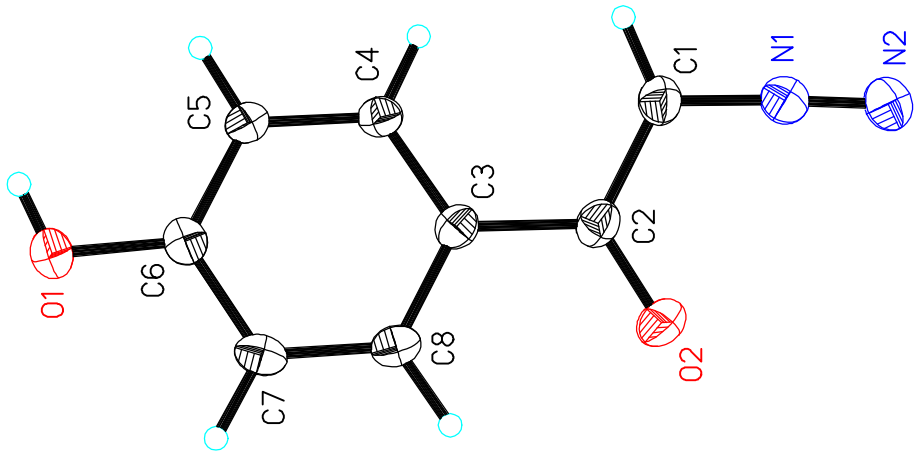

Figure 1.6 Packing of **1.165** in the Crystalline Lattice Cell

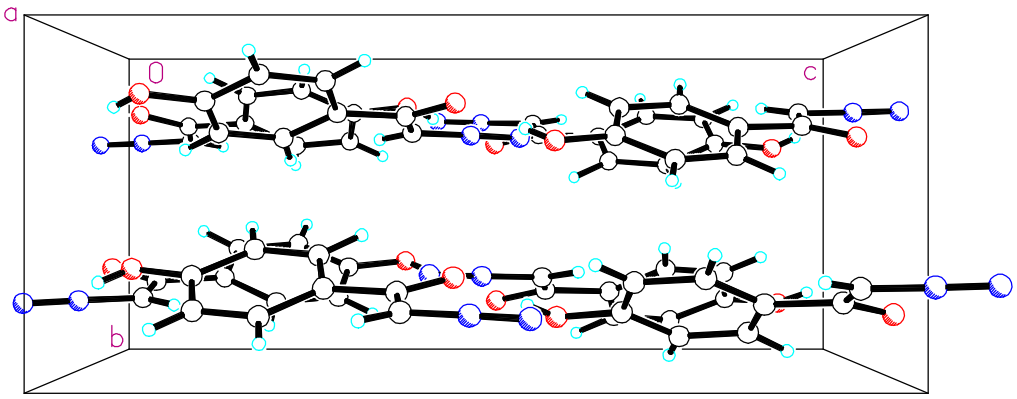

The bond angle between the diazo group (N1, N2), and the diazo carbon (C1) is 177.5° which indicates a nearly linear arrangement (Table 1.10). The dihedral angle between the diazo group (N1), the diazo carbon (C1), the carbonyl carbon (C2), and the ipso carbon (C3) is nearly 180°. This confirms that the diazo group ($C1=N1^{+}=N2^{-}$) is antiperiplanar to the phenyl ring and synperiplanar to the carbonyl group (C=O).[151]

Table 1.10 Measured Structural Parameters of **1.165** in the Crystalline Ground State

Bond length / Å		Bond angle / (°)		Dihedral angle / (°)	
N1-N2	1.110	N2-N1-C1	177.5	N2-N1-C1-C2	22
N1-C1	1.321	N1-C1-C2	116.8	N1-C1-C2-O2	2
C1-H1	0.950	C2-C1-H1	129	N1-C1-C2-C3	179.7
C1-C2	1.431	O2-C2-C1	120.7	O2-C2-C3-C4	-168.5
O2-C2	1.241	O2-C2-C3	121.7	C1-C2-C3-C4	13.8
C2-C3	1.480	C1-C2-C3	117.6	O2-C2-C3-C8	12.3
C3-C4	1.399	C2-C3-C4	122.7	C1-C2-C3-C8	-165.4

The measured bond length between the diazo carbon (C1) and the carbonyl carbon (C2) of 1.43 Å is shorter than that of a normal carbon-carbon single bond (ca. 1.54 Å),[151] suggesting partial double bond character. Furthermore, the bond length between the two

nitrogen atoms of the diazo group is only 1.11 Å, which is very close to the bond length of a nitrogen-nitrogen triple bond (ca. 1.10 Å)[151] These data confirm a partial positive charge build up on the nitrogen (N1) as a result of resonance stabilization. This, in turn, causes an electrostatic attractive interaction between the partially negatively charged carbonyl oxygen (O_2) and the partially positively charged nitrogen (N1) in this s-Z conformation.

Scheme 1.33 Conformer Analysis from Solid State, X-ray Results of **1.165**

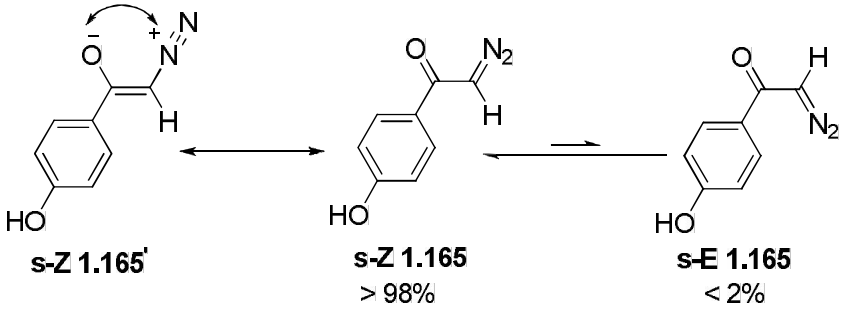

In addition, the methine proton of **1.165** gave only one peak (CD_3CN, δ ppm 6.30, 1H, s) in ^1H NMR spectroscopy. This indicates that there is a strong preference for only one conformer in solution. As noted above, the X-ray analysis shows that diazo *p*HP **1.165** preferentially adopts the s-Z conformation (**s-Z 1.165**) in the crystalline ground state (Scheme 1.33). These data, therefore, are in strong agreement with the ^1H NMR spectroscopy and X-ray crystallography data reported for similar *para*-substituted diazoacetophenones by Kaplan and Meloy[106,107] and by Sorriso and co-workers.[108,109] The semiemperical (AM1) and *ab initio* calculations [HF/6-31G(d)] by Muchall et al.[111,112] also support the s-Z conformation as the predominant conformation for the similar *para*-substituted diazoacetophenones (see **Introduction**). It is envisioned that the *anti* arrangement of the diazo group (leaving group) with the *p*-hydroxyphenyl ring in **s-Z 1.165** (Scheme 1.33) provides the proper orientation for the hypothesized photo-Favorskii-like rearrangement as well as the concerted ketene formation in the Wolff rearrangement (Scheme 1.33).

UV-vis Spectroscopic Studies of diazo *p*HP 1.165

The α-diazo-*p*-hydroxyacetophenone (**1.165**) chromophore absorbs farther into the visible region due to the extended conjugation with the diazo functionality. The resonance capability of this chromophore is greatly affected by the nature of the solvent and the pH of the solution. The absorption maximum (λ_{max}) in the UV-vis spectrum of diazo *p*HP **1.165** at pH 7 (ammonium acetate buffer) appears at 306 nm, with $\varepsilon = 14200\ M^{-1}\ cm^{-1}$ (Figure 1.7).

Figure 1.7 The UV/vis Spectrum of Diazo *p*HP **1.165** in 50 % Aqueous Acetonitrile

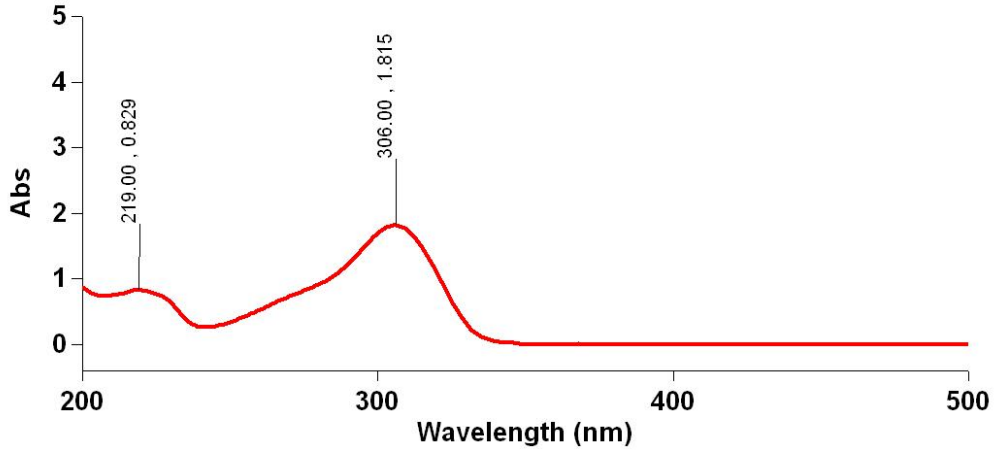

Different buffer solutions were used to study the pH dependence of diazo *p*HP **1.165**. UV/vis spectra in buffer solutions at pH 4, 7, and 10 were obtained (Figure 1.8). A sodium acetate/acetic acid buffer solution was used to obtain pH 4, whereas ammonium acetate/ammonia buffer solutions were used to achieve pH 7 and 10.

The $\lambda_{max,}$ did not change significantly upon changing the pH from 7 to 4 (Figure 1.8), suggesting that the cross-conjugated tautomeric form of diazo *p*HP, **s-Z 1.165**, is the major species in acidic and neutral media (Scheme 1.34). In contrast, the conjugate base form of diazo *p*HP **1.165** with its extended conjugation, as illustrated by the three resonance structures, was the dominant species at pH 10 (Scheme 1.34).

Figure 1.8 The UV-vis Spectra of Diazo *p*HP **1.165** at Different pH Values

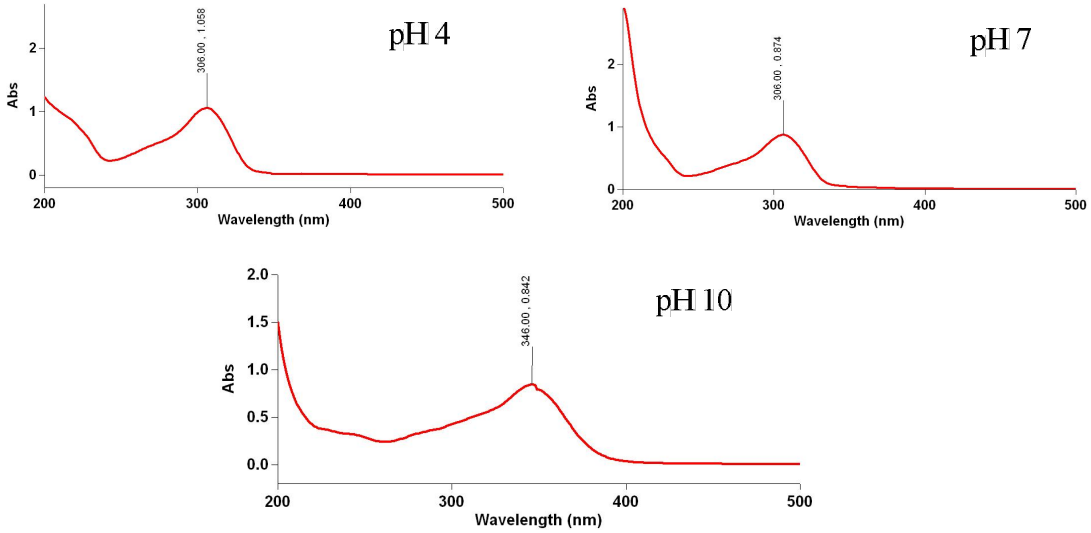

Scheme 1.34 Charge Distribution of Diazo *p*HP **1.165** at Different pH Values[a]

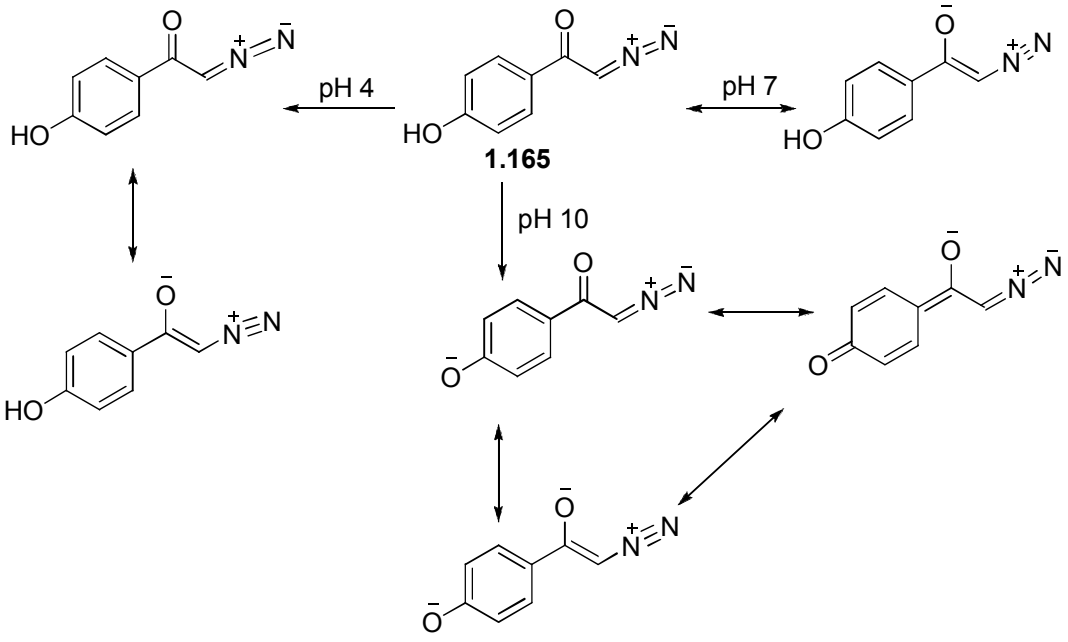

[a]The most stable conformer (**s-Z 1.165**) at neutral pH was employed to illustrate the charge distribution at different *p*H values.

The absorption maximum was red shifted from 306 nm to 346 nm in this case, with the absorption band tailing into the 400 nm region. The color of the solution of diazo *p*HP **1.165** changed from light yellow to bright yellow when the pH was changed from 4 to 10, indicating increased contribution from the conjugate base (Scheme 1.34). Interestingly, the extinction coefficient value (ε) decreased from 17100 M^{-1} cm^{-1} to 14200 M^{-1} cm^{-1} and further to 13600 M^{-1} cm^{-1} with increasing pH (4→7→10).

B. Product Studies and General Photochemistry of diazo *p*HP 1.165

The preliminary photolysis studies were performed on non-degassed aqueous acetonitrile (D_2O/CD_3CN, 1:1) and were monitored by ^1H NMR spectroscopy. The photolysis of diazo *p*HP **1.165** was carried out at 300 nm or 350 nm using sixteen 3000 Å or 3500 Å lamps, respectively. The release of nitrogen was observed as bubbles effervescing from the solution during the reaction. The disappearance of diazo *p*HP **1.165** and appearance of 4-hydroxyphenylacetic acid (PAA, **1.53**) were quantified by integrating the corresponding signals at 6.23 and 3.49 ppm in ^1H NMR. Regardless of the wavelength used, the rearranged acid **1.53** was observed as the major product (83%). Other minor products (combined NMR yield <5%) were not identified due to their low abundances (Equation 1.34).

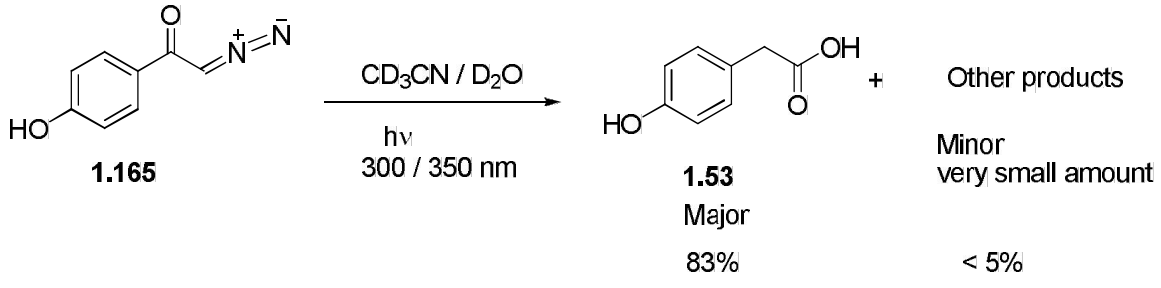

Eq. 1.34

However, the formation of *p*-hydroxyacetophenone, α-hydroxy-*p*-hydroxyacetophenone, and *p*-hydroxybenzyl alcohol were ruled out as minor products by spiking the photolysis sample

with these compounds. The formation of PAA was confirmed by spiking the photolysis mixture with an authentic sample which is commercially available. In contrast, photolysis of diazo *p*HP **1.165** performed in dry acetonitrile at 300 or 350 nm produced a complex mixture of products (Equation 1.35). Analysis of the ^{1}H NMR spectrum of the crude reaction mixture indicated the presence of four major products containing an aromatic ring.

1.165

Eq. 1.35

Similarly, the RP-HPLC analysis of the photolysis mixture revealed formation of several photoproducts. All attempts to identify the unknowns by spiking the mixtures with authentic samples of putative products and analyzing them by ^{1}H NMR, GC/MS, and RP-HPLC were unsuccessful (see **Experimental** section). The amount of water required to produce rearranged acid **1.53** was also determined by changing the percentage of water in the photolysis sample. It was found that decreasing water content below 5% leads to complete suppression of the rearrangement and formation of the complex mixture of products analogous to the reaction performed in dry acetonitrile.

The photochemistry of diazo *p*HP **1.165** was studied in solutions at pH 4, 7 and 10. The absorption maximum (λ_{max}) at pH 4 and 7 was 306 nm whereas the λ_{max} at pH 10 was 346 nm, indicative of the formation of the conjugate base (Scheme 1.34). The photolysis of diazo *p*HP **1.165** at different pH values was performed in D_2O/CD_3CN (1:1) at 300 nm or 350 nm with 16-3000 Å or 16-3500 Å lamps and analyzed by ^{1}H NMR. Irradiation at pH 4 and 7 gave the rearranged acid **1.53** as the major product, whereas a complex mixture of products was observed at pH 10 which appeared to be similar to the results for photolysis in

dry acetonitrile. Quantum yields for the disappearance of diazo *p*HP **1.165** and appearance of PAA **1.53** were determined by RP-HPLC from photolyses performed in aqueous acetonitrile (1:1) at 300 nm or 350 nm using 2-3000 Å or 16-3500 Å lamps. Quantum yields for the disappearance of the diazo *p*HP **1.165** (Φ_{dis} = 0.25) and the appearance of the rearranged acid **1.53** (Φ_{app} = 0.23) fall in the same range with the values obtained for similar diazoketones reported by Mazzucato et al. (Table 1.11).[152]

Table 1.11 Photolysis of *para* Substituted Diazo Ketones in Different Solvents[152]

Diazo compound	λ_{max}[a]/nm	Φ_{dis}[b]	Φ_{dis}[c]	Φ_{dis}[d]
C_6H_5-$COCHN_2$	294	0.55	0.46	0.40
p-CH_3-C_6H_4-$COCHN_2$	296	0.62	0.41	0.30
p-CH_3O-C_6H_4-$COCHN_2$	304	0.50	0.34	nd
p-Cl-C_6H_4-$COCHN_2$	299	0.62	0.41	nd
p-NO_2-C_6H_4-$COCHN_2$	307	0.31	0.18	nd

[a]Determined in methanol; [b]Determined in hexane at 300 nm; [c]Determined in methanol at 300 nm; [d]Determined in 20 % aqueous ethanol at 300 nm.

The authors studied the effects of para substituents and various solvents on the photolysis of diazoacetophenone at 300 nm. It was found that electron withdrawing groups at the *para* position and polar solvents diminished the efficiency of the photolysis reaction.

Triplet Sensitized photolysis studies of diazo *p*HP 1.165

The photolysis experiments in the presence of triplet sensitizers such as mangiferin,[153] **1.183**, which is a xanthone[154] derivative, and benzophenone-4,4'-dicarboxylic acid (**1.184**) were also performed (Figure 1.6). The derivatives of benzophenone[154-156] and xanthone were selected for their enhanced water solubility.

Figure 1.9 Triplet Sensitizers which were Used in the Photolysis of Diazo *p*HP **1.165**

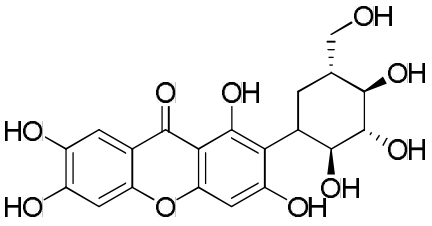

1.183

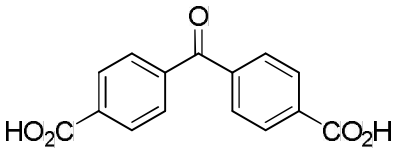

1.184

Despite being structurally similar to benzophenone, xanthone has a triplet energy close to that of acetophenone (E_T = 74 kcal/mol).[153-155,157,158] The triplet energy of xanthone is in the range of 71 - 74 kcal/mol[153, 159] and its photochemistry is highly solvent dependent.[154] For example, the triplet energy of xanthone in ethanolic ether was found to be close to its lower limit.[160] The triplet energy of benzophenone is 68.8 kcal/mol,[161] whereas the triplet energies of *p*HP derivatives are in the 69-71 kcal/mol range.[38] The triplet sensitization can be defined as a direct irradiation of a suitable donor molecule (D), such as benzophenone and xanthone, rather than that of the target substrate (or acceptor, A), such as the *p*HP derivative. The triplet energy difference (ΔE_T) between the donor and acceptor molecules must be either equal to or less than -3 kcal/mol for efficient energy transfer.[160,161]

$$\Delta E_T = E_T(A) - E_T(D) \leq -3 \text{ kcal/mol} \qquad \text{(Eq. 1.36)}$$

In addition, the donor should also absorb at longer wavelengths than the acceptor to enhance the possibility for exclusive excitation of the donor.[161] Sensitizers mangiferin **1.183** and benzophenone **1.184** absorb farther into the visible region, as compared to the diazo *p*HP **1.185**, and have triplet energy differences of near zero or less, which makes them suitable sensitizers for the photolysis of diazo *p*HP **1.185** in aqueous acetonitrile.

Interestingly, sensitization with magiferin **1.183** resulted in a drop in the quantum yields for disappearance of diazo *p*HP **1.185** (Φ_{dis}) and appearance of the rearranged acid

1.53(Φ_{app}), down by 40-50 % (Table 1.12). A similar behavior was observed in the photolysis reaction sensitized by benzophenone **1.184**. According to the RP-HPLC analysis, no side reactions were observed with these triplet sensitizers.

Table 1.12 Quantum Yield Values for Diazo *p*HP **1.165**

Photolysis condition	Excitation wavelength/(nm)	$\Phi^{a}_{dis.}$ (± 0.01)	$\Phi^{b}_{app.}$ (± 0.01)
Direct Irradiation	300	0.25	0.22
Non-degassed	350	0.10	0.08
Sensitization with **1.183**[c]	300	0.13	0.11
	350	0.06	0.04
Sensitization with **1.184**[d]	300	0.19	0.13
Purged with O_2	300	0.17	0.12
Degassed with Ar	300	0.28 ± 0.02	0.24

All solvents contained 50% H_2O. Photolyses were conducted for 8 min under the conditions indicated in the Table 1.12 with 2-3000/16-3500 Å lamps. a) Determined by RP-HPLC for the disappearance of the starting material at 300/350 nm; b) Determined with RP-HPLC for the appearance of PAA at 300/350 nm; c) The concentration of **1.183** was 4.76 x 10^{-3} M; d) The concentration of **1.184** was 3.70 x 10^{-3} M

The lowered efficiency may be attributed to incomplete capture of the excited triplet state energy of benzophenone or xanthone by the diazo *p*HP acceptor. Nonetheless, these results may suggest that a significant portion of the reaction proceeds through the triplet excited state.

Quenching studies with molecular oxygen

Quenching experiments were performed in the presence and absence of molecular oxygen, which is a well known triplet quencher.[154,156,161] The oxygen-free conditions were generated by purging the sample with argon for 30 min before the photolysis. The quartz tube was sealed with a rubber septum and an argon filled balloon with a needle was used to degas

the reaction solution while it was being cooled in an ice bath for 30 min. A needle syringe and an argon filled balloon were used to withdraw aliquots for HPLC analysis at time intervals while the photolysis reaction was being performed. Oxygen saturated conditions were obtained in the same way purging the sample with oxygen for 30 min before the photolysis.

In this experiment, oxygen is the quencher (Q) or ground state energy acceptor (A) and the diazo *p*HP derivative **1.185** is the excited state energy donor (D) or sensitizer (S). The stable ground state triplet molecular oxygen ($^3\Sigma^-_g$) has two low lying singlet excited states, $^1\Delta_g$ and $^1\Sigma^+_g$, which possess excitation energies of ~23 kcal/mol and ~38 kcal/mol, respectively.[154,155] In solution the upper excited state, $^1\Sigma^+_g$, is deactivated to the long-lived $^1\Delta_g$ state which is known as singlet oxygen. Because of these two low lying singlet excited states, triplet oxygen can efficiently quench the excited states. An excited sensitizer molecule ($^1S^*$) can potentially produce two molecules of singlet oxygen as depicted in Equation 1.37 and Equation 1.38.[154,155,161]

$$^1S^* + {}^3O_2 \longrightarrow {}^3S^* + {}^1O_2^* \text{ and}$$

$$^3S^* + {}^3O_2 \longrightarrow {}^1S_{gs} + {}^1O_2^* \qquad \text{Eq. 1.37}$$

The spin allowed reactions shown in Equation 1.37 are exothermic when the singlet-triplet energy gap of the sensitizer (ΔE_{ST}) is ≥ 23 kcal/mol which is sufficient for energy transfer to $^3O_2$. This process is called singlet quenching. When the ΔE_{ST} is small, the oxygen catalyzed intersystem crossing is always possible which is spin allowed if the encounter complex of ^3S and $^3O_2$ has overall triplet multiplicity, but no singlet oxygen will be formed. The reaction shown in the Equation 1.38 is known as triplet quenching which is spin allowed if the encounter complex of ^3S and $^3O_2$ has overall singlet multiplicity. In other words triplet

oxygen ($^3\Sigma^-_g$) can either add to the excited state or abstract an electron from the excited state. This process results in net quenching or energy transfer (Equation 1.38). The triplet photosensitization is a well known and synthetically useful process to generate singlet oxygen.[154,155,160]

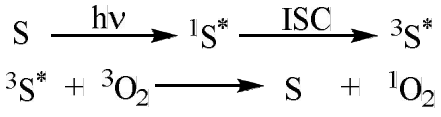

Eq. 1.38

Our quenching experiments with molecular oxygen (oxygen saturated conditions) resulted in an unexpected decrease in the rearrangement reaction rate, suggesting the involvement of the triplet excited state in the rearrangement of diazo *p*HP **1.165** (Table 1.12).[154,155] In oxygen saturated conditions the quantum yields for disappearance of diazo *p*HP **1.165** and appearance of the rearranged acid **1.53** decreased by 50% (i.e. Φ_{app} from 0.24 to 0.12).

It has been established that the photo-Wolff rearrangement occurs from the singlet excited state, whereas the photo-Favorskii rearrangement takes place from the triplet excited state to produce the rearranged acid (see **Introduction**).[46,52,55,56,99-101, 162] Accordingly, a Stern-Volmer quenching plot was constructed using the quantum yields shown in Table 1.12 to obtain an estimated lifetime and the reaction rate of the triplet state. The quantum efficiency as a function of the quencher concentration is given by,

$$\Phi_0/\Phi = 1 + K_{SV}[Q] \qquad \text{Eq. 1.39}$$

Where Φ_0 is the quantum efficiency for the appearance of 4-hydroxyphenyl acetic acid (PAA) in the absence of quencher (Q) and Φ is the same efficiency with the quencher present. The slope of the plot of Φ_0/Φ vs. the quencher concentration ([Q]) is defined as the Stern-Volmer constant K_{SV}. The lifetime of the triplet state ($^3\tau$) is determined from the equation:

$$K_{SV} = {}^3\tau \times k_{diff} \qquad \text{Eq. 1.40}$$

Where, k_{diff} is the bimolecular rate of diffusion in 50% aqueous acetonitrile (ca. 1.37 x 10^{10} M^{-1} s^{-1}). The rate constant for the appearance of PAA (k_r) can then be calculated by using the reciprocal triplet lifetime ($^3\tau$) of PAA assuming a triplet reaction is the only operating manifold.

Table 1.13 Oxygen Concentrations[155,156] in 50% Aqueous Acetonitrile and the Corresponding Φ_0/Φ Values of diazo *p*HP **1.165**

Experimental condition	$[O_2]$	Φ_{dis}	Φ_{app}	$(\Phi_0/\Phi)_{dis}$	$(\Phi_0/\Phi)_{app}$
Degassed	2.7×10^{-6}	0.28	0.24	1.000	1.000
Ambient conditions	2.7×10^{-4}	0.25	0.22	1.120	1.091
Purged with O_2	2.0×10^{-3}	0.17	0.12	1.647	2.000

Figure 1.10 Stern-Volmer Plot for the Photolysis of Diazo *p*HP **1.165** in 50% Aqueous Acetonitrile at 300 nm

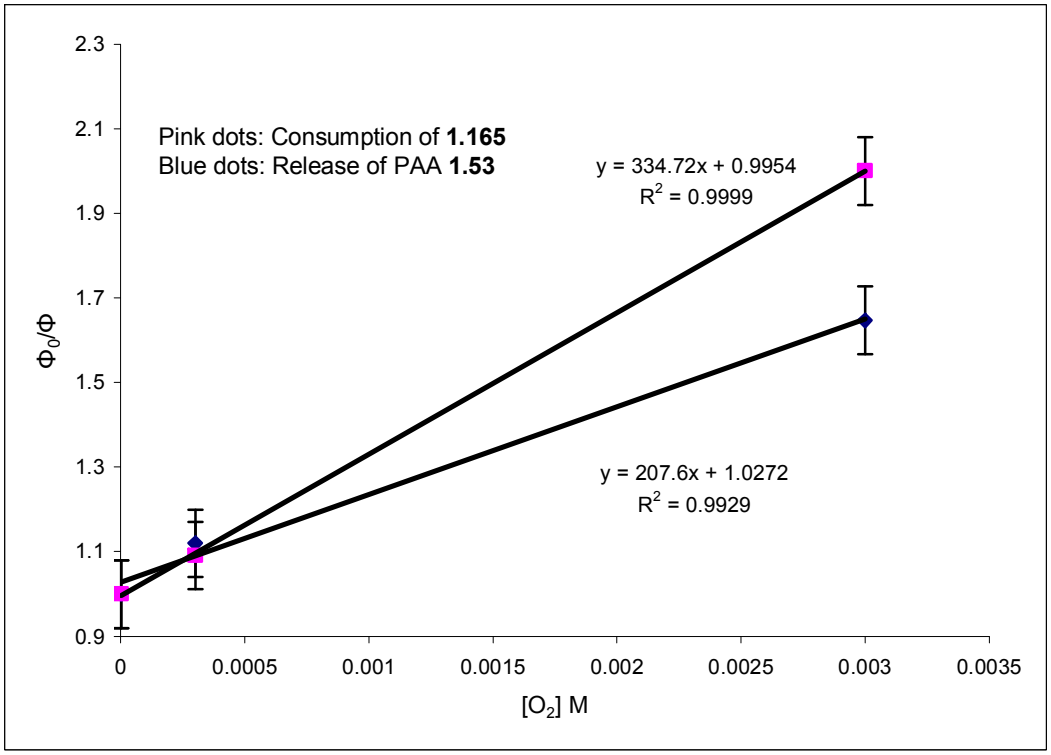

The oxygen concentration in a typical organic solvent at ambient pressure falls in the range of 10^{-3} to 10^{-4} M.[155] The oxygen concentration can be reduced to approximately 10^{-6} M by degassing the photolysis solution.[155] Using the quantum efficiency data from Table 1.12, the oxygen concentration in 50% aqueous acetonitrile, and the rate of diffusion in 50% aqueous acetonitrile, the lifetime of the triplet and the reaction rate can be determined (Table 1.13). The plot of Φ_0/Φ vs. oxygen concentration gave a straight line with a linear regression co-efficient of 0.993 (Figure 1.10). The lifetime of the triplet excited state and the rate of the appearance of PAA **1.53** were found to be 15 ns and 6.6×10^7 s^{-1}, respectively.

Time resolved-IR spectroscopy studies

This work was performed in collaboration with Prof. John P. Toscano and Anthony Evans at John Hopkins University, Baltimore, Maryland. [163] α-Diazo-*p*-hydroxy acetophenone[93] (**1.165**) was chosen as a model compound for mechanistic studies to identify whether formation of *p*-hydroxyphenylacetic acid **1.53** occurs via the photo-Favorskii or photo-Wolff rearrangement, or possibly a combination of these two pathways. To this end, the LFP studies of α-diazo-*p*-hydroxyacetophenone (**1.165**) were monitored by time-resolved IR spectroscopy (TRIR).[164,165] The method which was originally used by Hamaguchi and co-workers[166,167] has been followed to perform TRIR experiments on diazo *p*HP **1.165**. This technique allows the assessment of the entire mid-IR spectrum (4000-800 cm^{-1}) with sufficient time resolution (ca. 50 ns) and high sensitivity. In addition, TRIR spectroscopy probes a wide range of transient intermediate signals in solution. Excitation pulses (266 nm, 10 ns, 0.4 mJ) from a continuum HPO-300 diode-pumped Nd:YAG laser were crossed with

the broad-band output of a $MoSi_2$ infrared source. A MCT photovoltaic IR detector was used to monitor changes in infrared intensity.

Figure 1.11 Transient Absorption Spectra of the Ketene Intermediate

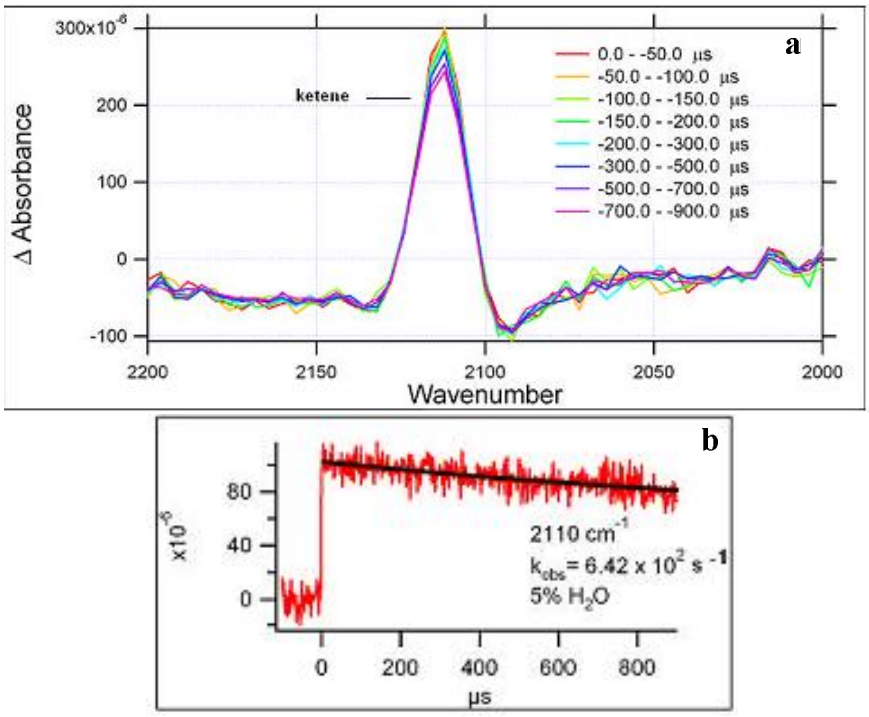

(a) TRIR spectrum of the ketene region obtained in LFP reaction of diazo *p*HP **1.165** (Nd:YAG laser; 266 nm, 10 ns, 0.4 mJ) ; (b) Observed kinetic trace at 2100 cm^{-1}.

The LFP studies have been performed in 5% aqueous acetonitrile to minimize the deleterious effect of water on TRIR measurements. Observation of a band at 2110 cm^{-1} characteristic of a ketene intermediate as well as its rate of formation [ca. 6.42×10^2 s^{-1} (Figure 1.11)] are in agreement with the literature reports[132,168-171] on absorption spectra and the rates of formation for analogous ketenes.

Wagner and co-workers[132] reported that the ketene intermediate derived from α-diazo-*p*-methoxyacetophenone absorbs at 2115 cm^{-1} whereas that derived from α-diazo-acetophenone has an absorption band at 2118 cm^{-1}. However, Wagner did not report the rate of formation of ketene intermediates. The ketene intermediate derived from α-diazo-*p*-

hydroxyacetophenone (**1.165**) absorbs at 2110 cm^{-1} which lies in the same region for ketenes studied by Wagner and co-workers within the error limits [(from 2100 cm^{-1} to 2122 cm^{-1}), see the Introduction; Table 1.8]. Ketene trapping experiments were performed using diazo *p*HP **1.165** as the source of the ketene with diethylamine as the trap in acetonitrile.

Scheme 1.35 Proposed Mechanism for the Amide **1.188** Formation

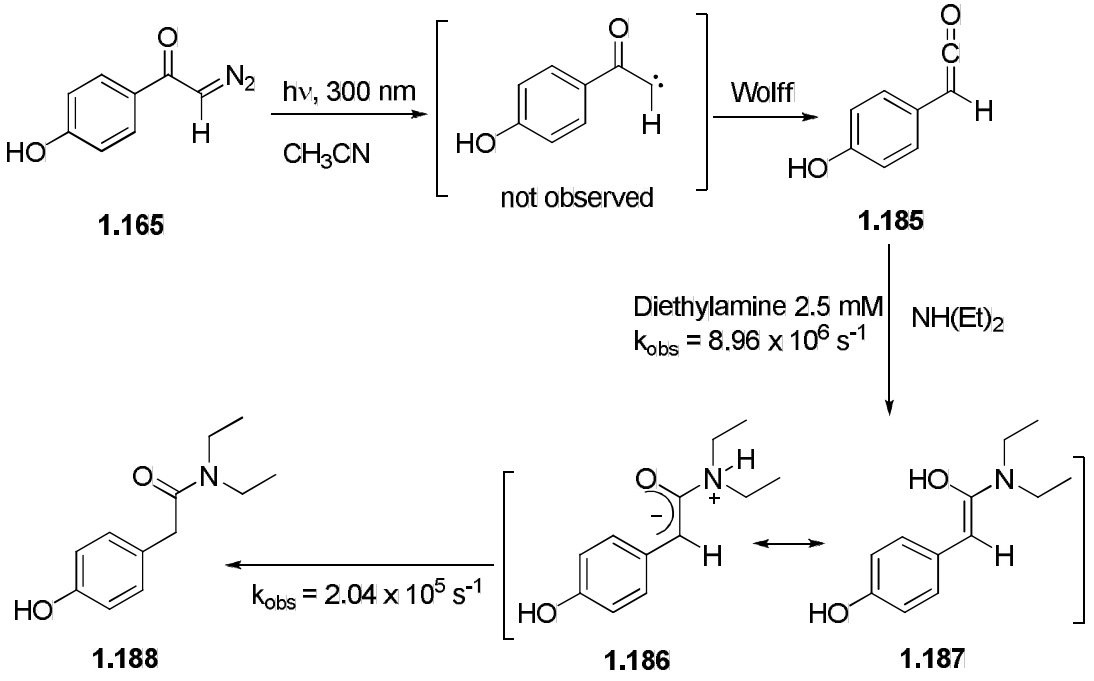

The LFP studies and time-resolved IR studies of the *p*-hydroxyphenyl ketene (**1.185**) performed in the presence of diethylamine produced an unstable intermediate at 1690 cm^{-1} which decayed to a stable product generating a band at 1645 cm^{-1} in the TRIR spectra (Figure 1.12). The former band was putatively assigned to either the zwitterionic ylide (**1.186**) or the amide enol (**1.187**) whereas the latter band was attributed to the amide **1.188** (Scheme 1.35). Quenching kinetics were measured at 1695 cm^{-1} for the observed first order (k_{obs}) formation of the relevant intermediate **1.186** or **1.187** as a function of diethylamine concentration [DEA]. The results are depicted in Table 1.16.

Figure 1.12 Formation of Amide **1.188** from either Intermediate **1.186** or **1.187** in the Presence of Diethylamine in Acetonitrile

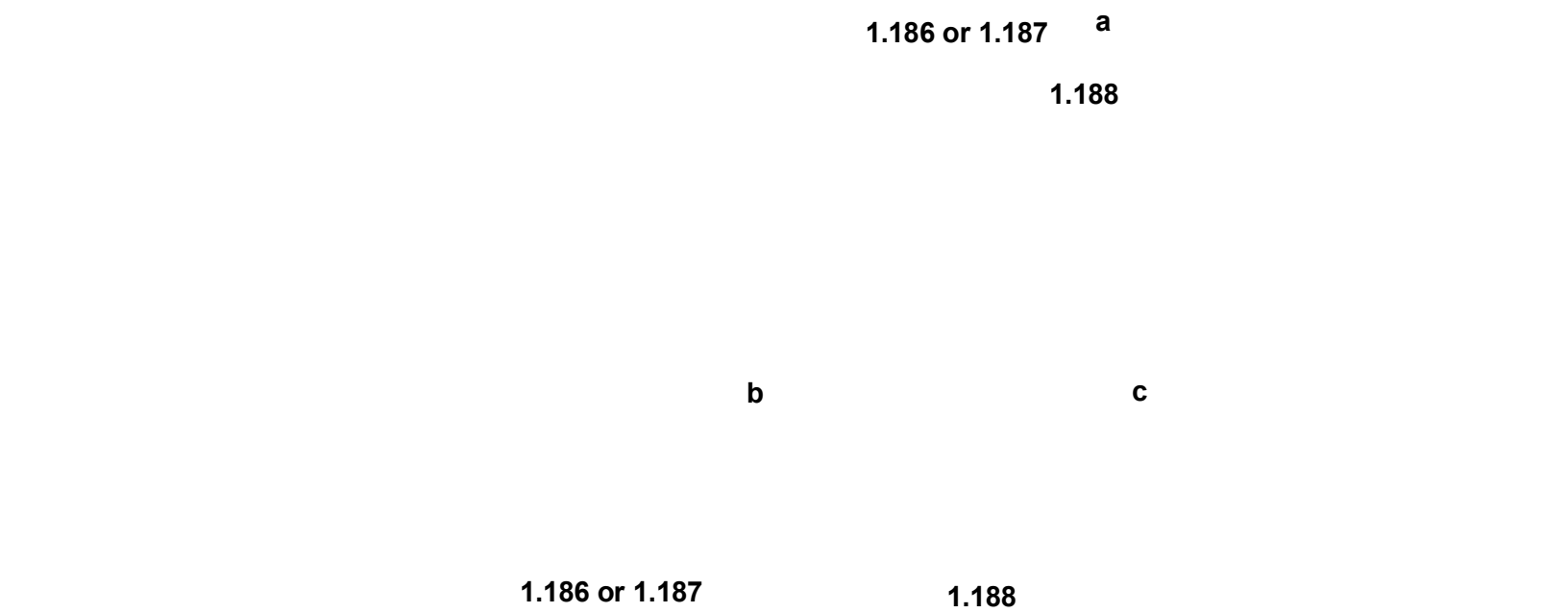

(a) TRIR spectrum for the formation of **1.188** at 1645 cm^{-1} (Nd:YAG laser; 266 nm, 10 ns, 0.4 mJ) ; (b) and (c) observed kinetic traces at 1695 cm^{-1} and 1645 cm^{-1}, respectively.

The observed rate constant of the relevant intermediate decay or formation (k_{obs}), as a function of added quencher concentration ([Q]), is given by

$$k_{obs} = k_0 + k_q[Q] \qquad \text{(Eq. 1.41)}$$

Where k_0 is the observed first order decay rate constant in the absence of quencher and k_q is the second-order quenching rate constant. The values of k_q were obtained from the slope of the graphs of k_{obs} vs [Q]. The quenching rate constant (k_q) was obtained from the plot of observed rate constant (k_{obs}) vs diethylamine concentration [DEA] (Figure 1.13). The k_q for the formation of the unstable intermediate **1.186** or **1.187** was obtained from the slope of the plot (Figure 1.10) and was found to be 2.72×10^6 M^{-1} s^{-1}.

Table 1.14 Observed Pseudo-first Order Kinetics (k_{obs}) for the Formation of Intermediate **1.186** or **1.187**

[DEA] / mM	ν/cm^{-1}	k_{obs}/ 10^6 s^{-1}
0.05	1695	0.544
0.10	1695	0.676
0.40	1695	1.490
0.80	1695	2.580

Figure 1.13 Observed Pseudo-first Order Formation Constant (k_{obs}) for Intermediate **1.186** or **1.187** vs. Concentration of Diethylamine [DEA] in CH_3CN.

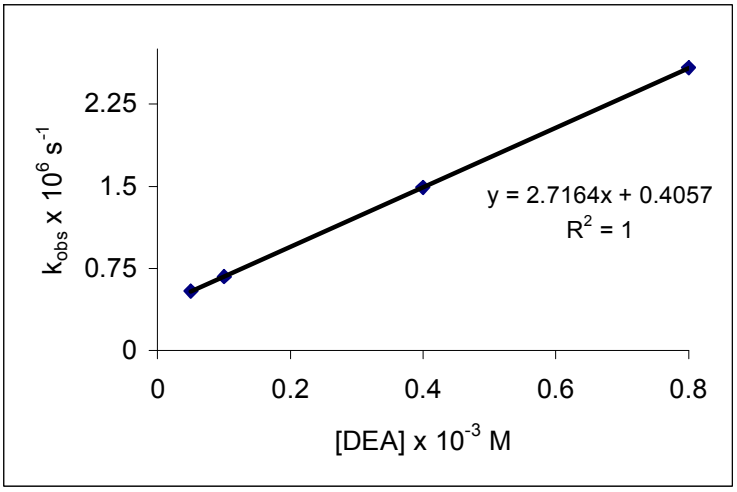

Quenching kinetics was also measured at 2110 cm^{-1} for the observed pseudo-first order decay (k_{obs}) of the *p*-hydroxyphenyl ketene as a function of diethylamine concentration in acetonitrile. The results are illustrated in Table 1.15.

Table 1.15 Observed Pseudo-first Order Kinetics (k_{obs}) for the Decay of the Ketene Intermediate **1.185**

[DEA] / mM	ν/cm^{-1}	k_{obs}/ 10^6 s^{-1}
0.05	2110	0.324
0.10	2110	0.678
0.20	2110	1.490
0.40	2110	2.539

The quenching rate constant (k_q) was obtained from the plot of observed rate constant (k_{obs}) vs diethylamine concentration [DEA] (Figure 1.11). The k_q for the decay of ketene **1.155** was determined from the slope of the plot (Figure 1.14) which was found to be 6.32×10^6 M^{-1} s^{-1}.

Figure 1.14 Observed Pseudo-first Order Decay Constant (k_{obs}) for Ketene **1.155** vs. the Concentration of Diethylamine [DEA] in CH_3CN.

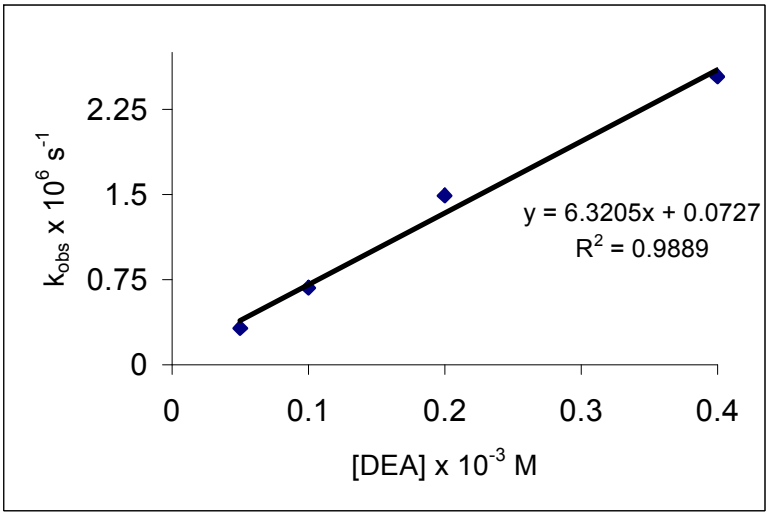

The quenching rate constant values (ca. 10^6 M^{-1} s^{-1}) are one order of magnitude lower than the values reported for similar ketenes by Wagner and co-workers (ca. 10^7 M^{-1} s^{-1}).[132] As mentioned earlier, this effect can be a result of trace amount of water present in the diethylamine or the acetonitrile. It is known that wet solvents and reagents decrease the rate of the quenching by 2 orders of magnitude.[139-141] This may be due to the decreased electrophilicity of ketene **1.185** resulting from the electron donating ability of the *p*-hydroxyl group. In addition, we argue that phenolic hydrogen of diazo-*p*HP can H-bond with the diethylamine thereby diminishing the nucleophilicity of the amine group. Another factor is the possibility of a competing photo-Favorskii rearrangement of the diazo *p*HP with traces of

water present in the solvent. This rearrangement would diminish formation of the ketene intermediate during the course of the reaction.

Quenching studies were also performed in Toscano's laboratories on the photochemistry of **1.165** in methanol, methanol/hydroxide, and acetonitrile/water to explore the multiplicity for the formation of the ketene. The results are illustrated in Table 1.16.

Table 1.16 Observed Rates for Ketene Quenching

Nucleophile/quencher	ν/cm^{-1}	k_{obs}/s^{-1}
5% aqueous CH_3CN	2110	6.42×10^2
10% aqueous CH_3CN	2110	6.66×10^2
MeOH	2110	6.37×10^2
$MeOH/OH^-$	2110	5.00×10^4

The amount of water and changing the solvent from aqueous acetonitrile to methanol had negligible effects on the ketene quenching rates whereas the observed rate increased by two orders of magnitude in the presence of hydroxyl ion.

If the photo-Favorskii rearrangement mechanism also operates in this transformation, the characteristic spirodienedione intermediate should have been formed in the course of the rearrangement of **1.165**. The cyclopropanone ring of the putative spirodienedione intermediate is expected to absorb in the IR 1800-1850 cm^{-1}.[67,68] The LFP of **1.165** followed by TRIR studies resulted in detection of a weak, very broad signal in the 1900 cm^{-1} region (Figure 1.15). The intensity of this transient is very low compared with the absorbance of the ketene intermediate **1.185**. Thus, this absorption band is unlikely to be due to the elusive spirodienedione intermediate sought in our studies. The nature of this transient species is unclear at this point. Future ultrafast LFP studies can potentially be helpful in identifying the nature of this intermediate.

Figure 1.15 TRIR Spectra for the Ketene and an Unknown Transient

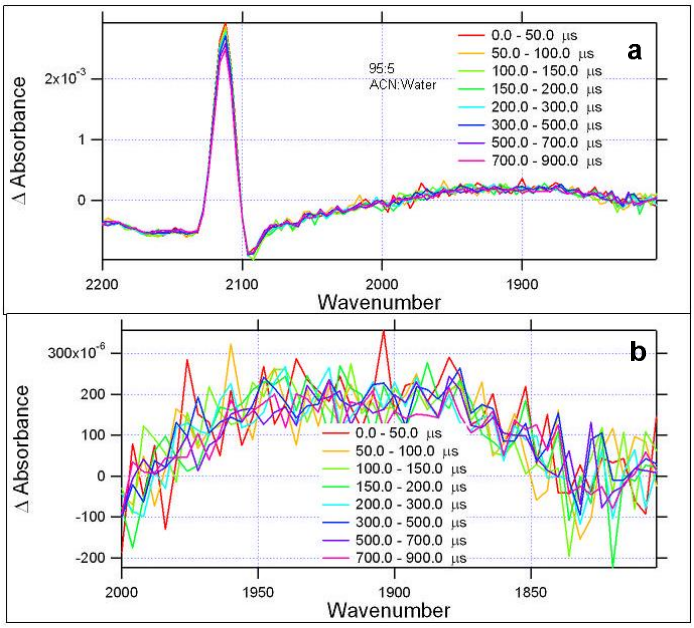

(a) TRIR spectrum for the formation of the ketene at 2110 cm^{-1}; (b) TRIR spectrum for the formation of the unknown transient around 1900 cm^{-1}.

Based on the LFP data obtained for the ketene intermediate and the lack of strong evidence for the spirodiendione intermediate **1.62** in the photo-Favorskii rearrangement, we have concluded that the photo-Wolff rearrangement must be the predominant and likely the sole pathway, for the described transformation (Scheme 1.36). The mechanism may, in part, follow the route previously suggested by Platz and co-workers.[101, 121,126 ,127] In applying his mechanism, the initial irradiation of diazo *p*HP **1.165** produces the singlet excited state of diazo *p*HP **1.165**, which undergoes nitrogen extrusion via either concerted or a stepwise pathway. In the case of a concerted pathway, the excited diazo *p*HP ^{1}**1.165** relaxes successively to the excited ketene (**1.189**) and then further to the ground state ketene **1.189** which can react with water to generate rearranged acid **1.53**.

In the stepwise pathway, the excited diazo *p*HP ^{1}(**1.165**) generates the singlet hot carbene ^{1}(**1.190**)*, which decays to the vibrationally relaxed singlet carbene ^{1}(**1.191**). The latter ^{1}(**1.191**) can either undergo ISC to the triplet excited state ^{3}(**1.192**) or isomerize to the vibrationally relaxed stable carbene **1.193** via an oxirene intermediate **1.194**. Both the relaxed singlet carbene ^{1}(**1.191**) and the stable carbene can also rearrange into the ground state ketene **1.189** which finally reacts with water to form the rearranged acid **1.53**.

Scheme 1.36 Photo-Wolff Rearrangement of α-Diazo-*p*-hydroxyacetophenone (**1.165**)

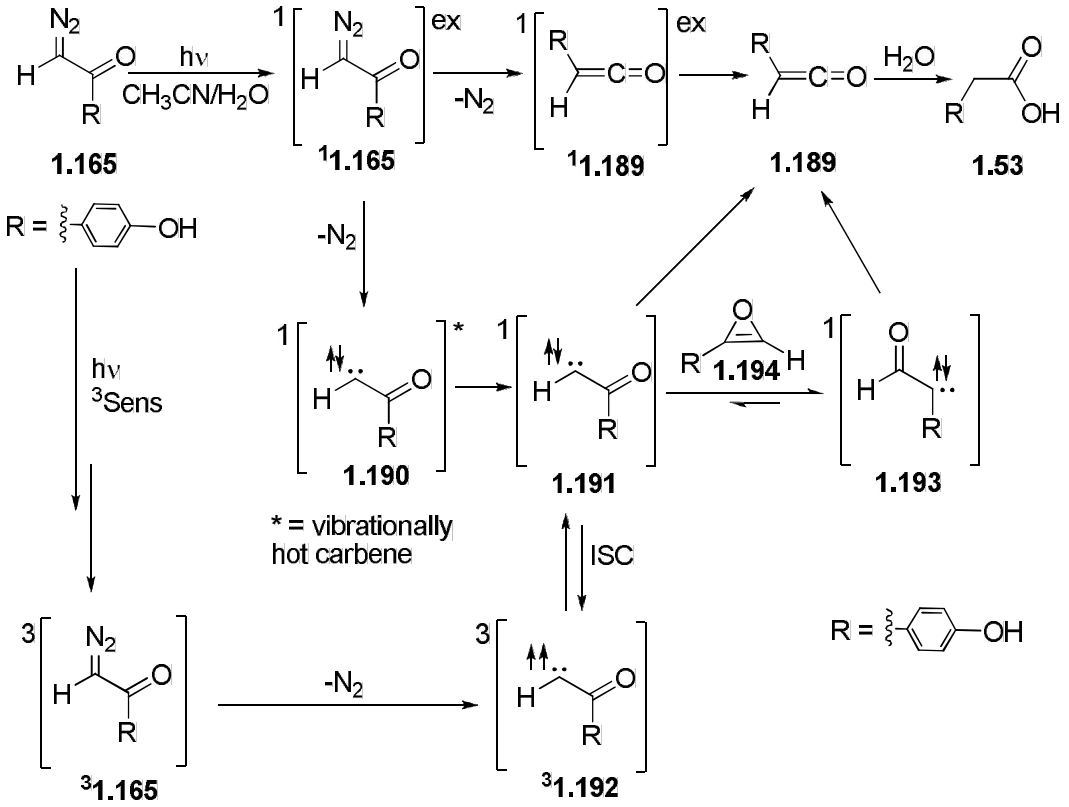

In the triplet sensitized photolysis, diazo *p*HP **1.165** will be generated in its excited triplet state ^{3}(**1.165**) and can undergo direct release of nitrogen generating the triplet excited carbene ^{3}**1.192**. The triplet excited carbene ^{3}**1.192** can undergo intersystem crossing to the singlet excited state followed by the photo-Wolff rearrangement as described earlier. The other, less likely pathway is that the triplet excited state of the diazo *p*HP ^{3}**1.165** may

undergo protonation to diazo species ^{3}**1.195** followed by photo-Favorskii rearrangement through the triplet biradical **1.69** with concomitant release of nitrogen (Scheme 1.37).

Scheme 1.37 Photo-Favorskii Rearrangement of α-Diazo-*p*-Hydroxyacetophenone (**1.165**)

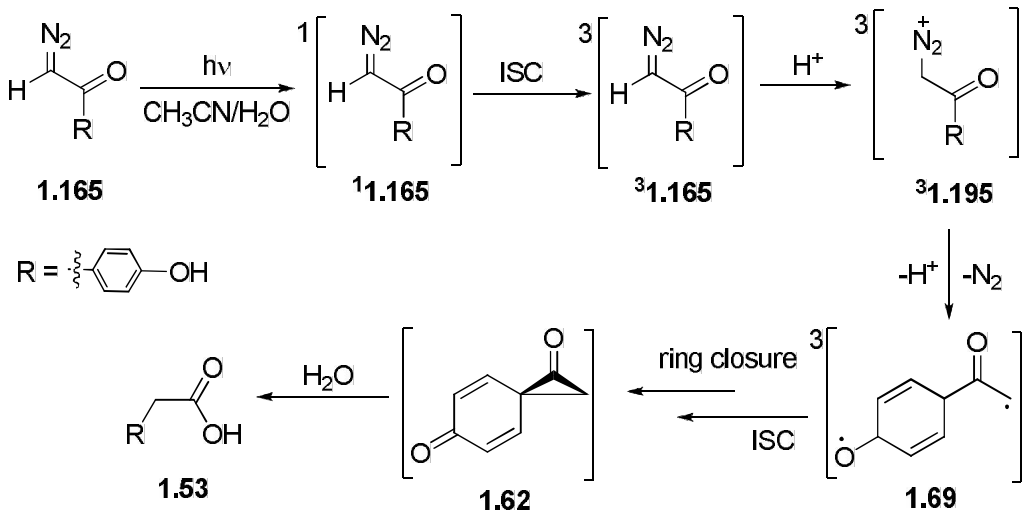

The triplet biradical **1.69** can undergo intersystem crossing and cyclization to produce the spirodienedione intermediate **1.62**. In the presence of water the putative intermediate **1.62** would collapse to generate the rearranged acid **1.53**. The protonation of the methine carbon of the triplet excited state of diazo *p*HP (^{3}**1.165**) is critical for the photo-Favorskii rearrangement to proceed, because there should be a twist or out-of-plane rotation of the substituted acetyl group (the leaving group, the diazo group) during the photorelease. This process is equivalent in effect to the formation of the oxyallyl-phenoxy triplet biradical **1.69** which is the key intermediate prior to the formation of the putative spirodienedione intermediate **1.62**. The carbanion or partial negative charge on the methine carbon (without protonation of the methine carbon) would not facilitate the possible out-of-plane rotation or twist of the substituted acetyl group (the diazo leaving group). Thus, we can argue that photo-Favorskii rearrangement would not proceed without protonation of the methine carbon of diazo *p*HP **1.165** prior to the release of nitrogen in the excited state.

As mentioned earlier, quenching studies with molecular oxygen support the photo-Favorskii rearrangement because the part of the excited state responsible for the photocleavage of diazo *p*HP is the triplet excited state. Moreover, oxygen can also quench either the triplet excited state of the diazo *p*HP precursor or triplet carbene derived from diazo *p*HP or both in the photo-Wolff rearrangement. However, Platz and co-workers demonstrated that aryldiazoketones undergo Wolff rearrangement via the singlet excited state both in acetonitrile and methanol (see the Introduction). Thus, we argue that molecular oxygen quenches the triplet excited state of the diazo *p*HP which may be responsible for both mechanisms.

In summarizing these results, it can be concluded that the photocatalyzed decomposition of **1.165** may follow two competing pathways to the rearranged acid; clearly, the photo-Wolff rearrangement is occurring and may originate from both the singlet and triplet excited states. The photo-Favorskii rearrangement, if it does occur, may emanate from the triplet excited state (Scheme 1.37). However, the lack of IR evidence of any cyclopropanone carbonyl limits support for a photo-Favorskii triplet pathway by sensitization. Direct irradiation gives only evidence for the ketene by TRIR. A plausible mechanistic scenario in accord with Platz and co-workers' results is illustrated in Scheme 1.38. As depicted in Scheme 1.37 the extrusion of nitrogen from diazo *p*HP mainly occurs through the Wolff rearrangement. In accord to Platz's results, *syn* conformation favored diazo *p*HP **1.165** may follow predominantly the concerted photo-Wolff rearrangement. Nonetheless, stepwise photo-Wolff rearrangement via carbene intermediates **1.190-1.193** may also contribute to the Wolff rearranged product **1.53**.

Scheme 1.38 Plausible Mechanisms for the Rearrangement of **1.165** in Aqueous Acetonitrile

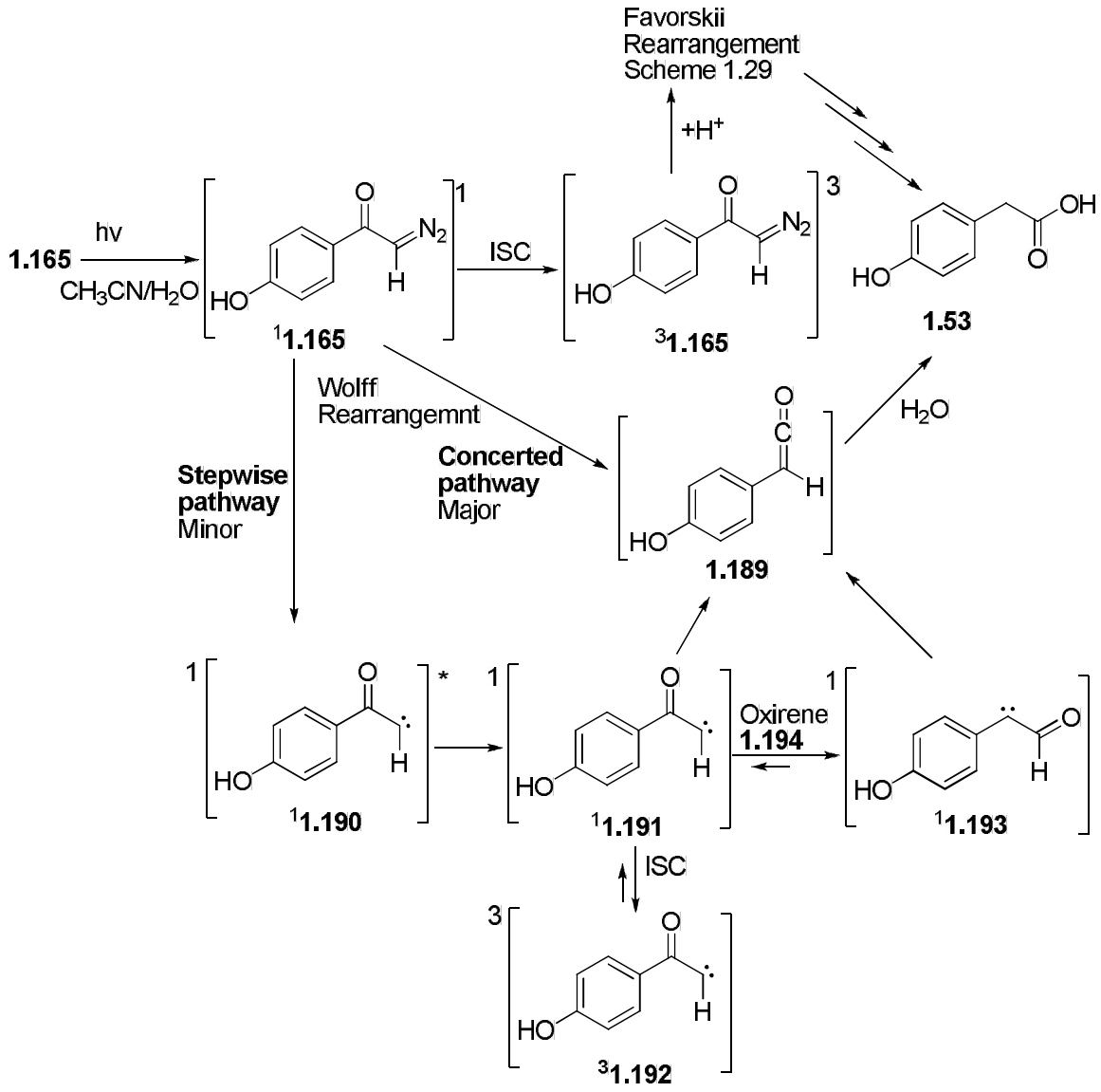

Since the quenchable triplet excited state in the photolysis of diazo *p*HP in aqueous acetonitrile was detected with molecular oxygen, the ISC is possible for both the singlet excited diazo *p*HP ^{1}**1.165** and vibrationally relaxed singlet carbene ^{1}**1.191** to generate triplet excited diazo *p*HP ^{3}**1.165** and triplet carbene ^{3}**1.192**. The triplet excited state of diazo *p*HP ^{3}**1.165** may follow the photo-Favorskii rearrangement as depicted in Scheme 1.37 whereas triplet carbene ^{3}**1.192** may follow the photo-Wolff rearrangement as illustrated in Scheme

1.36. Ultrafast LFP studies followed by either nanosecond TRIR or femtosecond UV-vis would be extremely informative in confirming the proposed mechanism.

Substituent Effects on *p*HP Photochemistry on Releasing Diethyl Phosphate

Previous studies by Givens and co-workers[65,69,70] on *p*HP-caged carboxylates have clearly indicated that *meta* methoxy substitution has a beneficial effect of shifting the *p*HP absorption significantly towards the visible region.

Figure 1.16 Methoxy Substituted *p*HP Diethyl Phosphates

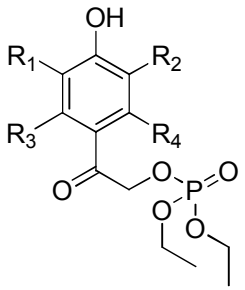

1.200a R_1 = H, R_2 = OMe, R_3, R_4 = H
1.200b R_1 = OMe, R_2= OMe, R_3, R_4 = H
1.200c R_1 = H, R_2 = $COCH_3$, R_3, R_4 = H
1.184a R_1, R_2 = H, R_3 = OMe, R_4 = H
1.184b R_1, R_2 = H, R_3 = OMe, R_4 = OMe

Therefore, caged compounds based on *meta* methoxy substitution can successfully be applied in biochemical studies because higher wavelengths (> 350 nm) can be used to excite the chromophore thus avoiding absorption of UV light by biological substrates such as aromatic amino acids in proteins and the bases in nucleotides. Accordingly, new methoxy substituted *p*HP phosphates were targeted and the neighboring group effects on their photochemistry were explored (Figure 1.16).

Synthesis of *meta*-methoxy- and a *meta*-acetyl substituted diethyl phosphates.

The new diazo *p*HP approach for the known *meta*-methoxy substituted *p*HP chromophores commenced with commercially available methoxy substituted *p*-hydroxybenzoic acids (Scheme 1.39).

Scheme 1.39 Synthesis of *meta* Methoxy Substituted and a *meta* Acetyl Substituted Diethyl Phosphates

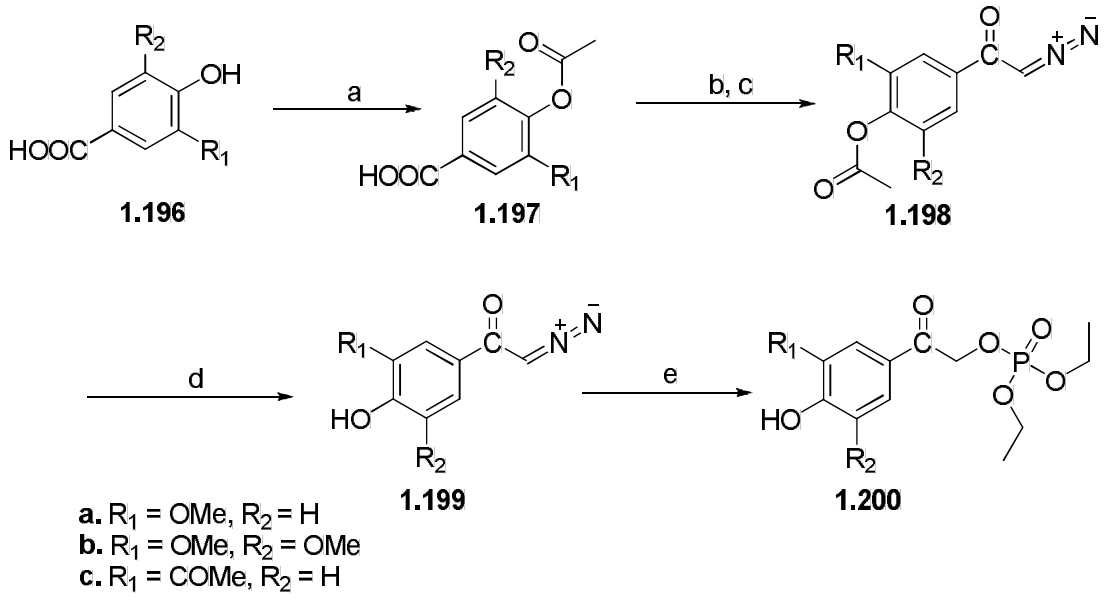

1.196 **1.197** **1.198** **1.199** **1.200**

a. R_1 = OMe, R_2 = H
b. R_1 = OMe, R_2 = OMe
c. R_1 = COMe, R_2 = H

Reagents and conditions; (a) CH_3COCl, Et_3N, CH_2Cl_2, 1 h, 60-70%; (b) $SOCl_2$, reflux, 8 h, 95-99%; (c) CH_2N_2, Et_2O, 0 °C to rt, overnight, 38-69%; (d) NH_4OAc, H_2O/MeOH, 1:4, 50 °C, 8 h, 90-96%; (e) HO-P(O)-$(OEt)_2$, benzene, 60 °C, 24 h, 75-79%.

For the acetyl analog, the Fries rearrangement of *p*-acetoxybenzoic acid **1.162a** was used to produce 3-acetyl-4-hydroxybenzoic acid **1.196c** in excellent yield. The phenol group of carboxylates **1.196** was protected as the acetate with acetyl chloride followed by refluxing in thionyl chloride to quantitatively give the corresponding acid chlorides. The acid chlorides were reacted with excess diazomethane in ether to generate the corresponding acetate protected diazoketones **1.198** in 65-69 % yield. A poor yield was obtained for *meta* acetyl

derivative **1.198c** (38%). The deprotection was quantitatively achieved with NH_4OAc in aqueous methanol followed by esterification with diethyl phosphoric acid which produced the *meta* substituted *p*HP phosphate esters **1.199** in 75-79% yield.

Synthesis of 2-diazo-1-(4-hydroxy-2-methoxyphenyl)ethanone

The synthesis began with commercially available 4-hydroxy-2-methoxybenzaldehyde, **1.201** (Scheme 1.40).

Scheme 1.40 Synthesis of 2-diazo-1-(4-hydroxy-2-methoxyphenyl)ethanone

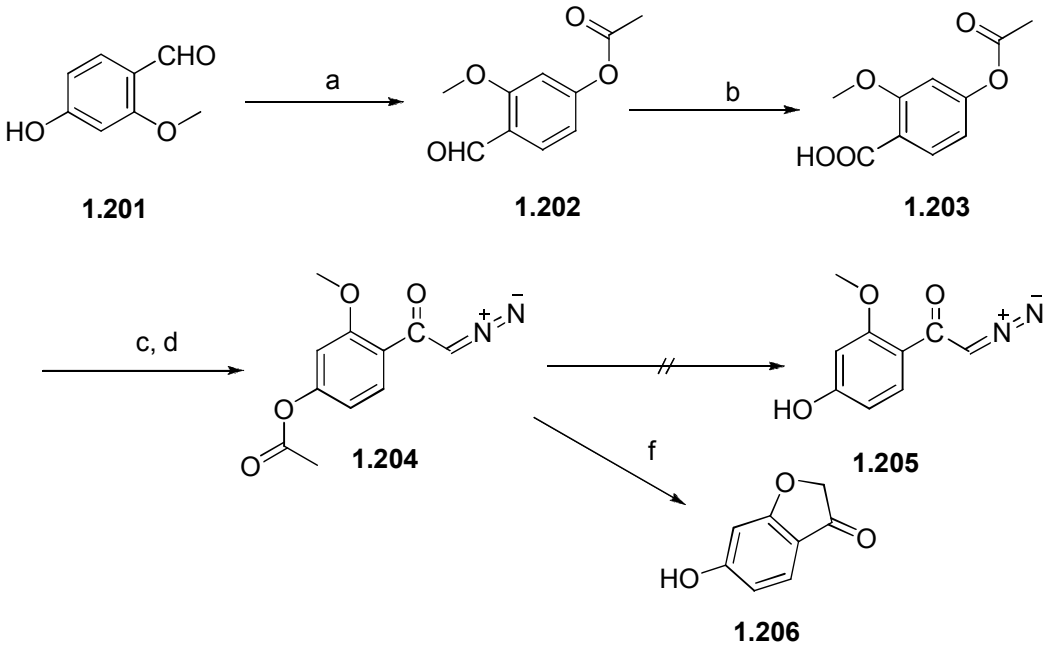

Reagents and conditions; (a) CH_3COCl, Et_3N, CH_2Cl_2, 1 h, 100%; (b) $KMnO_4$, acetone, rt. 4 h, 88%; (c) $SOCl_2$, reflux, 8 h; (d) CH_2N_2, Et_2O, 0 °C to rt, overnight; (e) NH_4OAc, H_2O/MeOH, 1:4, 50 °C, 8 h, lead to **1.206** in 100% yield; (f) NH_4OAc, H_2O/MeOH, 1:4, 50 °C, 8 h or H^+ or H_2O or OH^-, rt, 100%.

The acetate ester **1.202**was installed prior to oxidation of the aldehyde with $KMnO_4$. The acid chloride was generated by reacting acid **1.203** with thionyl chloride, followed by reacting with excess diazomethane in ether to produce the *ortho* or 2-methoxy diazoketone **1.204** in good yield (69%). It should be mentioned that exposure of **1.204** to silica gel, acids,

aqueous bases, and even water causes cyclization of **1.204** to 6-hydroxy-3-coumaranone (**1.206**) because of neighboring methoxy group participation. Accordingly, purification of *ortho*-methoxy diazo *p*HP **1.204** was achieved by passing the crude mixture quickly through silica gel treated with triethylamine.

Previuos studies by Gefflaut and Périé [172] demonstrated that the *o*-benzyloxy diazoketone **1.207** did not generate the corresponding phosphate ester with dibenzyl phosphoric acid. Instead, 3-coumaranone **1.208** was obtained as the exclusive product along with tribenzyl phosphate **1.209** (Equation 1.42). It is likely that protonation of the double bond produces the diazonium ion which undergoes neighboring group assisted rapid extrusion of nitrogen. Accordingly, the cyclization reaction takes place in competition with the desired intermolecular reaction with the phosphoric acid.

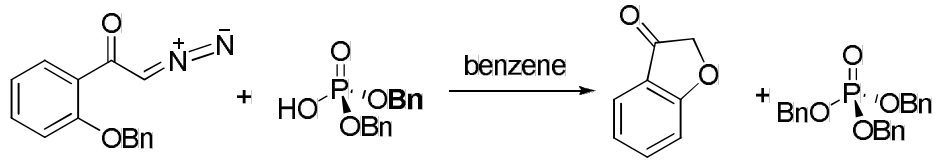

1.207 **1.208** **1.209**

Eq. 1.42

In contrast to the desired intermolecular process, the *ortho* methoxy diazo ketone **1.204** reacted with diethyl phosphoric acid (**1.30**) to give exclusively 3-coumaranone **1.206** which parallels the findings of Gefflaut and Périé[172] (Equation 1.43).

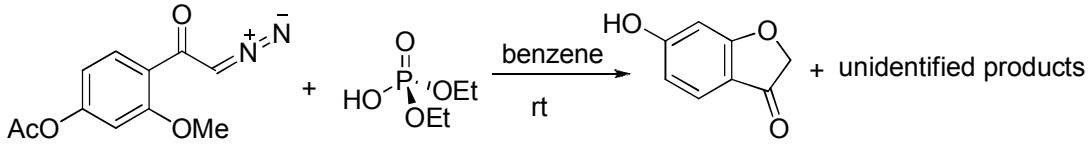

1.204 **1.30** **1.206**

Eq. 1.43

Thus, the diazo approach suffers limitations in the case of *ortho* methoxy substituted *p*HP diethyl phosphate generation, where the neighboring group participation dominates.

Synthesis of *ortho*-methoxy substituted diethyl phosphates

Since the diazo approach was unsuccessful in generating *ortho*-methoxysubstituted *p*HP phosphates, an alternative approach via α-haloketones was explored (Scheme 1.41).

Scheme 1.41 Synthesis of *ortho*-Methoxy Substituted Diethyl Phosphates

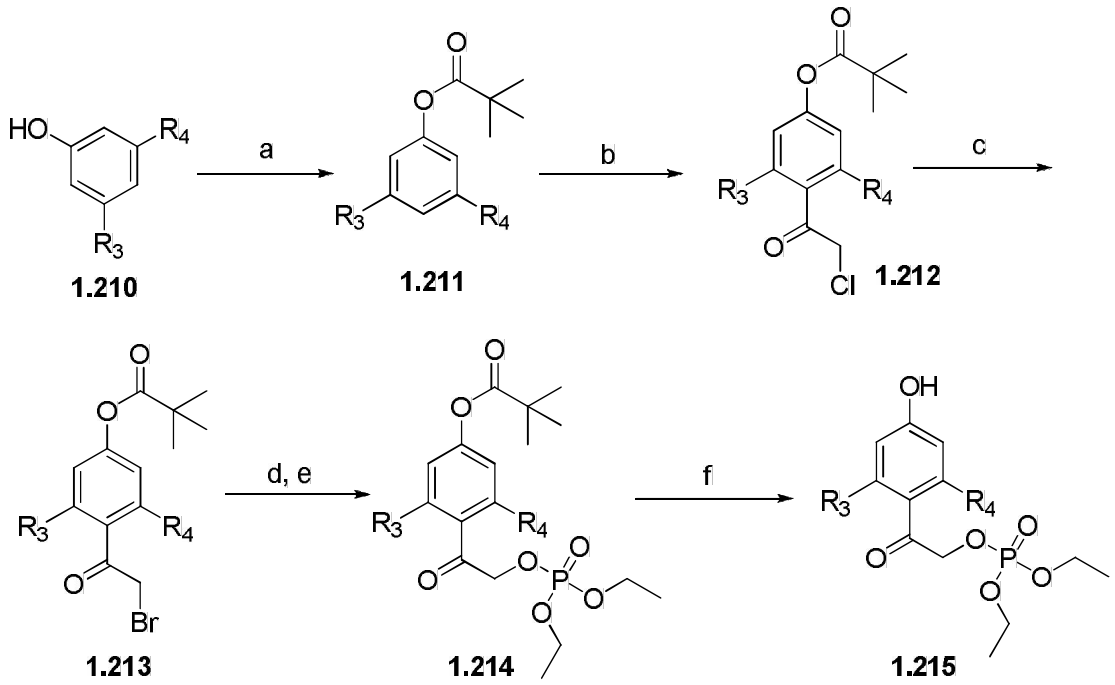

a. R_3 = OMe, R_4 = H
b. R_3 = OMe, R_4 = OMe

Reagents and conditions: (a) $(CH_3)_3COCl$, Et_3N, 0 °C to rt, overnight, 100%; (b) $ClCH_2COCl$, $AlCl_3$, 0 °C, 3 h, 20-50%; (c) NaBr, acetone, reflux, 24 h, 90-98%; (d) HO-P(O)-$(OEt)_2$, Ag_2O, CH_3CN, 60 °C, 16 h for **1.214a,** 76%; (e) K^+ $^-OP(O)(OEt)_2$, dibenzo-[18]-crown- 6, CH_3CN, reflux, 16 h for **1.214b,** 20%; (e) NH_4OAc, H_2O/MeOH, 1:4, 50 °C, 24 h, 90-95%.

Syntheses began with commercially available methoxy phenols **1.210.** 3-Methoxyphenol **1.210a** was esterified with pivaloyl chloride to block the substitution

reactions at the 2- and 5-positions of the aromatic ring. The Friedel-Crafts reaction of **1.211**with chloroacetyl chloride gave acetylated ortho-methoxy analogs **1.212a-b** in poor to moderate yield. The X-ray analysis was performed to confirmed the structure of the chloroacetyl group of **1.212a** (Figure 1.17), whereas the symmetrical nature of **1.212b** was established by NMR analysis. A Finkelstein reaction with NaBr was performed to obtain bromide **1.213**, which was subsequently esterified with diethyl phosphoric acid in the presence of Ag_2O to produce **1.214a** as a single product in 76% yield.

It was found that, at room temperature, deprotection of **1.214** proceeded very sluggishly (5 days) and required a large excess of NH_4OAc. However, raising the reaction temperature to 50 °C allowed for complete deprotection of **1.214a** within 24 h, producing **1.215a** in excellent yield (95%).

Figure 1.17 Crystal Structure of 4-(2-chloroacetyl)-3-methoxyphenyl pivalate (**1.212a**)[a]

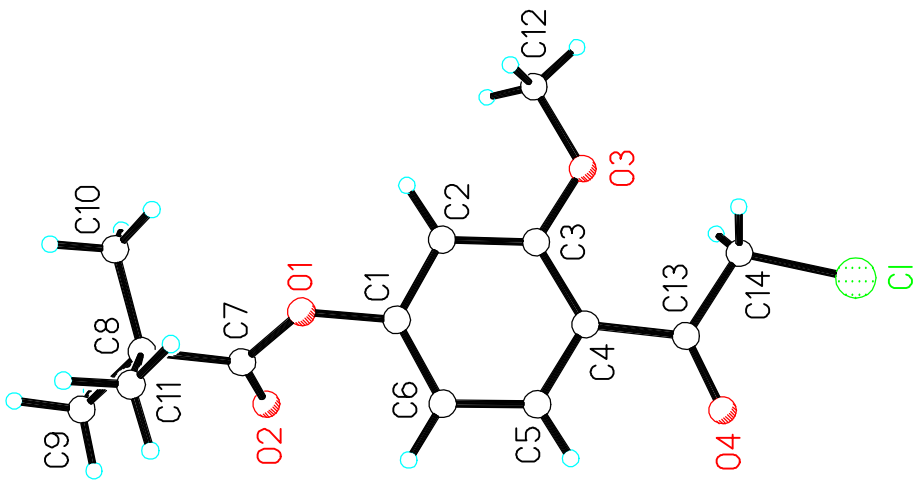

[a]Crystal structure of 4-(2-chloroacetyl)-3-methoxyphenyl pivalate **1.212a** which confirms the proper attachment of the acetyl chloride group after the Fridel-Crafts acylation reaction on 3-methoxyphenyl pivalate (**1.211a**) with chloroacetyl chloride.

In contrast, several attempts to phosphorylate **1.213b** using different conditions failed, presumably due to significant steric hindrance caused by the two *ortho* methoxy groups. However, employment of the potassium salt of diethylphosphoric acid in the presence of dibenzo-[18]-crown-6 provided crude phosphate **1.213b** in 20% yield. Subsequent deprotection of **1.214b** with NH_4OAc followed by purification of the product by preparative TLC provided *ortho*,*ortho'*-dimethoxy substituted *p*HP diethyl phosphate **1.215b** in 2% yield. Nonetheless, the amount of *ortho*-dimethoxy substituted *p*HP diethyl phosphate ester **1.215b** was enough to perform the subsequent photochemical analysis.

Spectroscopic Data Studies

The absorption maxima (λ_{max}) for all *ortho* and *meta* methoxy substituted *p*HP phosphates fall in the 300 nm region; however *meta* methoxy *p*HP derivatives have extended π-π^* absorption bands.[65,70] The UV/vis spectra of all compounds were determined in CH_3CN/H_2O (1:1) at ambient conditions. The absorption maxima and absorption coefficient values of methoxy substituted *p*HP diethyl phosphate esters **1.200a-c** and **1.215a-b** are shown in Table 1.17.

Table 1.17 The UV/vis Spectral Data for *meta* and *ortho* Methoxy Substituted *p*HP Diethyl Phosphates and for the m*eta* Acetyl *p*HP Diethyl Phosphate

*p*HP ester	λ_{max}/nm, (log ε/ M^{-1} cm^{-1})
1.200a *(m*-OMe)	271 (3.71), 310 (3.68)
1.200b (*m,m'*-OMe)	305 (3.21)
1.215a (*o*-OMe)	278 (3.98), 307 (3.93)
1.215b (*o,o'*-OMe)	283 (3.70)
1.200c (*m*-COMe)	274 (3.39), 319 (3.06)

A tailing of the absorption bands into the 400 nm region was observed for monosubstituted *ortho*- and *meta*-methoxy *p*HP diethyl phosphates **1.200a** and **1.215a** at acidic and neutral pH values (Figure 1.18). Furthermore, it was observed that there were two absorption maxima for the neutral form of *p*HP phosphate esters **1.200a** and **1.215a** at pH 4 and 7. These, bands may presumably be assigned to π-π* absorptions of the neutral form of unsymmetrical monosubstituted *ortho*- and *meta*-methoxy *p*HP diethyl phosphates **1.200a** and **1.215a**. A weak π-π* absorption band was observed for the *m*-COMe *p*HP derivative **1.203c** at 319 nm with an absorption coefficient (ε) of 1140 M^{-1} cm^{-1} [(log ε = 3.06), Table 1.19]. On the other hand, only one π-π* absorption band was observed for disubstituted *ortho*- and *meta*-methoxy *p*HP diethyl phosphates **1.200b** and **1.215b**. This may presumably be due to the symmetry of dimethoxy substituted phosphate esters **1.200b** and **1.215b**.

Figure 1.18 UV/vis Absorption Spectra of *o*- and *m*-Methoxy Substituted *p*HP Diethyl Phosphates and the *m*-Acetyl *p*HP Diethyl Phosphate

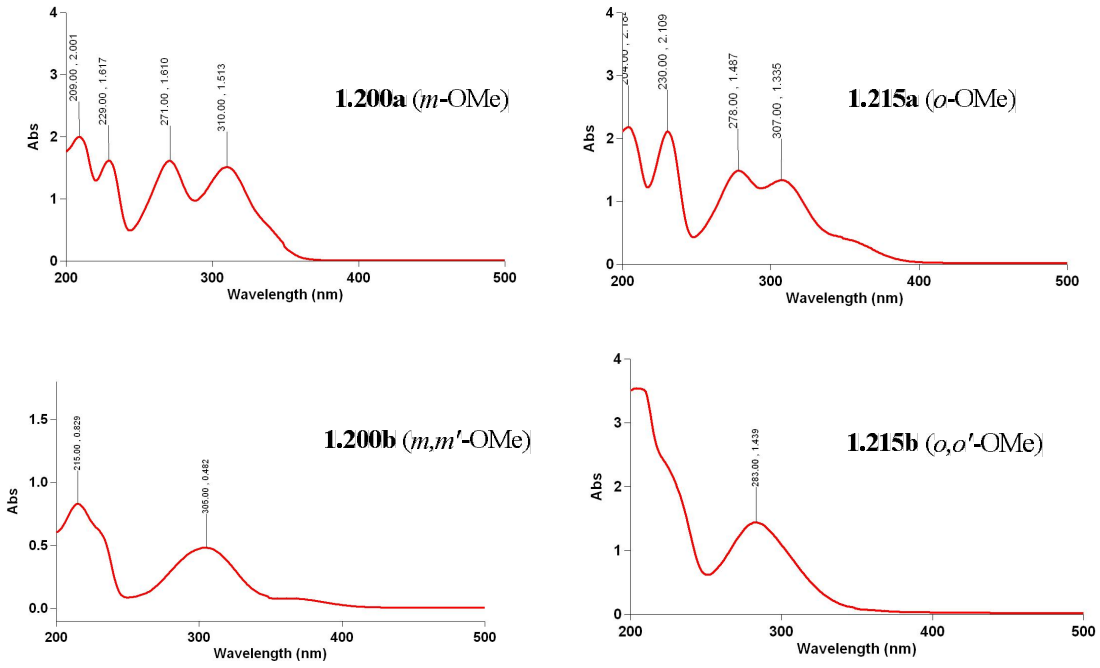

The pH dependence of *o*-MeO-*p*HP HDEP **1.215a** was studied in Tris buffer solution at pH 9 using UV/vis spectroscopy. In this case the absorption maxima were shifted to longer wavelengths, becoming a single band around 350 nm assigned to the conjugate base of *p*HP phosphate ester **1.215a**.

Neighboring group participation in the photochemistry of α-diazo ketones

The photochemistry of methoxy substituted diazo *p*HPs **1.198a** and **1.204** was investigated to study the effect of the methoxy group on the release of nitrogen in the excited state (Figure 1.19). Due to complications with neighboring group participation in the synthesis of unprotected *o*-methoxy diazo *p*HP, the acetate protected *o*-methoxy substituted diazo *p*HP **1.204** was used in our photochemical studies. The photochemistry of the acetate protected *m*-methoxy substituted diazo *p*HP **1.198a** was examined for comparative purposes.

Figure 1.19 Methoxy Substituted α-Diazoketones

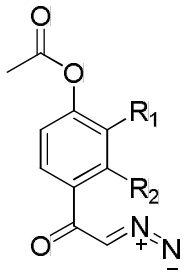

1.198a R_1 = OMe, R_2 = H
1.204 R_1 = H, R_2 = OMe

The photolysis was performed in a Pyrex NMR tube at 300 nm in D_2O/CD_3CN (1:1) using 2-3000 Å lamps. Acetyl protected *m*-methoxy diazo *p*HP **1.198a** produced rearranged acid **1.217** as the major product, whereas the acetyl-protected *o*-methoxy diazo *p*HP **1.204** gave rearranged acid **1.219** and cyclized ketone **1.222** in equal amounts (Schemes 1.41, 1.42, and 1.43). The formation of two photoproducts, the rearranged acid **1.219** and the cyclized

ketone **1.222,** was confirmed by chromatographic separation of individual photoproducts on silica gel followed by spectroscopic characterization. Based on these results, it would be reasonable to propose that photorelease from *m*-methoxy substituted **1.198a** follows the same pathway discussed above for the unsubstituted diazo *p*HP **1.165** via the photo-Wolff rearrangement to a ketene intermediate **1.216** (Scheme 1.42).

Scheme 1.42 Photolysis of **1.198a** in Aqueous Acetonitrile

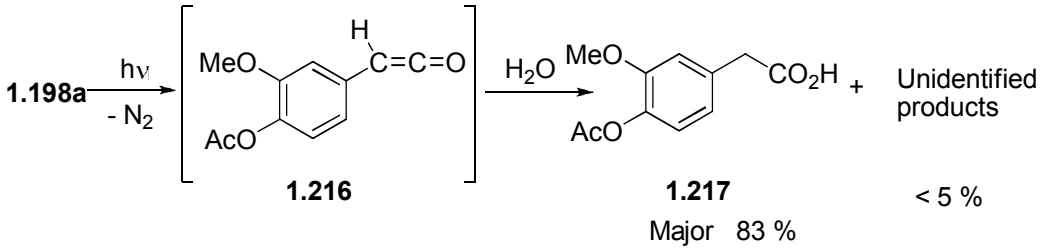

In contrast, photolysis of the *o*-methoxy substituted diazo *p*HP **1.204** follows two competing pathways to produce 6-acetoxy-3-coumaranone (**1.222**) and the rearranged acid **1.219** (Scheme 1.43).

Scheme 1.43 Two Competing Pathways for Product Formation from Diazo *p*HP **1.204**

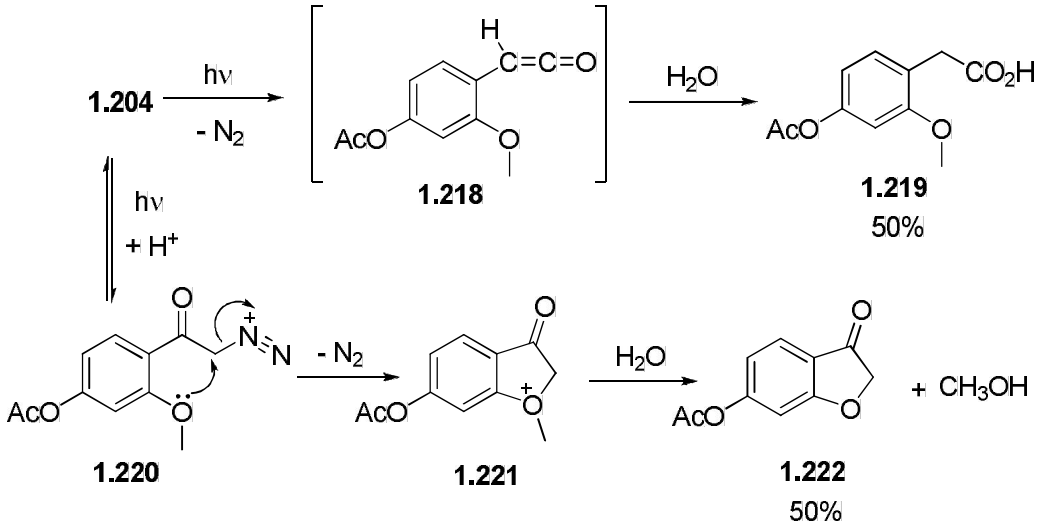

The latter product is produced by the photo-Wolff rearrangement discussed above. Alternatively, protonation of the carbon-nitrogen double bond in aqueous media can produce

diazonium ion **1.220**, which upon nucleophilic attack by the methoxy group cyclizes to give oxonium intermediate **1.221**. The latter rearranges to 6-acetoxy-3-coumaranone (**1.222**) generating methanol as the side product.

Another mechanistic scenario can also be put forward for the formation of cyclic ketone **1.222** (Scheme 1.44). In both pathways depicted in Scheme 1.43, a carbene **1.223** is formed with loss of nitrogen prior to ketene formation. Furthermore, the methoxy oxygen in *o*-methoxy substituted diazo *p*HP **1.204** can add to the carbene **1.223** in competition with ketene **1.218** formation. The resulted zwitterion **1.224** can be protonated on carbon to produce the cyclic ketone **1.222** along with methanol as the side product (Scheme 1.44). However, in accord with studies by Platz and co-workers the stepwise Wolff rearrangement (the mechanism via carbene formation) is the minor contributor to the rearrangement in aryldiazoketones which predominantly exist in the *syn* conformation.

Scheme 1.44 Formation of Products via the Carbene Intermediate **1.223**

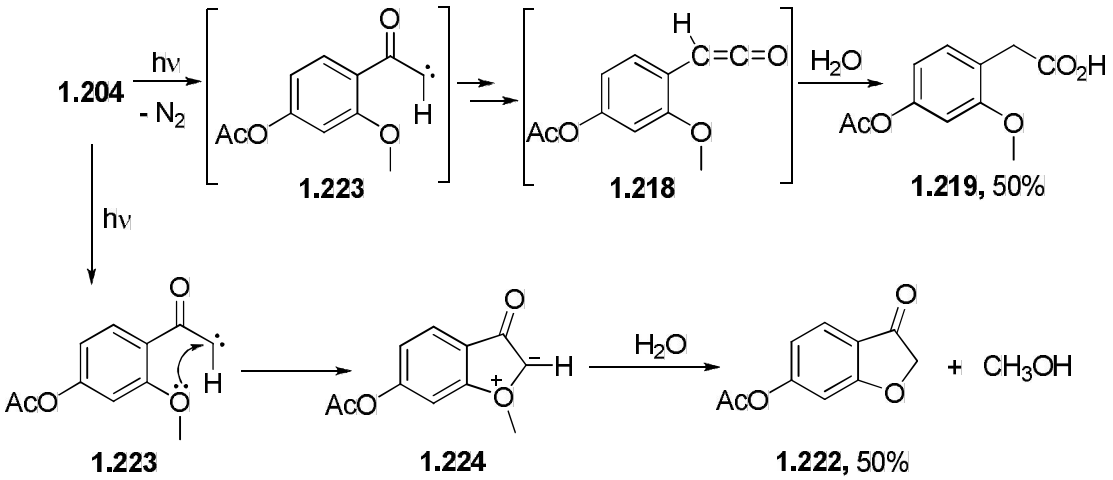

Accordingly, the concerted pathway would be the major contributor to the Wolff rearrangement-derived products from diazo *p*HP **1.204**. Thus, we argue that the mechanism

depicted in Scheme 1.43 is more appropriate for the formation of cyclic ketone **1.222** than that of illustrated in Scheme 1.44.

As discussed in the Introduction, an analogous cyclization was previously observed in photolysis of *o*-substituted *p*HP derivatives by Anderson and Reese in 1962.[50] It was shown that upon irradiation, *o*-hydroxy substituted α-chloro ketones cyclized to produce 3-coumaranone as the major product, whereas *o*-methoxy substituted derivatives gave the rearranged acid as the major product (see Introduction). In contrast to these observations, the acetyl-protected *o*-methoxy diazo *p*HP **1.204** produced equal amounts of cyclized product **1.222** and rearranged acid **1.219** because the diazo group is a better leaving group than the chloride. We can also argue that the oxygen atom of the *o*-methoxy group can attack the carbene which is derived from *o*-methoxy substituted diazo *p*HP **1.204** in competition with the Wolff rearrangement to form the ketene. Nonetheless, carbene formation was not be observed in Anderson and Reese studies of *o*-methoxy substituted α-chloro ketones, thereby the rearranged acid was produced as the major product.

Photoproduct Analysis and Photochemistry of *meta*-and *ortho*-Substituted *p*HP Diethyl Phosphates

Preliminary photolysis studies of *o*- and *m*-methoxy substituted *p*HP diethyl phosphates in D_2O/CD_3CN (1:1) at 300 nm or 350 nm were performed using 8 × 3000 Å or 16 × 3500 Å lamps. The photolysis reactions were monitored by ^1H NMR spectroscopy at time intervals using DMF as the internal standard. The released diethyl phosphoric acid, benzyl alcohol (< 5%), and the rearranged acid were observed (Equation 1.44).

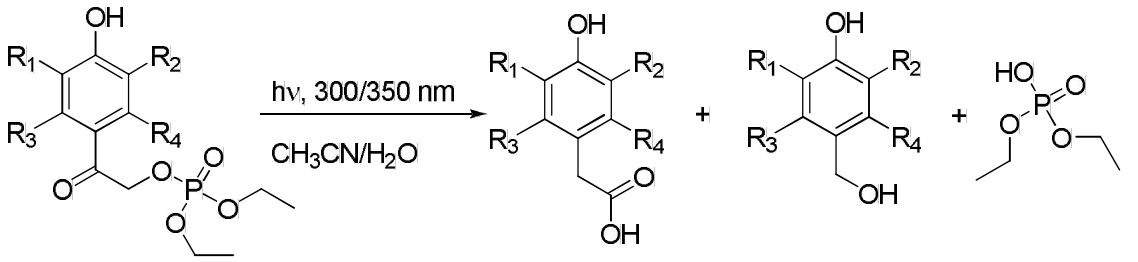

Major Minor, < 5 %

1.200a R_1 = H, R_2 = OMe, R_3, R_4 = H
1.200b R_1 = OMe, R_2 = OMe, R_3, R_4 = H
1.200c R_1 = H, R_2 = COMe, R_3, R_4 = H
1.215a R_1, R_2 = H, R_3 = OMe, R_4 = H
1.215b R_1, R_2 = H, R_3 = OMe, R_4 = OMe
1.57e R_1, R_2, R_3, R_4 = H

1.223 **1.224** **1.31**

Eq. 1.44

The formation of diethyl phosphoric acid **1.31** was confirmed by spiking the photolysis sample with the authentic compound. The identities of other photoproducts, the rearranged acid analogs **1.223** and benzyl alcohol analogs **1.224**, were confirmed by spiking the photolysis samples of unsubstituted *p*HP diethyl phosphate, **1.57e** (HDEP)**,** with authentic compounds (4-hydroxyphenylacetic acid **1.53**, benzyl alcohol **1.71**). The results and product distributions were similar to those obtained previously by Givens and co-workers[70] on releasing GABA and L-Glu from *m*-trifluoromethoxy substituted *p*HP derivative. It was found that *m*-acetyl *p*HP diethyl phosphate analog **1.200c** (3-COMe-*p*HP HDEP) produced the same photoproducts, but at a lower efficiency even at 300 nm (Equation 1.44). Generally, the quantum yields for the photolysis of methoxy substituted diethyl phosphates **1.200a-b**, **1.215a-b** in D_2O/CD_3CN, 1:1 are much lower at 350 nm than at 300 nm. Quantum efficiencies for the disappearance of starting diethyl phosphate esters **1.200a-c** and **1.215a-b** (Φ_{dis}) were determined by RP-HPLC analysis at 300 nm using 2 × 3000 Å lamps. The quantum yield for the disappearance (Φ_{dis}) was also determined at 350 nm for 3-COMe-HDEP **1.200b** using 16 × 3500 Å lamps to examine the efficiency of the photocleavage at a higher wavelength. The results are summarized in Table 1.18.

Table 1.18 Quantum Yields for Disappearance of the Starting Material ($\Phi_{dis.}$) for Methoxy Substituted *p*HP Diethyl Phosphates and a *m*-Acetyl *p*HP Diethyl Phosphate

Compound	Wavelength /nm	% conversion[a]	$\Phi_{dis.}$
1.200a *(m - OMe)*	300	10[b]	0.39 ± 0.02[b]
1.200b (*m,m'*-OMe)	300	11[b]	0.44 ± 0.02[b]
1.200b (*m,m'*-OMe)	350	04[b]	0.13 ± 0.02[b]
1.215a (*o* - OMe)	300	18[b]	0.59 ± 0.03[b]
1.215b (*o,o'*- OMe)	300	36[c]	0.69 ± 0.03[c]
1.200c (*m*-COMe)	300	02[b]	0.03 ± 0.005[b]

[a] Determined after 2 min of photolysis; [b] Determined by RP-HPLC in CH_3CN/H_2O, 1:1

[c] Determined by ^1H NMR in CH_3CN/H_2O, 1:1

The quantum yield for the release of diethyl phosphoric acid from *m*-methoxy *p*HP diethyl phosphate **1.200a** was 0.39 ± 0.03 (Table 1.18). The values are identical to those reported by Phillips and co-workers[62] in the photolysis of unsubstituted *p*HP caged diethyl phosphate (0.40 ± 0.09) which indicates that a single methoxy group in the 3-position does not significantly affect the efficiency of photorelease. Installation of two methoxy groups (at both *meta*-positions) also does not statistically increase the efficiency of the reaction: The quantum yield for the disappearance of 3,5-dimethoxy *p*HP diethyl phosphate **1.200b** was found to be 0.44 ± 0.02. It should be mentioned that the quantum yield values for *m*-methoxy *p*HP HDEP are greater than those reported for *m*-methoxy *p*HP GABA derivatives because the phosphate group is a better leaving group.

Surprisingly, the *o*-methoxy substituted diethyl phosphates **1.215a-b** showed a large increase in quantum yields (> 50%) compared to both the *m*-methoxy **1.200a-b** series and unsubstituted **1.57e** (Table 1.18, Introduction). Thus, the quantum yield for the disappearance of *o*-methoxy **1.215a** was 0.59 ± 0.03, and the observed value for *o,o'*-dimethoxy **1.215b** was

0.69 ± 0.03. However, the quantum yield for the disappearance of *o,o'*-dimethoxy **1.200b** was dramatically diminished when the excitation wavelength was changed from 300 nm to 350 nm (Table 1.18).

Table 1.19 Chemical Shift Values for the Methylene Peak in Methoxy Substituted *p*HP Diethyl Phosphate Derivatives in CD_3COCD_3

*p*HP ester	chemical shift for the methylene peak /ppm
1.57e (H)	5.29 - 5.31
1.200a (*m*-OMe)	5.31 - 5.34
1.200b (*m,m'*-OMe)	5.34 - 5.37
1.215a (*o*-OMe)	5.09 - 5.12
1.215b (*o,o'*-OMe)	4.78 - 4.81

Analysis of the ^{1}H NMR spectra of the *o*-methoxy substituted diethyl phosphates **1.215a-b** revealed a significant shielding of the two methylene hydrogens adjacent to the carbonyl in the phenacyl group. The chemical shifts of the methylene peak in CD_3COCD_3 for *o*-OMe **1.215a** and *o,o'*-OMe **1.215b** are 5.10 ppm and 4.79 ppm, respectively (Table 1.19).

The efficiency for the disappearance of *m*-COMe *p*HP diethyl phosphate **1.200c** was ca. 0.03± 0.005, which is one order of magnitude lower than that of the methoxy substituted derivatives. It was reported that the quantum yield for the release of GABA was higher (ca. 0.31-0.38) when electron withdrawing substituents such as $CONH_2$ and CO_2Me were introduced at the *m*-position of the *p*HP chromophore.[5] However, the reported quantum efficiency value for the *m*-CO_2H-substituted *p*HP GABA is 0.04, which is identical within experimental error to the value obtained for the *m*-COMe *p*HP **1.200c** (ca. 0.03 ± 0.005). The reason for the low quantum yields could be the intramolecular hydrogen bonding between the carbonyl oxygen and the phenolic hydrogen (Figure 1.20). The intramolecular hydrogen

bonding could greatly diminish the formation of the phenoxide anion in the excited state, which is a crucial step in the photo-Favorskii rearrangement. The excited state acidity would thus be lower in **1.200c** as compared to the methoxy substituted *p*HP derivatives **1.200a-b** and **1.215a-b**.

Figure 1.20 Intramolecular H-bond Formation in **1.200c**

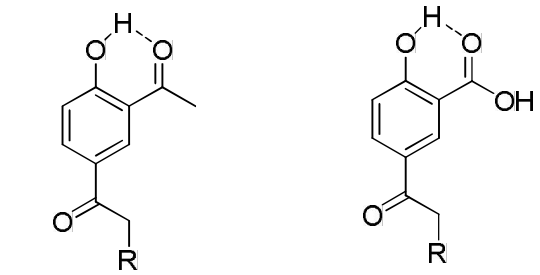

R = $-OP(O)(OEt)_2$ **1.200c**

R = GABA

The different effect of *m*-$CONH_2$ and -CO_2Me vs *m*-COMe and -CO_2H substitution may be a result of the resonance stabilization within the amide and the ester, which can reduce the intramolecular hydrogen bonding ability of the carbonyl moiety in these groups. This, in turn, can increase the propensity for generation of the phenoxide anion by releasing the less H-bonded phenolic hydrogen in the excited state for *m*-$CONH_2$ and –CO_2Me, which diminishes the acidity in the excited state and subsequently increases the efficiency of the photoreaction in the case of the *m*-$CONH_2$ and -CO_2Me.

Summarizing the substituent effects and the results of recent studies on the photo-Favorskii rearrangement using LFP,[5,66,69,70] the mechanism for the photorelease of methoxy substituted and a *m*-acetyl substituted *p*HP diethyl phosphate can be illustrated as follows (Scheme 1.45).

Scheme 1.45 Proposed Mechanism After Initial formation of the Excited Singlet of the *p*HP Chromophore

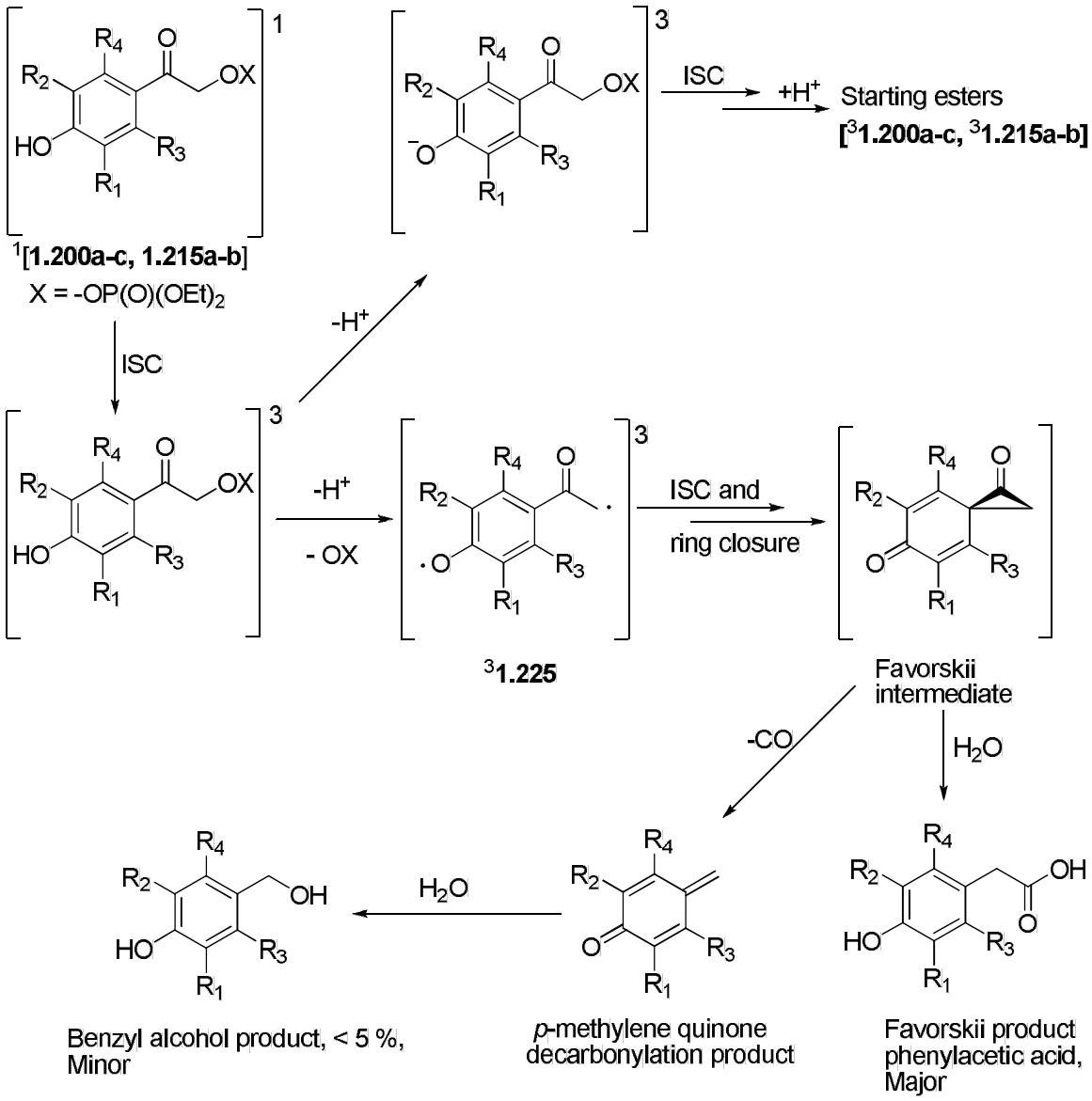

Irradiation of esters **1.200a-c** and **1.215a-b** are initially converted to their singlet excited state species (not shown) and this is followed by the intersystem crossing to the triplet excited state ester.[53,54,56,69,70] From this point the triplet excited state esters can either undergo the photo-Favorskii rearrangement by concomitantly releasing the phenolic proton

and the leaving group generating an oxyallyl-phenoxy triplet biradical (^{3}**1.225**) (λ_{max} = 445, 420, and 330 nm; $\tau \sim 0.6$ ns).[66,70] or the triplet can be diverted to an energy wasting pathway by releasing the phenolic proton generating the triplet phenoxide anion. The triplet phenoxide anion then intersystem crosses to the singlet ground state and protonates to reform the starting esters (**1.200a-c, 1.215a-b**). The oxyallyl-phenoxy triplet biradical (^{3}**1.225**) also intersystem crosses to the singlet excited state and cyclizes to form the Favorskii intermediate spirodienedione (Scheme 1.45).[69,70]

The putative spirodienedione intermediate then either can react with water to produce the rearranged acid as the major product or can decarbonylate to form the *p*-quinone methide intermediate (λ_{max} = 276 nm; TRIR absorption (λ_{max}) at 1647 cm^{-1}) which then reacts with water to generate *p*-hydroxybenzyl alcohol as the minor product (< 5 %).[69,70]

A key feature of the photo-Favorskii rearrangement is the possible out-of-plane rotation or twist of the substituted acetyl group (the leaving group) during the photorelease.[69,70] In the triplet excited state this process would be equivalent in effect to the formation of the oxyallyl-phenoxy triplet biradical ^{3}**1.225**. An initial partial rotation of the bichromophoric starting ketophenol was originally proposed by Phillips and co-workers[173] using time-resolved resonance Raman spectra of the triplet state of *p*HP phosphate and acetate esters. This suggestion, however, was later retracted. Recently, Givens, Stensrud, and co-workers[69] reexamined the out of plane motion of the oxyallyl group computationally [MP3 (6-31G* basis set)] using a series of the fluorinated oxyallyl-phenoxy triplet biradicals. The authors computed the energy and conformations of fluorinated triplet biradicals. Twist angles and triplet biradical/singlet energy differences were calculated for the lowest energy conformation of the phenoxy-oxyallyl triplet biradical in each case. It was found out that

triplet biradicals were generated through out-of-plane rotation of the acyl group with rotations that ranged from 8.0° for the *m*-fluoro substituted triplet biradical to 41.8° for the tetrafluoro substituted triplet biradical. The authors argued that the large twist angle of the tetrafluoro substituted triplet biradical may be the reason for the high efficacies for the *o*-fluoro substituted *p*HP GABA derivatives (see Introduction, Table 1.7). The *o*-fluoro substituted derivative stabilizes the oxyallyl-phenoxy triplet biradical which is the key intermediate prior to the putative spirodienedione intermediate in the Favorskii rearrangement pathway. This may be the case with the *o*-methoxy substituted *p*HP diethyl phosphates **1.215a-b** which have high quantum yields compared with the *meta*-methoxy derivatives **1.200a-b**. Thus, we argue that a better stabilization of the oxyallyl-phenoxy triplet biradical ^{3}**1.225** results from *o*-substitution by methoxy groups than from *m*-substitution of methoxy groups (Table 1.19). However, DFT calculations and Stern-Volmer quenching studies would be necessary and informative in elaborating our hypothesis.

Future work

All attempts to develop a procedure to isolate purified samples of caged biologically active phosphates such as ATP, cAMP, and NADPH, with *p*HP group were unsuccessful via the diazo approach. However, there may be alternative approaches to overcome this problem. For example, by protecting both the free amine and sugar hydroxyl groups for the above mentioned phosphates might lead to better reactions and more approachable separations using the α-diazo-*p*-hydroxyacetophenone approach to produce *p*HP protected phosphates. If the diazo approach continued to be unsuccessful, a parallel synthetic strategy may also be attempted with α-haloketones such as α-bromo-*p*-hydroxyacetophenone using the tetrabutyl

ammonium salts of the biologically active phosphates which are acyl protected at the amine functions and ketal protected on the sugar hydroxyl groups. The separation of individual products from the crude mixture may be better accomplished by either RP-HPLC or DEAE cellulose chromatography or DEAE Sephadex chromatography as described by Park et al.[51,52] The substituent effects on release of nitrogen (N_2) from α-diazo-*p*-hydroxyacetophenone deserve further elaboration. The effect of electron donating groups (OMe) and electron withdrawing groups (COMe) at the *meta* position of the *p*HP chromophore should provide insight into the mechanism of N_2 photorelease. In addition, quenching studies on the photochemistry of α-diazo-*p*-hydroxyacetophenone should be tested with suitable quenchers other than molecular oxygen. It was reported that piperylene quenches effectively the triplet excited state reactivity of α-diazoketones.[113,124,174] Thus, piperylene may be a better candidate to solve the mechanistic dilemma which has been discussed in this work. In addition, DFT calculations would be informative to obtain electron distribution in the excited states of the methoxy substituted *p*HP diethylphosphate derivatives, particularly at the methylene group, to provide a better explanation for the faster photorelease of diethyl phosphoric acid especially for *o*-methoxy substituted derivatives (the propensity of bond breaking in the excited state).

Conclusions

A simple esterification procedure to install phosphates and other sensitive functionalities (carboxylates, sulfonates, phenol esters and amino acids) has been accomplished using the α-diazo-*p*-hydroxyacetophenone (diazo *p*HP) which was found to be a widely applicable precursor for generating *p*HP protected esters in high yields, especially certain simple phosphate esters. Accordingly, convenient, high yields, one-pot syntheses were developed for other *p*HP derivatives through their corresponding α-diazo-*p*-hydroxyacetophenones.

ortho and *meta* substituents on the *p*HP chromophore were synthesized, particularly the electron donating methoxy substituents, through the diazo-*p*-hydaroxyphenacyl and other, previously developed routes, to explore the substitutent effects on extending the absorption range of the chromophore toward the visible region and on the efficiency of the photorelease. It was found that that photorelease of diethyl phosphate from *o*-methoxy *p*HP derivatives is more than 50% higher than *m*-methoxy. The quantum yield for the *m*-acetyl *p*HP diethyl phosphate derivative is an order of magnitude lower than that of other *o*- and *m*-methoxy *p*HP diethyl phosphates. The mechanism of photorelease appears to follow a photo-Favorskii pathway to generate the phenylacetic acid and benzyl alcohol derivatives. When nitrogen is the leaving group, the photo-Wolff rearrangement is the predominant pathway to the rearranged acid in the case of *m*-methoxy diazo *p*HP. In contrast, neighboring methoxy group participation by the *o*-methoxy substituent diazo *p*HP derivative cyclizes to give 6-hydroxy-3-coumaranone along with rearrangement to the Favorskii acid.

The light induced release of nitrogen (N_2) from diazo *p*HP in aqueous acetonitrile was studied. Uv/vis spectroscopic studies on solvent and pH effects, effects of triplet sensitization

and quenching provided useful information regarding the mechanism of N_2 release. Extensive time-resolved IR spectroscopy studies revealed that the dominant photochemical pathway was through the singlet excited state into the Wolff rearrangement to a ketene. However, quenching experiments with molecular oxygen suggested a quenchable triplet excited state may also contribute to the reaction in direct photolysis reactions. It is uncertain whether this pathway proceeds through the photo-Wolff or photo-Favorskii rearrangement or both. The Stern-Volmer quenching studies with molecular oxygen produced a triplet life time of 15 ns and the rate of 6.6×10^7 s^{-1} for the triplet photoreaction in aqueous acetonitrile (1:1). These preliminary results suggest that the rate constant for the release nitrogen is one or two orders of magnitude slower than the reported values for other *p*HP caged substrates. A detectable cyclopropanone moiety situated in the putative spirodienedione intermediate was not observed in accord all previous time-resolved IR and UV-vis studies. Thus, it unlikely that the diazo-p-hydroxyacetophenone follows a photo-Favorskii rearrangement pathway upon photorelease of N_2.

Experimental Methods

General Methods

All compounds were prepared by literature procedures unless indicated otherwise. All reagents were purchased from commercial sources (Aldrich, Acros Organics, Alfa Acer and Fisher) and used without further purification unless otherwise noted. Nitrobenzene and dichloromethane (DCM) were distilled prior to use. ^{1}H NMR spectra were recorded on a Bruker 400 MHz instrument unless otherwise noted. IR spectra were recorded on a Shimadzu FTIR-8400S spectrophotometer; results are reported in cm^{-1}. UV/vis spectra were recorded on a Cary 100 spectrophotometer (Varian, Inc., Palo Alto, CA). HPLC analyses were performed with a C18 Econosphere 250 x 4.6 mm analytical column (Altech Associates, Inc., Deerfield, IL) connected to a Rainin dual pump system for preliminary studies. Mass spectrometry was performed on a Sciex API-1 Plus quadrupole mass spectrometer with an electrospray ionization (ESI) source. pH values of solutions were measured using a Fisher Science pH 510 meter calibrated with certified Fisher buffer solutions of pH 4, 7, and 10. A Labconco FreezeZone device set was used for lyophilization (at -52 °C and 0.04 mbar). Thin layer and column chromatography were performed on precoated silica gel plates (Sorbent Technologies, Atlanta, GA) and standard grade (32-63 μm) silica gel (Sorbent Technologies, Atlanta, GA), respectively. Melting points were determined on a Thomas-Hoover melting point apparatus (Arthur H. Thomas Company, PA) and are uncorrected.

4-(Chlorocarbonyl)phenyl acetate (1.163a)

The general method of Adam and Binder [175] was followed with modifications. *p*-Acetoxybenzoic acid (**1.162a**, 1.0 g, 5.6 mmol) was dissolved in $SOCl_2$ (15.0 mL). The resulting mixture was refluxed at 45 °C for 9 h. Thionyl chloride was evaporated under

reduced pressure to afford crude 4-(chlorocarbonyl)phenyl acetate (**1.163a**) as a colorless oil. This acid chloride was used in the next step without any further purification (1.06 g, 5.35 mmol, 97% yield): ^{1}H NMR ($CDCl_3$) δ ppm 8.14-8.11 (1H, dd, *J* = 8.6 Hz, 3.3 Hz), 7.26-7.24 (1H, dd, *J* = 8.7 Hz, 1.8 Hz), 2.33 (3H, s); ^{13}C NMR (100 MHz, $CDCl_3$) δ (ppm) 168.0, 167.3, 156.3, 133.3, 132.3, 130.5, 122.6, 122.3, 21.2. The spectroscopic data are in strong agreement with the literature.[176]

α-Diazo-*p*-acetoxyacetophenone (1.164a)

The general methods of Arndt[177]and Mander et al.[93] were applied with modifications. To a solution of KOH (678 mg, 12.1 mmol) in 2-methoxyethanol (5 mL) and water (5 mL), diazold (1.17 g, 5.4 mmol) in diethylether (50 mL) was added carefully. The resulting mixture was gently heated to reflux temperatures (40-50 °C). The ether layer was distilled into a collection flask that was kept in an ice bath at 0 °C. The ether distillate was sequentially dried over KOH pellets for 1 h at 0 °C and with Na pieces for 1 h at 0 °C. Then a solution of the acid chloride (200 mg, 1.00 mmol) in dry ether (10 mL) was added to the distillate with vigorous stirring at -5 °C. The reaction mixture was allowed to come to 0 °C and stirred for 4 h. The solvent was evaporated, and the yellow colored residue was purified by flash chromatography using a gradient solvent system-EtOAc/hexane (1:4), EtOAc/hexane (1:3), and EtOAc/hexane (1:2) to afford α-diazo-*p*-acetoxyacetophenone (**1.164a**) as yellow needles (112 mg, 0.55 mmol, 55% yield): mp 105-107 °C; ^{1}H NMR ($CDCl_3$) δ ppm 7.81-7.79 (1H, dd, *J* = 6.8 Hz, 1.8 Hz), 7.20-7.18 (1H, dd, *J* = 6.8 Hz, 1.8 Hz), 5.88 (1H, s), 2.33 (3H, s); ^{13}C NMR (100 MHz, $CDCl_3$) δ (ppm) 185.3, 169.1, 154.2, 134.4, 128.4, 122.1, 54.4, 21.4; IR (KBr, cm^{-1}) 3067, 2114, 1757, 1609, 1574, 1417, 1392, 1369,

1103, 1167, 916, 860; MS (ESI (+)) *m/z* calcd for $(C_{10}H_8N_2O_3 + H)^+$ 205.0613, found 205 **α-Diazo-*p*-hydroxyacetophenone (1.165)**

The general method of Das et al.[178] was followed with modifications. To a stirred solution of α-diazo-*p*-acetoxyacetophenone (**1.164a**, 60 mg, 0.29 mmol) in aqueous MeOH (H_2O:MeOH, 1:4, 10 mL), NH_4OAc (181 mg, 2.4 mmol) was added. The resulting mixture was warmed to 50 °C and the progress of the reaction was monitored by TLC. After 4 h, the reaction mixture was concentrated and the residue was extracted with EtOAc (10 mL x 5). Combined organic layers were dried over anhydrous $MgSO_4$ and the solvent was evaporated to afford α-diazo-p-hydroxyacetophenone (**1.165**) as a yellowish orange colored crystalline solid that was further purified on silica gel (hexane:EtOAc, 1:1) to generate the pure compound as yellow colored crystals (48 mg, 0.30 mmol, 100% yield), mp = 144-150 °C (dec.): ^{1}H NMR (CD_3COCD_3) δ ppm 9.20 (1H, s), 7.77-7.75 (2H, d, *J* = 8.8 Hz), 6.92-6.90 (2H, d, *J* = 8.8 Hz), 6.47 (1H, s); ^{13}C NMR (100 MHz, CD_3COCD_3) δ (ppm) 185.4, 162.7, 129.9, 129.7, 116.2, 53.2; IR (KBr, cm^{-1}) 3263, 2170, 2123, 1605, 1560, 1508, 1261, 1230, 1173, 1099, 1028, 802; UV/Vis (CH_3CN/H_2O), λ_{max} (ε $Lmol^{-1}cm^{-1}$) 306 (14165); MS (ESI (+)) m/z calcd for $(C_8H_6N_2O_2 + H)^+$ 163.0507, found 163.1299; *m/z* calcd for $(C_8H_6N_2O_2 + Na)^+$ 185.1118, found 185.1129. .0606.

4-(2-(diphenoxyphosphoryloxy)phenyl acetate (1.167a)

The target molecule was synthesized by the method that was used by Epstein and Garrossian[48] with slight modifications. To a stirred solution of α-diazo-*p*-acetoxyacetophenone (**1.165**, 102 mg, 0.50 mmol) in benzene (5 mL), diphenyl phosphate (250 mg, 1.0 mmol) in benzene (5 mL) was added dropwise. The resulting mixture was refluxed at 70 °C. The progress of the reaction was monitored by the TLC. After 16 h, the

benzene layer was washed sequentially with saturated $NaHCO_3$ (40 mL) and water (40 mL) and dried over anhydrous $MgSO_4$. The solvent was evaporated to afford 4-(2-(diphenoxyphosphoryloxy)phenyl acetate (**1.167a**) as a yellow colored oil.(185 mg, 0.43 mmol, 87% yield): ^{1}H NMR ($CDCl_3$) δ ppm 7.90-7.87 (2H, d, *J* = 8.7), 7.35-7.31 (4H, m), 7.27-7.25 (4H, m), 7.19-7.17 (4H, m), 5.41-5.38 (2H, d, *J* = 10.0 Hz); ^{31}P NMR (162 MHz, $CDCl_3$) δ ppm -10.96; ^{13}C NMR (100 MHz, $CDCl_3$) δ (ppm) 190.3, 168.8, 155.2, 150.6, 131.4, 130.0, 129.7, 129.5, 125.7, 122.3, 120.4, 70.0, 21.28; MS (ESI (+)) m/z calcd for $(C_{22}H_{19}O_7P + H)^+$ 427.0947, found 427.0948; m/z calcd for $(C_{22}H_{19}O_7P + Na)^+$ 449.0766, found 449.0761; *m/z* calcd for $(C_{22}H_{19}O_7P + NH_4)^+$ 444.1212, found 444.1217

2-(4-Hydroxyphenyl)-2-oxoethyl diphenyl phosphate[9] (1.167b)

The general methods of Epstein and Garrossian[48] and Périé et al.[172] were used with modifications. To a stirred solution of α-diazo-*p*-hydroxyacetophenone (**1.165**, 11 mg, 0.068 mmol) in benzene (5 mL), diphenyl phosphate (34 mg, 0.14 mmol) in benzene (5 mL) was added dropwise. The resulting mixture was stirred at rt and the progress of the reaction was monitored by TLC. After 30 min, the benzene layer was washed sequentially with saturated $NaHCO_3$ (20 mL) and water (20 mL) and dried over anhydrous $MgSO_4$. The solvent was evaporated to afford 2-(4-hydroxyphenyl)-2-oxoethyl diphenyl phosphate[58] (**1.167b**) as a yellowish white solid that was chromatographed on silica gel (hexane:EtOAC, 1:1) to produce the pure compound (24 mg, 92% yield): ^{1}H NMR ($CDCl_3$) δ ppm 7.57-7.55 (2H, d, *J* = 8.6 Hz), 7.40-7.36 (4H, m), 7.32-7.30 (4H, m), 7.26-7.22 (2H, m), 5.33-5.30 (2H, d, *J* = 11.6 Hz); ^{31}P NMR (162 MHz, $CDCl_3$) δ ppm -11.10; ^{13}C NMR (125 MHz, $CDCl_3$) δ (ppm) 189.4, 162.4, 150.5, 130.4, 130.1, 126.0, 125.8, 120.5, 116.1, 70.3; MS (ESI (+)) m/z calcd

for $(C_{20}H_{17}O_6P + H)^+$ 385.0841, found 385.0845; *m/z* calcd for $(C_{20}H_{17}O_6P + NH_4)^+$ 402.1106, found 402.1107

Diethyl 2-(4-hydroxyphenyl)-2-oxoethyl phosphate[58] (**1.168**)

To a stirred solution of α-diazo-*p*-hydroxyacetophenone (**1.165**, 100 mg, 0.62 mmol) in benzene (5 mL), diethyl phosphate (190 mg, 1.23 mmol) in benzene (5 mL) was added dropwise. The resulting mixture was stirred at 60 °C and the progress of the reaction was monitored by TLC. After 24 h the benzene layer was washed sequentially with saturated $NaHCO_3$ (20 mL) and water (20 mL) and dried over anhydrous $MgSO_4$. The solvent was evaporated to afford diethyl 2-(4-hydroxyphenyl)-2-oxoethyl phosphate[58] (**1.168**) as yellowish white solid that was chromatographed on silica gel (hexane:EtOAC, 1:1) to produce the pure compound as a white solid (149 mg, 84% yield): ^{1}H NMR (400 MHz, CD_3COCD_3) δ ppm 9.33 (1H, s), 7.89-7.92 (2H, d, *J* = 6.8 Hz), 6.94-6.97 (2H, d, *J* = 6.8 Hz), 5.29-5.31 (2H, d, *J* = 10.6 Hz), 4.12-4.19 (4H, m), 1.29-1.33 (6H, m). The spectroscopic data are in strong agreement with the literature.[176]

2-(4-Hydroxyphenyl)-2-oxoethyl benzoate[179] **(1.169)**

To a stirred solution of α-diazo-*p*-acetoxyacetophenone (**1.165**, 20 mg, 0.098 mmol) in benzene (5 mL), benzoic acid (24 mg, 0.20 mmol) in benzene (5 mL) was added dropwise. The resulting mixture was refluxed at 70 °C. The progress of the reaction was monitored by TLC. After 42 h the benzene layer was washed sequentially with saturated $NaHCO_3$ (40 mL) and water (40 mL) and dried over anhydrous $MgSO_4$. The solvent was evaporated to afford a mixture of acetoxy benzoate and unprotected benzoate as a yellowish brown colored solid. (30 mg, 0.10 mmol, 100% yield). To a solution of the above mixture (30 mg, 0.147 mmol) in aqueous MeOH (1:4, 10 mL), NH_4OAc (92 mg, 1.19 mmol) was added. The resulting

mixture was warmed at 50 °C and the progress of the reaction was monitored by TLC. After 4 h, the reaction mixtuture was concentrated and the residue was extracted with EtOAc (10 mL x 5). The combined organic layers were dried over anhydrous $MgSO_4$ and the solvent was evaporated to afford the crude benzoate ester as a yellowish orange colored crystalline solid. The crude compound was further purified on silica gel (EtOAc/hexane 1:1) to give pure 2-(4-hydroxyphenyl)-2-oxoethyl benzoate[179] (**1.169**) as a white solid (25 mg, 0.098 mmol, 97% yield), ^{1}H NMR (CD_3COCD_3) δ ppm 9.33 (1H, s), 8.12-8.09 (2H, m), 7.98-7.95 (2H, m), 7.70-7.66 (1H, m), 7.57-7.53 (2H, m), 7.00-6.97 (2H, m), 5.65 (2H, s); ^{13}C NMR (125 MHz, CD_3COCD_3) δ (ppm) 191.12, 166.47, 163.31, 134.20, 131.27, 131.07, 130.55, 129.54, 127.66, 116.44, 116.36, 67.34. The spectroscopic data are in strong agreement with the reported data.[179]

2-(4-Hydroxyphenyl)-2-oxoethyl acetate (1.170)

To a stirred solution of α-diazo-*p*-hydroxyacetophenone (**1.165**, 10 mg, 0.062 mmol) in acetonitrile and water (10 mL, 4:1), glacial acetic acid (1 mL, 16 mmol) was added dropwise at rt. The resulting mixture was stirred at rt and the progress of the reaction was monitored by TLC. After 16 h the reaction mixture was concentrated and ethyl acetate (10 mL) was added. The organic layer was washed sequentially with saturated $NaHCO_3$ (20 mL) and water (20 mL) and dried over anhydrous $MgSO_4$. The solvent was evaporated to afford crude acetate ester as a yellowish brown solid that was chromatographed on silica gel (EtOAc/hexane 1:1) to give the pure 2-(4-hydroxyphenyl)-2-oxoethyl acetate (**1.170**) as a white solid (11.8 mg, 0.061 mmol, 98% yield): mp 128-131 °C; ^{1}H NMR (400 MHz, CD_3COCD_3) δ ppm 9.28 (1H, s), 7.91-7.88 (2H, dd, J = 9.5 Hz, 2.7 Hz), 6.97-6.94 (2H, dd, J = 9.5 Hz, 2.7 Hz), 5.35 (2H, s), ^{13}C NMR (125 MHz, CD_3COCD_3) δ (ppm) 191.2, 170.6, 163.3, 131.2, 130.13, 127.6,

116.4, 66.7, 20.5; IR (KBr, cm^{-1}) 3229, 1734, 1666, 1605, 1576, 1383, 1219, 1178, 841, 609; MS (ESI (+)); *m*/*z* calcd for $(C_{10}H_{10}O_4 - H)^+$ 193.0501, found 193.0497.

2-(4-Hydroxyphenyl)-2-oxoethyl 2,2,2-trifluoroacetate (1.171)

To a cooled (0 °C), stirred solution of α-diazo-*p*-hydroxyacetophenone (**1.165**, 10 mg, 0.062 mmol) in benzene (6 mL), trifluoroacetic acid (14 mg, 0.12 mmol) was added dropwise at 0 °C. The resulting mixture was stirred at 0 °C to rt and the progress of the reaction was monitored by TLC. After 1 h the benzene layer was washed sequentially with saturated $NaHCO_3$ (20 mL) and water (20 mL) and dried over anhydrous $MgSO_4$. The solvent was evaporated to give the crude trifluoroacetate ester as a yellowish brown solid that was chromatographed on silica gel (EtOAc/hexane 1:1) to give pure 2-(4-hydroxyphenyl)-2-oxoethyl 2,2,2-trifluoroacetate (**1.171**) as a white solid (14 mg, 0.056 mmol, 94% yield): mp = 128-131 °C; ^{1}H NMR (CD_3COCD_3) δ ppm 9.43 (1H, s), 7.95-7.93 (2H, dd, *J* = 6.8 Hz, 2 Hz), 7.00-6.98 (2H, dd, *J* = 6.8 Hz, 2 Hz), 5.81 (2H, s), ^{19}F NMR (376 MHz, $CDCl_3$) δ ppm -75.71 (3F, s); ^{13}C NMR (125 MHz, CD_3COCD_3) δ (ppm) 191.2, 170.6, 163.3, 131.2, 127.6, 116.4, 66.7, 20.6; IR (KBr, cm^{-1}) 3240, 1782, 1674, 1605, 1574, 960, 845, 725; MS (ESI (+)); *m*/*z* calcd for $(C_9H_{10}O_5\ S - H)^+$ 231.0334, found 231.0334.

α-Tosyloxy-*p*-hydroxyacetophenone (1.172)

To a cooled (0 °C), stirred solution of α-diazo-*p*-hydroxyacetophenone (**1.165**, 100 mg, 0.6 mmol) in dry CH_3CN (7 mL) under Ar was added *p*-toluenemethanesulfonic acid monohydrate (118 mg, 0.6 mmol) dropwise in CH_3CN (2 mL). The reaction mixture was allowed to stir for 30 min at 0 °C, brought to room temperature and stirred for 30 min. At that point, another portion of diazo ketone (50 mg, 0.3 mmol) in CH_3CN (1 mL) was added and the reaction mixture allowed to stir at room temperature for another 60 min. The reaction

mixture was evaporated to dryness and ethyl acetate (10 mL) was added, followed by washing the organic layer with a saturated aqueous solution of $NaHCO_3$ (15 mL x 3). The organic phase was separated, dried over anhydrous $MgSO_4$, filtered, and the supernatant concentrated under reduced pressure to afford the crude sulfonate ester. The crude product was purified by column chromatography on silica gel (EtOAc/hexane 1:1) to provide *p*-hydroxyphenacyl tosylate **1.172** as a brownish white solid (134 mg, 71%): mp 131-134 °C; ^{1}H NMR (500 MHz, CD_3COCD_3): δ 9.38 (1H, s), 7.83-7.88 (4H, m), 7.47-7.48 (2H, dd, *J* = 6.6 Hz, 8.0 Hz), 6.92-6.94 (2H, d, *J* = 6.8 HZ), 5.39 (2H, s), 2.46 (3H, s); ^{13}C NMR (125 MHz, CD_3COCD_3): δ 189.4, 163.4, 146.1, 134.4, 131.5, 130.9, 128.9, 127.2, 116.3, 71.4, 21.6; IR (KBr) 3310, 1682 and 964 cm^{-1}; MS (ESI (+)); *m/z* calcd for $(C_{15}H_{14}O_5SNa - H)^+$ 329.0460, found 329.0467.

2-(4-hydroxyphenyl)-2-oxoethyl trifluoromethanesulfonate (1.173)

To a stirred solution of α-diazo-*p*-hydroxyacetophenone (**1.165**, 10 mg, 0.062 mmol) in benzene (6 mL), triflic acid (10 mg, 0.068 mmol) in benzene (4 mL) was added dropwise at 0 °C under Ar. The reaction mixture was allowed to stir for 30 min at 0 °C, and then brought to room temperature. At that point, ethyl acetate (10 mL) was added to the reaction mixture and the organic phase was washed with saturated $NaHCO_3$ solution (15 mL x 3) and water (20 mL). The organic layer was separated, dried over anhydrous $MgSO_4$ and filtered. The solvent was evaporated to afford 2-(4-hydroxyphenyl)-2-oxoethyl trifluoromethanesulfonate as a yellowish brown solid which was run through a small pad of silica gel (hexane/EtOAc, 1:1) to afford the 2-(4-hydroxyphenyl)-2-oxoethyl trifluoromethanesulfonate (**1.173**) as a white solid which decomposed with time at room temperature (16 mg, 0.056 mmol, 91% yield)], ^{1}H NMR (400 MHz, CD_3COCD_3) δ ppm 9.48 (1H, s), 7.96-7.94 (2H, dd, *J* = 6.8 Hz,

2 Hz), 7.00-6.98 (2H, dd, J = 6.8 Hz, 1.96 Hz), 5.81 (2H, s); ^{19}F NMR (376 MHz, CD_3COCD_3) δ (ppm) -76.47 (3F, s). Product was really unstable and decomposed slowly at room temperature. Thus, the other spectroscopic data was not obtained on the target compound. This is in agreement with reported data.[147]

α-Mesyloxy-*p*-hydroxyacetophenone (1.174)

To a cooled (0 °C), stirred solution of α-diazo-*p*-hydroxyacetophenone (**1.165**, 100 mg, 0.6 mmol) in dry benzene (10 mL) under Ar was added methanesulfonic acid (60 µL, 0.9 mmol) dropwise. The reaction mixture was allowed to stir for 30 min at 0 °C, brought to room temperature and stirred for additional 60 min. At that point, ethyl acetate (10 mL) was added to the reaction mixture and the organic phase was washed with saturated $NaHCO_3$ solution (15 mL x 3). The organic phase was separated, dried over anhydrous $MgSO_4$, filtered, and the supernatant concentrated under reduced pressure to afford the crude *p*-hydroxyphenacyl methanesulfonate which is 95% pure according to ^{1}H NMR. The product was further purified by column chromatography on silica gel (EtOAc/hexane 1:1) to provide *p*-hydroxyphenacyl mesylate **1.174** as a white solid (139 mg, 98%): mp 162-164 °C; ^{1}H NMR (500 MHz, CD_3COCD_3): δ 9.41 (1H, s), 7.91-7.93 (2H, d, J = 6.8 Hz), 6.96-6.97 (2H, d, J = 6.8 HZ), 5.59 (2H, s), 3.25 (3H, s); ^{13}C NMR (125 MHz, CD_3COCD_3): δ 190.4, 163.6, 131.4, 127.1, 116.4, 71.7, 38.6; IR (KBr) 3365, 1691 and 962 cm^{-1}; MS (ESI (+)); *m*/*z* calcd for ($C_9H_{10}O_5S$-H^+) 329.0460, found 329.0467.

O-(4-Hydroxyphenacyl) γ-aminobutyrate, trifluoroacetate salt[53] (1.175a)

The general method of Shinada et al.[91] was followed with modifications. To a stirred solution of α-diazo-*p*-hydroxyacetophenone (**1.165**, 50 mg, 0.31 mmol) in toluene (10 mL), 4-(tert-butoxycarbonylamino) butanoic acid (Boc-GABA, 75 mg, 37 mmol) in toluene (2 mL)

was added dropwise at rt. A catalytic amount of copper acetylacetonate (8 mg, 0.031 mmol) was added to the reaction mixture. The resulting mixture was stirred at 60 °C and the progress of the reaction was monitored by TLC. After 2 h ethyl acetate (10 mL) was added. The organic layer was washed sequentially with saturated $NaHCO_3$ (20 mL) and water (20 mL) and dried over anhydrous $MgSO_4$. The solvent was evaporated to afford crude boc-GABA ester as a yellowish brown solid which was chromatographed on silica gel (hexane:EtOAc, 1:1) to give the *p*HP Boc-GABA as a yellowish brown solid. To a stirred solution of the above compound in CH_2Cl_2 (5mL), freshly distilled TFA (5 mL) was added. The reaction mixture was allowed to stir for 15 min and concentrated under reduced pressure. The residue was dissolved in water and CH_2Cl_2 (20 mL, 1:1). The water layer was extracted, frozen, and then lyophilized to afford *p*HP GABA **1.175a** as a white solid[11] (81 mg, 75% overall yield): ^{1}H NMR (400 MHz, D_2O) δ ppm 7.86 (2H, d, J = 8.8 Hz), 6.94 (2H, d, J = 8.8 Hz), 5.44 (2H, s), 3.07 (2H, t, J = 7.8), 2.66 (2H, t, J = 7.2 Hz), 2.00 (2H, m); ^{13}C NMR (100 MHz, D_2O) δ (ppm) 197.4, 192.7, 177, 164.7, 133.6, 130.6, 128.4, 118.4, 69.4, 41.3, 33.0, 24.8. The spectroscopic data are in strong agreement with literature.[53]

γ-O-*p*-Hydroxyphenacyl D- glutamate[53] (1.175b)

The general method of Shinada et al.[91] was followed with modifications. To a stirred solution of α-diazo-*p*-hydroxyacetophenone (20 mg, 0.12 mmol) in toluene (10 mL), 5-tert-butoxy-2-(tert-butoxycarbonylamino)-5-oxopentanoic acid (Boc-D-Glu(O^{t}Bu)-OH - 56 mg, 0.18 mmol) in toluene (2 mL) was added dropwise at rt. A catalytic amount of copper acetoacetonate (3 mg, 0.012 mmol) was added. The resulting mixture was stirred at 60 °C and the progress of the reaction was monitored by TLC. After 2 h ethyl acetate (10 mL) was added. The organic layer was washed sequentially with saturated $NaHCO_3$ (20 mL) and water (20 mL) and dried

over anhydrous $MgSO_4$. The solvent was evaporated to afford the crude protected glutamate ester that was chromatographed on silica gel (hexane:EtOAc, 1:1) to produce protected glutamate ester as a yellowish brown solid that was then used in the deprotection step. To a stirred solution of the above compound in CH_2Cl_2 (5 mL), freshly distilled TFA (5 mL) was added. The reaction mixture was allowed to stir for 15 min and concentrated under reduced pressure. Then residue was dissolved in water and CH_2Cl_2 (20 mL, 1:1). The water layer was extracted, frozen, and then lyophilized to afford *p*HP-glutamate **1.175b** as a white solid[53] (35 mg, 71% overall yield): mp = 134-136 °C; ^{1}H NMR (400 MHz, D_2O) δ ppm 7.87 (2H, d, , *J* = 8.4 Hz), 6.94 (2H, d, *J* = 8.4 Hz), 5.46 (2H, s), 4.14 (2H, t, *J* = 6.6 Hz), 2.79 (2H, t, 7.3 Hz), 2.23 (2H, m); ^{13}C NMR (100 MHz, D_2O) δ (ppm) 190.12, 174.23, 162.23, 156.92, 131.11, 128.93, 125.21, 116.82, 64.34, 51.45, 26.42. The spectroscopic data are in strong agreement with reported data.[53]

2-(4-Methoxyphenoxy)-*p*-hydroxyacetophenone (1.177a)

The general method of Shinada et al.[91] was followed with modifications. To a stirred solution of α-diazo-*p*-acetoxyacetophenone (**1.165**, 20 mg, 0.098 mmol) in toluene (10 mL), and *p*-methoxy phenol (24 mg, 0.19 mmol) in toluene (2 mL) was added dropwise at rt. A catalytic amount of rhodium(II) acetate dimer (4 mg, 0.01 mmol) was added to the reaction mixture. The resulting mixture was stirred at 60 °C overnight. The reaction mixture was concentrated and the yellow colored crude product was used for the deprotection step without further purification. To a stirred solution of the crude acetate in aqueous MeOH (1:4, 10 mL), NH_4OAc (60 mg, 0.78 mmol) was added. The resulting mixture was warmed at 50 °C and the progress of the reaction was monitored by TLC. After 8 h, the reaction mixture was concentrated and the residue was extracted with EtOAc (10 mL x 5). The combined organic

layers were dried over anhydrous $MgSO_4$ and the solvent was evaporated to afford 2-(4-methoxyphenoxy)-*p*-hydroxyacetophenone (**1.177a**) as a brownish white solid which was further purified on silica gel (hexane:EtOAc, 1:1) to generate the pure compound as a white solid (18 mg, 56% overall yield): mp = 132-134 °C; ^{1}H NMR (500 MHz, CD_3COCD_3) δ ppm 9.28 (1H, s), 7.97-7.96 (2H, d, *J* = 6.8 Hz), 6.96-6.95 (2H, d, *J* = 6.7 Hz), 6.91-6.89 (2H, d, *J* = 6.6 Hz), 6.84-6.82 (2H, d, *J* = 6.8 Hz), 5.29 (2H, s), 3.72 (3H, s); ^{13}C NMR (125 MHz, CD_3COCD_3) δ (ppm) 193.58, 163.15, 155.20, 153.61, 131.59, 131.51, 128.16, 116.53, 116.25, 115.38, 71.78, 55.88; IR (KBr, cm^{-1}) 3150, 1668, 1610, 1572, 1248, 1169, 987, 843, 636; MS (ESI (+)); *m*/*z* calcd for $(C_{15}H_{13}O_4 - H)^+$ 257.0814, found 257.0810. The spectroscopic data are in strong agreement with reported data.[180]

1-(4-hydroxyphenyl)-2-(4-(trifluoromethyl)phenoxy)ethanone (1.177b)[180]

To a stirred solution of α-diazo-*p*-acetoxyacetophenone (**1.165**, 40 mg, 0.20 mmol) in toluene (10 mL), and *p*-trifluoromethyl phenol (64 mg, 0.39 mmol) in toluene (2 mL) was added dropwise at rt. A catalytic amount of rhodium(II) acetate dimer (9 mg, 0.02 mmol) was added to the reaction mixture. The resulting mixture was stirred at 60 °C overnight. The reaction mixture was concentrated and the yellow colored crude product was used for the deprotection step without any purification. To a stirred solution of the crude 1-(4-acetoxyphenyl)-2-(4-(trifluoromethyl)phenoxy)ethanone in aqueous MeOH (1:4, 10 mL), NH_4OAc (120 mg, 1.6 mmol) was added. The resulting mixture was warmed to 50 °C and the progress of the reaction was monitored by TLC. After 8 h, the reaction mixture was concentrated and the residue was extracted with EtOAc (10 mL x 5). The combined organic layers were dried over anhydrous $MgSO_4$ and the solvent was evaporated to afford the 1-(4-hydroxyphenyl)-2-(4-

(trifluoromethyl)phenoxy)ethanone as a brownish white solid which was further purified on silica gel (hexane:EtOAc, 1:1) to generate the pure 1-(4-hydroxyphenyl)-2-(4-(trifluoromethyl)phenoxy)ethanone (**1.177b**) as a brownish white solid (49 mg, 68% overall yield): mp = 173-175 °C; ^{1}H NMR (500 MHz, CD_3COCD_3) δ ppm 9.34 (1H, s), 7.99-7.97 (2H, d, *J* = 7.0 Hz), 7.63-7.62 (2H, d, *J* = 8.5 Hz), 7.15-7.13 (2H, d, *J* = 8.6 Hz), 6.98-6.97 (2H, d, *J* = 6.8 Hz), 5.57 (2H, s); ^{13}C NMR (125 MHz, CD_3COCD_3) δ (ppm) 192.4, 163.4, 162.4, 131.5, 127.7, 127.7, 116.4, 116.3, 116, 70.9; IR (KBr, cm^{-1}) 3150, 1668, 1610, 1572, 1248, 1169, 987, 843, 636; MS (ESI (+)); *m/z* calcd for $(C_{15}H_{11}F_3O_2 - H)^+$ 295.0582, found 295.0567. The spectroscopic data are in strong agreement with reported data.[180]

α-hydroxy-*p*-hydroxyacetophenone[52] (**1.178**)

The title compound was obtained as a byproduct in the synthetic procedures given above. α-Hydroxy-*p*-hydroxyacetophenone[52] (**1.178**) was also generated in the decomposition of α-diazo-*p*-hydroxyacetophenone (**1.165**) in aqueous media. ^{1}H NMR (400 MHz, CD_3COCD_3) δ (ppm) 9.30 (1H, s), 7.91-7.88 (2H, dd, *J* = 6.9 Hz, 2 Hz), 6.97-6.94 (2H, dd, *J* = 6.9 Hz, 2 Hz), 4.80-4.79 (2H, d, *J* = 5.1); ^{13}C NMR (125 MHz, CD_3COCD_3)) δ (ppm) 197.8, 163.5, 131.2, 127.2, 116.4, 65.8. The spectroscopic data are in strong agreement with the literature.[52]

Photochemistry:

General methods:

Photolyses were performed in a Rayonet RPR-100 photochemical reactor (Southern New England Ultraviolet Company, Branford, CT) fitted with a Merry-go-round apparatus and with 16-350 nm (RPR 3500 Å) or 16-300 nm (RPR 3000 Å) lamps. The Rayonet reactor was

turned on to warm up the lamps for 15 minutes prior to irradiation of the sample. Samples were irradiated in NMR tubes or Pyrex test tubes at 40–45 °C in the Rayonet reactor in the presence or absence of oxygen. The tubes were placed in a RPR merry-go-round apparatus and a counter was started at the onset of exposure to record the time of irradiation. Exposure times were controlled by manual removal of the sample from the reactor or alternately by turning the lamps on or off. The light output for the determination of quantum efficiencies was measured by using the potassium ferrioxalate method.[181] Photolysis samples were analyzed using ^{1}H NMR and RP-HPLC methods. HPLC analyses were performed with a Waters XTerra MS-C18 analytical column (column size: 2.1 x 150 mm, particle size: 5 μm) connected to a Waters Alliance HT 2795 or a Waters Aquity UPLC. The solvent system for the separation was 99% CH_3CN, 1% H_2O, 0.06% formic acid and 99% H_2O, 1% CH_3CN, 0.08% formic acid. The detection wavelengths were 250 nm and 280 nm. The flow rate was 0.2 mL/min and the injection volume was 5 μL. Each sample was run three times.

Photolysis of α-diazo-p-hydroxyacetophenone (1.165) in aqueous acetonitrile

An NMR tube was charged with α-diazo-*p*-hydroxyacetophenone (6 mg, 0.037 mmol) and dissolved in CD_3CN (500 μL), D_2O (500 μL), and DMF (2 μL) and the contents were mixed thoroughly. DMF was used as an internal standard. The resulting sample mixture was photolyzed without degassing at 300 or 350 nm with 16-3000 or 16-3500 Å lamps. ^{1}H NMR spectra (16 scans) were collected after 0, 5, 10, 15, 20, and 25 min of photolysis. The depletion of α-diazo-*p*-hydroxyacetophenone (**1.165**) and the appearance of released *p*-hydroxyphenylacetic acid were quantified from the NMR integrations of the signals at δ 6.23 and 3.49 ppm, respectively. The results are shown in Equation 1.33.

Photolysis of α-diazo-*p*-hydroxyacetophenone (1.165) in dry acetonitrile

An NMR tube was charged with α-diazo-*p*-hydroxyacetophenone (**1.165**, 6 mg, 0.037 mmol) and dissolved in CD_3CN (1000 μL) and DMF (2 μL) and contents were mixed thoroughly. DMF was used as an internal standard. The resulting sample mixture was photolyzed without degassing at 300 or 350 nm with 16-3000 or 16-3500 Å lamps and ^1H NMR spectra (16 scans) were collected after 0, 5, 10, 15, 20, and 25 min of photolysis. The results are shown in Equation 1.34.

Photolysis of α-diazo-*p*-hydroxyacetophenone at different pD values: an NMR study

An NMR tube was charged with α-diazo-*p*-hydroxyacetophenone (6 mg, 0.037 mmol) and dissolved in CD_3CN (500 μL), D_2O (500 μL), and DMF (2 μL) and the contents mixed thoroughly. DMF was used as an internal standard. Different pD values were achieved by changing the pD of the D_2O (500 μL) before mixing with CD_3CN. A pD = 4 was achieved by careful addition of formic acid to D_2O. The pD = 7 was accomplished with solid NH_4OAc. The pD = 10 was achieved with solid Na_2CO_3. The resulted samples were photolyzed without degassing at 300 or 350 nm with 16-3000 or 16-3500 Å lamps and ^1H NMR spectra (16 scans) were collected after 0, 5, 10, 15, and 20 min of photolysis. The results are discussed in the Results and Discussion section.

Photolysis of α-diazo-*p*-hydroxyacetophenone (1.165) at different pH values; RP-HPLC analysis

A qualitative analysis of photoproducts was achieved with RP-HPLC. A quartz tube was charged with α-diazo-*p*-hydroxyacetophenone (**1.165**, 10 mg, 0.062 mmol). The ketone was

dissolved in HPLC grade CH_3CN (2.0 mL) and H_2O (2.0 mL), and the contents were mixed thoroughly before the photolysis. Different pH values were obtained by changing the pH of the H_2O (2.0 mL) before mixing with CH_3CN (2.0 mL). A buffer solution of sodium acetate/acetic acid in water was used to get the pH value of 4. Buffer solutions of tris(hydroxylmethyl)aminomethane/hydrochloric acid, and ammonium acetate/ammonia were used to achieve pH 7 and 10, respectively. The sample was irradiated at 300 or 350 nm with 16-3500 Å lamps, and sample aliquots (50 μL) were collected after 0, 5, 10 15, 20 min of photolysis. Each aliquot was diluted with 950 μL of HPLC grade CH_3CN/H_2O, 1:1, and was analyzed by HPLC using an Econosphere C18 analytical column. The solvent system for the separation was 70% CH_3CN and 30% H_2O with 0.1% H_3PO_4. The detection wavelength was 238 nm and flow rate was 1.0 mL/min. The distribution of products in each case was observed and attempts to identify the photoproducts were made by side by side injections of authentic compounds. The results are discussed in the Results and Discussion section.

Photolysis of α-diazo-*p*-hydroxyacetophenone (1.165): photoproduct analysis by ^{1}H NMR

A Pyrex NMR tube was charged with α-diazo-*p*-hydroxyacetophenone (**1.165**, 6 mg, 0.037 mmol) and dissolved in CD_3CN (500 μL) and D_2O (500 μL). The contents were mixed thoroughly. The resulting sample was photolyzed with air at 300 or 350 nm with 2-3000 Å or 16-3500 Å lamps and the ^{1}H NMR spectrum (16 scans) was collected after 10 min of photolysis. The depletion of α-diazo-*p*-hydroxyacetophenone and the appearance of released 4-hydroxyphenylacetic acid (PAA) were characterized from the NMR signals at δ 6.23 and 3.49 ppm, respectively. The photolysis sample was spiked with an authentic sample of PAA. The intensity of the methylene peak at 3.49 ppm increased dramatically. In addition,

intensities of peaks of PAA within the aromatic region (7.10-7.12 and 6.76-6.78 ppm) increased. These observations confirmed the formation of PAA from the photolysis. Bubbles evolved while the sample was being irradiated. This could be due to nitrogen extrusion.

Photolysis of α-diazo-*p*-hydroxyacetophenone (1.165): photoproduct analysis by RP-HPLC

A quartz tube was charged with α-diazo-*p*-hydroxyacetophenone (**1.165**, 10 mg, 0.062 mmol) that had been dissolved in HPLC grade CH_3CN (2.0 mL) and H_2O (2.0 mL). The contents were mixed thoroughly before the photolysis. The sample was irradiated at 300 or 350 nm with 2-3000 Å or 16-3500 Å lamps. Sample aliquots (100 μL) were collected after 10 min of photolysis. The aliquot was diluted with 950 μL of HPLC grade CH_3CN/H_2O, 1:1 and analyzed by HPLC using a C18 analytical column (qualitative analysis). The photoproducts were identified by co-injections with authentic samples of the unknown compounds.

Photolysis of α-diazo-*p*-hydroxyacetophenone (1.165) in dry CH_3CN: photoproduct analysis by GC/MS

A quartz tube was charged with α-diazo-*p*-hydroxyacetophenone (**1.165**, 20 mg, 0.12 mmol) that was dissolved in dry HPLC grade CH_3CN (4.0 mL). The contents were mixed thoroughly before the photolysis. The sample was irradiated at 300 nm with 2-3000 Å lamps and sample aliquots (100 μL) were collected after 0, 2, 4, 6, and 8 min of photolysis. These sample aliquots were diluted with 950 μL of HPLC grade CH_3CN and analyzed by GC/MS. Possible photoprudusts (*p*-hydroxybenzyl alcohol, *p*-hydroxyacetophenone, α-hydroxy-*p*-hydroxyacetophenone, *p*-hydroxyphenylacetic acid, *p*-hydroxybenzoic acid etc.), were also injected into the GC/MS under the same conditions, and the retention times and mass of each compound were determined. These GC/MS data were compared with the GC/MS retention

times and MS values of the authentic samples to attempt to assign the structures for the photoproducts.

Photolysis of α-diazo-*p*-hydroxyacetophenone (1.165) in dry CH_3CN: photoproduct analysis by RP-HPLC

A quartz tube was charged with α-diazo-*p*-hydroxyacetophenone (**1.165**, 20 mg, 0.12 mmol) that was dissolved in HPLC grade CH_3CN (4.0 mL). The contents were mixed thoroughly before the photolysis. The sample was irradiated at 300 nm with 2-3000 Å lamps and sample aliquots (100 μL) were collected after 0, 2, 4, 6, and 8 min of photolysis. The aliquots were diluted with 950 μL of HPLC grade CH_3CN and analyzed by HPLC using an Econosphere C18 analytical column. The solvent system for the separation was 70% CH_3CN and 30% H_2O with 0.1% H_3PO_4. The detection wavelength was 238 nm, the flow rate 1.0 mL/min, and the injection volume was 50 μL. Four major products were observed, and the identities of the photoproducts were determined by co-injections of authentic samples of the known compounds (*p*-hydroxybenzyl alcohol, *p*-hydroxyacetophenone, α-hydroxy-*p*-hydroxyacetophenone, *p*-hydroxyphenylacetic acid, *p*-hydroxybenzoic acid, etc.).

Photolysis of α-diazo-*p*-hydroxyacetophenone (1.165): Quantum yield determination by RP-HPLC

A stock solution was prepared for the biphenyl standard by dissolving biphenyl (160 mg, 1.04 mmol) in HPLC grade CH_3CN (90 mL) in a 100 mL volumetric flask and diluting it to the mark with HPLC grade H_2O (10 mL). A quartz tube was charged with α-diazo-*p*-hydroxyacetophenone (**1.165**, 10 mg, 0.062 mmol) that was dissolved in HPLC grade CH_3CN (1.0 mL) and H_2O (1.0 mL). The biphenyl internal standard solution (2.0 mL from the stock solution, 3.2 mg, 0.021 mmol) was added to the quartz tube and the contents were

mixed thoroughly. The sample was irradiated at 300 or 350 nm with 2-3000 Å or 16-3500 Å lamps and aliquots (100 μL) were collected after 0, 2, 4, 6, and 8 min of photolysis. Each aliquot was diluted with 950 μL of HPLC grade CH_3CN:H_2O (1:1), and was analyzed by HPLC using a Waters XTerra MS-C18 analytical column. The calibration curves were made for both α-diazo-*p*-hydroxyacetophenone and PAA under the same reaction conditions. The correction factor (R) for each compound was calculated. The depletion of the starting material and appearance of the PAA were quantified using average peak areas from three injections of each aliquot corresponding to the average peak area of the internal standard. Scatter plots were created by plotting mmol of α-diazo-*p*-hydroxyacetophenone vs, irradiation time (in min) and mmol of PAA vs. irradiation time (in min). The slope (*m*) of the best fit line from the linear regression analysis was determined for each plot. The light output (*L*) in units of millieinsteins per minute of the 2-3000 and 16-3500 Å lamps in the photoreactor was determined separately using the potassium ferrioxalate method.[181] The quantum yields (Φ) for the disappearance of α-diazo-*p*-hydroxyacetophenone and appearance of PAA were then calculated using following equation.

$$\Phi = |m| / L$$

Where *m* is the slope of the plot and L is the light output from lamps which were used in the actinometry. Results are shown in Table 1.12.

Sensitization Experiments:

Photolysis of α-diazo-*p*-hydroxyacetophenone with benzophenone-4,4-dicarboxylic acid (3.70×10^{-3} M and 9.25×10^{-3} M)

A quartz tube was charged with α-diazo-*p*-hydroxyacetophenone (**1.165**, 10 mg, 0.062 mmol) dissolved in HPLC grade CH_3CN (1.0 mL) and H_2O (1.0 mL). Biphenyl (2.0 mL from the

internal standard stock solution, (3.2 mg, 0.021 mmol) and benzophenone-4,4-dicarboxylic acid (4 mg, 0.015 mmol, sensitizer) were added to the quartz tube. The resulting mixture was shaken thoroughly until a clear solution was obtained. The sample was irradiated at 300 or 350 nm with 2-3000 Å lamps and aliquots (100 μL) were collected after 0, 2, 4, 6, and 8 min of photolysis. Each aliquot was diluted with 950 μL of HPLC grade CH_3CN/H_2O, 1:1, and was analyzed by HPLC using a Waters XTerra MS-C18 analytical column. The quantum yields of the disappearance of α-diazo-*p*-hydroxyacetophenone and appearance of PAA were calculated following the same procedure described for compound **1.165** alone. The experiment was repeated with the sensitizer concentration of 9.25×10^{-3} M. The results are shown in Table 1.12.

Photolysis of α-diazo-*p*-hydroxyacetophenone with a xanthone sensitizer, Mangiferin (4.76×10^{-3} M and 1.19×10^{-2} M)

A quartz tube was charged with α-diazo-*p*-hydroxyacetophenone (10 mg, 0.062 mmol) dissolved in HPLC grade CH_3CN (1.0 mL) and H_2O (1.0 mL). Biphenyl internal standard (2.0 mL from the stock solution, 3.2 mg, 0.021 mmol) and mangiferin (8 mg, 0.019 mmol, sensitizer) were added to the quartz tube. The resulting mixture was stirred thoroughly until a clear solution was obtained. The sample was irradiated at 300 or 350 nm with 2-3000 Å or 16-3500 Å lamps, and aliquots (100 μL) were collected after 0, 2, 4, 6, and 8 min of photolysis. Each aliquot was diluted with 950 μL of HPLC grade CH_3CN/H_2O, 1:1, and analyzed by HPLC using a a Waters XTerra MS-C18 analytical column. The quantum yields of the disappearance of α-diazo-*p*-hydroxyacetophenone and appearance of PAA were calculated following the same procedure described with compound **1.165** alone. The

experiment was repeated with the sensitizer concentration of 1.19 x 10^{-2} M. The results are shown in Table 1.12.

Photolysis of α-diazo-*p*-hydroxyacetophenone (1.165) under Ar

A quartz tube was charged with α-diazo-*p*-hydroxyacetophenone (**1.165**, 10 mg, 0.062 mmol) dissolved in HPLC grade CH_3CN (1.0 mL) and H_2O (1.0 mL). Biphenyl as the internal standard (2.0 mL from the stock solution, 3.2 mg, 0.021 mmol) was placed in the quartz tube and the contents were mixed thoroughly. The tube, fitted with a rubber septum, was cooled in an ice bath, purged with Ar for 30 min, and irradiated at 300 nm with 2-3000 Å bulbs. Aliquots (100 μL) were collected after 0, 2, 4, 6, and 8 min of photolysis through the rubber septum using a syringe and an Ar filled balloon to avoid the introduction of air into the tube. Each aliquot was diluted with 950 μL of HPLC grade CH_3CN/H_2O (1:1) and analyzed by HPLC using a a Waters XTerra MS-C18 analytical column. The quantum yields of the disappearance of α-diazo-*p*-hydroxyacetophenone (**1.165**) and appearance of PAA were calculated following the same procedure described above. The same procedure was repeated three times. The results are shown in Table 1.12.

Quenching Experiments:

Photolysis of α-diazo-*p*-hydroxyacetophenone in an oxygen atmosphere.

A quartz tube was charged with α-diazo-*p*-hydroxyacetophenone (**1.165**, 10 mg, 0.062 mmol) dissolved in HPLC grade CH_3CN (1.0 mL) and H_2O (1.0 mL). Biphenyl as the internal standard (2.0 mL from the stock solution, 3.2 mg, 0.021 mmol) was added to the quartz tube and the contents mixed thoroughly. The tube was fitted with a rubber septum and sealed, cooled in an ice bath, and purged with pure oxygen for 30 min. The sample was irradiated at 300 nm with 2-3000 Å lamps, and aliquots (100 μL) collected after 0, 2, 4, 6, and 8 min of

photolysis with a needle syringe. Each aliquot was diluted with 950 μL of HPLC grade CH_3CN/H_2O, 1:1, and analyzed by HPLC using a a Waters XTerra MS-C18 analytical column. The quantum yields of the disappearance of α-diazo-*p*-hydroxyacetophenone (**1.165**) and appearance of PAA were calculated following the same procedure described above. The same procedure was repeated three times. The results are shown in Table 1.12. A Stern-Volmer quenching plot was prepared using the oxygen concentration values which were obtained from the literature and the quantum yields.

X-Ray Crystallographic structure for the α-diazo-*p*-hydroxyacetophenone (1.165)

The needle shaped light yellow color crystals of diazo *p*HP **1.165** were produced from hexane/EtOAc solvent system. Colorless rectangular parallelepiped-shaped crystals of $C_8H_6N_2O_2$ are, at 100(2) K, orthorhombic, space group Pbca – D_{2h}^{15} (No. 61)[182] with **a** = 13.729(2) Å, **b** = 6.795(1) Å, **c** = 16.111(2) Å, V = 1503.1(3) $Å^3$ and Z = 8 molecules [d_{calcd} = 1.433 g/cm^3; μ_a(MoKα) = 0.106 mm^{-1}] A full hemisphere of diffracted intensities (1850 40-second frames with a ω scan width of 0.30°) was measured for a single-domain specimen using graphite-monochromated MoKα radiation (λ= 0.71073 Å) on a Bruker SMART APEX CCD Single Crystal Diffraction System.[183] X-rays were provided by a fine-focus sealed X-ray tube operated at 50kV and 30mA. Lattice constants were determined with the Bruker SAINT software package using peak centers for 5566 reflections. A total of 12759 integrated reflection intensities having 2θ((MoKα)< 58.23° were produced using the Bruker program SAINT[184]; 1932 of these were unique and gave R_{int} = 0.063 with a coverage which was 95.5% complete. The data were corrected empirically for variable absorption effects using equivalent reflections; the relative transmission factors ranged from 0.722 to 1.000. The Bruker software package SHELXTL was used to solve the structure using "direct

methods" techniques. All stages of weighted full-matrix least-squares refinement were conducted using F_o^2 data with the SHELXTL Version 6.10 software package.[185]

The final structural model incorporated anisotropic thermal parameters for all nonhydrogen atoms and isotropic thermal parameters for all hydrogen atoms. All hydrogen atoms were located in a difference Fourier and included in the structural model as independent isotropic atoms whose parameters were allowed to vary in least-squares refinement cycles. A total of 133 parameters were refined using no restraints, 1932 data and weights of $w = 1/ [\sigma^2(F^2) + (0.0870 P)^2 + 0.7647 P]$, where $P = [F_o^2 + 2F_c^2] / 3$. Final agreement factors at convergence are: R_1(unweighted, based on F) = 0.064 for 1835 independent absorption-corrected "observed" reflections having $2\theta(MoK\alpha) < 58.23°$ and $I > 2\sigma(I)$; R_1(unweighted, based on F) = 0.067 and wR_2(weighted, based on F^2) = 0.165 for all 1932 independent absorption-corrected reflections having $2\theta(MoK\alpha) < 58.23°$. The largest shift/s.u. was 0.000 in the final refinement cycle. The final difference map had maxima and minima of 0.42 and -0.35 $e^-/Å^3$, respectively.

UV/Vis study of α-diazo-p-hydroxyacetophenone (1.165) at different pH values

A 10 mL volumertric flask was charged with α-diazo-*p*-hydroxyacetophenone (10 mg, 0.062 mmol) and dissolved in CH_3CN (5.0 mL) and H_2O (5.0 mL). The pH was adjusted by changing the pH of H_2O (5.0 mL) before mixing it with CH_3CN (5.0 mL). A buffer solution of sodium acetate/acetic acid in water was used to obtain pH 4. A buffer solution of ammonium acetate/ammonia was used to achieve pH 7 and 10, respectively. The UV/vis scans were performed under ambient conditions with suitable dilutions at each pH value.

Substituent Effects on *p*HP Photochemistry on Releasing Diethyl Phosphates

3-Methoxy-4-acetoxybenzoic acid (1.197a)

The general method of Qin et al.[186] was followed with modifications. To a stirred solution of 3-methoxy-4-hydroxybenzoic acid (**1.196a**,1.0 g, 5.9 mmol) in dry CH_2Cl_2 (15 mL) under Ar, triethylamine (907 µL, 6.5 mmol) was added dropwise followed by acetyl chloride (506 µL, 7.1 mmol) dropwise. The reaction mixture was allowed to stir for 1 h at room temperature, then ethyl acetate (40 mL) was added, and the organic phase was washed with 10 % HCl (25 mL x 3) followed by a saturated $NaHCO_3$ solution (25 mL x 3). The aqueous fractions from $NaHCO_3$ extraction were combined, acidified with 10% HCl and re-extracted with EtOAc (25 mL x 3). The EtOAc fractions were combined, dried over anhydrous $MgSO_4$, filtered, and the supernatant concentrated under reduced pressure to afford 3-methoxy-4-acetoxybenzoic acid (**1.197a**) as a white solid (840 mg, 67%): mp 145-148 °C; ^{1}H NMR (500 MHz, CD_3COCD_3): δ 11.34 (1H, s), 7.69-7.66 (2H, m), 7.20-7.18 (1H, d, J = 8.1 Hz), 3.90 (1H, s), 2.27 (3H, s); ^{13}C NMR (125 MHz, CD_3COCD_3): δ 168.8, 167, 152.4, 144.9, 130.1, 123.9, 123.4, 114.3, 56.5, 20.6; IR (KBr, cm^{-1}) 3084-2544(br), 1759, 1686, 1597, 1470, 1221, 901, 762, 669; MS (ESI (-)) calcd for $(C_{15}H_{11}F_3O_2 - H)^+$ 209.0450, found 209.0448.

4-(2-Diazoacetyl)-2-methoxyphenyl acetate (1.198a)

The general methods of Adams and Binder[175] and Arndt[177] were followed with modifications. A flame dried 50 mL round bottomed flask was charged with 3-methoxy-4-acetoxybenzoic acid (**1.197a**, 0.840 g, 2.8 mmol) and freshly distilled $SOCl_2$ (20 mL) was added under Ar. The resulting mixture was refluxed at 80 °C for 8 h and concentrated under reduced pressure to afford 3-methoxy-4-acetoxybenzoyl chloride as colorless oil. This acid chloride was used in the next step without any purification.

General method A for preparation of diazomethane: To a solution of KOH (3.0 g, 53.5 mmol) in 2-methoxyethanol (17 mL) and water (5 mL), diazold (5.0 g, 23.3 mmol) in diethyl ether (75 mL) was added carefully. The resulting mixture was gently heated at reflux (40 - 45 °C). The ether layer was distilled into a collection flask kept in an ice bath at 0 °C. The ether distillate containing diazomethane was sequentially dried over KOH pellets for 1 h at 0 °C and with Na pieces for 1 h at 0 °C.

A solution of acid chloride (910 mg, 3.9 mmol) in dry ether (10 mL) was added dropwise to the dried ether distillate containing the diazomethane with vigorous stirring at -5 °C. The reaction mixture was allowed to come to 0 °C and stirred overnight. The solvent was evaporated, and the yellow residue was purified by flash chromatography with a gradient solvent system. [EtOAc/hexane (1:4), EtOAc/hexane (1:3), and EtOAc/hexane (1:2)] to afford 4-(2-diazoacetyl)-2-methoxyphenyl acetate (**1.198a**) as a yellow crystalline solid (645 mg, 69% yield): mp = 96-99 °C; ^{1}H NMR (500 MHz, CD_3COCD_3) δ ppm 7.56 (1H, d, J = 2 Hz), 7.47-7.45 (1H, d, J = 8.2 Hz), 7.18-7.16 (1H, d, J = 8.2 Hz), 6.63 (1H, s), 3.90 (3H, s), 2.26 (3H, s); ^{13}C NMR (125 MHz, $CDCl_3$) δ ppm 185.6, 168.8, 152.6, 144.5, 136.5, 124, 120.4, 111.6, 56.5, 54.4, 20.5; IR (KBr, cm^{-1}) 3078, 2112, 1765, 1582, 1508, 1420, 1367, 1192, 904, 785; MS (ESI (-)) calcd for $(C_{11}H_9N_2O_4 - H)^-$ 233.0562, found 233.0553.

2-Diazo-1-(4-hydroxy-3-methoxyphenyl)ethanone (1.199a)

The general method of Das et al.[178] was applied with modifications. To a stirred solution of 4-(2-diazoacetyl)-2-methoxyphenyl acetate (**1.198a**, 600 mg, 2.56 mmol) in aqueous MeOH (H_2O:MeOH, 1:4, 20 mL), was added NH_4OAc (1.578 g, 20.49 mmol). The resulting mixture was warmed at 50 °C and the progress of the reaction was monitored by TLC. After 8 h, the reaction mixture was concentrated and the residue was extracted with acetone (10 mL x 5).

The combined organic layers were dried over anhydrous $MgSO_4$ and the solvent was evaporated to afford 2-diazo-1-(4-hydroxy-3-methoxyphenyl)ethanone (**1.199a**) as a yellow-orange oil which was further purified on silica gel (hexane: EtOAc, 1:1) to generate the pure compound as a yellow oil (473 mg, 96% yield): ^{1}H NMR (500 MHz, CD_3COCD_3) δ ppm 8.45 (1H, s), 7.40-7.38 (1H, d, *J* = 2.1 Hz), 6.88-6.86 (2H, d, *J* = 8.4 Hz), 6.53 (1H, s), 3.90 (3H, s); ^{13}C NMR (125 MHz, CD_3COCD_3) δ (ppm) 185.4, 152.1, 148.5, 130, 122, 115.6, 110.8, 56.4, 53.3; IR (Teflon film, cm^{-1}) 3279, 3008-2839, 2106, 1688, 1591, 1516, 1356, 1277, 1200, 1028, 777; MS (ESI (-)) calcd for $(C_9H_8N_2O_3 - H)^-$ 191.0457, found 191.0438.

Diethyl phosphoric acid (1.30)

The general method of Barret, et al.[187] was followed with modifications. To a cooled, stirred solution of NaOH (4.0 g, 0.1 mol) in water (25 mL), diethyl chlorophosphate (7.2 mL, 0.05 mol) was added dropwise. The resulting mixture was stirred at 20-30 °C for 1 hr. Then, the reaction mixture was acidified with conc. H_2SO_4 acid and extracted with EtOAc (25 mL x 3). EtOAc fractions were combined, dried over anhydrous $MgSO_4$, filtered, and the supernatant concentrated under reduced pressure to afford diethyl phosphoric acid (**1.30**) as a colorless liquid which was lyophilized for 24 h and dried under reduced pressure for 24 h (6.54 g, 85%): ^{1}H NMR (400 MHz, CD_3COCD_3) δ ppm 13.52 (1H, s), 4.09-4.12 (4H, m), 1.36-1.32 (6H, m); ^{31}P NMR (162 MHz, CD_3COCD_3) δ ppm -1.94; ^{13}C NMR (125 MHz, CD_3COCD_3) δ (ppm) 64.1, 16.4; MS (ESI (-)) calcd for $(C_4H_{11}O_4P - H)^-$ 153.0317, found 153.0325.

Diethyl 2-(4-hydroxy-3-methoxyphenyl)-2-oxoethyl phosphate (1.200a)

The general method of Epstein and Garrossian[48] was followed some modifications. To a stirred solution of 2-diazo-1-(4-hydroxy-3-methoxyphenyl)ethanone (**1.199a**, 250 mg, 1.3 mmol) in benzene (10 mL) was added dropwise diethyl phosphoric acid (401 mg, 2.6 mmol)

in benzene (5 mL). The resulting mixture was stirred at 60 °C and the progress of the reaction was monitored by TLC. After 24 h, EtOAc (20 mL) was added to the reaction mixture. The organic layer was washed sequentially with saturated $NaHCO_3$ (40 mL) and water (20 mL) and dried over anhydrous $MgSO_4$. The solvent was evaporated to afford the crude product as a brown-yellow solid which was chromatographed on silica gel (with a gradient solvent system) EtOAc/hexane (1:2), EtOAc/hexane (1:1), and EtOAc/hexane (2:1)) to produce pure diethyl 2-(4-hydroxy-3-methoxyphenyl)-2-oxoethyl phosphate (**1.200a**) as yellow plates (323 mg, 78% yield): mp 75-78 °C; ^{1}H NMR (400 MHz, CD_3COCD_3) δ ppm 8.62 (1H, s) 7.58 (1H, s), 7.56 (1H, s), 6.95-6.93 (2H, d, J = 8 Hz), 5.34-5.31 (2H, d, J = 10.7 Hz); 4.18-4.14 (2H, m), 3.93 (3H, s), 1.33-1.29 (6H, m); ^{31}P NMR (162 MHz, CD_3COCD_3) δ ppm -0.13; ^{13}C NMR (125 MHz, CD_3COCD_3) δ (ppm) 191.7-191.6, 153.1, 148.7, 127.6, 123.6, 115.8, 111.5, 69.4, 64.5-64.4, 56.4, 16.5-16.4; IR (KBr, cm^{-1}) 3115, 3022-2872, 1688, 1587, 1526, 1400, 1271, 1236, 1034, 879, 748; UV/vis [H_2O/CH_3CN (1:1)], λ_{max} (ε $M^{-1}cm^{-1}$) 310 (4815), 271 (5146); MS(ESI (-)) *m/z* calcd for $(C_{13}H_{19}O_7P - H)^-$ 317.0790, found 317.0786.

3,5-Dimethoxy-4-acetoxybenzoic acid (1.197b)

To a stirred solution of 3,5-dimethoxy-4-hydroxybenzoic acid (**1.196a**, 1.5 g, 7.6 mmol) in dry CH_2Cl_2 (15 mL) under Ar was added triethylamine (2.1 mL, 15.1 mmol) followed by acetyl chloride (645 μL, 9.1 mmol) dropwise. The reaction mixture was allowed to stir for 30 min at room temperature. At that point ethyl acetate (40 mL) was added to the reaction mixture, and the organic phase was washed with 10% HCl (25 mL x 3) followed by saturated $NaHCO_3$ solution (25 mL x 3). The aqueous fractions from $NaHCO_3$ extraction were combined, acidified with 10% HCl and extracted with EtOAc (25 mL x 3). The EtOAc fractions were combined, dried over anhydrous $MgSO_4$, filtered, and the supernatant

concentrated under reduced pressure to afford the 3-methoxy-4-acetoxybenzoic acid (**1.197b**) as a brownish white solid (1.085 g, 60%): mp 167-170 °C; ^{1}H NMR (400 MHz, CD_3COCD_3): δ 7.36 (2H, s), 3.88 (6H, s), 2.26 (3H, s); ^{13}C NMR (125 MHz, CD_3COCD_3): δ 168.3, 167.1, 153.3, 133.6, 129.4, 107.1, 56.7, 20.3; IR (KBr, cm^{-1}) 3458-2536 (br), 1762, 1686, 1616, 1518, 1470, 1425, 1333, 1123, 943, 904, 764; MS(ESI (-)) *m*/*z* calcd for $(C_{11}H_{12}O_6 - H)^-$ 239.0556, found 239.0544.

2-Diazo-1-(4-hydroxy-3,5-dimethoxyphenyl)ethanone (1.199b)

A flame dried 50 mL round bottomed flask was charged with 3,5-dimethoxy-4-acetoxybenzoic acid (**1.197b**, 1.085 g, 4.5 mmol) and freshly distilled $SOCl_2$ (20 mL) was added under Ar. The resulting mixture was refluxed at 80 °C for 8 h and concentrated under reduced pressure to afford 3,5-dimethoxy-4-acetoxybenzoyl chloride as a colorless oil. This acid chloride was used in the next step without any further purification. General method A was used to generate diazomethane in excess by distillation in dry ether. Then a solution of acid chloride (1.165 g, 4.5 mmol) in dry ether (10 mL) was added dropwise to the distillate (diazomethane) with vigorous stirring at -5 °C. The reaction mixture was allowed to come to 0 °C and stirred overnight. The solvent was evaporated, and the dark yellow colored residue was used in the next step without purification. To a stirred solution of crude 4-(2-diazoacetyl)-2,6-dimethoxyphenyl acetate (690 mg, 2.61 mmol) in aqueous MeOH (H_2O:MeOH, 1:4, 20 mL), NH_4OAc (1.61 g, 20.89 mmol) was added. The resulting mixture was warmed at 50 °C and the progress of the reaction was monitored by TLC. After 8 h, the reaction mixture was concentrated and the residue was extracted with acetone (10 mL x 5). The combined organic layers were dried over anhydrous $MgSO_4$ and the solvent was evaporated to afford 2-diazo-1-(4-hydroxy-3,5-dimethoxyphenyl)ethanone (**1.199b**) as a

yellow-brown oil which was further purified on silica gel (hexane:EtOAc, 1:1) to generate the pure compound as a thick yellow oil (545 mg, 94% yield): ^{1}H NMR (400 MHz, CD_3COCD_3) δ ppm 8.03 (1H, s), 7.20 (2H, s), 3.88 (6H, s); ^{13}C NMR (125 MHz, CD_3COCD_3) δ (ppm) 185.5, 148.6, 128.6, 105.5, 56.8, 53.3; IR (KBr, cm^{-1}) 3313, 2115, 1601, 1564, 1518, 1456, 1371, 1194, 1114, 762, 733, 669; MS (ESI (-)) *m*/*z* calcd for $(C_{10}H_{10}N_2O_4 - H)^-$ 221.0562, found 221.0558.

Diethyl 2-(4-hydroxy-3,5-dimethoxyphenyl)-2-oxoethyl phosphate (1.200b)

To a stirred solution of 2-diazo-1-(4-hydroxy-3,5-dimethoxyphenyl)ethanone (**1.199b**, 500 mg, 2.25 mmol) in benzene (10 mL), diethyl phosphoric acid (694 mg, 4.5 mmol) in benzene (5 mL) was added dropwise. The resulting mixture was stirred at 60 °C and the progress of the reaction was monitored by the TLC. After 24 h, EtOAc (20 mL) was added to the reaction mixture. The organic layer was washed sequentially with saturated $NaHCO_3$ (40 mL) and water (20 mL) and dried over anhydrous $MgSO_4$. The solvent was evaporated to afford the crude product as a brown-yellow oil which was chromatographed on silica gel with a gradient solvent system; EtOAc/hexane (1:2), EtOAc/hexane (1:1), EtOAc/hexane (2:1), and EtOAc/hexane (3:1)) to produce the pure diethyl 2-(4-hydroxy-3-methoxyphenyl)-2-oxoethyl phosphate (**1.200b**) as a thick yellow oil (588 mg, 75% yield): ^{1}H NMR (400 MHz, CD_3COCD_3) δ ppm 8.26 (1H, s) 7.32 (2H, s), 5.37-5.34 (2H, d, J = 10.8 Hz); 4.20-4.13 (2H, m), 3.91 (3H, s), 1.33-1.29 (6H, m); ^{31}P NMR (162 MHz, CD_3COCD_3) δ ppm -0.12; ^{13}C NMR (125 MHz, CD_3COCD_3) δ (ppm) 191.8-191.7, 148.7, 142.6, 106.6, 69.5, 64.5-64.4, 56.8, 16.50; IR (Teflon film, cm^{-1}) 3242, 2982-2848, 1693, 1605, 1518, 1460, 1327, 1194, 1115, 1045, 802; UV/vis [H_2O/CH_3CN (1:1)], λ_{max} (ε $M^{-1}cm^{-1}$) 305 (1617); MS (ESI (-)) *m*/*z* calcd for $(C_{14}H_{21}O_8P - H)^-$ 347.0896, found 347.0889.

3-Methoxyphenyl pivalate (1.211a)

The general method of Gorobets et al.[188] was followed with modifications. To a cooled (0 °C), stirred solution of 3-methoxyphenol (**1.210a**, 2.0 g, 16.1 mmol) in dry CH_2Cl_2 (10 mL), freshly distilled triethylamine (3.350 mL, 24.2 mmol) and a catalytic amount of 4-dimethylaminopyridine (20 mg, 0.16 mmol) were added under Ar. After 10 min, pivaloyl chloride (2.98 mL, 24.2 mmol) was added dropwise to the reaction mixture. The reaction mixture was allowed to stir for 30 min at 0 °C, brought to room temperature and stirred overnight. At that point, water (10 mL) and ethyl acetate (30 mL) were added to the reaction mixture, and the organic phase was washed sequentially with 10% HCl (25 mL x 3), water (25 mL x 2), saturated $NaHCO_3$ solution (25 mL x 3) and brine (25 mL x 2). The organic phase was separated, dried over anhydrous $MgSO_4$, filtered, and the supernatant concentrated under reduced pressure to produce 3-methoxyphenyl pivalate (**1.211a**) as a thick yellow oil (3.335 g, 100%): ^{1}H NMR (500 MHz, CD_3COCD_3) δ ppm 7.31-7.28 (1H, t, J = 8.1 Hz), 6.82-6.82 (1H, d, J = 2.3 Hz), 6.81-6.80 (1H, d, J = 2.4 Hz), 6.69-6.66 (1H, m), 3.79 (3H, s), 1.33 (9H, s); ^{13}C NMR (125 MHz, CD_3COCD_3) δ (ppm) 177, 161.6, 153.4, 130.6, 114.7, 112.1, 108.7, 55.8, 39.6, 27.4; IR (Teflon film, cm^{-1}) 2972-2837, 1753, 1606, 1593, 1490, 1140, 1115, 1043, 766; MS (ESI (+)) *m/z* calcd for $(C_{12}H_{16}O_3 + H)^+$ 209.1178, found 209.1182. ^{1}H NMR data were similar to the literature values.[189]

4-(2-Chloroacetyl)-3-methoxyphenyl pivalate (1.212a)

The general method of Gonzalez-Gomez[190] was followed with modifications. To a cooled (0 °C), stirred solution of $AlCl_3$ (4.73 g, 35.4 mmol) in chloroacetyl chloride (10 mL) under Ar was added 3-methoxyphenyl pivalate (**1.211a**, 3.355 g, 16.1 mmol). The reaction mixture was allowed to stir for 3 h at 0 °C under Ar. Then, water (20 mL) was added cautiously to

quench the reaction, and the mixture extracted with EtOAc (25 mL x 4). The organic phase was washed sequentially with saturated $NaHCO_3$ solution (25 mL x 3) and brine (25 mL x 2). The organic phase was separated, dried over anhydrous $MgSO_4$, filtered, and the supernatant concentrated under reduced pressure to afford the crude product which was chromatographed on silica gel (EtOAc/hexane/CH_2Cl_2, 1:2:2) to give 4-(2-chloroacetyl)-3-methoxyphenyl pivalate (**1.212a**) as green-white crystalline solid (2.32 g, 50%): mp 58-61 °C; ^{1}H NMR (500 MHz, CD_3COCD_3): δ ppm 7.85.7.84 (1H, d, *J* = 8.6 Hz), 7.01-7.00 (1H, d, *J* = 2 Hz), 6.86-6.83 (1H, d, *J* = 8.6 Hz), 4.90 (2H, s), 4.01 (3H, s), 1.34 (9H, s); ^{13}C NMR (125 MHz, CD_3COCD_3): δ ppm 190.4, 176.7, 161.3, 157.6, 132.6, 123.4, 115.4, 107.2, 56.8, 51.8, 39.8, 27.3; IR (KBr, cm^{-1}) 2980-2854, 1757, 1686, 1606, 1420, 1271, 1186, 1117, 897, 791; MS (ESI (+)) *m*/*z* calcd for ($C_{14}H_{17}O_4Cl + H^+$) 285.0894, found 285.0912.

4-(2-Diethoxyphosphoryloxyacetyl)-2-methoxyphenyl pivalate (1.214a)

The general methods of Finkelstein[191] and Yogh, et al.[192] were utilized with modifications. A 50 mL round bottomed flask was charged with 4-(2-chloroacetyl)-3-methoxyphenyl pivalate (**1.212a**, 500 mg, 1.8 mmol) and NaBr (1.08 g, 10.5 mmol). Acetone (20 mL) was added and the resulting mixture was refluxed at 60 °C for 24 h. Then, the reaction mixture was concentrated and the resulting residue was suspended in ethyl acetate (20 mL) and washed sequentially with brine (20 mL x 2) and water (20 mL). The ethyl acetate layer was separated, dried over anhydrous $MgSO_4$, filtered, and the supernatant concentrated under reduced pressure to afford 4-(2-bromoacetyl)-3-methoxyphenyl pivalate (**1.213a**) as a white solid (95% conversion to α-bromo ketone analog according to ^{1}H NMR). This compound was used directly in the next step without purification. To a stirred solution of 4-(2-bromoacetyl)-3-methoxyphenyl pivalate (**1.213a**, 548 mg, 1.66 mmol) in CH_3CN (10 mL), diethyl

phosphoric acid (641 mg, 4.16 mmol) and Ag_2O (772 mg, 3.33 mmol) were added. The resulting mixture was stirred at 60 °C and the progress of the reaction was monitored by the TLC. After 16 h, the black colored suspension was filtered through a plug of Celite, the filtrate concentrated, and EtOAc (20 mL) was added. The organic layer was washed sequentially with saturated $NaHCO_3$ (40 mL) and water (20 mL) and dried over anhydrous $MgSO_4$. The solvent was evaporated to afford the crude product as a yellow-brown liquid which was chromatographed on silica gel using a gradient solvent system [EtOAc/hexane (1:2), EtOAc/hexane (1:1), EtOAc/hexane (2:1), and EtOAc/hexane (3:1) EtOAc/MeOH (19:1)] to produce the 4-(2-(diethoxyphosphoryloxy) acetyl)-2-methoxyphenyl pivalate (**1.214a**) as a yellow-brown solid (468 mg, 76%): mp 80-84 °C: ^{1}H NMR (500 MHz, CD_3COCD_3) δ ppm 7.93-7.91 (1H, d, J = 8.6 Hz), 7.01 (1H, d, J = 2 Hz), 6.86-6.84 (1H, d, J = 8.5 Hz), 5.18-5.16 (2H, d, J = 10.8 Hz), 4.18-4.12 (4H, m), 4.00 (3H, s), 1.34 (9H, s), 1.32-1.29 (6H, m); ^{31}P NMR (162 MHz, CD_3COCD_3) δ ppm -0.24; ^{13}C NMR (125 MHz, $CDCl_3$) δ (ppm) 193.0-192.9, 176.7, 161.7, 157.7, 132.4, 122.8, 115.4, 107.1, 73.0, 64.4-64.3, 56.8, 39.8, 27.3, 16.5; IR (KBr) 2982-2852(br), 1747, 1686, 1605, 1261, 1124, 1028, 854, 798 cm^{-1} MS (ESI (+)) *m/z* calcd for $(C_{18}H_{26}O_8PNa + H)^+$ 425.1341, found 425.1323.

Diethyl 2-(4-hydroxy-3-methoxyphenyl)-2-oxoethyl phosphate (1.215a)

To a stirred solution of 4-(2-(diethoxyphosphoryloxy)acetyl)-2-methoxyphenyl pivalate (**1.214a**, 468 mg, 1.16 mmol) in aqueous MeOH (H_2O:MeOH, 1:4, 20 mL), NH_4OAc (1.435 g, 18.61 mmol) was added. The resulting mixture was warmed at 50 °C and the progress of the reaction was monitored by TLC. After 36 h, the reaction mixture was concentrated and the residue was extracted with EtOAc (10 mL x 5). Combined organic layers were dried over anhydrous $MgSO_4$ and the solvent was evaporated to afford diethyl 2-(4-hydroxy-3-

methoxyphenyl)-2-oxoethyl phosphate (**1.215a**) as a dark yellow solid which was further purified on silica gel using a gradient solvent system [EtOAc/hexane (3:1), and EtOAc/MeOH (19:1)] to isolate the pure compound as a white crystalline solid (340 mg, 92% yield): mp 95-98 °C: ^{1}H NMR (400 MHz, CD_3COCD_3) δ ppm 9.40 (1H, s) 7.83-7.7.81 (2H, d, *J* = 8.8 Hz), 6.56 (2H, m, including a doublet), 5.12-5.09 (2H, d, *J* = 11.2 Hz); 4.20-4.13 (4H, m), 3.94 (3H, s), 1.33-1.29 (6H, m); ^{31}P NMR (162 MHz, CD_3COCD_3) δ ppm -0.37; ^{13}C NMR (125 MHz, CD_3COCD_3) δ (ppm) 191.5, 164.97, 162.9, 133.4, 117.3, 109.4, 99.7, 73.1-73.0, 64.4, 56.1, 16.5; IR (KBr, cm^{-1}) 3134, 1672, 1602, 1473, 1383, 1337, 1231, 1032, 984, 849; UV/vis [H_2O/CH_3CN (1:1)], λ_{max} (ε $M^{-1}cm^{-1}$) 307 (8498), 278 (9465); MS (ESI (+)) *m*/*z* calcd for $(C_{13}H_{19}O_7P - H)^-$ 317.0790, found 317.0795.

3,5-Dimethoxyphenyl pivalate (1.211b)

To a cooled (0 °C), stirred solution of 3,5-methoxyphenol (**1.210b**, 2.0 g, 12.97 mmol) in dry CH_2Cl_2 (10 mL), freshly distilled triethylamine (2.70 mL, 19.45 mmol) and a catalytic amount of 4-dimethylaminopyridine (16 mg, 0.13 mmol) were added under Ar. After 10 min, pivaloyl chloride (2.40 mL, 19.4 mmol) was added dropwise to the reaction mixture. The reaction mixture was allowed to stir for 30 min at 0 °C, brought to room temperature and stirred overnight. At that point, water (10 mL) and ethyl acetate (30 mL) were added to the reaction mixture and the organic phase was washed sequentially with 10% HCl (25 mL x 3), water (25 mL x 2), saturated $NaHCO_3$ solution (25 mL x 3) and brine (25 mL x 2). The organic phase was separated, dried over anhydrous $MgSO_4$, filtered, and the supernatant concentrated under reduced pressure to produce 3,5-dimethoxyphenyl pivalate (**1.211b**) as a thick yellow colored oil (3.09 g, 100%): ^{1}H NMR (500 MHz, CD_3COCD_3) δ ppm 6.38-6.37 (1H, t, *J* = 2.3 Hz), 6.29 (1H, s), 6.28 (1H, s), 3.77 (6H, s), 1.32 (9H, s); ^{13}C NMR (125 MHz,

CD_3COCD_3) δ (ppm) 176.9, 162.2, 154, 101.8, 98.4, 55.9, 39.6, 27.4; IR (Teflon film, cm^{-1}) 2968-2839, 1751, 1618, 1475, 1130, 1063, 895, 835, 681; MS (ESI (+)) *m*/*z* calcd for $(C_{13}H_{18}O_4 + Na)^+$ 261.1103, found 261.1100.

4-(2-Bromoacetyl)-3,5-dimethoxyphenyl pivalate (1.213b)

To a cooled (0 °C), stirred solution of $AlCl_3$ (3.695 g, 27.70 mmol) in chloroacetyl chloride (10 mL) under Ar was added 3,5-dimethoxyphenyl pivalate (**1.211b**, 3.0 g, 12.59 mmol)]. The reaction mixture was allowed to stir for 3 h at 0 °C under Ar. Then, water (20 mL) was added cautiously to quench the reaction and the mixture was extracted with EtOAc (25 mL x 4). The organic phase was washed sequentially with saturated $NaHCO_3$ solution (25 mL x 3) and brine (25 mL x 2) and then dried over anhydrous $MgSO_4$, filtered, and the supernatant concentrated under reduced pressure to afford 4-(2-chloroacetyl)-3,5-dimethoxyphenyl pivalate (**1.212b**) as a yellow-white solid which was used in the next step without purification. A 50 mL round-bottomed flask was charged with 4-(2-chloroacetyl)-3,5-dimethoxyphenyl pivalate (**1.212b**, 3.95 g, 12.54 mmol) and NaBr (7.75 g, 75.29 mmol). Acetone (25 mL) was added and the resulting mixture was refluxed at 60 °C for 24 h. Then, the reaction mixture was concentrated and resulted residue was suspended in ethyl acetate (30 mL) and washed sequentially with brine (25 mL x 2) and water (25 mL). The ethyl acetate layer was separated, dried over anhydrous $MgSO_4$, filtered, and the supernatant concentrated under reduced pressure to afford 4-(2-bromoacetyl)-3,5-dimethoxyphenyl pivalate (**1.213b**) as a yellow-white solid which was purified using flash chromatography on silica gel (hexane:CH_2Cl_2:EtOAc, 2:2:1) to produce a white solid (925 mg, 20%): mp 125-128 °C; ^{1}H NMR (500 MHz, CD_3COCD_3): δ ppm 6.53 (2H, s), 4.59 (2H, s), 3.81 (6H, s), 1.33 (9H, s); ^{13}C NMR (125 MHz, CD_3COCD_3): δ ppm 193.9, 176.8, 158.9, 155.6, 114.9,

99.7, 56.8, 51, 39.7, 27.4; IR (KBr, cm^{-1}) 3018-2841, 1749, 1732, 1597, 1464, 1412, 1221, 1128, 997, 892; MS (ESI (+)) *m/z* calcd for ($C_{15}H_{19}O_5Br + Na^+$): 381.0314, found 381.0312.

Diethyl 2-(4-hydroxy-2,6-dimethoxyphenyl)-2-oxoethyl phosphate (1.215b)

The general methods of Knopik et al.[193] and Das et al.[178] were followed with some modifications. To a stirred solution of 4-(2-bromoacetyl)-3,5-dimethoxyphenyl pivalate (**1.213b**, 500 mg, 1.40 mmol) in CH_3CN (10 mL), the potassium salt of diethyl phosphoric acid (535 mg, 2.78 mmol) and dibenzo-[18]-crown-6 (50 mg, 0.14 mmol) were added. The resulting mixture was stirred at 80 °C, and the progress of the reaction was monitored by TLC. After 16 h, the reaction mixture was concentrated and EtOAc (20 mL) was added. The organic layer was washed sequentially with saturated $NaHCO_3$ (40 mL) and water (20 mL) and dried over anhydrous $MgSO_4$. The solvent was evaporated to afford the crude product as a yellow-white solid which was chromatographed on silica gel using a gradient solvent system; EtOAc/hexane (1:2), EtOAc/hexane (1:1), EtOAc/hexane (2:1), EtOAc/hexane (3:1) EtOAc/MeOH (19:1) to isolate the crude diethyl 2-(4-hydroxy-2,6-dimethoxyphenyl)-2-oxoethyl phosphate (**1.214b**) as a dark yellow thick oil. Several attempts were made to purify the product on silica gel but they were unsuccessful. Therefore, the crude product was used in the deprotection step without further purification. To a stirred solution of the crude phosphate from the previous step (160 mg) in aqueous MeOH (H_2O:MeOH, 1:4, 10 mL) was added NH_4OAc (456 mg, 5.92 mmol). The resulting mixture was warmed at 50 °C and the progress of the reaction monitored by TLC. After 36 h, the reaction mixture was concentrated and the residue was extracted with EtOAc (10 mL x 5). The combined organic layers were dried over anhydrous $MgSO_4$ and the solvent was evaporated to afford diethyl 2-(4-hydroxy-

2,6-dimethoxyphenyl)-2-oxoethyl phosphate (**1.215b**) as a yellow-brown thick oil which was further purified by preparative TLC (hexane:isopropanol:chloroform, 1:1:11) to produce the pure product as a thick yellow oil (10 mg, overall 2%): ^{1}H NMR (400 MHz, CD_3COCD_3) δ ppm 9.04 (1H, s), 6.18 (1H, s), 4.81-4.79 (2H, d, J = 9.3 Hz); 4.13-4.05 (2H, m), 3.75 (3H, s), 1.30-1.27 (6H, m); ^{31}P NMR (162 MHz, CD_3COCD_3) δ ppm -0.75; ^{13}C NMR (125 MHz, CD_3COCD_3) δ ppm 196, 162.4, 160.2, 108.8, 92.9, 72.2, 64.4, 56.2, 16.5; IR (Teflon film, cm^{-1}) 2959-2852, 1738, 1593, 1462, 1342, 1261, 1211, 1153, 1028, 800; UV/vis [H_2O/CH_3CN (1:1)], λ_{max} (ε $M^{-1}cm^{-1}$) 283 (5013); MS(ESI (-)) m/z calcd for ($C_{14}H_{21}O_8P$ - H)$^-$ 347.0896, found 347.0887.

3-Acetyl-4-hydroxybenzoic acid (1.196c)

The general method of Nagano and Matsumura [194] was followed with modifications. Aluminum chloride (2.96 g, 22.2 mmol) was added into a flame dried 3-neck round bottomed flask containing a solution of 4-hydroxybenzoic acid (1.0 g, 5.55 mmol) in nitrobenzene (10 mL) under Ar. The reaction mixture was kept stirring vigorously at 150 °C for 14 h in the 3-neck flask fitted with a $CaCl_2$ tube. On cooling some crushed ice and 10% HCl (50.0 mL) were added to the rection and the separated nitrobenzene was removed by distillation. The aqueous phase was extracted with EtOAc (25 mL x 3) and washed with saturated $NaHCO_3$ solution (25 mL x 3). The alkaline aqueous phase was acidified with 10% HCl and extracted again with EtOAc (25 mL x 3). The combined organic layers were dried over anhydrous $MgSO_4$, filtered, and the supernatant concentrated under reduced pressure to afford 3-acetyl-4-hydroxybenzoic acid (**1.196c**) as a pink solid (980 mg, 98%): mp 227-230 °C; ^{1}H NMR (400 MHz, CD_3COCD_3): δ 12.71 (1H, s), 8.56 (1H, s), 8.17-8.15 (1H, s, J = 8 Hz), 7.05-7.03 (1H, s, J = 8 Hz), 2.77 (3H, s); ^{13}C NMR (125 MHz, CD_3COCD_3): δ (ppm) 166.7, 166.6,

138.1, 134.6, 122.4, 120.2, 119.1, 119, 27; IR (KBr, cm^{-1}) 3433, 1684, 1643, 1610, 1578, 1420, 1325, 1296, 1215, 1122, 943, 825, 771; MS(ESI (-)) m/z calcd for $(C_9H_7O_4 - H)^-$: 179.0344, found 179.0323.

4-Acetoxy-3-acetylbenzoic acid (1.197c)

To a stirred solution of 3-acetyl-4-hydroxybenzoic acid (**1.196c**, 950 mg, 5.27 mmol) in dry CH_2Cl_2 (15 mL) under Ar was added triethylamine (1.465 mL, 10.55 mmol) followed by dropwise addition of acetyl chloride (564 µL, 7.91 mmol). The reaction mixture was allowed to stir for 45 min at room temperature. At that point, ethyl acetate (40 mL) was added to the reaction mixture and the organic phase was washed with 10% HCl (25 mL x 3) followed by saturated $NaHCO_3$ (25 mL x 3). The aqueous fractions from the $NaHCO_3$ extraction were combined, acidified with 10% HCl and extracted with EtOAc (25 mL x 3). The EtOAc fractions were combined, dried over anhydrous $MgSO_4$, filtered, and the supernatant concentrated under reduced pressure to afford the 4-acetoxy-3-acetylbenzoic acid (**1.197c**) as a pink solid (820 mg, 70%): mp 125-145 °C (dec.); ^{1}H NMR (400 MHz, CD_3COCD_3) δ ppm 10.44 (1H, s), 8.48 (1H, d, *J* = 1.8 Hz), 8.23-8.21 (1H, d, *J* = 8.4 Hz), 7.35-7.33 (1H, d, *J* = 8.4 Hz), 2.60 (3H, s), 2.33 (3H, s); ^{13}C NMR (125 MHz, CD_3COCD_3) δ (ppm) 197.3, 169.4, 166.4, 153.5, 138.1, 135.1, 132.3, 129.3, 125.4, 119.1, 27, 21.2; IR (KBr, cm^{-1}) 3078-2552 (br), 1767, 1689, 1647, 1429, 1296, 1192, 918, 735; MS (ESI (-)) *m/z* calcd for $(C_{11}H_{10}O_5 - H)^-$ 221.0450, found 221.0440.

1-(3-Acetyl-4-hydroxyphenyl)-2-diazoethanone (1.199c)

A flame dried 50 mL round bottomed flask was charged with 4-acetoxy-3-acetylbenzoic acid (**1.197c**, 830 mg, 3.74 mmol) and freshly distilled $SOCl_2$ (20 mL) was added under Ar. The resulting mixture was refluxed at 80 °C for 8 h and concentrated under reduced pressure to

afford 4-acetoxy-3-acetylbenzoyl chloride as colorless oil. This acid chloride was used in next step without further purification. General method A was used to generate diazomethane in excess by distillation in dry ether. Then a solution of acid chloride (899 mg, 3.74 mmol) in dry ether (10 mL) was added dropwise to the distillate (diazomethane) with vigorous stirring at -5 °C. The reaction mixture was allowed to come to 0 °C and stirred overnight. The solvent was evaporated, and the dark yellow thick oil was used in the deprotection step without purification. To a stirred solution of crude 2-acetyl-4-(2-diazoacetyl)phenyl acetate (340 mg, 1.38 mmol) in aqueous MeOH (H_2O: MeOH, 1:4, 20 mL) was added NH_4OAc (852 mg, 11.05 mmol). The resulting mixture was warmed at 50 °C and the progress of the reaction was monitored by TLC. After 8 h, the reaction mixture was concentrated and the residue was extracted with acetone (10 mL x 5). The combined organic layers were dried over anhydrous $MgSO_4$ and the solvent was evaporated to afford 1-(3-acetyl-4-hydroxyphenyl)-2-diazoethanone (**1.199c**) as a dark yellow oil which was further purified on silica gel (hexane: EtOAc, 1:1) to isolate the pure compound as a yellow oil (254 mg, 21% overall yield): ^{1}H NMR (400 MHz, CD_3COCD_3) δ ppm 12.68 (1H, s), 8.40 (1H, d, J = 2.2 Hz), 8.04-8.01 (1H, d, J = 8.8 Hz), 7.03-7.01 (1H, d, J = 8.8 Hz), 6.69 (1H, s), 2.76 (3H, s); ^{13}C NMR (125 MHz, CD_3COCD_3) δ (ppm) 197.5, 185, 169.5, 153.2, 135.3, 132.2, 129.6, 125.4, 54.9, 21.2; IR (Teflon film, cm^{-1}) 3364, 2112, 1761, 1690, 1614, 1418, 1362, 1196, 1150, 1011, 914, 847, 733; MS (ESI (-)) *m/z* calcd for $(C_{10}H_8N_2O_3 - H)^-$ 203.0457, found 203.0452.

2-(3-Acetyl-4-hydroxyphenyl)-2-oxoethyl diethyl phosphate (1.200c)

To a stirred solution of 1-(3-acetyl-4-hydroxyphenyl)-2-diazoethanone (**1.199c**, 240 mg, 1.18 mmol) in benzene (10 mL) was added dropwise diethyl phosphoric acid (362 mg, 2.35 mmol)

in benzene (5 mL). The resulting mixture was stirred at 60 °C and the progress of the reaction was monitored by TLC. After 24 h, EtOAc (20 mL) was added to the reaction mixture. The organic layer was washed sequentially with saturated $NaHCO_3$ (40 mL) and water (20 mL) and dried over anhydrous $MgSO_4$. The solvent was evaporated to afford the crude product as a brown-yellow oil which was chromatographed on silica gel using a gradient solvent system [EtOAc/hexane (1:2), EtOAc/hexane (1:1), EtOAc/hexane (2:1), and EtOAc/hexane (3:1)] to give 2-(3-acetyl-4-hydroxyphenyl)-2-oxoethyl diethyl phosphate (**1.200c**) as a thick brown oil (306 mg, 79% yield): ^{1}H NMR (400 MHz, CD_3COCD_3) δ ppm 12.81 (1H, s), 8.59-8.58 (1H, d, *J* = 2.2 Hz), 8.17-8.14 (1H, d, *J* = 8.8 Hz), 7.08-7.06 (1H, d, *J* = 8.8 Hz), 5.42-5.39 (2H, d, *J* = 10.6 Hz), 4.18-4.13 (4H, m), 2.79 (3H, s), 1.33-1.30 (6H, m); ^{31}P NMR (162 MHz, CD_3COCD_3) δ ppm -0.14; ^{13}C NMR (125 MHz, CD_3COCD_3) δ (ppm) 191.6, 167.2, 136.5, 133.3, 126.8, 120.2, 119.4, 119.3, 69.5, 64.6-64.6, 27.2, 16.5-16.4; IR (Teflon film, cm^{-1}) 3443, 2985-2872, 1703, 1643, 1597, 1369, 1265, 1209, 1153, 1030, 820; UV/vis [H_2O/CH_3CN (1:1)], λ_{max} (ε $M^{-1}cm^{-1}$) 319 (1143), 274 (2474); MS (ESI (-)) *m/z* calcd for $(C_{14}H_{19}O_7P - H)^-$ 329.0790, found 329.0772.

4-Acetoxy-2-methoxybenzaldehyde (1.202)

The general method of Wuennemann[195] was followed with modifications. Triethylamine (956 μL, 6.9 mmol) and a catalytic amount of 4-dimethylaminopyridine (56 mg, 0.46 mmol) were added into a flame dried 50 mL round bottomed flask containing a solution of 4-hydroxy-2-methoxybenzaldehyde (**1.201**, 700 mg, 4.6 mmol) in dry CH_2Cl_2 (10 mL) under Ar. After 10 min, acetyl chloride (490 μL, 6.9 mmol) was then added dropwise to the reaction mixture. The reaction mixture was allowed to stir for 30 min, and EtOAc (30 mL)

was added to the reaction mixture. The organic phase was extracted with 10% HCl (20 mL x 3) and washed with saturated $NaHCO_3$ (20 mL x 3) followed by brine (40 mL) and then dried over anhydrous $MgSO_4$, filtered, and the supernatant concentrated under reduced pressure to afford 4-acetoxy-2-methoxybenzaldehyde (**1.202**) as a white solid (893 mg, 100%): mp 77-80 °C; ^{1}H NMR (500 MHz, CD_3COCD_3): δ ppm 10.37 (1H, s), 7.79-7.77 (1H, d, J = 8.4 Hz), 7.00 (1H, d, J = 2 Hz), 6.85-6.83 (1H, m), 3.97 (3H, s), 2.29 (3H, s); ^{13}C NMR (125 MHz, CD_3COCD_3): δ ppm 188.4, 169.2, 163.9, 158.1, 129.7, 123.5, 115.3, 107.3, 56.7, 21.1; IR (KBr, cm^{-1}) 2984-2872, 1763, 1684, 1606, 1589, 1497, 1375, 1267, 1213, 901, 810; MS (ESI (-)) m/z calcd for $(C_{10}H_{10}O_4\text{-}H)^-$: 193.0501, found 193.0498.

4-Acetoxy-2-methoxybenzoic acid (1.203)

The method of Adamski-Werner[196] was followed with modifications. A 50 mL round bottomed flask was charged with 4-acetoxy-2-methoxybenzaldehyde (**1.202**, 890 mg, 4.6 mmol) and was dissolved in acetone (30 mL). $KMnO_4$ (1.45 g, 9.2 mmol) in water (20 mL) was added dropwise to the reaction mixture. The reaction mixture was allowed to stir for 4 h and was concentrated under reduced pressure. The resulted solid was dissolved in a mixture of EtOAc (20 mL) and warm water (30 mL). The pH of the aqueous layer was adjusted to 2. Then, the aqueous phase was extracted with EtOAc (20 mL x 3) and the combined organic layers were extracted with saturated $NaHCO_3$ (20 mL x 3). The combined aqueous layers were acidified with 10% HCl and re-extracted with EtOAc (20 mL x 3). The combined organic layers were dried over anhydrous $MgSO_4$, filtered, and the supernatant concentrated under reduced pressure to afford 4-acetoxy-2-methoxybenzoic acid (**1.203**) as a white solid (850 mg, 88%): mp 80-82 °C; ^{1}H NMR (500 MHz, CD_3COCD_3): δ ppm 7.94-7.92 (1H, d, J

= 8.5 Hz), 7.01-7.00 (1H, d, *J* = 2 Hz), 6.87-6.84 (1H, d, *J* = 8.5 Hz), 3.99 (3H, s), 2.28 (3H, s); ^{13}C NMR (125 MHz, CD_3COCD_3): δ ppm 169.3, 165.9, 160.75, 156.4, 134, 117.8, 115.2, 107.4, 57, 21.1; IR (KBr, cm^{-1}) 3321-2852 (br), 1725, 1700, 1542, 1502, 1460, 1288, 1210, 1104, 1020, 890, 815, 770; MS (ESI (-)) *m*/*z* calcd for $(C_{10}H_{10}O_5\text{-}H)^-$: 209.0450, found 209.0444.

4-(2-Diazoacetyl)-3-methoxyphenyl acetate (1.204)

A flame dried 50 mL round bottomed flask was charged with 4-acetoxy-2-methoxybenzoic acid (**1.203**, 840 mg, 4.0 mmol) and freshly distilled $SOCl_2$ (20 mL) was added under Ar. The resulting mixture was refluxed at 80 °C for 8 h and concentrated under reduced pressure to afford 4-acetoxy-2-methoxybenzoyl chloride as a colorless oil. This acid chloride was used in the next step without further purification. General method A was used to generate diazomethane in excess by distillation in dry ether. Then a solution of acid chloride (913 mg, 4.0 mmol) in dry ether (10 mL) was added dropwise to the distillate containing the diazomethane in ether with vigorous stirring at -5 °C. The reaction mixture was allowed to come to 0 °C and stirred overnight. The solvent was evaporated, and the yellow solid was purified by flash chromatography on triethylamine saturated silica gel with a gradient solvent system [EtOAc/hexane (1:4), EtOAc/hexane (1:3), and EtOAc/hexane (1:2)] to afford 4-(2-diazoacetyl)-3-methoxyphenyl acetate (**1.204**) as a yellow solid (645 mg, 69% yield): mp 87-90 °C; ^{1}H NMR (500 MHz, CD_3COCD_3) δ ppm 7.90-7.88 (1H, d, *J* = 7.8 Hz), 6.94 (1H, d, *J* = 2 Hz), 6.84-6.82 (1H, d, *J* = 8.5), 6.63 (1H, s), 3.95 (3H, s), 2.27 (3H, s); ^{13}C NMR (125 MHz, CD_3COCD_3) δ (ppm) 169.3, 156.1, 131.8, 115, 107.1, 58.1, 56.6, 21.1; IR (KBr, cm^{-1}) 3126-3032, 2102, 1765, 1618, 1601, 1418, 1358, 1261, 1207, 1016, 962, 906, 690; MS (ESI (+)) *m*/*z* calcd for $(C_{11}H_{10}N_2O_4 + H)^+$ 235.0719, found 235.0728.

Characterization of photoproducts:

6-Hydroxybenzofuran-3(2H)-one (1.206)

6-Hydroxybenzofuran-3(2H)-one (**1.206**) was produced unintentionally by deprotection of 4-(2-diazoacetyl)-3-methoxyphenyl acetate (**1.204**, 280 mg, 1.47 mmol) with NH_4OAc (898 mg, 11.65 mmol) in H_2O/MeOH, 1:4 (20 mL) at 50 °C for 8 h. The off-white compound was characterized by NMR and mass spectroscopy as 6-hydroxybenzofuran-3(2H)-one [**1.206**, (218 mg, 100% yield)]: mp 239 °C (dec.); ^{1}H NMR (500 MHz, CD_3COCD_3) δ ppm 9.67 (1H, s, 9.67), 7.48-7.46 (1H, d, *J* = 8.4 Hz), 6.65-6.63 (1H, d, *J* = 8.4 Hz), 6.54-6.53 (1H, d, *J* = 2.0 Hz), 4.61 (2H, s); ^{13}C NMR (125 MHz, CD_3COCD_3) δ (ppm) 197.4, 177, 167.3, 125.9, 114.8, 112.4, 99.4, 76.1; IR (KBr, cm^{-1}) 3068-2526 (br), 1662, 1618, 1585, 1460, 1277, 1115, 1007, 870, 768; MSvv(ESI (-)) *m*/*z* calcd for $(C_8H_6O_3 - H)^-$149.0239, found 149.0224.

2-(4-Acetoxy-2-methoxyphenyl)acetic acid (1.219)

The 2-(4-Acetoxy-2-methoxyphenyl)acetic acid (**1.219**) was produced by photolysis of 4-(2-diazoacetyl)-3-methoxyphenyl acetate (**1.204**, 40.0 mg, 0.17 mmol) in CH_3CN/H_2O, 1:1 at 300 nm using 2-3000 Å lamps at ambient conditions. After 10 min, the photolysis mixture was concentrated and the resulting residue was chromatographed on silica gel (EtOAc:hexane (1:3), EtOAc:hexane (1:2), EtOAc:hexane (1:1), and EtOAc:hexane (2:1)) to afford 2-(4-acetoxy-2-methoxyphenyl)acetic acid (**1.219**) as a yellow solid (10 mg, 0.045 mmol, 26% yield): mp 94-104 °C (dec.); ^{1}H NMR (500 MHz, CD_3COCD_3) δ ppm 7.22-7.20 (1H, d, *J* = 8 Hz), 6.70 (1H, s), 6.61-6.60 (1H, d, *J* = 7.2 Hz), 3.75 (3H, s), 3.54 (2H, s), 2.23 (3H, s); ^{13}C NMR (125 MHz, CD_3COCD_3) δ (ppm) 169.7, 159.1, 151.8, 132, 117.7, 114.7, 114.1, 105.8, 56.2, 27.4, 21.1; IR (KBr, cm^{-1}) 3396-2554 (br), 1763, 1705, 1608, 1506, 1419,

1209, 1146, 1016, 960, 899, 804; MS (ESI (+)) *m/z* calcd for $(C_{11}H_{12}O_5 + Na)^+$ 247.0583, found 247.0575.

3-Oxo-2,3-dihydrobenzofuran-6-yl acetate (1.222)

Method A; The general method of Wuennemann[195] was followed with modifications. Triethylamine (20 mg, 0.20 mmol) and catalytic amount of 4-dimethylaminopyridine (2 mg, 0.46 mmol) were added into a flame dried 50 mL round bottomed flask containing a solution of 6-hydroxybenzofuran-3(2H)-one (**1.206**, 20 mg, 0.13 mmol) in dry CH_2Cl_2 (10 mL) under Ar. After 10 min, acetyl chloride (11 μL, 0.16 mmol) was added dropwise to the reaction mixture. The reaction mixture was allowed to stir for 30 min and EtOAc (30 mL) was added to the reaction mixture. The organic phase was extracted with 10% HCl (20 mL x 3) and washed with saturated $NaHCO_3$ solution (20 mL x 3) followed by brine (40 mL) and then dried over anhydrous $MgSO_4$, filtered, and the supernatant concentrated under reduced pressure to afford 3-oxo-2,3-dihydrobenzofuran-6-yl acetate (**1.222**) as a white crystalline solid (25.3 mg, 0.13 mmol, 100%).

Method B; 3-Oxo-2,3-dihydrobenzofuran-6-yl acetate (**1.222**) was also produced by photolysis of 4-(2-diazoacetyl)-3-methoxyphenyl acetate (**1.204**, 40.0 mg, 0.17 mmol) in CH_3CN/H_2O, 1:1 at using 2-3000 Å lamps under ambient conditions. After 10 min, the photolysis mixture was concentrated and the resulting residue was chromatographed on silica gel (EtOAc/hexane (1:3), EtOAc/hexane (1:2), and EtOAc/hexane (1:1)) to afford 3-oxo-2,3-dihydrobenzofuran-6-yl acetate (**1.222**) as white crystalline solid (12 mg, 0.062 mmol, 36% yield), mp 122-124 °C: ^{1}H NMR (500 MHz, CD_3COCD_3) δ ppm 7.65-7.64 (1H, d, J = 8.3 Hz), 7.02 (1H, d, J = 1.8 Hz), 6.92-6.90 (1H, d, J = 8.3 Hz), 4.75 (2H, s), 2.30 (3H, s); ^{13}C NMR (125 MHz, CD_3COCD_3) δ (ppm) 198.6, 175.4, 169.2, 159.5, 125.3, 119.9, 117.4, 108.1,

76.3, 21.1; IR (KBr, cm^{-1}) 3113-2943, 1759, 1707, 1618, 1454, 1194, 1015, 906, 829, 688; MS (ESI (-)) *m/z* calcd for $(C_{10}H_8O_4 - H)^-$ 191.0344, found 191.0359.

Photochemistry:

General methods:

Photolyses were performed in a Rayonet RPR-100 photochemical reactor (Southern New England Ultraviolet Company, Branford, CT) fitted with a merry-go-round apparatus and with 16-350 nm (RPR 3500 Å) or 16-300 nm (RPR 3000 Å) lamps. The Rayonet reactor was turned on to warm up the lamps for 15 min prior to irradiation of the sample. Samples were irradiated in NMR tubes or Pyrex test tubes or quartz test tubes at 40 – 45 °C in the Rayonet reactor in the presence or absence of oxygen. The tubes were placed in a RPR merry-go-round apparatus and a counter was started at the onset of exposure to record the time of irradiation. Exposure times were controlled by manual removal of the sample from the reactor or alternately by turning the lamps on or off. The light output for the quantum yields were measured by the potassium ferrioxalate method.[181] Photolysis samples were analyzed using ^{1}H NMR and RP-HPLC methods. HPLC analyses were performed with a Waters XTerra MS-C18 analytical column (column size: 2.1 x 150 mm, particle size: 5 μm) connected to a Waters Alliance HT 2795 or a Waters Aquity UPLC. The solvent system for the separation was 99% CH_3CN, 1% H_2O, 0.01% formic acid and 99% H_2O,1 % CH_3CN, 0.01% formic acid. The detection wavelengths were 250 nm and 280 nm. The flow rate was 0.2 mL/min and the injection volume was 5 μL. Each sample was run three times.

Photolysis of diethyl 2-(4-hydroxy-3-methoxyphenyl)-2-oxoethyl phosphate (1.200a): photoproduct analysis by ^{1}H NMR

A Pyrex NMR tube was charged with diethyl 2-(4-hydroxy-3-methoxyphenyl)-2-oxoethyl phosphate (**1.200a** (8 mg, 0.025 mmol)) dissolved in CD_3CN (500 μL) and D_2O (500 μL). DMF (2.0 μL) was added as an internal standard and the contents were mixed thoroughly. The resulting solution was photolyzed without degassing at 300 or 350 nm with 2-3000 Å or 16-3500 Å lamps and the ^{1}H NMR spectra (16 scans) were collected after 0, 2, 4, 6, 8, and 10 min of photolysis at 300 nm. The depletion of diethyl 2-(4-hydroxy-3-methoxyphenyl)-2-oxoethyl phosphate (**1.200a**) and the appearance of released 4-hydroxy-2-methoxyphenylacetic acid were determined by the integration of the NMR signals at δ 5.07-5.09 ppm and 3.44 ppm, respectively. The photolysis sample was spiked with authentic samples of 4-hydroxy-2-methoxy-phenylacetic acid and diethyl phosphoric acid. The intensity of the methylene peak at 3.44 ppm (4-hydroxy-2-methoxyphenylacetic acid) and at 3.90-3.94 ppm (diethyl phosphoric acid) increased dramatically with the addition of the known acids. In addition, intensities of peaks of 4-hydroxy-2-methoxy-phenylacetic acid within the aromatic region (6.93-6.95, 6.41 and 6.32-6.35 ppm) increased. These observations confirmed the formation of 4-hydroxy-2-methoxy-phenylacetic acid and diethyl phosphoric acid by photolysis.

UV/vis study of diethyl 2-(4-hydroxy-3-methoxyphenyl)-2-oxoethyl phosphate (1.200a)

A 10 mL volumertric flask was charged with 2-(4-hydroxy-3-methoxyphenyl)-2-oxoethyl phosphate (**1.200a**, 10.0 mg, 0.031 mmol) dissolved in CH_3CN (5.0 mL) and H_2O (5.0 mL). The pH was adjusted by changing the pH of the H_2O portion (5.0 mL) before mixing with CH_3CN (5.0 mL). A buffer solution of sodium acetate/acetic acid in water was used to obtain

the pH value of 4. A buffer solution of tris(hydroxylmethyl)aminomethane /hydrochloric acid in water was used to achieve the pH 7 and 9 values, respectively. UV/vis scans were performed under ambient conditions with suitable dilutions at each pH value. The results are shown in Table 1.17.

Photolysis of diethyl 2-(4-hydroxy-3-methoxyphenyl)-2-oxoethyl phosphate: Quantum yield determination by RP-HPLC

A biphenyl stock solution was prepared by dissolving biphenyl (160 mg, 1.04 mmol) in HPLC grade CH_3CN (90 mL) in a 100 mL volumetric flask and diluted to the mark with HPLC-grade H_2O (10 mL). A quartz tube was charged with diethyl 2-(4-hydroxy-3-methoxyphenyl)-2-oxoethyl phosphate (**1.200a**, 10 mg, 0.031 mmol) dissolved in HPLC-grade CH_3CN (1.0 mL) and H_2O (1.0 mL). Biphenyl (2.0 mL from the stock solution, 3.2 mg, 0.021 mmol) was added to the quartz tube as an internal standard, and the contents were mixed thoroughly. The sample was irradiated at 300 nm with 2-3000 Å lamps, and sample aliquots (100 μL) were collected after 0, 2, 4, 6, and 8 min of photolysis. Each aliquot was diluted with 950 μL of HPLC-grade CH_3CN:H_2O (1:1) and analyzed by RP-HPLC. A calibration curve was made for diethyl 2-(4-hydroxy-3-methoxyphenyl)-2-oxoethyl phosphate (**1.200a**) under the same reaction conditions. The correction factor (R) for the compound was calculated. A scatter plot was created by using the number of mmol of 2-(4-hydroxy-3-methoxyphenyl)-2-oxoethyl phosphate vs. irradiation time. The slope (*m*) of the best fit line from the linear regression analysis was determined for each series. The light output (*L*) of the 2-3000 Å lamps in the photoreactor was determined separately using the potassium ferrioxalate method[181] in units of millieinsteins per min. The quantum yield (Φ)

for the disappearance of diethyl 2-(4-hydroxy-3-methoxyphenyl)-2-oxoethyl phosphate (**1.200a**) was then calculated using following equation:

$$\Phi = |m| / L$$

where *m* is the slope of the plot (mmol/min) and L is the light output from the lamps (miliEinstein/min) which were used for both the reaction and the actinometry. The same procedure was repeated three times. The results are given in Table 1.18.

Photolysis of *diethyl* 2-(4-hydroxy-3,5-dimethoxyphenyl)-2-oxoethyl phosphate (1.200b): Quantum yield determination by RP-UPLC

The same procedure was repeated as above.

Photolysis of diethyl 2-(4-hydroxy-2-methoxyphenyl)-2-oxoethyl phosphate (1.215a): Quantum yield determination by RP-UPLC

The same procedure was repeated as for diethyl 2-(4-hydroxy-3-methoxyphenyl)-2-oxoethyl phosphate (**1.200a**).

Photolysis of diethyl 2-(4-hydroxy-2,6-dimethoxyphenyl)-2-oxoethyl phosphate (1.215b): Quantum yield determination by ^{1}H-NMR

A Pyrex NMR tube was charged with diethyl 2-(4-hydroxy-2,6-dimethoxyphenyl)-2-oxoethyl phosphate (**1.215b**, 2 mg, 0.0057 mmol) and dissolved in CD_3CN (250 μL) and D_2O (250 μL). DMF (0.50 μL) was added as an internal standard. The contents were mixed thoroughly. The resulting sample was photolyzed without degassing at 300 nm with 2-3000 Å lamps, and the ^{1}H NMR spectra (24 scans, 64 scans, and 124 scans) were collected after 0, 20, 60, and 120 s. The depletion of diethyl 2-(4-hydroxy-2,6-dimethoxyphenyl)-2-oxoethyl phosphate (**1.215b**) was determined by integration of the 1H NMR signals at δ 5.12 ppm compared to the DMF peaks which gave the disappearance of starting material. Scatter plots were created by plotting the number of mmol of 2-(4-hydroxy-2,6-dimethoxyphenyl)-2-

oxoethyl phosphate (**1.215b**) vs. irradiation time for each scan. The slope (*m*) of the best fit line from the linear regression analysis was determined for each series. The light output (*L*) of the 2-3000 Å lamps in the photoreactor was determined separately using the potassium ferrioxalate method[181] in units of millieinsteins per min. The quantum yield (Φ) for the disappearance of diethyl 2-(4-hydroxy-2,6-dimethoxyphenyl)-2-oxoethyl phosphate (**1.215b**) was then calculated using followi

$$\Phi = |m| / L$$

Where *m* is the slope of the plot and L is the light output from bulbs which were used in the actinometry. The results are shown in Table 1.18.

Photolysis of diethyl 2-(3-acetyl-4-hydroxyphenyl)-2-oxoethyl diethyl phosphate (1.200c): photoproduct analysis by ^{1}H NMR

A Pyrex NMR tube was charged with 2-(3-acetyl-4-hydroxyphenyl)-2-oxoethyl diethyl phosphate (**1.200c**, 5 mg, 0.015 mmol) and dissolved in CD_3CN (500 μL) and D_2O (500 μL). DMF (2.0 μL) was added as an internal standard and the contents mixed thoroughly. The resulting sample was photolyzed without degassing at 300 nm with 8-3000 Å lamps and the ^{1}H NMR spectra (16 scans) collected after 0, 10, 20, 30, and 40 min. The depletion of 2-(3-acetyl-4-hydroxyphenyl)-2-oxoethyl diethyl phosphate (**1.200c**) and the appearance of released 3-acetyl-4-hydroxy-phenylacetic acid were from the ^{1}H NMR signal integrations at δ 5.33-5.36 ppm and 3.60 ppm, respectively. The photolysis sample was spiked with authentic samples of 3-acetyl-4-hydroxy-phenylacetic acid and diethyl phosphoric acid. The intensity of the methylene peak at 3.60 ppm (3-acetyl-4-hydroxy-phenylacetic acid) and at 3.85-3.92 ppm (diethyl phosphoric acid) increased dramatically. In addition, intensities of peaks for 3-acetyl-4-hydroxy-phenylacetic acid within the aromatic region (7.77, 7.41-7.44

and 6.90-6.92 ppm) increased. These observations confirmed the formation of 3-acetyl-4-hydroxyphenylacetic acid and diethyl phosphoric acid from the photolysis.

Photolysis of 2-(3-acetyl-4-hydroxyphenyl)-2-oxoethyl diethyl phosphate (1.200c): Quantum yield determination by RP-HPLC.

The same procedure was repeated as in diethyl 2-(4-hydroxy-3-methoxyphenyl)-2-oxoethyl phosphate (**1.200a**).

Photolysis of 4-(2-diazoacetyl)-2-methoxyphenyl acetate (1.198a): photoproduct analysis by ^{1}H- NMR

A pyrex NMR tube was charged with 4-(2-diazoacetyl)-2-methoxyphenyl acetate (**1.198a**, 8 mg, 0.034 mmol) and dissolved in CD_3CN (500 μL) and D_2O (500 μL). The contents were mixed thoroughly. The resulting sample mixture was photolyzed without degassing at 300 nm with 2-3000 Å lamps and ^{1}H NMR spectra (16 scans) were collected after 10 min of photolysis. Bubbles evolved while the sample was being irradiated due most likely to nitrogen evolution. The depletion of 4-(2-diazoacetyl)-2-methoxyphenyl acetate and the appearance of released 4-acetoxy-3-methoxy-phenyl acetic acid were characterized by the NMR signals at δ 6.23 and 3.49 ppm, respectively. The photolysis sample was spiked with an authentic sample of 4-acetoxy-3-methoxy-yphenyl acetic acid. The intensity of the methylene peak at 3.49 ppm increased dramatically. This observation confirmed the formation of 4-acetoxy-3-methoxy-yphenyl acetic acid as the major product from the photolysis.

Photolysis of 4-(2-diazoacetyl)-3-methoxyphenyl acetate (1.204): photoproduct analysis by ^{1}H- NMR

A Pyrex NMR tube was charged with 4-(2-diazoacetyl)-3-methoxyphenyl acetate (**1.204**, 20 mg, 0.085 mmol) and dissolved in CD_3CN (500 μL) and D_2O (500 μL). The contents were mixed thoroughly. The resulting sample was photolyzed without degassing at 300 nm with 2-3000 Å and ^{1}H NMR spectra (16 scans) were collected after 10 min. Bubbles evolved during the irradiation due to nitrogen evolution. The depletion of 4-(2-diazoacetyl)-3-methoxyphenyl acetate (**1.204**) and the appearance of released 4-acetoxy-3-methoxy-phenyl acetic acid were characterized from the NMR signals at δ 6.50 and 3.52 ppm, respectively. The photolysis sample was spiked with an authentic sample of 4-acetoxy-2-methoxyphenyl acetic acid. The intensity of the methylene peak at 3.52 ppm increased dramatically upon the irradiation. This observation confirmed the formation of 4-acetoxy-2-methoxyphenyl acetic acid as the major product from the photolysis. However, because of neighboring group (*o*-OMe) participation, another major photoproduct, 6-acetoxy-3-coumaranone, was formed. The methylene peak of this compound came under the D_2O peak and could not be integrated in ^{1}H-NMR spectrum. The aromatic region showed the formation of 6-acetoxy-3-coumaranone which was confirmed by spiking with an authentic sample. The authentic sample, 6-acetoxy-3-coumaranone, was separately synthesized by acetylation of 6-hydroxy-3-coumaranone to confirm the formation of the 6-acetoxy-3-coumaranone (see the Experimental; synthesis of **1.222**).

Photolysis of 4-(2-diazoacetyl)-3-methoxyphenyl acetate (1.204): photoproduct analysis by column chromatography.

A quartz tube was charged with 4-(2-diazoacetyl)-3-methoxyphenyl acetate (**1.204**, 150 mg, 0.64 mmol) and dissolved in CH_3CN (2 mL) and H_2O (2.0 mL). The contents were mixed thoroughly before the photolysis. The resulting sample was photolyzed without degassing at 300 nm with 8-3000 Å lamps to 85% completion as determined by RP-HPLC. Two major products were observed by RP-HPLC and TLC (hexane/EtOAc, 1:1) analysis. The photolysis was stopped and the sample solution was concentrated to give a yellow residue that was chromatographed on silica gel (neutralized with triethylamine) with a gradient solvent system (EtOAc:hexane (1:2), EtOAc:hexane (1:1), EtOAc:hexane (2:1)). The cyclized product, 6-acetoxy-3-coumaranone, was obtained as a white crystalline solid (mp 122-124 °C). The rearranged product, 4-acetoxy-3-methoxyphenyl acetic acid, was generated as a dark yellow solid: mp. 94-104 °C (dec.). The structures of these two compounds were characterized by comparison with authentic compounds using ^{1}H NMR and MS data.

References:

1. Hanson, J. R. *Protecting Groups in Organic Synthesis*, Sheffield Academic Press, Sheffield, **1999**.
2. Corey, E. J.; Cheng, X. –M, *The Logic of Chemical Synthesis*; John Wiley and Sons: New York, **1995**.
3. Sheehan, J. C.; Umezawa, K. *J. Org. Chem*, **1973**, *38*, 3771-3774.
4. Givens, R. S.; Conard, P. G., II; Yosef, A. L.; Lee, J, -I. In *CRC Handbook of* Organic Photochemistry and Photobiology; 2nd Ed.; CRC press, New York, **2004**.
5. Givens, R. S.; Lee,J. -I.; Kotala, M. Mechanistic overview of phototriggers and cage release, In *Dynamic Studies in Biology: Phototriggers, Photoswitches, and caged Biomolecules*; Wiley-VCH: Weinheim, **2005**, Ch. 2, pp. 95-129.
6. Greene's Protective Groups in Organic Synthesis, 4th ed.; Wutts, P. G. M., Greene, T. W., Eds.; Wiley Interscience-John Wiley and Sons: New York, **2007**.
7. Pelliccioli, A. P.; Wirz, J. Photochem. Photobiol. Sci. **2002**, *1*, 441-458.
8. Ni, J.; Auston, D. A.; Frelich, D. A.; Muralidharan, S.; Sobie, E. A.; Kao, J. P. Y. *J. Am. Chem. Soc*. **2007**, *129*, 5316-5317.
9. Adams, S. R.; Tsien, R. Y.; *Annu. Rev. Physiol*. **2000**, *18*, 755-784.
10. Barltrop, J. A.; Schofield, P.; Tetrahedron Lett. **1962**, *16*, 697-699.
11. Kaplan, J. H.; Forbush, B., III; Hoffman, J. F.; *Biochemistry*, **1978**, *17*, 1929-1935.
12. Givens, R. S.; Weber, J. F. W.; Jung, A. H.; Park, C. –H. New Photoprotecting Groups: Desyl and p-Hydroxyphenacyl Phosphate and carboxylate Esters. *Methods Enzymol*; Academic Press, **1998**; pp 1-29.
13. Baldwin, J. E.; McConnaughie, A. W.; Moloney, M. G.; Pratt, A. J.; Shim, S. B. *Tetrahedron,* **1990**, *46*, 6879-6884.
14. Wang, B.; Zheng, A. *Chem. Pharm. Bull*. **1997**, *45*, 715-718.
15. Koenigs, P. M.; Faust, B. C.; Porter, N. A. *J. Am. Chem. Soc*. **1993**, *115*, 9371-9379.
16. Lester, H. A.; Nerbonne, J. M. *Ann. Rev. Biophys. Bioeng*. **1982**, *11*, 151-175.
17. Barltrop, J. A.; Plant, P. J.; Schofield, P. *J. Chem. Soc., Chem. Comm*. **1966**, 822-823.
18. Ried, V. W.; Wilk, M.; *Justus Liebigs Ann. Chem*. **1954**, *590*, 91-110.
19. Walker, J. W.; Reid, J. P.; McCray, J. A.; Trentham, D. R. *J. Am. Chem. Soc*. *110*, 7170-7177.
20. Parkesh, R.; Vasudevan, S. R.; Berry, A.; Galione, A.; Dowden, J.; Churchill, G. C. *Org. Biomol. Chem*. **2007**, *5*, 441-443.
21. Cohen, B. E.; Stoddard, B. L.; Koshland, D. E., Jr. *Biochemistry*, **1997**, *36*, 9035-9044.
22. Lee, H. C.; Aarhus, R.; Gee, K. R.; Kestner, T. *J. Biol. Chem*. **1997**, *272*, 4172-4178.
23. Franchetti, P.; Cappellacci, L.; Pasqualini, M.; Grifantini, M.; Lorenzi, T.; Raffaelli, N.; Magni, G. *Nucleos. Nucleot. Nucl*. **2003**, *22*, 865-868.
24. Lee, H. C.; Aarhus, R. *J. Biol. Chem*. **1995**, *270*, 2152-2157.
25. Wlcox, M.; Viola, R. W.; Johnson, K. W.; Billington, A. P.; Carpenter, B. K.; McCray, J. A.; Guzikowski, A. P.; Hess, G. P. *J. Org. Chem*. **1990**, *55*, 1585-1589.

26. Il'ichev, Y. V.; Schworer, M.; Wirz, J. *J. Am. Chem. Soc*. **2004**, *126*, 4581-4595.
27. Helrung, B.; Kamdzhilov, Y.; Schworer, M.; Wirz, J. *J. Am. Chem. Soc*. **2005**, *127*, 8934-8935.
28. Zimmerman, H. E.; Sandel, V. R. *J. Am. Chem. Soc*. **1963**, *85*, 915-922.
29. Zimmerman, H. E. *J. Phys. Chem. A* **1998**, *102*, 7725.
30. Zimmerman, H. E. *J. Phys. Chem. A* **1998**, *102*, 5616-5621.
31. DeCosta, D. P.; Pincock, J. A. *J. Am. Chem. Soc*. **1993**, *115*, 2180-2190.
32. Pincock, J. A. *Accounts Chem. Res*. **1997**, *30*, 43-49.
33. Givens, R. S.; Matuszewski, B. *J. Am. Chem. Soc*. **1984**, *106*, 6860-6861.
34. Suzuki, A. Z.; Watanabe, T.; Kawamoto, M.; Nishiyama, K.; Yamashita, H.; Ishii, M.; Iwamura, M.; Furuta, T. *Org. Lett*. **2003**, *5*, 4867-4870.
35. Lu, M.; Fedoryak, O. D.; Moister, B. R.; Dore, T. M. *Org. Lett*. **2003**, *5*, 2119-2122.
36. Furuta, T.; Takeuchi, H.; Isozaki, M.; Takahashi, Y.; Kanehara, M.; Sugimoto, M.; Watanabe, T.; Noguchi, K.; Dore, T. M.; Kurahashi, T.; Iwamura, M.; Tsien, R. Y. *Chem. Bio. Chem* **2004**, *5*, 1119-1128.
37. Lin, W.; Lawrence, D. S. *J. Org. Chem*. **2002**, *67*, 2723-2726.
38. Dore, T. M. In *Dynamic studies in Biology: Phototriggers, photoswitches and caged Biomolecules*: Givens, R. S. Goeldner, M., Eds.; Wiley-VCH: Weinheim, Germany, **2005**.
39. Furuta, T.; Wang, S. S. H.; Dantzker, J. L.; Dore, T. M.; Bybee, W. J.; Callaway, E. M.; Denk, W.; Tsien, R. Y. *Proc. Natl. Acad. Sci*. U.S.A. **1999**, *96*, 1193-1200.
40. Ando, H.; Furuta, T.; Tsien, R. Y.; Okamoto, H. *Nat. Genet*. **2001**, *28*, 317-325.
41. Hagen, V.; Bendig, J.; Frings, S.; Eckardt, T.; Helm, S. *Angewandte Chemie Int. Ed. Engl.* **2001**, *40*, 1046-1048.
42. Sheehan, J. C.; Wilson, R. M. *J. Am. Chem. Soc*. **1964**, *86*, 5277-5281.
43. Sheehan, J. C.; Wilson, R. M. Oxford, A. W. *J. Am. Chem. Soc*. **1971**, *93*, 7222-7228.
44. Givens, R. S.; Athey, P. S.; Kueper, L. W., III; Matuszewski, B.; Xue, J, -Y. *J. Am. Chem. Soc.* **1992**, *114*, 8708-8710.
45. Givens, R. S.; Athey, P. S.; Matuszewski, B.; Kueper, L. W., III; Xue, J, -Y. J. Am. Chem. Soc. **1993**, *115*, 6001-6012.
46. Rajesh, C. S.; Givens, R. S.; Wirz, J. *J. Am. Chem. Soc*. **2000**, *122*, 611-618.
47. Corrie, J. E. T.; Trentham, D. R. *J. Chem. Soc., Perkin Trans. 1* **1992**, 2409-2417.
48. Epstein, W, W.; Garrossian, M. *J. Chem. Soc., Chem. Commun*. **1987**, *8*, 532-533.
49. Dhavale, D. D.; Mali, V. P.; Sudrik, S. G.; Sonawane, H. R. *Tetrahedron*, **1997**, *53*, 16789-16794.
50. Anderson, J. C.; Reese, C. B. *Tetrahedron Lett*. **1962**, *1*, 1-4.
51. Givens, R. S.; Park, C. –H, *Tetrahedron Lett*. **1996**, *35*, 6259-6266.
52. Park, C. –H.; Givens, R. S. *J. Am. Chem. Soc*. **1997**, *119*, 2453-2463.
53. Givens, R. S.; Jung, A.; Park, C. –H, Weber, J.; Bartlett, W. *J. Am. Chem. Soc*. **1997**, *119*, 8369-8370.
54. Givens, R. S.; Weber, J. F. W.; Conard, P. G., II; Orosz, G.; Donahue, S. L. *J. Am. Chem. Soc*. **2000**, *122*, 2687-2697.
55. Givens, R. S.; Lee, J. –I. *Journal of Photoscience* **2003**, *10*, 37-48.

56. Conrad, P. G., II; Givens, R. S.; Hellrung, B.; Rajesh, C. S.; Ramseir, M. *J. Am. Chem. Soc.* **2000**, *122*, 9346-9347.
57. Ma, C.; Zuo, P.; Kwok, W. M.; Chan, W. S.; Kan, J. T. Z.; Toy, P. H.; Phillips, D. L. *J. Org. Chem*. **2004**, *69*, 6641-6657.
58. Ma, C.; Kwok, W. M.; Chan, W. S.; Zuo, P.; Kan, J. T. W.; Toy, P. H.; Phillips, D. L. *J. Am. Chem. Soc*. **2005**, *127*, 1463-1472.
59. Chan, W. S.; Kwok, W. M.; Phillips, D. L. *J. Phys. Chem. A* **2005**, *109*, 3454-3469.
60. Ma, C.; Kwok, W. M.; Chan, W. S.; Du, Y.; Kan, J. T. W.; Phillips, D. L. *J. Am. Chem. Soc*. **2006**, *128*, 2558-2570.
61. Zuo, P.; Ma, C.; Kwok, W. M.; Chan, W.; Phillips, D. L. *J. Org. Chem*. **2005**, *70*, 8661-8675.
62. Chen, X. B; Ma, C.; Kwok, W. M.; Guan, X.; Du, Y.; Phillips, D. L. *J. Phys. Chem. A* **2006**, *110*, 12406-12413.
63. Hagen, V.; Bendig, J.; Frings, S.; Eckardt, T.; Helm, S.; Reuter, D.; Kaupp, U. B. *J. Am. Chem. Soc*. **1997**, *119*, 4149-4159.
64. Zhang, K.; Corrie, J. E. T.; Munasinghe, V. R. N.; Wan, P.; J. Am. Chem. Soc. **1999**, *121*, 5625-5632.
65. Conrad, P. G., II; Givens, R. S.; Weber, J. F. W.; Kandler, K. *Org. Lett*. **2000**, *2*, 1545-1547.
66. Givens, R. S.; Heger, D.; Hellrung, B.; Kamdzhilov, Y.; Mac, M.; Conrad, P. G.; Cope, E.; Lee, J. –I.; Mata-Segreda, J. F.; Schowen, R. L.; Wirtz, J. *J. Am. Chem. Soc.* **2008**, *130*, 3307-3309.
67. Turro, N. J.; Hammond, W. B. *J. Am. Chem. Soc*. **1966**, *88*, 3672-3673.
68. Turro, N. J. *Accounts Chem. Res*. **1969**, *2*, 25-32.
69. Stensrud, K. F.; Heger, D.; Sebej, P.; Wirz, J.; Givens, R. S. *Photochem. Photobiol. Sci*. **2008**, *7*, 614-624.
70. Stensrud, K.; Noh, J.; Kandler, K.; Wirz, J.; Heger, D.; Givens, R. S. *J. Org. Chem.* **2009**, *74*, 5219-5227.
71. Bochet, C. G.; *J. Chem. Soc., Perking Trans. 1* **2002**, 441-458.
72. Hsien-Ming, L.; Larson, D. R.; Lawrence, D. S. *ACS Chem. Biol*. **2009**, *4*, 409-427.
73. Curtius, T. *Ber.* **1883**, *16*, 2230-2231.
74. Doyle, M. P.; McKervey, M. A.; Ye, T. *Modern Catalytic Methods for Organic* Synthesis with Diazo Compounds; **1998**, Wiley; New York; pp 433-486.
75. Wolff, L. *Justus Liebigs Ann. Chem*. **1902**, *325*, 129-195.
76. Wolff, L.; Hall, A. H. *Ber. Dtsh. Chem. Ges*. **1903**, *36*, 3612-3618.
77. Wolff, L. *Justus Liebigs Ann. Chem*. **1904**, *333*, 1-21.
78. Staudinger, H. *Ber. Dtsh. Chem. Ges*. **1905**, *38*, 1735-1739.
79. Schröter, G. *Ber. Dtsh. Chem. Ges*. **1909**, *42*, 2336-2349.
80. Wolff, L. *Ber. Dtsh. Chem. Ges*. **1912**, *394*, 23-59.
81. Arndt, F.; Eistert, B.; Partale, W. *Ber*. **1927**, *60B*, 1364-1370.
82. Arndt, F.; Eistert, B.; Amende, J. *Ber*. **1928**, *61B*, 1949-1953.
83. Bradley, W.; Robinson, R. *J. Chem. Soc*. **1928**, 1310-1318.
84. Süs, O. *Justus Liebigs Ann. Chem*. **1944**, *556*, 65-84.
85. Süs, O. *Justus Liebigs Ann. Chem*. **1944**, *556*, 85-90.

86. Horner, L. ; Spietschka, E. ; Gross, A. W. *Justus Liebigs Ann. Chem*. **1951**, *573*, 17-30.
87. Kirmse, W.; Horner, L. *Chem. Ber*. **1956**, *89*, 2759-2765.
88. Noels, A. F.; Demonceau, A.; Petiniot, N.; Hubert, A. J.; Teyssie, P. *Tetrahedron*, **1982**, *38*, 2733-2739.
89. Polozov, A. M.; Polezhaeva, N. A.; Mustaphin, A, H.; Khotinen, A. V.; Arbuzov, B. A. *Synthesis*, **1990**, 515-517.
90. Tan, Z.; Qu, Z.; Chen, B.; Wang, J. *Tetrahedron*, **2000**, *56*, 7457-7461.
91. Shinada, T.; Kawakami, T, Sakai, H.; Takada, I.; Ohfune, Y. *Tetrahedron Lett*. **1998**, *39*, 3757-3760.
92. Newman, M. S.; Beal, P. F. *J. Am. Chem. Soc*. **1950**, *72*, 5161-5163.
93. Mander, L. N.; Beames, D. *J. Aust. Chem*., **1974**, *27*, 1257-1268.
94. Corrie, J. E. T.; Reid, G. P.; Trentham, D. R.; Mazid, M. A.; Hursthouse, M. B. *J. Chem. Soc., Perkin Trans 1* **1992**, 1015-1019.
95. Hoard, D. E.; Ott, D. G. *J. Am. Chem. Soc*. **1965**, *87*, 1785-1788.
96. Coulson, A. B. W.; Knowles, J. R. *J. Chem. Soc., Chem. Commun*. **1970**, 7
97. Motiu-DeGrood, R.; Hunt, W.; Wilde, J.; Hupe, D. J. *J. Am. Chem. Soc*. **1978**, *101*, 2182-2190.
98. Gefflaut, T.; Périé, J. *Syn. Commun*. **1994**, *24*, 29-33.
99. Kirmse, W. *Eur. J. Org. Chem*. **2002**, 2193-2256.
100. Toscano, J. In *Review of reactive intermediate chemistry*; Platz, M. S., Moss, R. A., Jones, M., Eds.; Wiley-Interscience; **2007**.
101. Wang, J.; Burdzinski, G.; Kubicki, J.; Platz, M. S. *J. Am. Chem. Soc*. **2008**, *130*, 11195-11209.
102. Popik, V. V. *Can. J. Chem*. **2005**, *83*, 1382-1390.
103. Ye, T.; McKervey, M. A. *Chem. Rev*. **1994**, *94*, 1091-1160.
104. Tidwell, T. T.; *Ketenes*, Wiley, New York, **1995**, pp. 77-100.
105. Meier, H.; Zeller, K. –P. *Angew. Chem. Internat. Edit*. **1975**, *14*, 32-43.
106. Kaplan, F.; Meloy, G. K. Tetrahedron Lett. **1964**, 2427-2430.
107. Kaplan, F.; Meloy, G. K. *J. Am. Chem. Soc*. **1966**, *88*, 950-956.
108. Paliani, G.; Sorriso, S.; Cataliotti, R. *J. Chem. Soc., Perkin Trans. 2* **1976**, 707-710.
109. Sorriso, S.; Piazza, G.; Foffani, A. *J. Chem. Soc. B* **1971**, 805-809.
110. Aliev, Z. G.; Atovmyan, L. O.; Kartsev, V. G. *Bull. Acad. Sci. USSR Div. Chem. Sci*. **1985**, *34*, 1866-1868.
111. Werstiuk, N. H.; Muchall, H. M.; Ma, J.; Liu, M. T. H. *Can. J. Chem*. **1998**, *76*, 1162-1173.
112. Muchall, N. H.; Pitters, M. S.; Workentin, M. S. *Tetrahedron*, **1999**, *55*, 3767-3778.
113. Celius, T. C.; Wang, Y.; Toscano, J. P. In *CRC Handbook of Organic Photochemistry and Photobiology*; 2nd Ed.; Ch. 90, CRC press, New York, **2004**.
114. Tidwell, T. T. *Ketenes*, Wiley, New York, **1995**.
115. Torres, M.; Lown, E. M.; Gunning, H. E.; Strausz, O. P. *Pure Appl. Chem*. **1980**, *52*, 1623-1643.
116. Lewars, E. G. *Chem. Rev*. **1983**, *83*, 519-534.
117. Frater, G.; Strausz, O. P. *J. Am. Chem. Soc*. **1970**, *92*, 6654-6656.
118. Zeller, K. P.; Meier, H. *Angew. Chem. Int. Ed. Engl*. **1977**, *16*, 835-851.

119. Tomioka, H.; Okuno, H.; Kondo, S.; Izawa, Y. *J. Am. Chem. Soc*. **1980**, *102*, 7123-7125.
120. Bachmann, C.; N'Guessan, T. Y.; Debu, F.; Monnier, M.; Pourcin, J.; Aycard, J. P. ; Bodot, H. *J. Am. Chem. Soc*. **1990**, *112*, 7488-7497.
121. Wang, J.; Burdzinski, G.; Kubicki, J.; Gustafson, T. L.; Platz, M. S. *J. Am. Chem. Soc*. **2008**, *130*, 5418-5419.
122. Jones, M., Jr. Ando, W. *J. Am. Chem. Soc*. **1968**, *90*, 2200-2201.
123. Tomioka, H.; Kitagawa, H.; Izawa, Y. *J. Org. Chem*. **1979**, *44*, 3072-3075.
124. Tomioka, H, Okuno, H.; Izawa, Y. *J. Org. Chem*. **1980**, *45*, 5278-5283.
125. Hutton, R. S.; Roth, H. D. *J. Am. Chem. Soc*. **1978**, *100*, 4324-4325.
126. Burdzinski, G.; Platz, M. S. *J. Phys. Org. Chem*. **2010**, Early View.
127. Burdzinski, G.; Wang, J.; Gustafson, T. L.; Platz, M. S. *J. Am. Chem. Soc*. **2008**, *130*, 3746-3747.
128. Likhtvorik, I. R.; Zhu, Z.; Tae, E. L.; Tippman, E.; Hill, B. T.; Platz, M. S. *J. Am.* Chem. Soc. **2001**, 123, 6061-6068.
129. Wang, J.; Kubicki, J.; Peng, H.; Platz, M. S. *J. Am. Chem. Soc.* **2008**, *130*, 6604-6609.
130. Zhang, Y.; Kubicki, J.; Wang, J.; Platz, M. S. *J. Phys. Chem. A* **2008**, *112*, 11093-11098.
131. Scott, A. P.; Platz, M. S.; Radom, L. *J. Am. Chem. Soc*. **2001**, *123*, 6069-6076.
132. Wagner, B. D.; Arnold, B. R.; Brown, G. S.; Lusztyk, J. *J. Am. Chem. Soc*. **1998**, *120*, 1827-1834.
133. Barra, M.; Fisher, T. A.; Cernigliaro, G. J.; Sinta, R.; Scaiano, J. C. *J. Am. Chem. Soc*. **1992**, *114*, 2630-2634.
134. Wang, J. –L.; Toscano, J. P.; Platz, M. S.; Nikolaev, V.; Popic, V. *J. Am. Chem. Soc.* **1995**, *117*, 5477-5483.
135. Visser, P.; Zuhse, R.; Wong, M. W.; Wentrup, C. *J. Am. Chem. Soc*. **1996**, *118*, 12598-12602.
136. Qiao, G. G.; Andraos, J.; Wentrup, C. *J. Am. Chem. Soc*. **1996**, *118*, 5634-5638.
137. Rodler, M.; Blom, C. E.; Bauder, A. *J. Am. Chem. Soc*. **1984**, *106*, 4029-4035.
138. Schaumann, E.; Sieveking, S.; Walter, W. *Chem. Ber*. **1974**, *107*, 3589-3601.
139. Andraos, J.; Kresge, A. J. *J. Am. Chem. Soc*. **1992**, *114*, 5643-5646.
140. Andraos, J.; Chiang, Y.; Huang, C. –G.; Kresge, A. J.; Scaiano, J. C. *J. Am. Chem. Soc*. **1993**, *115*, 10605-10610.
141. McClelland, R. A.; Kanagasabapathy, V. M.; Banait, N. S.; Steenken, S. *J. Am. Chem.* Soc. **1992**, *114*, 1816-1823.
142. March, J. Advanced Organic Chemistry: Reactions, Mechanisms and Structure, 4th ed., Wiley-Interscience, New York, **1992**.
143. Pitters, J. L.; Griffiths, K.; Kovar, M.; Norton, P. R.; Workentin, M. S. *Angew. Chem. Int. Ed. Engl*. **2000**, *39*, 2144-2147.
144. Reiser, A. *Photoreactive polymers: The Science and Technology of Resists*, Wiley, New York, **1989**.
145. Purchased from Sigma-Aldrich, St Louis, MO, USA.
146. Sci Finder Scholar, **2009**.

147. Happer, D. A. R.; Hayman, C. M.; Storer, M. K.; Lever, M. *Aust. J. Chem*. **2004**, *57*, 467-472.
148. Smith, A. B., III. *Tetrahedron*, **1981**, *37*, 2407-2439.
149. Eckardt, T.; Hagen, V.; Schade, B.; Schmidt, R.; Schweitzer, C.; Bendig, J. *J. Org. Chem.* **2002**, *67*, 703-710.
150. Hagen, V.; Dekowski, B.; Nache, V.; Schmidt, R.; Geibler, D.; Lorenz, D.; Eichhorst, J.;Keller, S.; Kaneko, H.; Benndorf, K.; Wiesner, B. *Angew. Chem. Int. Ed*. **2005**, *44*, 7887-7891.
151. March, J. *Advanced Organic Chemistry*; Wiley: 4th ed.: New York: **1992**.
152. Mazzucato, U.; Cauzzo, G.; Foffani, A. *Tetrahedron Lett*. **1963**, *23*, 1525-1529.
153. Andreu, G. L.; Delgado, R.; Velho, J. A.; Curti, C.; Vercesi, A. E. *Arch. Biochem. Biophys*. **2005**, *439*, 184-193.
154. Murov, S. L., Carmichael, I., Hug, G. L. *Handbook of Photochemistry*; Marcel Dekker Inc.: New York, **1993**.
155. Turro, N. J. *Modern Molecular Photochemistry*; Benjamin/Cummings Publishing Co., Inc.: Menlo Park, **1978**.
156. Pastor-Pérez, L, Wiebe, C.; Pérez-Prietto, J.; Stiriba, S. –E. *J. Org. Chem*. **2007**, *72*, 1541-1544.
157. Scaiano, J. C. *J. Am. Chem. Soc*. **1980**, *102*, 7747-7753.
158. Herkstroeter, W. G.; Lamola, A. A.; Hammond, G. S. *J. Am. Chem. Soc*. **1964**, *86*, 4537-4540.
159. Calvert, J. G.; Pitts, J. N. *Photochemistry*; Wiley: New York, **1966**.
160. Gut, I. G.; Wood, P. D.; Redmond, R. W. *J. Am. Chem. Soc*. **1996**, *118*, 2366-2373.
161. Klan, P.; Wirz, J. *Photochemistry of Organic Compounds From Concepts to* Practice; Wiley, **2009**.
162. Candeias, N. R. ; Afonso, C. A. M. *Curr. Org. Chem*. **2009**, *13*, 763-787.
163. Toscano, J. P.; Evans, A. unpublished results
164. Srivastava, S.; Toscano, J. P. *J. Am. Chem. Soc*. **1997**, *119*, 11552-11553.
165. Wang, Y.; Yuzawa, T.; Hamaguchi, H.; Toscano, J. P. *J. Am. Chem. Soc*. **1999**, *121*, 2875-2882.
166. Iwata, K.; Hamaguchi, H., *Appl. Spectrosc*. **1990**, *44*, 1431-1437.
167. Yuzawa, T.; Kato, C.; George, M. W.; Hamaguchi, H. *Appl. Spectrosc*. **1994**, *48*, 684-690.
168. Allen, A. D.; Colomvakos, J. D.; Diederich, F.; Eagle, I.; Hao, X.; Liu, R.; Lusztyk, J.; Ma, J.; McAllister, M. A.; Rubin, Y.; Sung, K.; Tidwell, T. T.; Wagner, B. D. *J. Am. Chem. Soc*. **1997**, *119*, 12125-12130.
169. Camara de Lucas, N.; Netto-Ferreira, J. C.; Andraos, J.; Lusztyk, J.; Wagner, B. D.; Scaiano, J. C. *Tetrahedron Lett*. **1997**, *38*, 5147-5150.
170. Wagner, B. D.; Zgierski, M. Z.; Lusztyk, J. *J. Am. Chem. Soc*. **1994**, *116*, 6433-6434.
171. Chiang, Y.; Fedorov, A. V.; Kresge, A. J.; Onyido, I. Tidwell, T. T. *J. Am. Chem. Soc*. **2004**, *126*, 9382-9386.
172. Périé, J.; Gefflaut, T. *Synth. commun*. **1994**, *24*, 29-33.
173. Ma, C.; Chan, W. S.; Kwok, W. M.; Zuo, P.; Phillips, D. L. *J. Phys. Chem. B*, **2004**, *108*, 9264-9276 and references therein

174. Tomioka, H.; Okuno, H.; Kondo, S.; Izawa, Y. *J. Am. Chem. Soc*. **1980**, *102*, 7123-7125.
175. Adams, R.; Binder, L. O. *J. Am. Chem. Soc*. **1941**, *63*, 2773-2776.
176. Darvesh, S.; McDonald, R. S.; Darvesh, K. V.; Mataija, D.; Conrad, S.; Gomez, G.; Walsh, R.; Martin, E. *Bioorg. Med. Chem*. **2007**, *15*, 6367-6378.
177. Arndt, F. *Organic Synthesis, Collective Vol. II*; Wiley: New York, **1943**; pp 165-167.
178. Das, B.; Ravindranath, N.; Mahender, G.; Ramesh, C. *Tetrahedron*, **2003**, *59*, 1049-1054.
179. Cope, E. Doctoral dissertation, The University of Kansas, **2008**.
180. Ma, C.; Givens R. S. unpublished results.
181. Hatchard, C. G.; Parker, C. A. *Proc. R. Soc. London A*, **1956**, *A220*, 518.
182. *International Tables for Crystallography*; 4th ed., Vol A, Kluwer: Boston, **1996**.
183. *Data Collection: SMART Software Reference Manual*; Bruker-AXS, Madison, WI, USA, **1998**.
184. *Data Reduction: SAINT Software Reference Manual*; Bruker-AXS, Madison, WI, USA, **1998**.
185. Sheldrick, G. M. *SHELXTL Version 6.10 Reference Manual*; Bruker-AXS, Madison, WI, USA, **2000**.
186. Qin, J.; Xie, M.; Hu, Z.; Zhao, H. *Synth. Commun*. **1992**, *22*, 2253-2258.
187. Barret, R.; Daudon, M. *Tetrahedron Lett*., **1990**, *31*, 4871-4872.
188. Gorobets, E.; Sun, G.; Wheatley, B. M. M.; Parvez, M.; Keay, B. A. *Tetrahedron Lett*. **2004**,*45*,3597-3601.
189. Miyashitha, M.; Shiina, I.; Miyoshi, S.; Mukaiyama, T. *Bull. Chem. Soc. Jpn*., **1993**, *66*, 1516-1527..
190. Gonzalez-Gomez, J.; Santana, L.; Uriarte, E. *Synthesis*, **2002**, *1*, 43-46.
191. Finkelstein, H. *Ber. Dtsh. Chem. Ges*. **1910**, *43*, 1528.
192. Yoh, S. D.; Park, K. H.; Kim, S. H.; Cheong, D. Y. *Tetrahedron*. **1989**, *45*, 3321-3328.
193. Knopik, P.; Bruzik, K. S.; Stec, W. J. *Org. Prep. Proced. Int*. **1991**, *23*, 214-216. 3328.
194. Nagano, T.; Matsumura, K. *J. Am. Chem. Soc*. **1953**, *75*, 6237-6238.
195. Wuennemann, S.; Froehlich, R.; Hoppe, D. *Organic Lett*. **2006**, *8*, 2455-2458.
196. Adamski-Werner, S. L.; Palaninathan, S. K.; Sacchettini, J. C.; Kelly, J. W. *J. Med. Chem*. **2004**, *47,* 355-374

Part II

Exploratory Studies of Hydroxyquinoline-Based Phototriggers

Introduction

Over the past three decades researchers have successfully used photo-removable protecting groups, also known as "cage" compounds, to control the spatial and temporal release of a substrate in studies of fast biological processes.[1-5] It has been said of this fascinating chemistry that 'light is a "traceless" reagent'.[1-3,5] Over the past several years many researches have made a considerable effort to come up with better absorbing chromophores that could be applied in biological studies without disturbing or destroying the physiological environment.[1-5] It has been reported that caged compounds have been employed to examine fast processes in neurobiology. For example, the controlled release of GABA, deactivated by the *p*HP chromophore, was used to activate GABA release upon photolysis in whole-cell patch clamp studies in neurons in cortical slices of mice.[6] The biological role of nicotinic acid adenine dinuclotide phosphate ($NAADP^+$) in intact sea-urchin eggs[7] was investigated by means of rapid release of caged $NAADP^+$. Caged cAMP was used to study cAMP dependent cellular processes,[8,9] i.e., the function of cAMP in the relaxation of distal muscle,[10] the ATP-induced mechanism of actomyosin in muscle contraction,[11] and the activation of pyrrolizidine alkaloids such as monocrotaline to highly reactive pyrrole intermediates responsible for DNA crosslinking reactions.[12]

The substituents on the chromophore can alter the extended conjugation thereby increasing or decreasing the effective absorption wavelength of the cage. For example, installation of carboxyl[13] and amino[14] substituents in the coumaryl chromophore resulted in a shift of its effective absorption to 405 nm (Equation 2.1). However, the coumaryl chromophore suffers from several disadvantages. One of the major drawbacks of the

coumaryl group as a photoremovable protecting group is that the coumaryl group is retained in the product **2.2** after the irradiation.

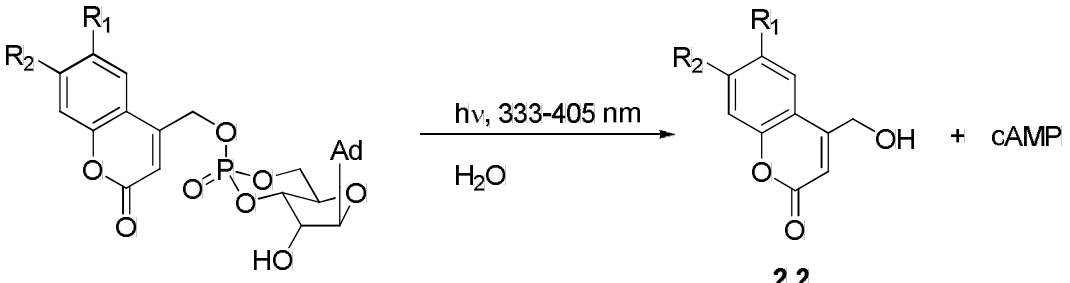

2.2

2.1a. $R_1 = R_2 = H$
b. $R_1 = OCH_3$, $R_2 = H$
c. R1 = H, R2 = OCH3
d. R1 = R2 = OCH3
e. R1 = H, $R_2 = N(CH_3)_2$
f. $R_1 = H$, $R_2 = Et_2N$
g. $R_1 = H$, $R_2 = OCH_2COOH$
h. $R_1 = R_2 = OCH_2COOH$

Eq. 2.1

In contrast, the *p*-hydroxyphenacyl group (*p*HP), developed by Givens and co-workers,[15,16] satisfies several Sheehan[17] and Lester[18] criteria for a successful photoremovable protecting group. Among them, increased water solubility, fast release rates, good quantum yields, and quantitative conversion to products whose chromophores experience a hypsochromic shift make the *p*HP group a versatile, well-suited photoremovable protecting group for biologically relevant substrates such as phosphates (ATP[19,20] and GTP[21]), carboxylates (GABA[22] and Glu[23]) including the C terminus of bradykinin[24,25] (a nonapeptide), and thiols (protein kinase A[26] and glutathione[27]). In addition, the *p*HP group has successfully been employed as a protecting group in synthesis.[28,29] However, the usefulness of the *p*HP chromophore could be further enhanced if its effective wavelength range could be bathochromically shifted into the visible region. Toward this goal, *m*–methoxy substituents have been installed on the pHP group, which resulted in extending the π-π* absorption range

of the chromophore.[30] Unfortunately, the *m*-methoxy substitution diminished the quantum yield of the photorelease of GABA in aqueous media.

Later, Yousef and Givens[31] turned their attention to substituted naphthalenes as modified *p*HP chromophores. The photochemical and photophysical properties of a series of trifluoromethylnaphthol derivatives have been previously studied by Seiler and Wirz[32,33] (Equation 2.2).

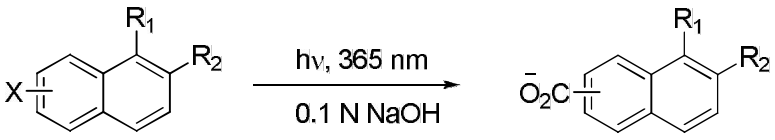

2.3a R_1 = OH, R_2 = H, X = 5-CF_3
b R_1 = OH, R_2 = H, X = 6-CF_3
c R_1 = OH, R_2 = H, X = 7-CF_3
d R_1 = OH, R_2 = H, X = 8-CF_3
e R_1 = OH, R_2 = H, X = 6-CF_3
f R_1 = H, R_2 =OH, X = 3-CF_3
g R_1 = H, R_2 =OH, X = 4-CF_3
h R_1 = H, R_2 =OH, X = 5-CF_3
i R_1 = H, R_2 =OH, X = 6-CF_3

2.4

Eq. 2.2

The authors proposed a photo-hydrolysis mechanism that proceeds through a heterolytic C-F bond cleavage from the singlet excited state of **2.3**, which was confirmed by quenching and laser flash photolysis (LFP) studies. Recently, Wan, Corrie and co-workers[34] investigated the photochemistry of 1-naphthol and its alkylated derivatives in aqueous media. Photolyses performed in acidic or neutral D_2O resulted in hydrogen/deuterium exchange at positions 5 and 8 of the naphthalene ring (Scheme 2.1). It was postulated that hydrogen-deuterium exchange occurs via a water-mediated excited state intramolecular proton transfer (ESIPT) process via a keto-tautomer intermediate **2.6a** (Scheme 2.1). According to this proposal, irradiation of compound **2.5a** produces a singlet excited state from which the molecule can follow three different pathways.

Scheme 2.1 Wan and Corrie Mechanism for H/D Exchange in 1-Naphthol in D_2O/CH_3CN (1:1)[34]

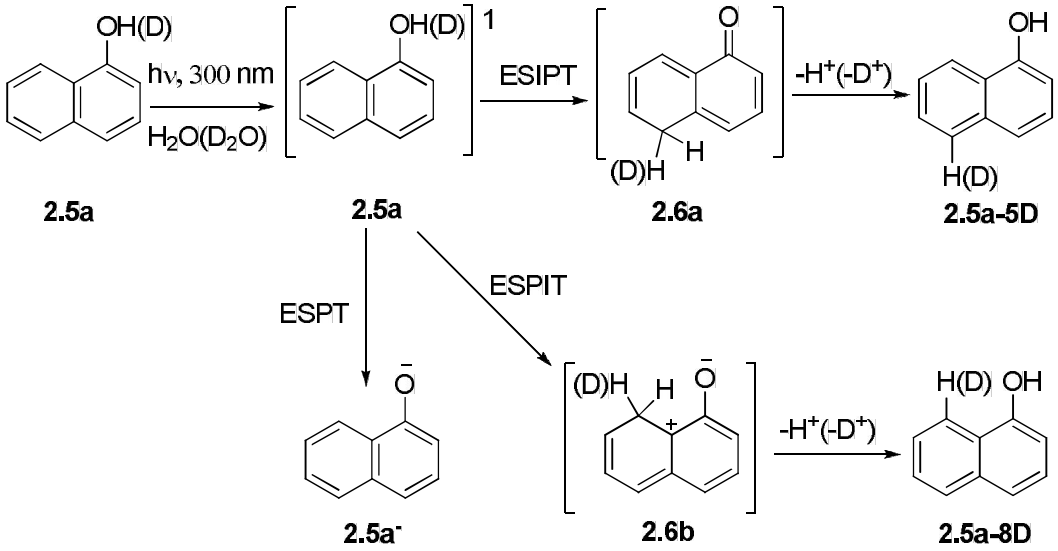

The laser flash photolysis studies (LFP) suggest that the hydrogen/deuterium exchange occurs at 5-position to give the keto-tautomer **2.6a** whereas the same process at the 8-postion of the naphthalene ring occurs to a lesser extent via the non-Kekulé intermediate **2.6b**. The third pathway leads to the formation of a 2-naphthyloxy anion through the excited state proton transfer (ESPT) from the OH group to solvent H_2O, a manifestation of the enhanced naphthol excited singlet state's acidity. Interestingly, there was no H/D exchange observed upon direct irradiation of anionic species **2.5a**$^-$.

The authors have also investigated photolysis of 1,5-disubstituted naphthol **2.7** in aqueous methanol at 300 nm. It was found that the quantum yield for the dehydration of **2.7** to **2.9** proceeding via a quinone methide intermediate (**2.8**) was very high (ca. 0.84). The formation of the photostable phenoxide intermediate **2.10** was also confirmed by LFP (Scheme 2.2).

Scheme 2.2 Photodehydration of Alcohol **2.7** in Aqueous Methanol[34]

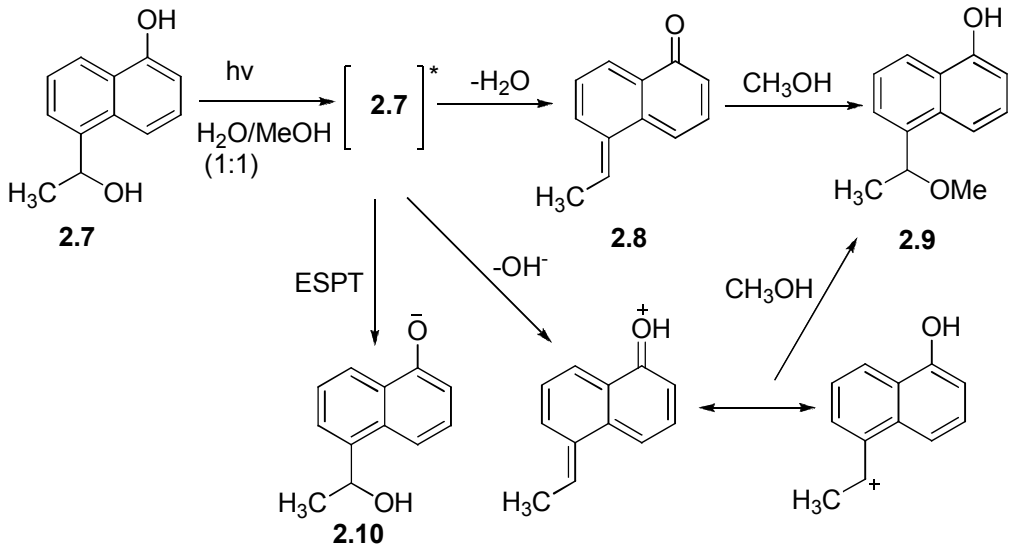

In contrast, no dehydration was observed with 1,4-substituted naphthol **2.11**. The photosubstitution reactions of **2.11** arise through the enhanced localized charge transfer from the naphtholic OH to the 5- and 8- ring positions. No reaction occurred at the 4-position of **2.11** confirming the crucial role of this charge transfer intermediate.

Scheme 2.3 Photodehydration of **2.11** in Aqueous Methanol[34]

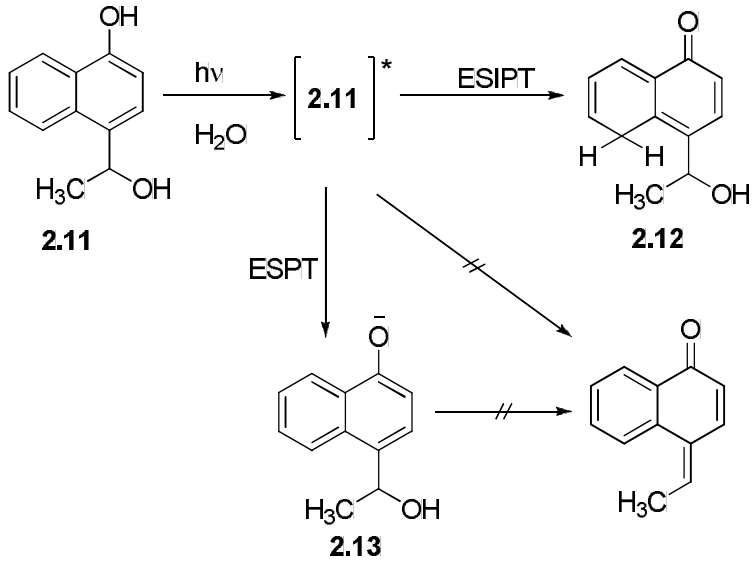

The formation of the phenoxide intermediate **2.13** and the products resulting from the H/D exchange at the 5 and 8 positions were the only compounds detected in this reaction (Scheme 2.3). This result indicates that **2.11** reacts via an ESIPT pathway similar to that observed for **2.5a**. Thus, the observed chemistry in Scheme 2.3 was dominated by the localized charge transfer to the 5- and 8- ring positions despite a potentially reactive substituent at the 4-position. Interestingly, the 1,5-substituted acetate ester **2.14** was found to be inert after prolonged irradiation at 300 nm in 50% aqueous acetonitrile (Equation 2.3). This observation contrasts with the demonstrated activity of other naphthalene derivatives at the substituted 5-position. It was suggested that the starting material may undergo ESPT or ESPIT processes but does not result any chemical transformations.

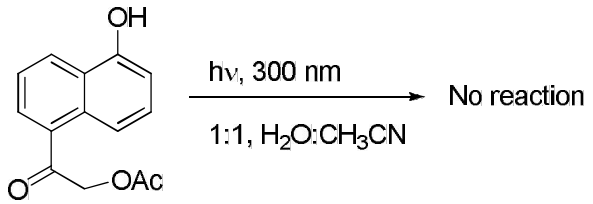

2.14

Eq. 2.3

Based on this information, Yousef and Givens[31] designed and synthesized a series of 1,4- and 2,6-disubstituted naphthalene-based photoremovable protecting groups and explored their photochemistry (Figure 2.1).

Figure 2.1 Naphthalene-based Photoremovable Protecting Groups

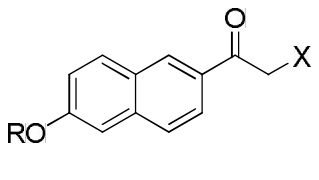

2,6 series

2.15 R = CH_3, X = GABA
2.16 R = H, X = GABA
2.17 R = H, X = -O-P(O)$(OEt)_2$

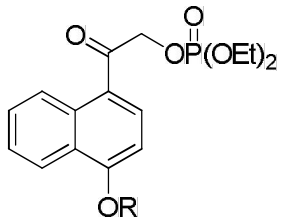

1,4 series

2.18 R = CH_3
2.19 R = H

Extension with an additional aromatic ring on the chromophore helped to bathochromically shift its absorption wavelength toward the visible region due to extended conjugation. However, this modification also resulted in decreased aqueous solubility. The photolysis of 1,4- and 1,6-substituted naphthyl esters revealed that the 1,4-substitued analogs (**2.18** and **2.19**) followed a photo-Favorskii rearrangement pathway, similar to the parent *p*HP chromophore, producing the rearranged acid **2.21** as a major product. In contrast, 2,6-substituted naphthyl esters (**2.15-2.17**) underwent photolysis via the photoreduction pathway, generating the corresponding acetylnaphthol **2.20** as a major photoproduct (Scheme 2.4).

Scheme 2.4 The Photochemistry of 1,4- and 2,6-Substituted Naphthyl Esters

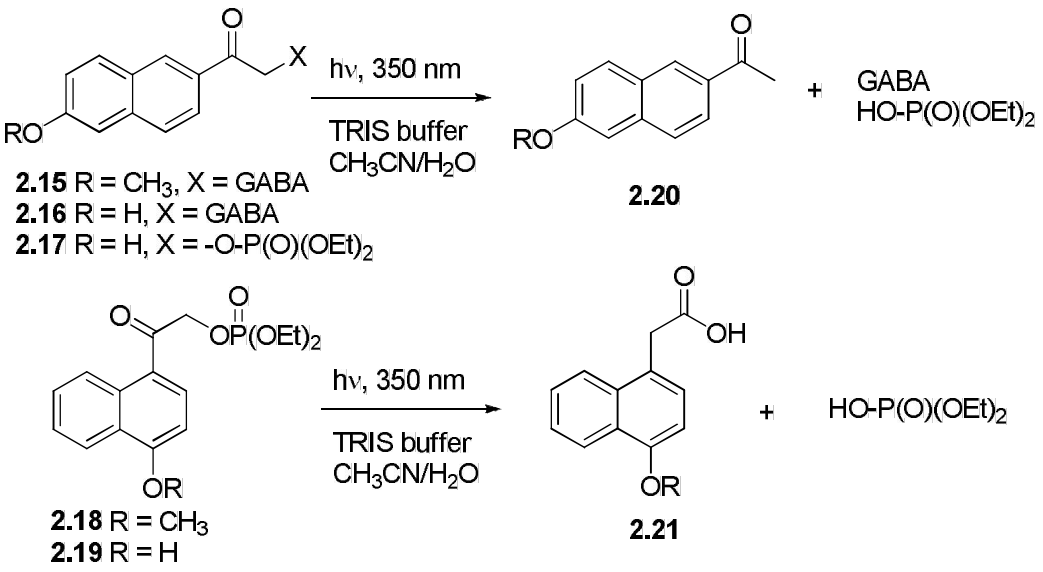

The suggested mechanism for the photolysis of the 2,6-substituted naphthyl esters involves a radical C-O bond homolysis to give 2-methylnaphthol radicals (Scheme 2.5), which upon hydrogen atom transfer affords 2-acetyl-6-naphthol.

Scheme 2.5 Proposed Mechanism for the Photolysis of 2,6-Substituted Naphthyl Esters

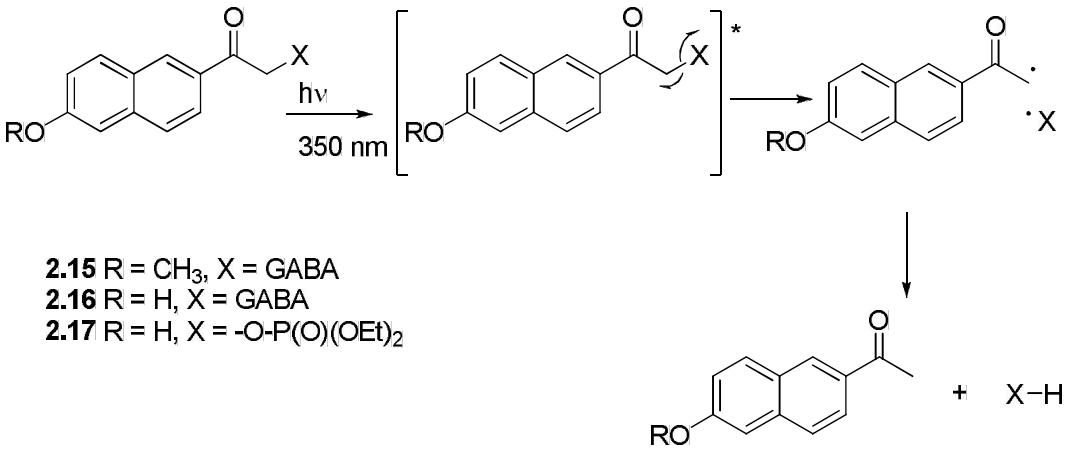

Table 2.1 The Quantum Yields and Conversions for Substrate Release in the Naphthyl Ester Series[31]

compound	λ_{max}[b]	% conversion[c,d,e]	Φ_{dis}[f] (x 10^{-2})
2.15 R = CH_3, X = GABA	317	56	0.67
2.16 R = H, X = GABA	319	70	0.91
2.17 R = H, X = -O-P(O)$(OEt)_2$	315	67	3.10
2.18 R = CH_3, X = -O-P(O)$(OEt)_2$	319	40	0.76
2.19 R = H, X = -O-P(O)$(OEt)_2$	325	98	2.80
*p*HP-O(PO)$(OEt)_2$[a]	306	Nd	38.0

[a]The diammonium salt of the monoester in TRIS buffer at 300 nm; 10% CH_3CN was added to the solvent; [b]Determined in H_2O for **2.15** and **2.16**; in CH_3CN for **2.17-19**; [c]Determined by RP-HPLC in 50 mM TRIS buffer with 10% CH_3CN, pH 7.3, after 1 h of photolysis at 350 nm for **2.15** and **2.16**; [d]Determined in 1% aqueous CH_3CN after 1 h of photolysis at 350 nm for **2.17**; [e]Determined in 1% aqueous MeOH after 1 h of photolysis at 350 nm for **2.18** and **2.19**; [f]Determined using RP-HPLC. Nd = not determined.

The efficiency of the substrate release was found to be one or two orders of magnitude lower than that for the parent *p*HP chromophore (Table 2.1). Evidence for a Favorskii-like rearrangement was observed on photolysis of the 1,4-substituted naphthyl ester series, which proceeded via the triplet excited state. The rate of the photorelease (ca. 10^6

s^{-1}) was also found to be two to three orders of magnitudes lower than the reported values for *p*HP-caged substrates.

Therefore, 5-acetyl-8-hydroxyquinoline (HAQ), which can also be described as a subtle change of the 1,4-substituted naphthyl chromphore, was proposed as an alternative chromophore that would extend the scope of the biological applications of the *p*HP chromophore. The presence of the N atom in the unsubstituted aromatic ring contributes some unique features to the HAQ chromophore. Among them, enhanced water solubility, metal chelating ability, and absorption at longer wavelengths bring added advantages those noted above for the naphthyl ester series. Thus, it is very important to explore the photochemistry which has been already reported on both the 8-hydroxyquinoline derivatives and related compounds in order to understand the photochemistry of HAQ based esters.

Kuzmin and Nekipelova[35-37] reported that the photochemical and photophysical processes of alkyl and alkoxy substituted 1,2-dihydroquinolines are very sensitive to the solvent. The reaction pathway in photolysis of substituted 1,2-dihydroquinolines changes when aprotic nonpolar solvents (hexanes) are replaced by water or methanol. The homolytic cleavage of the N-H bond to generate the corresponding amine radicals has been observed in aprotic solvents and alcohols other than methanol, and the photoinduced addition of solvent to the double bond of the heterocycle has been observed in water and methanol. It was reported that both of these reactions occur from the singlet excited state.

It is well known that transition metals can easily be employed to increase the intersystem crossing (by a heavy atom effect) of the HAQ esters because of the enhanced metal chelating ability of 8-hydroxyquinline. [38-40,40-42] However, it was demonstrated that metal chelation enhanced the fluorescence capabilities of 8-hydroxyquinoline and its

analogs.[41,42] Thus, the reported photochemical and photophysical processes of metal chelated 8-hydroxyquinoline and its derivatives would be useful to better understand the behavior of the HAQ chromophore. Soroka and co-workers[38] have reported the fluorescence properties of metal complexes of 8-hydroxyquinoline-5-sulfonic acid (HQSA) in aqueous media (Figure 2.4). In accord with their results, cadmium forms the most fluorescent complex (Cd-$HQSA_3$), whereas some other metals such as Mg^{2+}, Zn^{2+} (Mg or Zn-$HQSA_3$), and In^{3+} (In-$HQSA_3$) produce relatively low fluorescent complexes.

Figure 2.2 Structures of Some Metal Complexes of 8-hydroxyquinoline-5-sulfonic Acid[38]

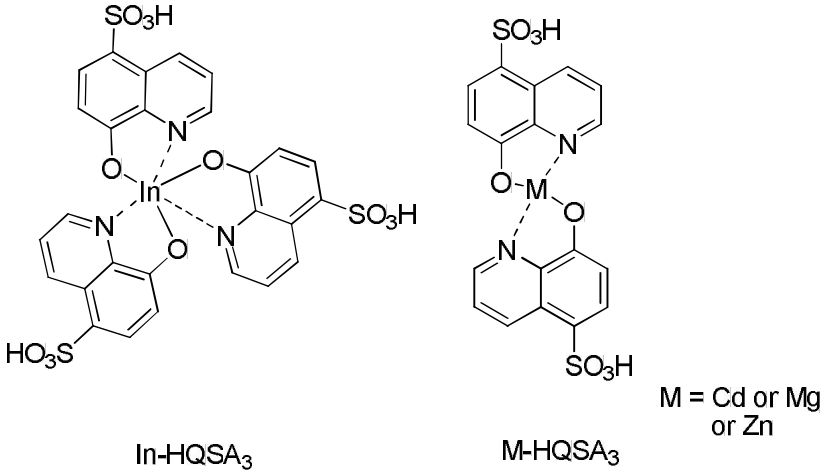

In the 1990s, Hopkins et al.[42] examined the photo- and electroluminescent properties of aluminum and zinc quinolate complexes 8-hydroxy-5-piperydinyl quinolinesulfonamide complexes (Al-PDQS and Zn-PDQS) vs. complexes with 8-hydroxyquinoline ((AlQ_3 and ZnQ_3) Figure 2.3). The authors demonstrated that the electron withdrawing sulfonamide group at the 5-position of the quinoline ring induced a blue-shift of the photo- and electroluminescence of Al-PDQS and Zn-PDQS compared to AlQ_3 and ZnQ_3.

Figure 2.3 Structures of Aluminum and Zinc Complexes of 8-Hydroxyquinoline and 8-Hydroxy-5-piperydinylquinolinesulfonamide[42]

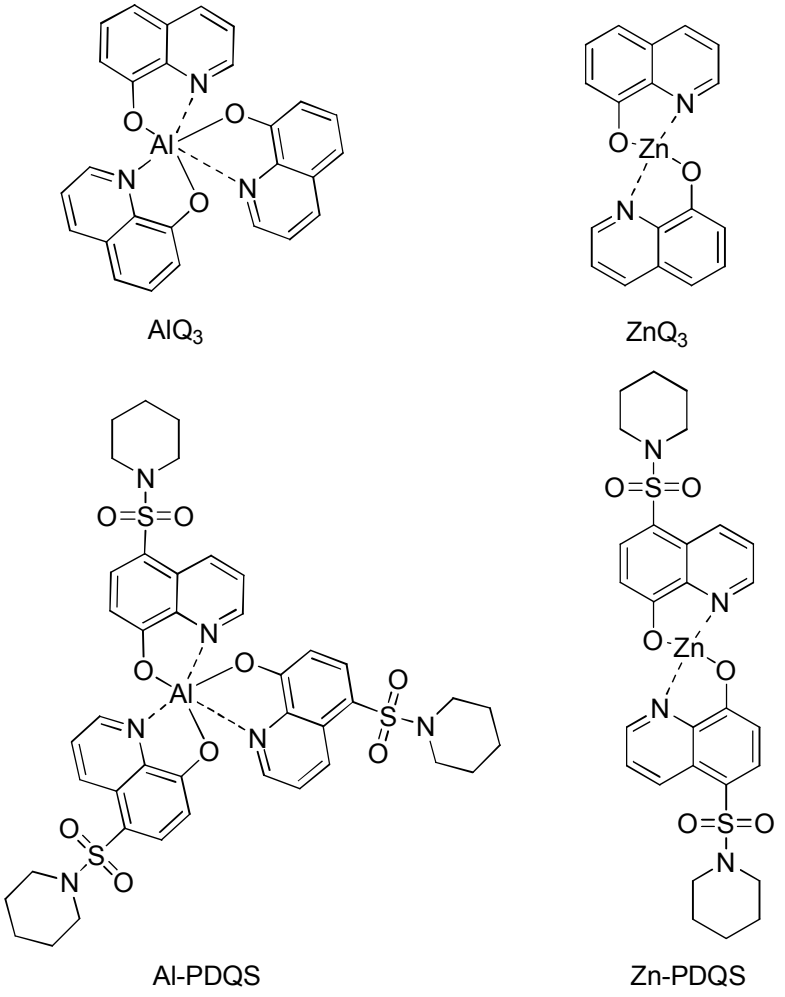

Heavy atom effect

Generally, aromatic hydrocarbons are considered to have very weak spin-orbit coupling which makes them ideal candidates for spin-orbit perturbation studies.[40,41] A spin-orbit perturbation is required to observe spin-forbidden transitions between states of different spin multiplicities such as an electronic transition from a singlet to a triplet state in an aromatic hydrocarbon. The rates of various multiplicity-forbidden, photophysical processes can be increased with an introduction of heavy atoms either within the aromatic structure of a

hydrocarbon or by the surrounding media (e.g. carbon tetrabromide and halogenated solvents or a xenon matrix).[40-42] These two types of heavy atom effects have been termed 'internal heavy atom effects,' where the heavy atom is directly affixed to the molecule. and 'external heavy atom effects,' where the heavy atom is not directly affixed but is in the proximity the molecule. The heavy atom can either increase the singlet-triplet mixing already present in the molecule or induce new configurations or both through spin perturbation. Likewise, the rate of the intersystem crossing can be dramatically increased for a particular chromophore with substitution of heavy atoms such as Br, I, and transition metals.[40-42] For example, a bromine atom substituted coumaryl derivatives exhibit the internal heavy atom effect.[43]

In the course of investigating of various coumaryl derivatives ((Bhc-X and Bhc-diol-X) Figure 2.4), it was found that a bromine atom substituted at the 8 position (i.e. 8-bromo-7-hydroxycoumarin) of the coumarin chromophore leads to efficient substrate release via the one-photon or two-photon excitation.[43] A variety of substrates have been released using the coumaryl photoremovable protecting group, including alcohols,[44] ketones and aldehydes,[45] cyclic nucleotide monophosphates,[46] diols,[47] neurotransmitters,[1,48] and DNA and RNA.[49]

Figure 2.4 8-Bromo-7-Hydroxycoumarin Analogs

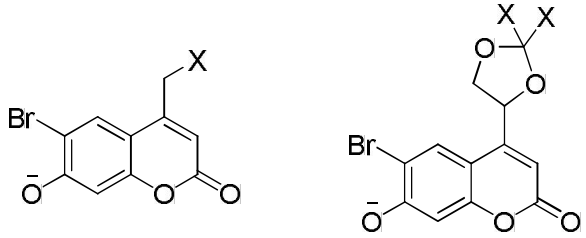

Bhc-X Bhc-diol-X

However, many coumaryl derivatives exhibit low solubility in aqueous solutions and in buffer solutions of high ionic strength. Furthermore, these cages were not compatible with

some fluorescent detection techniques (e.g. with a fluorescent indicator) because of high level of fluorescence of the coumaryl chromophore itself.

To overcome these difficulties, Toscano and co-workers[43] discovered the 8-bromo-7-hydroxyquinolinyl group (BHQ, **2.22)** which has good solubility in buffers at physiological conditions and exhibits low fluorescence. It was also found that bromine help to lower the pK_a of the phenolic proton thereby inducing a shift of the absorption maximum to the visible region. In addition, the formation of the triplet excited state by intersystem crossing would be facilitated by the presence of bromine in BHQ derivatives. Thus, BHQ derivatives which have good sensitivity to two-photon excitation can be used extensively in biological studies.

Scheme 2.6 Single and Two Photon Photolysis of BHQ[43] Derivatives[a]

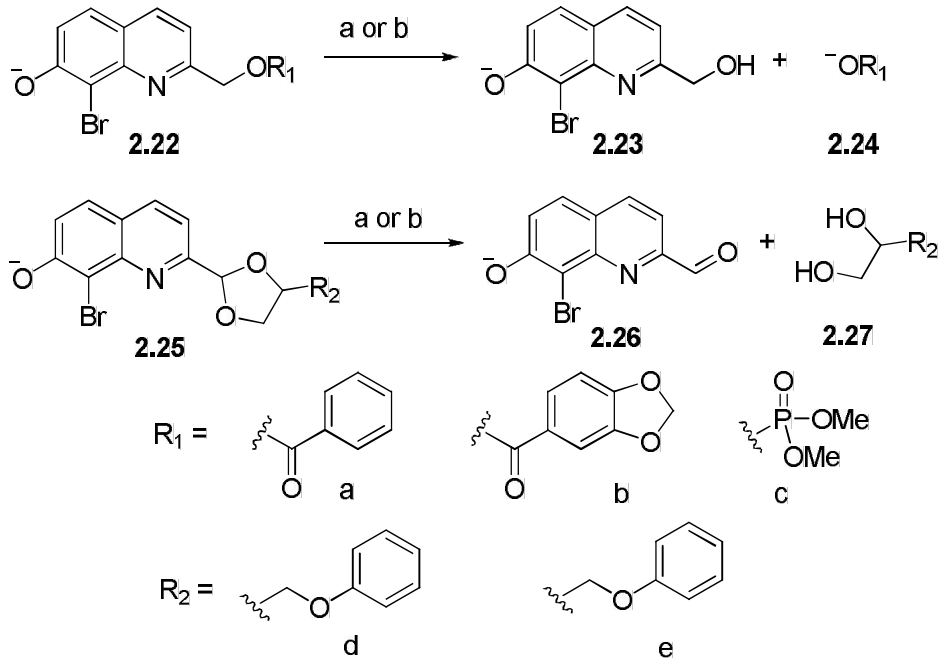

[a]Reagents and conditions; (a) hν, 365 nm (mercury lamp), KMOPS buffer, pH 7.2; (b) hν, 740 nm (a fs-pulsed and mode-locked Ti:sapphire laser), KMOPS buffer, pH 7.2

The absorption of the chromophore is red shifted and shows good sensitivity toward both one- and two-photon excitations The photolysis of BHQ derivatives **2.22** and **2.25** in aqueous

media released functional groups illustrated by **2.24** and **2.27** with good quantum yields (Scheme 2.6, Table 2.2).

Table 2.2 Photochemical and Photophysical Properties of BHQ[43] Derivatives[a]

Compound	λ_{max}	ε_{max} /(M^{-1} cm^{-1})	Q_u[b]	δ_u[c] / (GM)	τ_{dark}/(h)[d]
BHQ-OAc	369	2600	0.29	0.59	71
2.22a	368	2400	0.30	0.64	100
2.22b	296	6400	0.32	0.76	94
2.22c	370	3900	0.31	0.43	105
2.25d	375	2300	0.37	0.78	79
2.25e	374	2400	0.39	0.90	69

[a]Determined in KMOPS buffer, pH 7.2; [b]Determined at 365 nm (mercury lamp; 1-photon); [c]Determined at 740 nm (a fs-pulsed and mode-locked Ti:sapphire laser; two photon), GM = 10^{-50} ($cm^4 \times s$)/photon; [d]Time constant for the hydrolysis in the dark.

The one-photon uncaging efficiency for the BHQ derivatives (BHQ-OAc, **2.22a-e**) can be determined from the following relationship.

$$Q_u = (I\sigma t_{90\%})^{-1}$$

Where, I is the irradiation intensity which is determined by potassium ferrioxalate actinometry, σ is the decadic extinction coefficient (1000ε, the molar extinction coefficient) at 365 nm, and the $t_{90\%}$ is the irradiation time for 90% conversion to product.

The one-photon uncaging efficiency for the BHQ derivatives was found to be in the 0.30-0.39 range (Table 2.2).

The sensitivity of the BHQ derivatives (BHQ-OAc, **2.22a-e**) to undergo a photochemical reaction initiated by two-photon excitation (δ_u), the two-photon uncaging cross section, is determined in the Goeppert-Mayer, GM, unit which is defined as 10^{-50} ($cm^4 \times s$)/photon). This value is related to two-photon absorption cross-section, δ_a, by $\delta_u = Q_u \times \delta_a$. The pulse

parameters of the laser can be determined by using fluorescein as an external standard. The two-photon uncaging cross section can be determined from the following relationship.

$$\delta_u = N_p Q_{fF} \delta_{aF} C_F / \langle F(t) \rangle C_s$$

Here, Q_{fF} is the fluorsecenec quantum yield of fluorescein, δ_{aF} is the two-photon absorbance cross-section of fluorescein, $\langle F(t) \rangle$ is the time-averaged fluorescence photon flux (determined from the two-photon excitation of fluorescein in the same setup), N_p is the number of molecules photolyzed (determined from the initial rate of photolysis), is the collection efficiency of the detector, and C_s is the concentration of the BHQ-protected substrate. The values for the two-photon uncaging cross section for BHQ-OAc and **2.22a-e** ranged from 0.43 to 0.90 GM (Table 2.2). Interestingly, the quantum yield for the release of dimethyl phosphoric acid (**2.22c**) upon two-photon excitation was the lowest among all substrates, despite being the best leaving group.

These data suggested that BHQ derivatives are well-suited candidates for the one and two photon excitations. Mechanistic studies on the reaction mechanism were performed using Stern-Volmer quenching, isotope labeling studies, and DFT calculations. The obtained data supported a solvent assisted photoheterolysis (S_N1) reaction mechanism proceeding from the singlet excited state (Scheme 2.7). Upon irradiation in aqueous media, both BHQ acetate and BHQ phosphate (**2.28**) are initially excited to the singlet excited state (**2.29**). Subsequent intersystem crossing to the triplet **2.30** followed by decay restores the starting material **2.28**. Either homolytic cleavage of the C-O bond followed by single electron transfer or heterolytic cleavage from singlet excited **2.29** generates the switterion-like intermediate **2.31**. Trapping of the carbocation by water produces alcohol **2.32** and the corresponding carboxylate or phosphate. The tautomeric zwitterionic intermediate **2.33** has

been suggested because hydroxyqunolines are amphoteric and are protonated at nitrogen in the excited state on the picosecond time scale even in 9 to 10 M NaOH.[50] However, the possible role of the protonated intermediate **2.33** is unclear.

Scheme 2.7 Toscano's Mechanism for the BHQ Photolysis

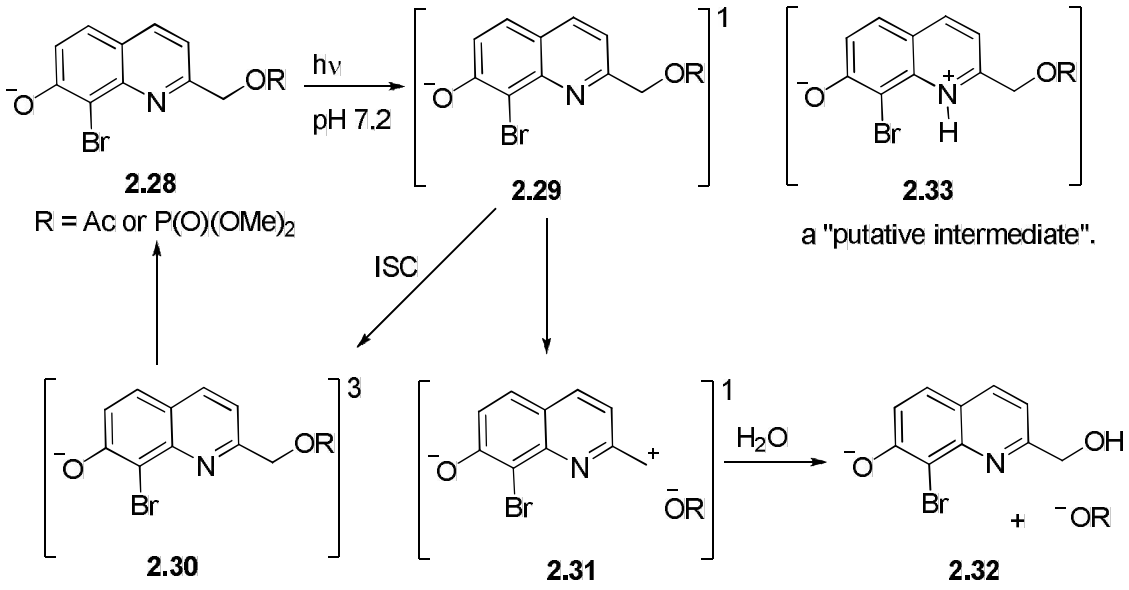

Toscano's efforts to develop a hydroxyquinolinyl-based photoremovable protecting groups were successful with the Br substitution at the 8 position. The quantum efficiency for the photorelease also can potentially be improved by substituting an electron-withdrawing group (an acetyl group at 5 position) which should facilitate the intersystem crossing like a heavy atom like Br and also lower the pK_a of the phenol. Therefore, we argue that 5-acetyl-8-hydroxyquinoline-based photoremovable protecting groups may have some added advantages in biological applications over the BHQ derivatives, because 8-hydroxyquinoline derivatives are well known fungicides and bactericides.[51,52] In addition, 8-hydroxyquinoline derivatives have been widely used in extraction of metal ions (i.e. Ca^{2+}, Mg^{2+}, Al^{3+}, Fe^{3+} etc.) from aqueous media.[38,39,54-56] and therefore, these chromophores may be biologically

important because divalent metal ions are readily available in the physiological environment. In accord with the pioneering studies on BHQ group by Toscano and co-workers[43] the HAQ chromophore may also be a good candidate for a two-photon excitation. Based on the results obtained with naphthalene-derived phototriggers and taking into account the interesting biological features and extended conjugation for a bathochromically shifted chromophore of 8-hydroxyquinoline, we strove to design a novel series of 5-acetyl-8-hydroxyquinoline-based photoremovable protecting groups. However, insufficient information is available from current literature on the photochemistry of 5,8-substituted quinoline derivatives, especially 5-acetyl-8-hydroxyquinolines, to rely on the analogies outlined earlier. Therefore, it is of interest to design, synthesize and explore the photochemistry of a model 5-acetyl-8-hydroxyquinoline based photoremovable protecting group.

Statement of Problem

In recent years, there has been a growing interest in employing of photoremovable protecting groups, also known as caging groups, in chemistry and biology. There are several key features that make a photoremovable protecting group a versatile cage, such as facile synthetic attachment to the substrate, efficient photorelease of the substrate, solubility of the caged substrate in aqueous media, and generation of stable photoproducts with a hypsochromic UV-vis shift of the photoreactive chromophore. The effective wavelength range of the chromophore is another crucial factor in biochemical applications of caged compounds because many biomolecules, including proteins and nucleotides, can absorb light at shorter wavelengths (< 280 nm), possibly resulting unwanted photoreactions. Therefore, chromophores that can absorb at longer wavelengths (> 300 nm) to enable efficient release of a substrate are particularly desirable for use in a physiological environment. The *p*-hydroxyphenacyl (*p*HP) photoremovable protecting group developed by Givens and co-workers, possesses several key features requisite of a versatile PPG, such as better solubility in both organic and aqueous media, fast release of the substrate, good quantum yields, ease of installation and quantitative conversion to products that are insensitive to radiation. However, the effective wavelength of the *p*HP group is a limiting factor for biochemical studies because the λ_{max} of this chromophore lies in the range of 280 - 320 nm. Therefore the possibility of extending the effective wavelength of the *p*HP chromophore towards the visible region has been explored. This would help expand the applicability of the *p*HP chromophore and its analogs. In 2000, Givens and co-workers introduced methoxy groups as substituents in the *meta*-position of the *p*HP chromophore. However, release of substrates, such as GABA and glutamate in aqueous media was significantly less efficient when compared to the

unsubstituted *p*HP chromophore in spite of a notable enhancement of π - π^* absorption of the chromophore.

Later, Yousef and Givens demonstrated that the 1,4- and 1,6-substituted naphthalene-based phototriggers increased the effective wavelength range but were also less efficient at releasing substrates (i.e., GABA and diethyl phosphoric acid) upon irradiation at 350 nm. Based on these results, it was proposed that 5-acetyl-8-hydroxyqunoline derivatives may be better candidates because of their effective wavelength ranges toward the visible region and their improved water solubility vis-à-vis the pyridine nitrogen. Furthermore, the 8-hydroxyquinoline is known to be an excellent chelating agent for divalent metal cations such as Ca^{2+} and Mg^{2+} which would enhance the rate of intersystem crossing by the heavy atom effect and would also be beneficial in biological arena. In addition to providing the necessary bathochromic shift, the added pyridyl ring may also help provide a substitution site for other functional groups to fine tune the physical and photochemical properties of this modified *p*HP chromophore.

Results and Discussion

A. Synthesis of 2-(8-hydroxyquinolin-5-yl)-2-oxoethyl benzoate

The proposed synthetic route to 2-(8-hydroxyquinolin-5-yl)-2-oxoethyl benzoate [HAQ benzoate, (**2.37**)] is shown in Scheme 2.8. The starting material, 8-hydroxyquinoline (**2.34**), which is readily available and inexpensive, was chosen for the starting point in the synthesis of HAQ benzoate **2.37**. Since it is well known that 8-hydroxyquinoline is a strong chelating agent with various divalent and trivalent metals such as Zn^{2+}, Mg^{2+}, Ca^{2+}, Al^{3+}, In^{3+},[43,44,55-57] care must be taken when working with metallic reagents especially during the purification processes of the product. We reasoned that an acetyl group can be introduced to the activated 5 position which is *para* to the hydroxyl group of the 8-hydroxyquinoline using the Friedel-Crafts acylation reaction. Subsequent α-bromination would generate bromide **2.36**. Finally, the benzoate ester **2.37** would be obtained via an S_N2 displacement by treating of bromide **2.36** with benzoic acid in the presence of a suitable base.

Scheme 2.8 Retrosynthetic Analysis for the Synthesis of HAQ Benzoate

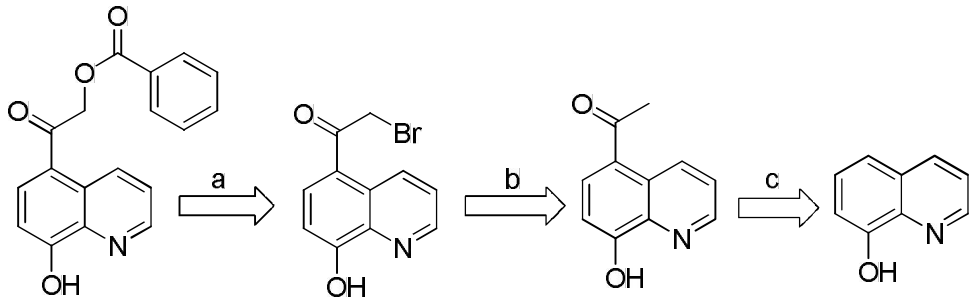

2.37 **2.36** **2.35** **2.34**

Retrosynthetic pathway: (a) S_N2 displacement with benzoic acid; (b) α-monobromination; (c) Friedel-Crafts acylation with acetyl chloride.

Following the synthetic plan described above, the Fridel-Crafts reaction[58] of 8-hydroxyquinoline with acetyl chloride produced 5-acetyl-8-hydroxyquinoline (HAQ), albeit

in moderate yield (40%). However, all attempts to effect α-bromination of **2.35** using several brominating reagents failed, including bromination with copper(II) bromide in $CHCl_3$/EtOAc,[59] dioxane dibromide (DDB) in dioxane/diethyl ether,[60] bromine in acetic acid,[61,62] bromine in diethyl ether,[63] N-bromosuccinimide (NBS) in the presence of catalytic amounts of *p*-toluenesulfonic acid in CH_3CN,[64] NBS with benzoyl peroxide in carbon tetrachloride (CCl_4)[65] and benzyltrimethylammonium tribromide in $CHCl_3$/MeOH.[66]

Accordingly, the Friedel-Crafts reaction was modified by replacing acetyl chloride with bromoacetyl chloride[67-69] (Scheme 2.9).

Scheme 2.9 Synthesis of 8-Hydroxy-5-Acetylquinoline Benzoates **2.37** and **2.39**

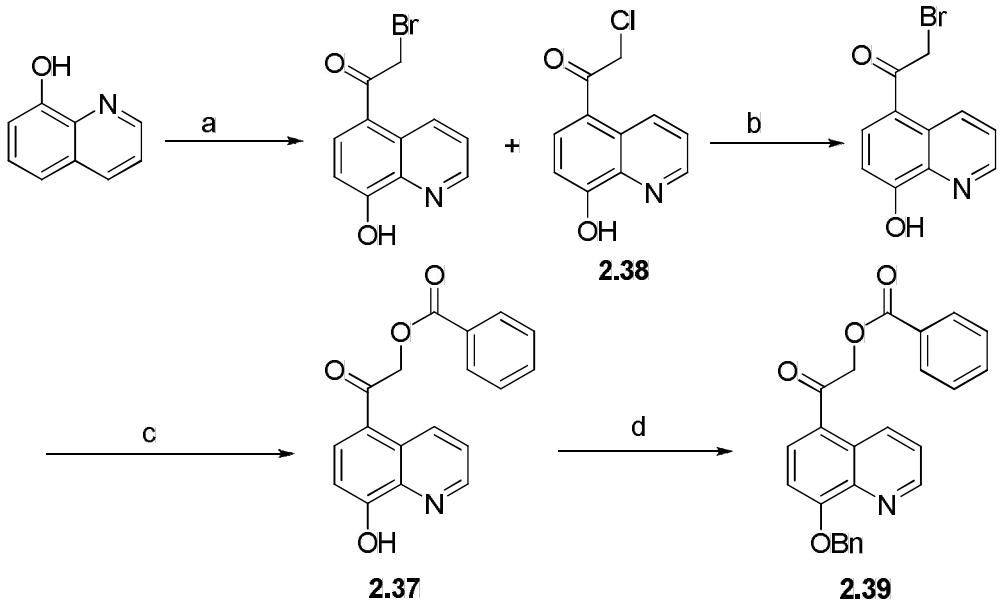

Reagents and conditions: (a) $BrCH_2COCl$, $AlCl_3$, CH_2Cl_2, 50 °C, 18 h, 45%; (b) NaBr, CH_3COCH_3, reflux, 12 h, 79%; (c) PhCOOH, DBU, dioxane/CH_2Cl_2 (1:1), rt, 12 h, 75%; (d) $PhCH_2Br$, K_2CO_3, DMF, rt, 12 h, 100%.

The reaction was carried out in dry CH_2Cl_2 in the presence of anhydrous $AlCl_3$ and bromoacetyl chloride to generate a mixture of the α-brominated and α-chlorinated 5-acetyl-8-hydroxyquinolines (formed by halogen exchange) in 45% yield. This mixture was then treated with an excess sodium bromide in acetone under reflux conditions[70] to produce 2-

bromo-1-(8-hydroxyquinolin-5-yl)ethanone (**2.36**). The latter was esterified[71] with benzoic acid in the presence of DBU in dioxane/CH_2Cl_2 (1:1) at room temperature to produce the benzoate ester **2.37** in 75% yield. Finally, benzyl protection was installed under standard conditions[72] to produce the benzoate ester **2.39** in quantitative yield (Scheme 2.9).

Synthesis of bis-[2-(8-Hydroxyquinolin-5-yl)-2-oxoethyl Benzoate] zinc(II) Dihydrate [($Zn(HAQ)_2$, 2.40]

The zinc chelated benzoate ester [$Zn(HAQ)_2$] **2.40** was obtained by treating the benzoate ester with diethyl zinc in THF at room temperature[56] (Equation 2.4). The resulting yellow residue was recrystallized from hot acetone/hexane to generate the desired product.

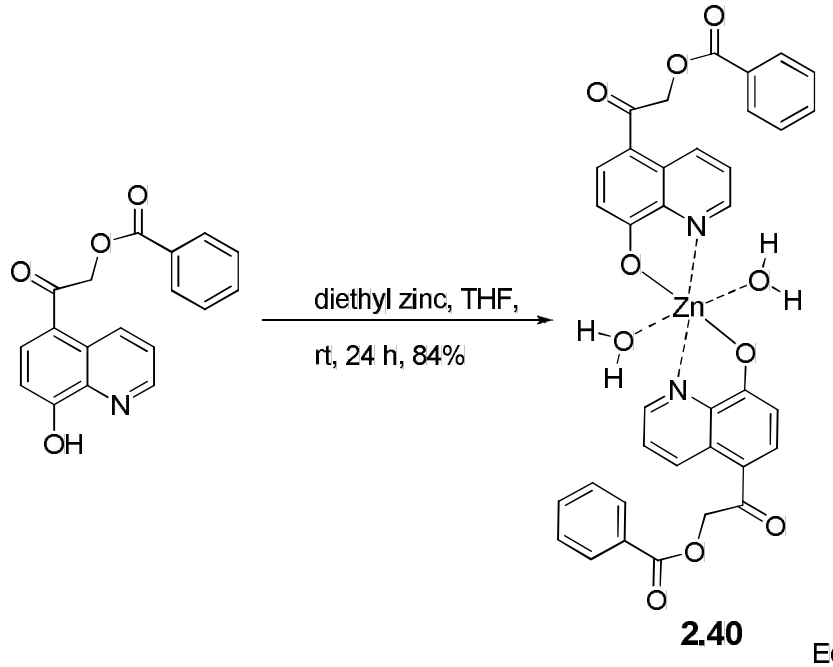

2.40 Eq. 2.4

Synthesis of benzyl protected 8-hydroxy-5-acetylquinoline diethyl phosphate (BnHAQ-DEP, 2.44)

The synthesis of the benzyl protected 8-hydroxy-5-acetylquinoline diethyl phosphate (Bn HAQ-DEP, **2.41**) from HAQ **2.35**[58] by protection of the hydroxyl group with benzyl bromide was followed by installation of ketal protection using iodobenzene diacetate in strongly alkaline methanol[73] to give **2.42**. The latter upon treatment with 50% acetic acid provided α-hydroxy ketone **2.43** in 88% overall yield. The α-hydroxy ketone **2.43** was esterified with diethyl phosphoryl chloride in pyridine[66] to afford the desired phosphate ester **2.44** in 30% yield (Scheme 2.10).

Scheme 2.10 Synthesis of Benzyl Protected 8-Hydroxy-5-acetylquinoline Diethyl Phosphate, **2.44**

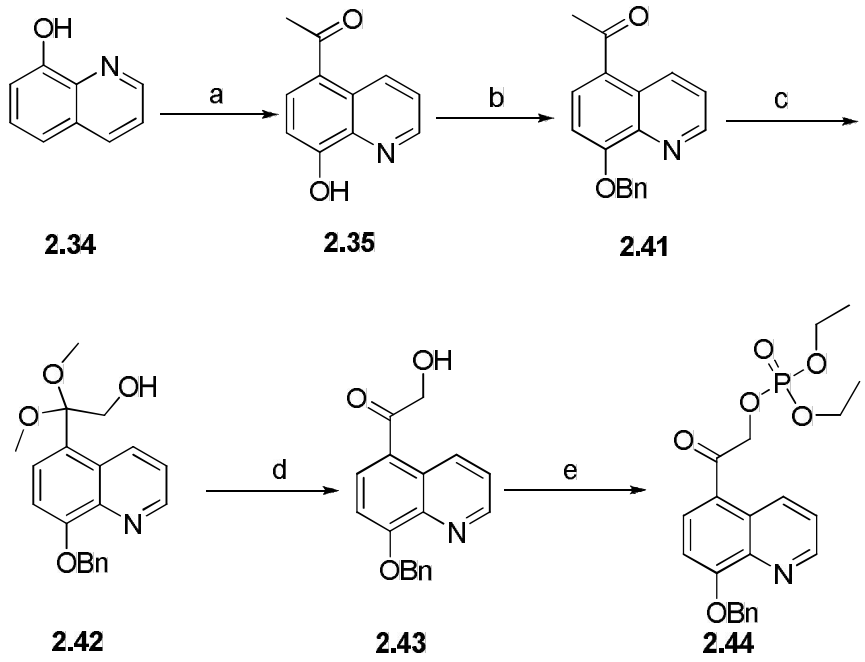

Reagents and conditions: (a) CH_3COCl, $AlCl_3$, nitrobenzene, 70 °C, 14 h, 40%; (b) $PhCH_2Br$, K_2CO_3, DMF, rt, 12 h, 100%; (c) $PhI(OAc)_2$, MeOH, KOH, 0 °C to rt, 14 h, 90%; (d) 50% CH_3COOH, rt, 12 h, 98%; (e) $P(O)Cl(OEt)_2$, pyridine, -5 °C to rt, 24 h, 30%.

Independent Synthesis of Putative Photoproducts

The synthesis of 2-(benzoyloxy)acetic acid (**2.46**) was accomplished by acylation of glycolic acid with benzoyl chloride (**2.45**) (Scheme 2.11).[74] The photo-oxidization product, quinoline-5,8-dione (**2.47**), was generated by iodobenzene diacetate oxidation[75] of 8-hydroxyquinoline in aqueous acetonitrile (CH_3CN:H_2O, 2:1) at 0 °C. The resulting yellowish-orange quinone **2.47** was air sensitive and should be stored under an inert atmosphere (under argon).

Scheme 2.11 Synthesis of Putative Photoproducts

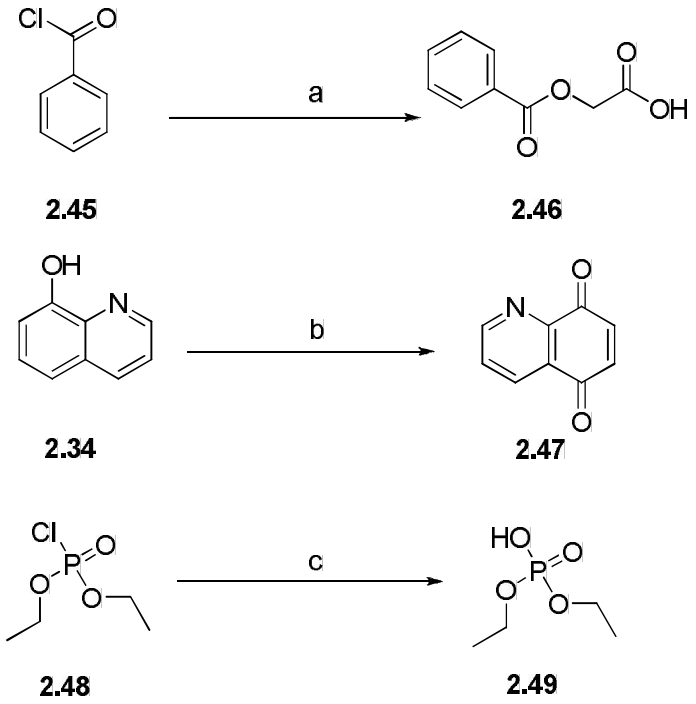

Reagents and conditions: (a) glycolic acid, anhydrous pyridine, Ar, overnight, rt, 69%; (b) $PhI(OAc)_2$, CH_3CN:H_2O (2:1), 0 °C, 3 h, 95%. (c) H_2O, NaOH, 3 h, < 30 °C, 30 min, 85%.

Diethyl phosphate[76] **2.49** was prepared by treatment of the corresponding acid chloride **2.48** with sodium hydroxide (Scheme 2.11).

B. Spectroscopic Studies

The OH-protected and unprotected 8-hydroxyquinoline derivatives have an extended resonance capability compared to other *p*-hydroxyphenacyl derivatives, which shifts their absorption maxima farther into the visible region. The absorption maximum (λ_{max}) of the UV-vis spectra of protected and unprotected benzoates **2.39** and **2.37** in aqueous acetonitrile at pH 7 range from 319 nm to 384 nm, respectively. These bands can be assigned to the π- π* transition from the filled orbital localized on the quinoline phenol ring to an antibonding molecular orbital localized on the pyridyl ring.[77]

Figure 2.5 The UV/vis Spectra of HAQ Benzoate **2.37** and BnHAQ Benzoate **2.39** in 10% H_2O in Acetonitrile

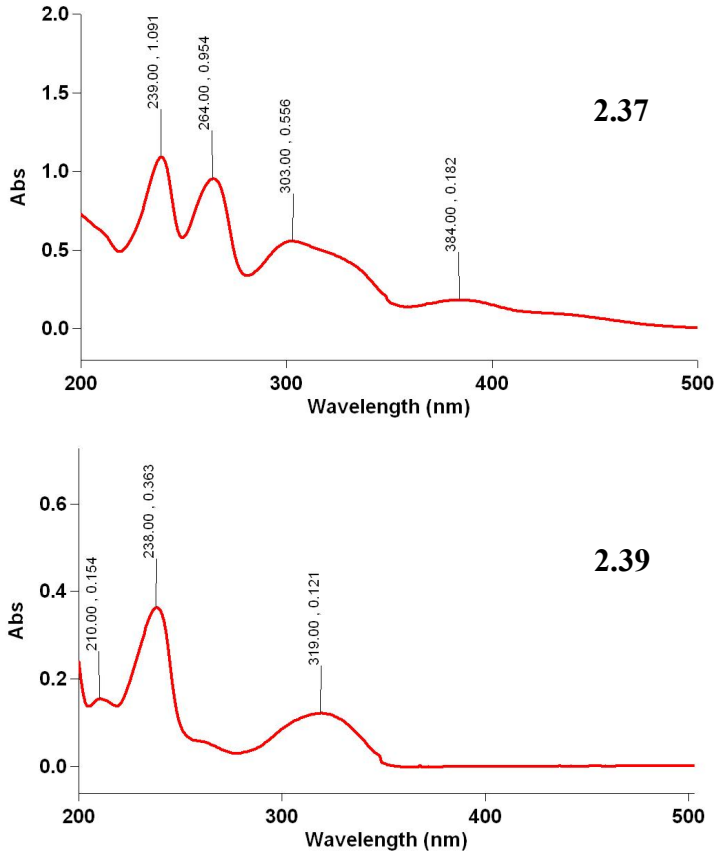

However, their absorption bands tail, which makes it difficult to predict the absorption maxima. The molar extinction coefficients (ε ($M^{-1}cm^{-1}$)) for the π-π* transitions of

2.37 and **2.39** were found to be 1620 (λ_{max} = 384 nm), and 8010 (λ_{max} = 319 nm), respectively. HAQ-benzoate ester **2.37** is more red-shifted due to the presence of a free hydroxyl group, whereas the benzyl protected analog **2.39** is blue–shifted (Figure 2.5). The pH dependence of the absorptivity of benzoate ester **2.37** was studied at pH 4, 7, and 10 by recording the UV/vis spectra in buffer solutions of sodium acetate/acetic acid, tris hydroxylmethyl) amino-methane/hydrochloric acid, and ammonium acetate/ammonia, respectively.

Figure 2.6 The UV/vis Spectra for the pH Dependence of Benzoate Ester **2.37**

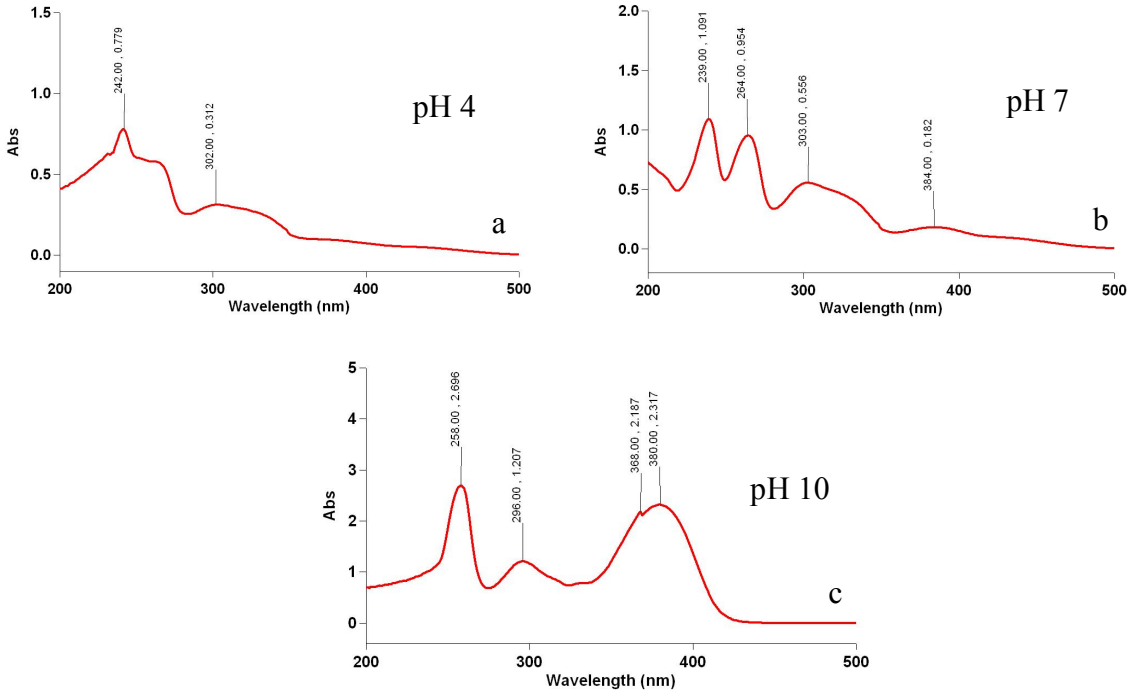

(a) Determined in sodium acetate/acetic acid buffer, (b) Determined in tris-(hydroxylmethyl)aminomethane /hydrochloric acid buffer, (c) Determined in ammonium acetate/ammonia buffer

Scheme 2.12 Charge Distribution of the Conjugate Acid and Conjugate Base of Hydroxyquinoline **2.37**

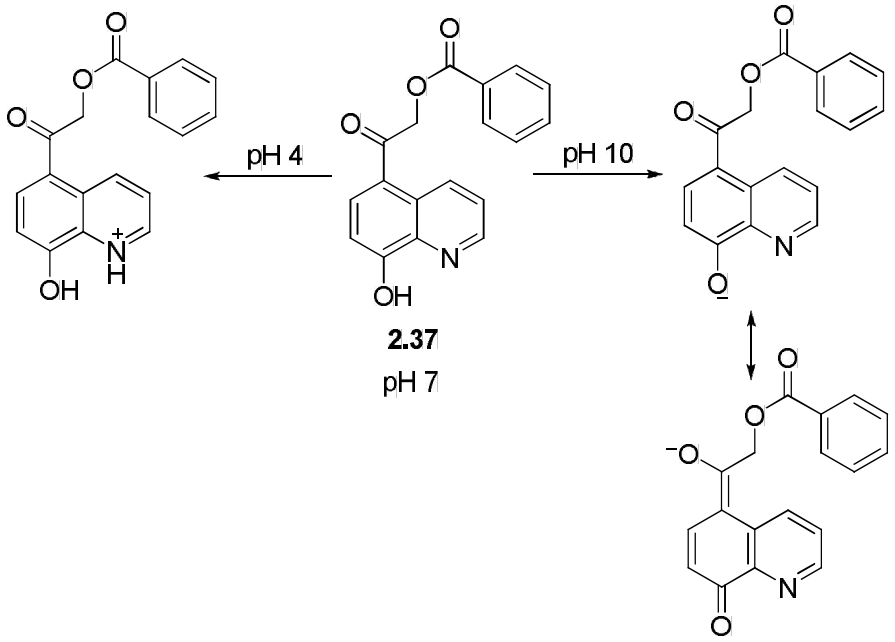

The absorption maximum of the 8-hydroxyquinoline was blue-shifted [λ_{max} ~302 nm (tailing)] at pH 4, and red-shifted [λ_{max} ~ 380 nm (sharp peak)] at pH 10 in accord with the degree of protonation or deprotonation of the chromophore (Figure 2.6 and Scheme 2.12). At low pH, hydroxyquinoline **2.37** exists as its conjugate acid and the phenoxide anion produced upon deprotonation of hydroxyquinoline **2.37** at high pH (conjugate base). At alkaline pH the energy the difference between HOMO and LUMO of the chromophore is reduced because of the extended conjugation of the phenoxide anion which lowers the energy difference between the n, π* and π, π* states at pH 9 (Scheme 2.12).

C. Stability Studies

The stability studies of the 8-hydroxyquinoline esters were performed with samples of the ester dissolved in aqueous acetonitrile and not exposed to the ultraviolet light. According to ^{1}H NMR and RP-HPLC analysis, no significant change was observed over 48 h. Since it was observed that the temperature inside the photoreactor increases as high as 40-45 ^{o}C during the photolysis reactions when performed at 300 nm with 16-3000 Å

lamps, the stability of 8-hydroxyquinoline esters was tested under these conditions as well. Control experiments with samples wrapped in aluminum foil in the merry-go-round photoreactor and illuminated for 2 h under the same conditions showed no significant change according to ^{1}H NMR and RP-HPLC analysis.

Product Studies and General Photochemistry of 8-Hydroxyquinoline Derivatives

8-Hydroxy and 8-Benzyloxy-5-acetylquinoline Benzoates (HAQ benzoate 2.37 and BnHAQ benzoate 2.39)

Photolyses of HAQ benzoate **2.37** and BnHAQ benzoate **2.39** in deuterated aqueous acetonitrile (10% D_2O in CD_3CN) were carried out in NMR tubes by photolyzing with and without argon degassing., and the reaction progress monitored by ^{1}H NMR (Equation 2.5 and Equation 2.6).

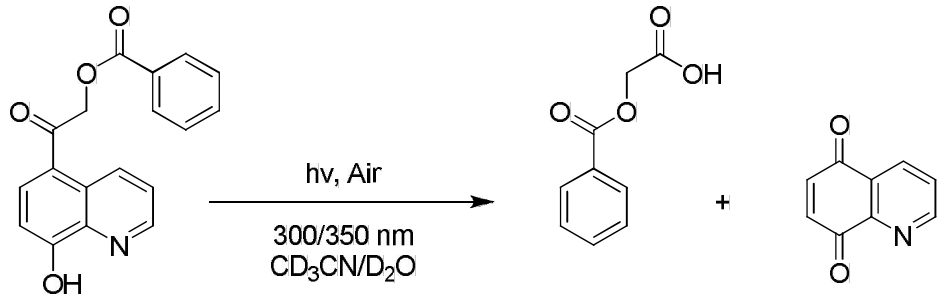

2.37 **2.46** 53% **2.47** 28%

Eq. 2.5

Oxygen-free conditions were accomplished by Ar purging the reaction sample in an NMR tube cooled in an ice bath for 30 min. After purging, the NMR tube was sealed and the degassed solution of 8-hydroxy-5-acetylquinoline benzoate (**2.37**) was photolyzed in a Merry-go-round apparatus at 300 nm or 350 nm with 16-3000 Å or 16-3500 Å lamps, respectively. The analyses were performed by ^{1}H NMR.

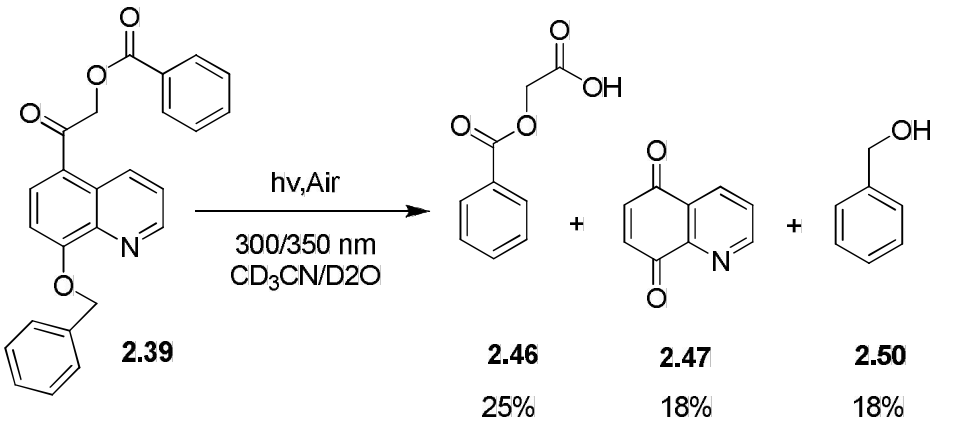

Eq. 2.6

Three major products were detected by HPLC. However, neither the release of benzoic acid nor the expected rearrangement product was observed by NMR analysis. During the course of the reaction, the color of the photolysis sample change from light yellow to bright yellow. Efforts were made to identify the photoproducts by comparison of their ^{1}H and ^{13}C NMR spectra and HPLC retention times with authentic or synthesized samples of several possible products, but these were unsuccessful. Accordingly, a photolysis experiment was carried out on a larger scale in order to separate the products by column chromatography and by acid-base extraction to isolate and further characterize the unknown products. After photolysis, EtOAc was added and the reaction mixture was first extracted with a saturated $NaHCO_3$ solution. The aqueous phase (combined $NaHCO_3$ layers) was acidified and extracted with EtOAc to isolate the acidic products. Surprisingly, instead of the expected product (benzoic acid), 2-(benzoyloxy)acetic acid (**2.46**) was isolated and identified by its characteristic ^{1}H NMR (the distinct methylene peak at 4.78 ppm) and confirmed by independent synthesis (see Experimental Section). The color change of the photolyzed sample from light yellow to bright yellow during the course of the reaction was attributed to the possible formation of quinoline-5,8-dione (**2.47**). The ^{1}NMR of quinone **2.47** has two characteristic doublets which correspond to two olefinic protons in the range of 7.1-7.2 ppm

(J = 10.0-11.0 Hz) which were observed in the crude photolysis mixture. However, all efforts to isolate quinone **2.47** from the photolysis mixture by column chromatography were unsuccessful. Therefore, this suspected photoproduct was also independently synthesized from commercially available starting materials through the route outlined in the Experimental Section. Analysis of the photolysis mixtures by spiking with the authentic sample of quinone **2.47** confirmed the formation of quinoline-5,8-dione in this reaction.

Samples of HAQ benzoate **2.37** were photolyzed using 16-3500 Å lamps for 3.5 h. Quantitative analysis of the photoproducts was carried out using ^{1}H NMR (Figure 2.7). The slopes (m) of the best fit line from the linear regression of the time-dependent concentrations of the reactant and product analyses were determined. The light output (L) of the 16-3500 Å lamps in the photoreactor was determined using the potassium ferrioxalate method in units of millieinsteins per minute**.** The quantum efficiencies (Φ) for the disappearance of hydroxyquinoline **2.37** and the appearance of the acid **2.46** were then calculated by $\Phi = |m| / L$. where m is the slope of the plot and L is the light output from lamps which were used in the actinometry. The results are shown in Table 2.3. The quantum yield for disappearance of hydroxyquinoline **2.37** in 10% aqueous acetonitrile was 4.0 ($\pm$ 0.5) $\times$ 10^{-4} and the appearance quantum yield for the acid product **2.46** was found to be 4.0 ($\pm$ 0.3) $\times$ 10^{-4} (Table 2.3). The reaction progress was also monitored by ^{1}H NMR. Depletion of hydroxyquinoline **2.37** and the appearance of the acid **2.46** were quantified by integration of the signals at δ 5.63 ppm and 4.78 ppm, respectively, for the methylene peak in each compound.

Figure 2.7 Photolysis of Non-degassed Sample of HAQ Benzoate **2.37** in 10% Aqueous Acetonitrile at 350 nm

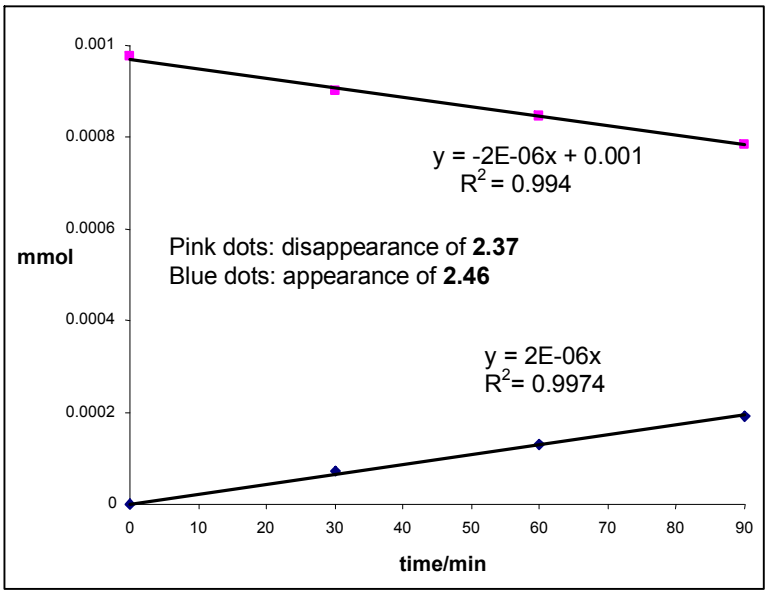

The photolysis of BnHAQ benzoate **2.39** was also performed as described above, in order to test the effect of the unprotected hydroxyl group versus a benzyloxy group on the photochemistry. It was found the that photochemical reaction of BnHAQ benzoate **2.39** proceeded much less efficiently, providing only 25% conversion to the acid **2.46** after 24 h, whereas conversion of HAQ benzoate **2.37** to the acid **2.46** reached 51-53% after 3.5 h (Table 2.3).

Photolysis of HAQ benzoate **2.37** was also performed in the absence of molecular oxygen to check its effect on this reaction. Degassed samples of HAQ benzoate **2.37** were inert to photolysis suggesting that molecular oxygen plays an important role in this photochemical transformation. The heavy atom effect on the photochemistry of $ZnHAQ_2$ **2.40** was explored by photolyzing the benzoate ester of the zinc chelated dimer **2.40** in aqueous acetonitrile, in the presence of oxygen and in a degassed solution at both 300 nm and 350 nm. It was found that in both cases the zinc chelated ester was inert to photolysis.

Table 2.3 Comparison of the Conversions and Quantum Yields in the Photolysis of Benzoate Esters (HAQ benzoate **2.37**, BnHAQ benzoate **2.39**, and Zinc Chelated Quinoline, $ZnHAQ_2$, **2.40**) under Ambient and Degassed Conditions

Compound	irradiated time /h	% conversion[a] degassed	% conversion[a] non-degassed	Φ_{dis}[b] / $x10^{-4}$	$\Phi_{dis.}$[c] / $x10^{-4}$	$\Phi_{app.}$[c] / $x10^{-4}$
2.37	3.5	51-53	51-53	4.0 ± 0.3	4.0 ± 0.5	4.0 ± 0.3
2.39	24	0.0	25	nd	1.2 ± 0.3	1.2 ± 0.2
2.40	24	0.0	0.0	0.0	0.0	0.0

Photolyses were conducted using 16-3000 Å or 16-3500 Å lamps. a) Determined using ^1H NMR in 10% D_2O in CD_3CN; b) Determined using RP-HPLC by the disappearance of the starting material at 350 nm; c) Determined using ^1H NMR at 350 nm

Photochemistry of BnHAQ-DEP **3**

Photolysis of the benzyl protected 8-hydroxy-5-acetylquinoline diethyl phosphate **2.44** (BnHAQ-DEP) was carried out with aqueous acetonitrile as the solvent and under ambient conditions at 300 nm and 350 nm. The products as evident by ^1H and ^{31}P NMR analysis were diethyl phosphoric acid along with unidentified products (Equation 2.7).

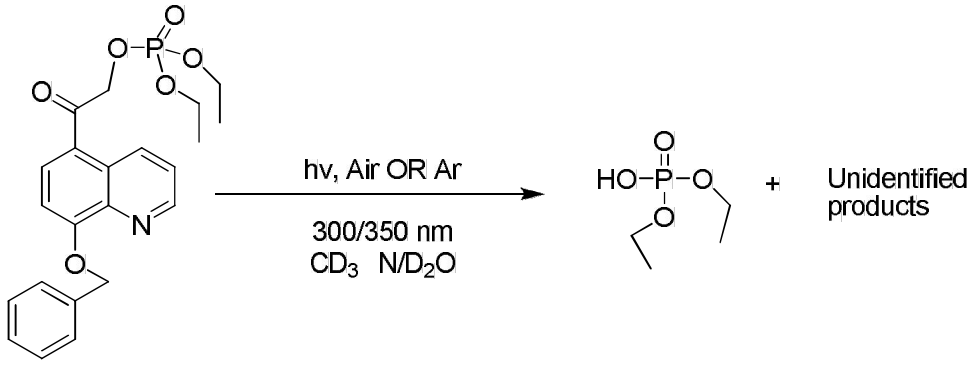

2.44 **2.49**

Eq 2.7

Photolysis of **2.44** was less efficient compared to that of the corresponding benzyl protected benzoate ester **2.39**. The released diethyl phosphoric acid was identified using ^{31}P NMR by spiking the photolysis reaction mixture with an authentic sample.

Interestingly, quinone formation was not observed as was the case in the photolysis of unprotected 8-hydroxy-5-acetylquinoline benzoate (**2.37**) and the benzyl protected benzoate **2.39.** At this point a detailed study on the photochemistry of HAQ derivatives would be necessary in order to learn more about the mechanisms for photorelease. However, the preferential photooxygenation reaction in the presence of air, the slow rates of reaction and the low quantum yields obtained for the HAQ series discouraged any further exploration of its photochemistry by our group.

Discussion

There is little known about the photochemistry of hydroxyquinolines. The photochemistry of acetylhydroxyquinolines themselves had not been investigated previously, despite parallel studies on 1,4- and 1,6-disubstituted naphthyl photoprotecting groups. Toscano and co-workers[43] have explored the photochemistry of 8-bromo-7-hydroxyquinolinyl group (BHQ) upon one photon and two photon excitations. Toscano suggested that these naphthyl analogs have π-π^* absorption bands that are extended toward the visible region, suggesting that they may be suitable chromophores for biochemical caging applications. Indeed, our studies of the 5-acetyl-8-hydroxyquinoline derivatives in aqueous media support this idea. We found that these derivatives have absorption maxima in the 320-400 nm range in aqueous acetonitrile. In 2001, Cossy and Belotti[77] developed an efficient protocol for generating substituted quinoline-5,8-quinones from the readily available substituted 8-hydroxyquinolines by photosensitized oxidation (Equation 2.8, Table 2.4).

These reactions were performed in CH_2Cl_2 in the presence of *meso*-tetraphenylporphine (TPP), an effective triplet state photosensitizer for producing singlet oxygen.[78,79] The resulting crude reaction mixture was treated with dry Na_2SO_4 to generate **2.52**.

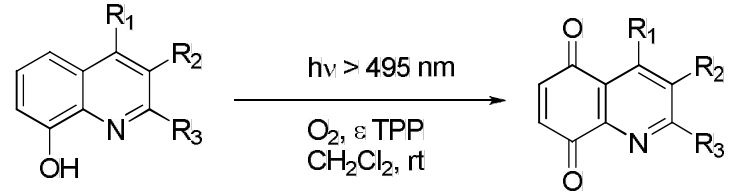

2.51a R_1 = H, R_2 = H, R_3 = H
b R_1 = H, R_2 = H, R_3 = CH_3
c R_1 = H, R_2 = CH_3, R_3 = H
d R_1 = CH_3, R_2 = H, R_3 = H
e R_1 = H, R_2 = H, R_3 = CN
f R_1 = H, R_2 = H, R_3 = CHO
g R_1 = H, R_2 = H, R_3 = CO_2Me
h R_1 = H, R_2 = H, R_3 = $CON(i\text{-}Pr)_2$
i R_1 = H, R_2 = H, R_3 = $CH_2N(Boc)CH_2Ph$
j R_1 = H, R_2 = H, R_3 = $CH_2N(Boc)CH_2CO_2Me$

2.52

Eq. 2.8

Table 2.4 Synthesis of 5,8-Quinolones **2.52**

2.51 derivatives.	Time[a] (h)	Yield % of **2.52**[b]
2.51a	2.5	82
b	2.5	80
c	2.0	82
d	2.0	72
e	8.0	73
f	5.5	51
g	2.0	81
h	2.0	89
i	2.5	53
j	2.0	50

Reactions were performed in CH_2Cl_2 on a 2 mmol scale at 20 °C (cooling with water) using visible light (1500 W xenon arc, filter for radiations > 495 nm) while sparging with oxygen; [b] Isolated yields.

The purpose of using the triplet sensitizer TPP in the reaction was to generate singlet molecular oxygen, i.e., $^1O_2$ ($^1\Delta_g$). The proposed mechanism for the product formation is depicted in Scheme 2.13.

Scheme 2.13 Cossy's Reaction Sequence for the Formation of **2.52**

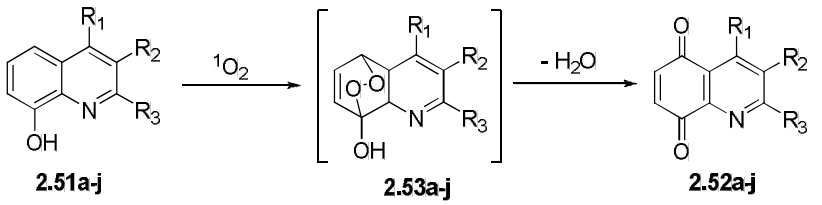

Initially, 8-hydroxyquinoline **2.51** reacts with singlet oxygen in the excited state to generate a non-isolatable, hydroxyendoperoxide intermediate **2.53** via a [4 + 2] cycloaddition reaction. Intermediate **2.53** undergoes ring opening and dehydration to produce 5,8-quinolone **2.52** in the presence of anhydrous Na_2SO_4.

Importance of quinoline-5,8-quinolone moiety

Substituted or unsubstituted 5,8-quinolones **2.52** and **2.46** are important synthetic intermediates en route to azaanthraquinones such as anthracyclines,[80] pluramycines,[81] antibiotics like dynemicin A and deoxydynemicin A,[82] cleistopholine,[83,84] and meridine[84] (Figure 2.8).

Figure 2.8 Compounds Possessing an Azaanthracenedione Moiety[83,84]

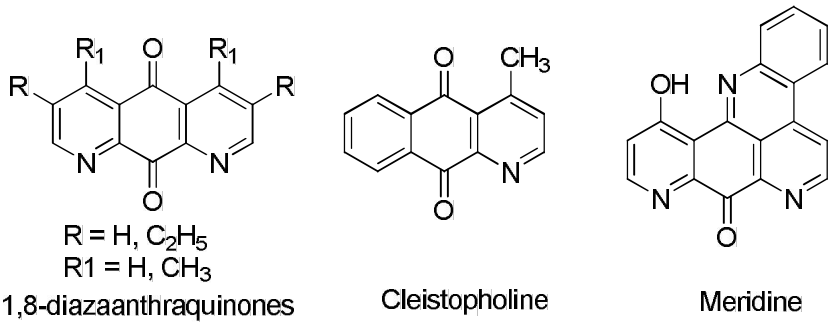

In addition, a variety of natural products can be found in which a carbon of the benzene ring of the anthraquinoline is replaced by nitrogen that also exhibit antibiotic and antitumor activity such as azabenzisochromanquinones,[85] cystodamine,[86] lavendamycin,[87] and streptonigrinone,[88] (Figure 2.9). Therefore, either substituted or unsubstituted quinoline-5,8-quinones **2.46** and **2.52** will be important synthetic intermediates to produce a variety of biologically active molecules such as azaanthraquinones.

Figure 2.9 Natural Products Bearing an Azaanthraquinoline Moeity[87,88]

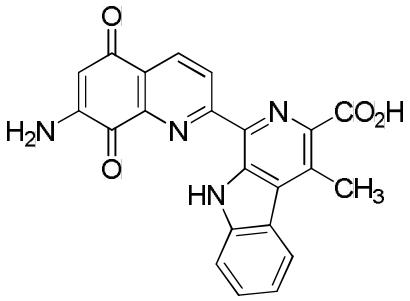

Lavendamycin

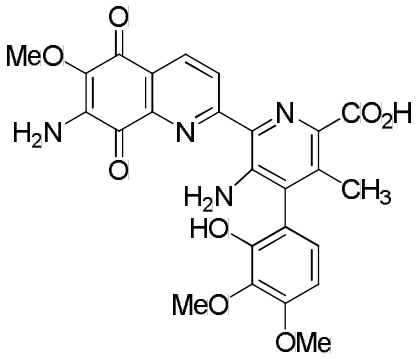

Streptonigrinone

On the basis of prior research on the *p*HP photoremovable protecting group, Yousef and Givens[31] designed and synthesized a series of novel 1,4- and 1,6-substituted naphthyl-based phototriggers and tested them in the release of GABA and diethyl phosphates in aqueous media. These studies prompted us to design and synthesize the 5-acetyl-8-hydroxyquinoline photoprotecting groups and to study their photochemistry in aqueous media (Figure 2.10). The only structural difference for the 8-hydroxyquinoline-based chromphore **2.54** compared to the 1,4-substituted naphthalene chromophore is the replacement of a CH group with a nitrogen atom at the position *para* to the hydroxyl group in the unsubstituted aromatic ring.

Figure 2.10 The 5-Acetyl-8-Hydroxyquinoline (HAQ) Based Phototriggers

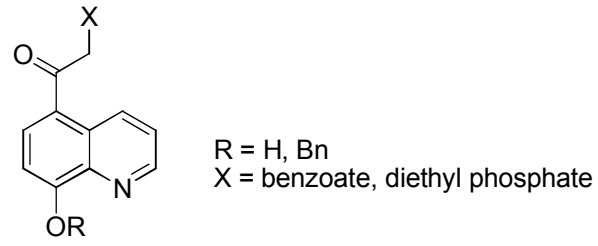

2.54

Likewise, the photoproducts **2.46** and **2.47** obtained on photolysis of HAQ benzoates suggest that the mechanism of photocleavage may arise from the photosensitized oxidation of the benzoate ester (Scheme 2.14).

Scheme 2.14 Proposed Mechanism for the HAQ Benzoate Photocleavage

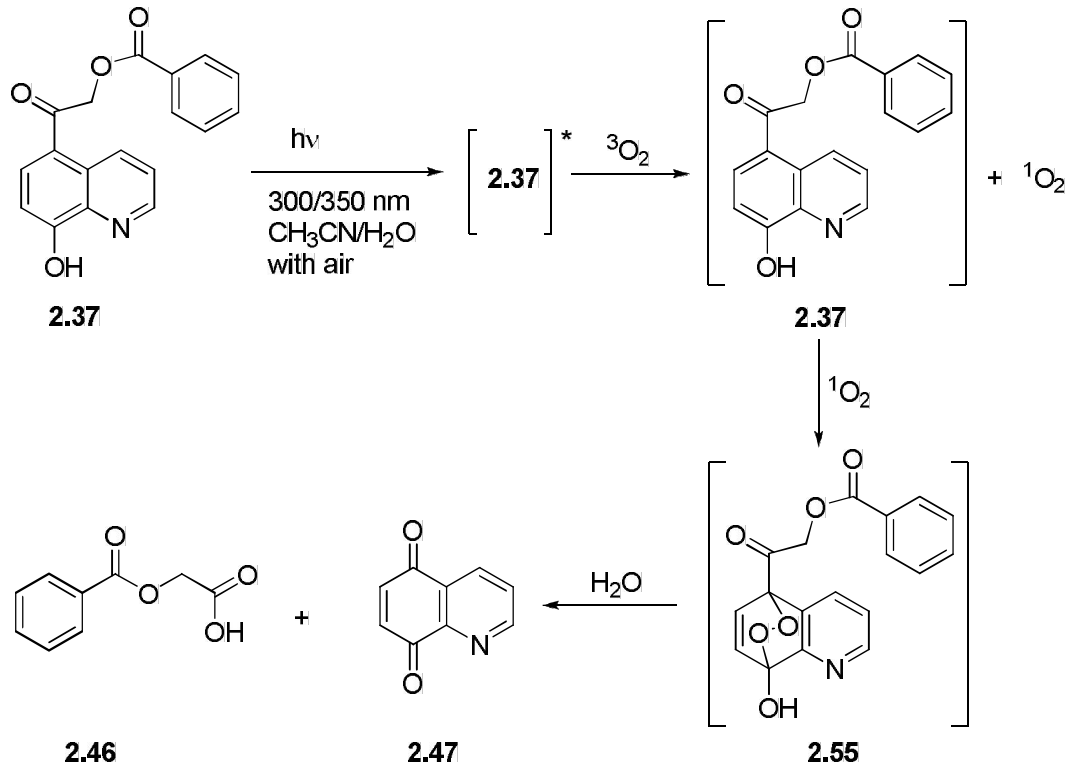

A similar mechanism had been proposed by Cossy and Belotti[77] in the formation of substituted quinoline-5,8-quinones from readily available substituted 8-hydroxyquinolines.

However, a triplet sensitizer (TPP) in CH_2Cl_2 at > 495 nm was used in those studies. Although no triplet sensitizer (TPP) was used in our studies as in the studies by Cossy and Belotti,[77] we argue that 8-hydroxyquinoline's excited triplet state can act as a photosensitizer, generating singlet oxygen $^1O_2$ ($^1\Delta_g$) under non-degassed conditions. The singlet oxygen $^1O_2$ ($^1\Delta_g$) reacts by a [4+2] cycloaddition reaction to generate the hydroxyl-5,8-endoperoxide intermediate **2.55**. This unstable intermediate fragments into photoproducts **2.46** and **2.47**. However, this mechanism, which models that proposed by Cossy and Belotti, must be refined in order to account for the quinone product and especially the 2-(benzoyloxy)acetic acid (**2.46)**. Therefore, an alternative mechanism is considered (Scheme 2.15).

Scheme 2.15 Revised Mechanism for the HAQ Benzoate Photocleavage

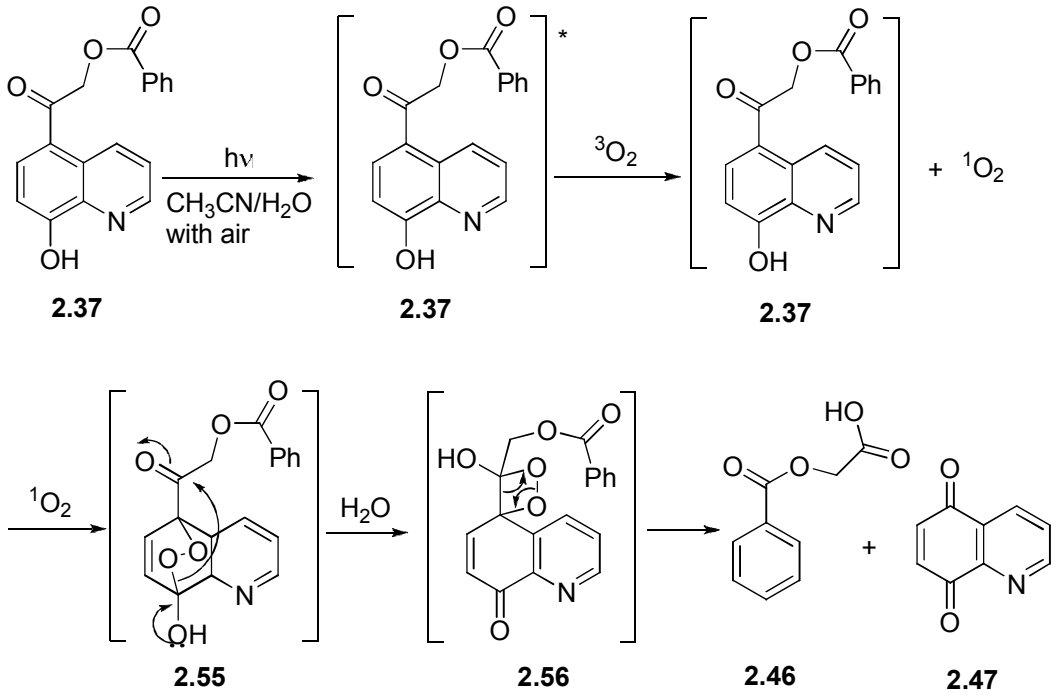

The ground state **2.37** can first react with singlet oxygen by the standard [2+2] cycloaddition to generate hydroxyendoperoxide intermediate **2.55**. The intermediate **2.55** rearranges to afford an oxetane, structure **2.56**. The unstable oxetane undergoes ring opening to generate the two observed products, the acid **2.46** and quinone **2.47** as the main photoproducts. Alternatively, irradiation of BnHAQ **2.39** can lead to 2-(benzoyloxy)acetic acid **2.46**, quinoline-5,8-dione **2.47**, and benzyl alcohol **2.50** (Scheme 2.16).

Scheme 2.16 Revised Mechanism for the BnHAQ Benzoate Photocleavage

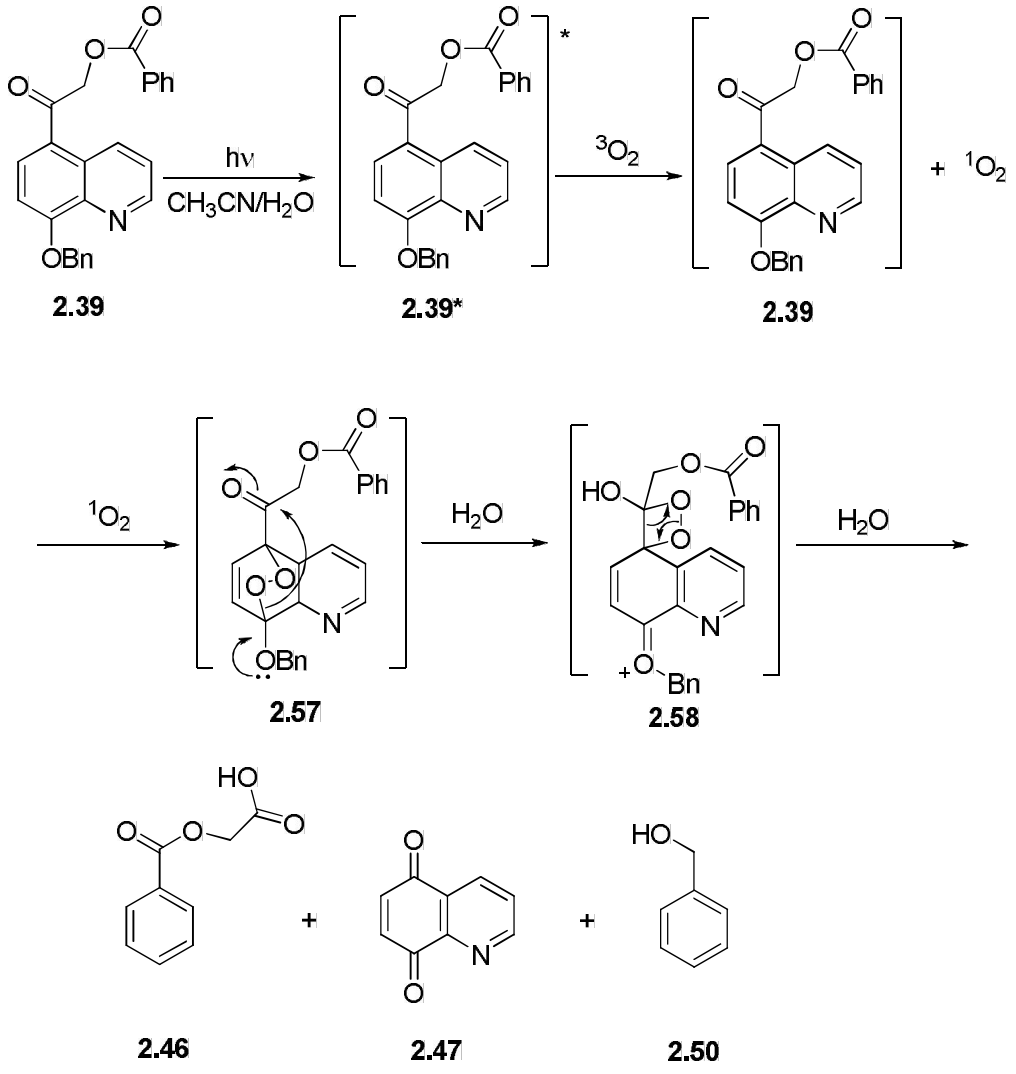

This mechanism is similar to that proposed for HAQ benzoate **2.37** except that the quninone formation is also accompanied by the release of benzyl alcohol **2.50**. However, the efficiency of this photoreaction is low due to a relatively slow formation of oxetane **2.58**, as the benzyl protection makes the oxygen lone pair less available for resonance stabilization or perhaps nucleophilic attack on $^1O_2$. The low reactivity of the HAQ benzoate **2.37** may also be due to the hydrogen bonding occurring between the OH-proton and the nitrogen atom. The intramolecular H-bonding diminishes the proton transfer, thereby reducing the acidity of the hydroxyl group in the excited state.

This explanation may also be advanced to rationalize the decreased likelihood of the photo-Favorskii rearrangement. The triplet excited state proton transfer from the phenolic hydroxyl group to the aqueous medium is purported to be necessary and occurs with a concomitant release of the substrate in the photo-Favorskii mechanism. This is crucial in the photo-Favorskii rearrangement generation of the triplet biradical that then rearranges to the produce putative Favorskii intermediate.[1,6] Thus, intramolecular H-bonding between the hydroxyl group and quinoline nitrogen diminishes the reactivity of the HAQ benzoate **2.37** upon irradiation.

Effect of zinc chelation

Employing zinc chelation on the hydroxyquinoline **2.40** nucleus was expected to influence the photolysis, possibly through a heavy atom effect.[40-42] It has been shown that a heavy atom such as zinc is capable of inducing the spin angular momentum changes for the excited state electron pair, thereby increasing the rate of intersystem crossing (especially for the transitions of S_1 to T_1 and T_1 to S_0). Our experiments demonstrated that the zinc chelated benzoate ester **2.40** was inert to the photolysis at ambient conditions in aqueous media. The

possible explanation for this observation may be the fluorescent enhancement of 8-hydroxyquinoline upon chelation with some metal ions[89,90] such as Zn^{2+}, Cu^{2+}, Pb^{2+}, and $Hg.^{2+}$ 8-Hydroxyquinoline, itself, is weakly fluorescent in aqueous media. There are two explanations for the origin of the strong fluorescent enhancement upon metal chelation. First, the photo-induced proton transfer from the phenolic hydroxyl to the quinoline nitrogen in the excited state [an excited state intramolecular proton transfer (ESIPT)] process results in fluorescent quenching.[89,91] Metal chelation interrupts this deprotonation process thereby deminishing the ESIPT channel.[92,93] Second, the low-lying excited state of 8-hydroxyquinoline (an n,π* transition occurs) is non-fluorescent due to rapid intersystem crossing. The metal complexation modulates the low-lying excited state to a lowest π state, leading to an π,π* transition. The transition from the π* singlet into its triplet state is not rapid due to a less favorable spin-orbit coupling of two π,π states. Therefore, the fluorescence emission channel becomes more probable.[94] Hence, the zinc chelation enhances the fluorescence energy dissipation from the singlet excited state.

HAQ benzoate **2.37** and BnHAQ benzoate **2.39** were inert to photolysis when degassed under argon saturated conditions even upon extended irradiation. These results are in accord with the results reported by Corrie and co-workers[34] for the 1,4-substituted naphthyl acetate **2.14**. Irradiation of HAQ benzoate **2.37** and BnHAQ benzoate **2.39** did not lead to generate any net chemistry even though ESPT or ESIPT could and probably does occur.

Photochemistry of BnHAQ-diethyl phosphate 2.44

Irradiation of BnHAQ-diethyl phosphate **2.44** in 10% aqueous acetonitrile released diethyl phosphoric acid both in the presence and absence of oxygen. The release of diethyl

phosphoric acid was not accompanied, however, with any products resulting from photooxygenation, as was the case with both benzoate **2.37** and benzoate **2.39**. This suggests that the release of diethyl phosphoric acid may proceed by a more traditional route. Either homolytic cleavage to produce radical species, heterolytic bond cleavage to generate ions, or alternatively, a photo-Favorskii rearrangement by the concerted loss of both the proton and the leaving group forming the spirodienedione intermediate **2.61** can be envisaged. However, the low quantum yields discouraged further analysis and identifications of the chromophore photoproducts. The photolysis of the oxygen-saturated aqueous acetonitrile solution of BnHAQ-DEP **2.44** did not produce any photooxygenated products. However, oxygen had a quenching effect on the quantum yield for the photodecomposition of BnHAQ-DEP **2.44**. This suggests that the triplet excited state of the diethyl phosphate ester **2.44** is involved in the photorelease of diethyl phosphoric acid, because oxygen is a well known triplet quencher.[41,42] In addition, Bailey and co-workers[95] observed shortened phosphorescence lifetimes (< 0.005 s) of 8-hydroxyquinoline in EPA revealing the possible involvement of the triplet excited state. Thus, a plausible mechanism for the release of diethyl phosphoric acid is depicted in Scheme 2.17. In accord with the studies by Suzuki et al.[44] on the photochemistry of 2-(alpha-bromoacetyl)naphthalene, the photorelease of diethylphosphoric acid can follow photohomolysis pathway, whereas the photorelease of diethylphosphoric acid from BnHAQ-DEP **2.44** can also follow both the photohomolyis pathway to the reduction product **2.62** and a photo-Favorskii rearrangement to the rearranged acid **2.63** and naphthyl alcohol **2.60** in accord with studies by Yousef and Givens[31] on the photochemistry of 1,4 substitutued naphthyl esters.

.

Scheme 2.17 Plausible Pathway for the Photolysis of **2.44** in Aqueous Acetonitrile

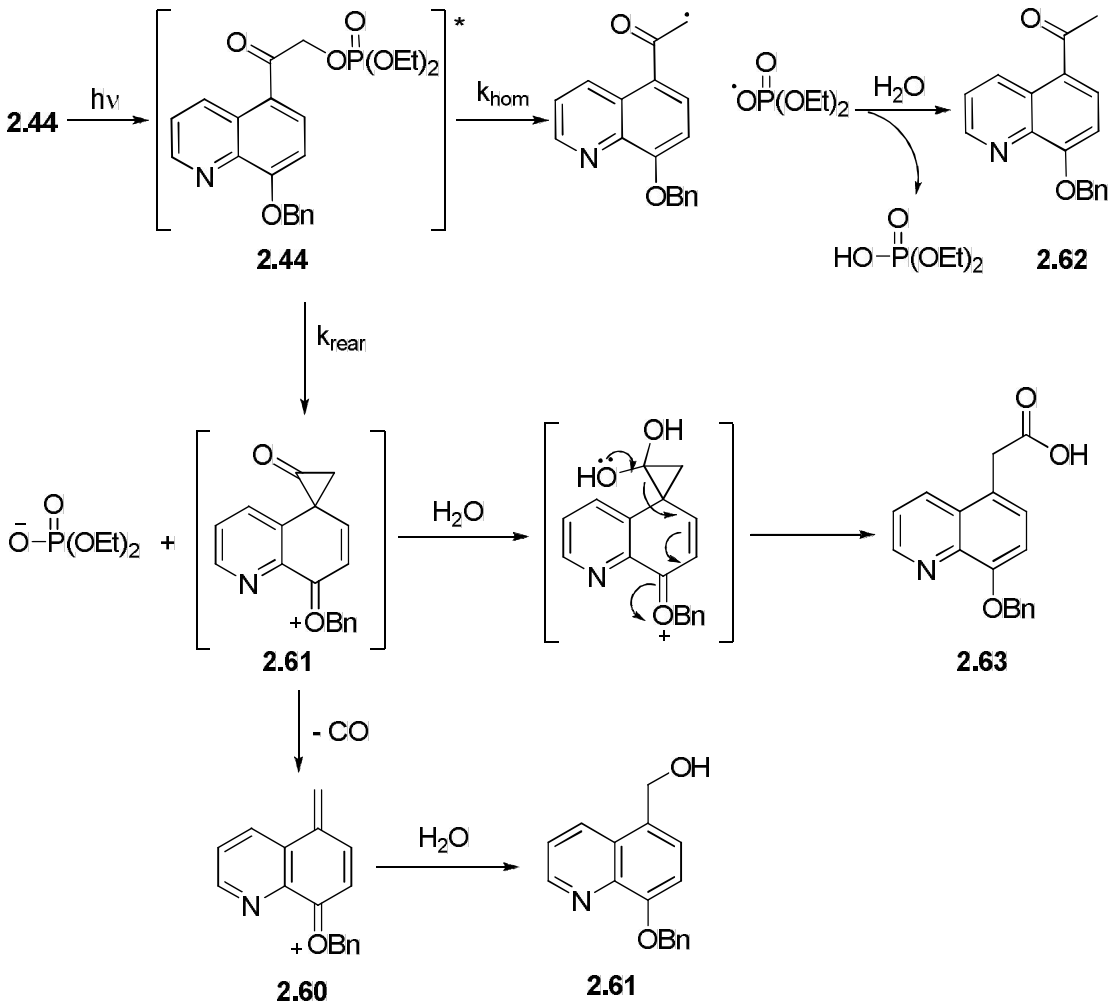

The quantum yield values for the photorelease of benzoic acid and diethyl phosphoric acid from HAQ benzoate **2.37** and BnHAQ-DEP **2.44** are three orders of magnitude lower than that of the corresponding known *p*HP derivatives and an order of magnitude lower than that those of the naphthalene-based phototrggers reported by Yousef and Givens.[31] There may be several reasons for the reduction of the quantum yields observed with HAQ derivatives. The intramolecular H-bonding of the phenolic hydrogen and the pyridine nitrogen in 5-acetyl-8-hydroxyquinoline (HAQ) noted above may be one of the major factors. Goldman and

Wehry[91] reported that singlet-triplet intersystem crossing is really inefficient for 8-hydroxyqunioline in various solvents including water and acetonitrile

The triplet energy of HAQ is similar to that of 1-acetylnaphthalene (ca. 57 kcal/mol)[96] and thus, even if intersystem crossing occurred, the energy of the resulting triplet may be too low for bond cleavage to compete with non-productive energy dispersal from the triplet state. The triplet energy of naphthalene (ca. 61 kcal/mol) drops by 2 kcal/mol with an introduction of an acetyl group at the 2-position.[41] The reported triplet energy of *p*-hydroxy acetophenone is 70.5 kcal/mol.[97] Therefore, the *p*HP group has excess triplet energy of 11.5 kcal/mol more than the 2-acetylnaphthalene. A similar trend could be expected for the HAQ series. In addition, it is known that 8-hydroxyquinoilne itself weakly fluoresces in the excited state due to excited state intramolecular proton transfer (ESIPT).[89-94] This effect could contribute to the lower quantum yields. The excess energy can dissipate via either non-radiative pathways or via phosphorescence,[95] thereby discouraging efficient bond lysis in the triplet excited state. These energy wasting exit channels are not as available to the *p*HP chromophore which reacts with higher quantum yields.

Future work

The photochemistry of diethyl 2-(8-hydroxyquinolin-5-yl)-2-oxoethyl phosphate (HAQ-DEP, **2.44)** revealed an effect by the free hydroxyl group on the photorelease of diethyl phosphoric acid. Time-resolved LFP studies of HAQ derivatives would be extremely informative in confirming the proposed mechanisms in this discussion. For example, especially under degassed conditions, the photochemical inertness of benzoate

esters **2.37** and **2.39** can be explained by examining the energy wasting processes in the excited state such as ESPT and ESIPT mechanisms.

Conclusions

The effective excitation wavelength range is an important criterion for selection of the proper photoremovable protecting group for successful applications in chemistry and biology. For biological applications, the system under study and the caged biomolecule may absorb and/or be photochemically activated by readiation in the mid UV range, < 300 nm. Our attempts to extend the range of the *p*-hydroxyphenacyl chromophore have shown that both substituents on the ring and expansion of the aromatic ring (i.e. naphthalene series) lead to lower quantum yields. This latest modification substituting 5-acetyl-8-hydroxyquinoline as the basic chromophore did move the absorption range into the visitble region. A series of caged derivatives with enhanced π-π^* absorption extending into the visible region were the subject of an exploratory photochemical and photophysical study. Photolysis of the benzoate series, however, gave unexpected results in aerated aqueous acetonitrile where photooxygenation of the chromophore was the sole reaction, producing a mixture of 2-(benzoyloxy)acetic acid and quinoline-5,8-dione. For the phosphate esters, however, release of diethyl phosphoric acid was realized. The efficiency of photorelease was three orders of magnitude lower compared to *p*HP-caged analogs.

8-Hydroxy-5-acetylquinoline as a photoreleasing chromophore is apparently limited to very good leaving groups (i.e. phosphates). Even with these, the chromophore is photochemically disintegrated during photorelease yielding a plethora of products. For poor leaving groups (i.e. benzoates), 5-acetyl-8-hydroxyquinoline self destructs by acting as a sensitizer of $^3O_2$ to form singlet oxygen. This degrades the chromophore to form a mixture of the 5,8-quinone and the α-substituted acetic acid of the substrate.

Experimental Methods

General Methods

All compounds were prepared by literature procedures unless indicated otherwise. All reagents were purchased from commercial sources (Aldrich, Acros Organics, Alfa Acer and Fisher) and used without further purification unless otherwise noted. Nitrobenzene and dichloromethane (DCM) were distilled prior to use. ^{1}H NMR spectra were recorded on a Bruker 400 MHz instrument unless otherwise noted. IR spectra were recorded on a Shimadzu FTIR-8400S spectrophotometer; results are reported in cm^{-1}. UV/vis spectra were recorded on a Cary 100 spectrophotometer (Varian, Inc., Palo Alto, CA). pH values of solutions were measured using a Fisher Science pH 510 meter calibrated with certified Fisher buffer solutions of pH 4, 7, and 10. HPLC analyses were performed with a C18 Econosphere 250 x 4.6 mm analytical column (Altech Associates, Inc., Deerfield, IL) connected to a Rainin dual pump system. Mass spectrometry was performed on a Sciex API-1 Plus quadrupole mass spectrometer with an electrospray ionization (ESI) source. Thin layer and column chromatography were performed on precoated silica gel plates (Sorbent Technologies, Atlanta, GA) and standard grade (32-63 μm) silica gel (Sorbent Technologies, Atlanta, GA), respectively. Melting points were determined on a Thomas-Hoover melting point apparatus (Arthur H. Thomas Company, PA) and are uncorrected.

5-Acetyl-8-hydroxyquinoline (2.35)

5-Acetyl-8-hydroxyquinoline (**2.35**) was prepared according to the method described by Matsumura[58] with some modifications. Acetyl chloride (1.14 g, 14.52 mmol) was added into a flame dried 3-neck round bottomed flask containing solution of 8-hydroxyquinoline (**2.34**, 2.0 g, 13.78 mmol) in nitrobenzene (15.3 mL, 149.4 mmol) under argon. Aluminum chloride

(11.50 g, 86.0 mmol) was added to the reaction mixture at a time with stirring. The reaction mixture was kept at 70 °C for 14 h in the 3-neck flask fitted with a $CaCl_2$ drying tube. On cooling, some crushed ice and 10% HCl (60 mL) were added and the nitrobenzene was removed by distillation. On standing overnight the separated hydrochloride of 5-acetyl-8-hydroxyquinoline was filtered. The residue was dissolved in water (50 mL) and sodium acetate (2.0 g) was added. The resulting crude product was recrystallized from hot water to afford 5-acetyl-8-hydroxyquinoline (**2.35**) as colorless hair-like needles (1.03 g, 5.51 mmol, 40% yield): mp 111-112 °C; ^{1}H NMR ($CDCl_3$) δ ppm 9.61-9.58 (1H, dd, J = 8.8 Hz, 1.2 Hz), 8.83-8.82 (1H, dd, J = 4.1 Hz, 1.2 Hz), 8.1.8 (1H, d, J = 8.2 Hz), 7.63-7.60 (1H, q, J = 4.2 Hz), 7.19 (1H, d, J = 8.2 Hz), 2.72 (3H, s); ^{13}C NMR (100 MHz, $CDCl_3$) δ (ppm) 199.5, 157.1, 148.6, 138.5, 136.7, 134.4, 127.6, 125.2, 124.6, 108.6, 29.2; IR (KBr, cm^{-1}) 3273(br), 1659, 1618, 1570, 1510, 1250, 835; UV/Vis (NH_4OAc, pH 7), λ_{max} (ε $Lmol^{-1}cm^{-1}$) 381 (3743), 301 (9345), 263 (15945), 240 (18465), 222 (13637); MS (ESI (+)) *m*/*z* calcd for $(C_{11}H_{10}NO_2 + H)^+$ 188.0711, found 188.0703.

2-Bromo-1-(8-hydroxyquinolin-5-yl)ethanone (2.36)

The method described by Babad et al.[69] was used with modifications. To a suspension of $AlCl_3$ (4.56 g, 34.44 mmol) in CH_2Cl_2 (12 mL) at reflux was added bromoacetyl chloride (1.34 mL, 16.53 mmol) in CH_2Cl_2 (3 mL) under an Ar atmosphere. The mixture was refluxed for 30 min at 50 °C. At this point, 8-hydroxyquinoline (**2.34**, 2.00 g, 3.78 mmol) in CH_2Cl_2 (5 mL) was added dropwise. The mixture was refluxed for 18 h and then carefully poured onto ice (50.0 g), water (10 mL), and CH_2Cl_2 (10 mL) with stirring. A yellow colored precipitate was obtained. 10% HCl (10 mL) was added to the reaction mixture resulting in a red colored precipitate that was suction filtered. After 48 h, the filtrate yielded a reddish-

yellow plate-like precipitate which was a mixture of 2-bromo-1-(8-hydroxyquinolin-5-yl)ethanone (**2.36**) and 2-chloro-1-(8-hydroxyquinolin-5-yl)ethanone (**2.38**,1.362 g, 45% overall yield). The crude product (500 mg) was dissolved in acetone (10 mL) and excess NaBr (1.34 g, 13.57 mmol) was added. The resulting mixture was refluxed for 12 h.[98] Water (10 mL) was added to the reaction mixture, which was then extracted with EtOAc (10 mL x 3), washed with water and brine, and dried over anhydrous $MgSO_4$. The solvent was evaporated to afford 2-bromo-1-(8-hydroxyquinolin-5-yl)ethanone (**2.36**) as a yellowish brown solid (474 mg, 1.78 mmol, 79% yield)), mp 122-125 °C (dec): ^{1}H NMR (400 MHz, $CDCl_3$) δ ppm 9.53-9.50 (1H, dd, *J* = 8.8 Hz, 1.3 Hz), 8.85-8.84 (1H, *J* = dd, 4.0 Hz, 1.4 Hz), 8.20 (1H, d, *J* = 8.2 Hz), 7.63-7.66 (1H, q, *J* = 4.2 Hz), 7.19 (1H, d, *J* = 8.2 Hz), 4.55 (2H, s); ^{13}C NMR (100 MHz, $CDCl_3$) δ (ppm) 191.9, 157.7, 148.6, 138.3, 136.1, 134.5, 127.9, 124.7, 121.4, 108.5, 32.6; IR (KBr, cm^{-1}) 2702(br), 1688, 1624, 1596; UV/Vis (CH_3CN), λ_{max} (ε $Lmol^{-1}cm^{-1}$) 328 (9140), 265 (5340), 240 (27700); MS (ESI (+)) m/*z* calcd for $(C_{11}H_8BrNO_2 + H)^+$ 265.9817 (^{79}Br) and 267.9817 (^{81}Br), found 265.9807 (^{79}Br) and 267.9758 (^{81}Br).

2-(8-Hydroxyquinolin-5-yl)-2-oxoethyl benzoate (2.37)

The benzoate ester was generated according to a method based upon a method used by Buu-Hoi et al.[71] 2-Bromo-1-(8-hydroxyquinolin-5-yl)ethanone (**2.36**, 474 mg, 1.78 mmol) was dissolved in mixture of 1,4-dioxane (5 mL) and CH_2Cl_2 (5 mL). Benzoic acid (326 mg, 2.67 mmol) was added, followed by DBU (325 mg, 2.14 mmol). The reaction mixture was stirred for 12 h. Water (5 mL) was added to the reaction mixture, which was extracted with EtOAc (10 mL x 5), washed sequentially with $NaHCO_3$ (10 mL x 3), brine (20 mL), and water (30 mL). The organic layer was dried over anhydrous $MgSO_4$ and the solvent was evaporated to afford 2-(8-hydroxyquinolin-5-yl)-2-oxoethyl benzoate (**2.37**) as a yellowish brown solid

(410 mg, 1.33 mmol, 75% yield): mp 176-179 °C; ^{1}H NMR ($CDCl_3$) δ ppm 9.54-9.52 (1H, dd, *J* = 8.8 Hz, 1.4 Hz), 8.84-8.82 (1H, dd, *J* = 4.2 Hz, 1.4 Hz), 8.18-8.16 (3H, m), 7.62-7.59 (2H, m), 7.51-7.47 (2H, m), 7.21 (1H, d, *J* = 8.2 Hz), 5.63 (2H, s); ^{13}C NMR (100 MHz, $CDCl_3$) δ (ppm) 192.6, 166.4, 157.5, 148.6, 138.3, 136, 133.6, 132.7, 130.2, 129.6, 128.7, 127.6, 124.6, 121.9, 108.5, 67.1; IR (KBr, cm^{-1}) 3414(br), 3300, 2924, 1724, 1682, 1566, 1506, 1450; UV/Vis (CH_3CN/H_2O), λ_{max} (ε $Lmol^{-1}cm^{-1}$) 384 (1620), 303 (2250), 264 (4920), 239 (5200); MS (ESI (+)) *m*/*z* calcd for $(C_{18}H_{13}NO_4 + H)^+$ 308.0923, found 308.0905.

2-(Benzoyloxy)acetic acid (2.46)

The general method of Shieh and Kuo[74] was followed. Glycolic acid (649 mg, 8.54 mmol) was dissolved in dry pyridine (5 mL). Benzoyl chloride (1.0 g, 7.11 mmol) was added dropwise. The reaction mixture was stirred overnight under Ar. Water (10 mL) and EtOAc (10 mL) were added to the reaction mixture. The EtOAc layer was separated, and the water layer was extracted with EtOAc (10 mL x 2). The combined organic layers were washed sequentially with 10% HCl (20 mL x 3), $NaHCO_3$ (20 mL x 3), and water (30 mL). The organic layer was dried over anhydrous $MgSO_4$. The solvent was evaporated, and the white residue was purified by flash chromatography with EtOAc/hexane (1:1) to afford 2-(benzoyloxy)acetic acid (**2.46**) as a white solid (886 mg, 4.92 mmol, 69% yield): mp 109-111 °C; ^{1}H NMR (500 MHz, $CDCl_3$) δ ppm 8.12-8.09 (2H, m), 7.63-7.59 (1H, m), 7.50-7.46 (2H, m), 4.92 (2H, s); ^{13}C NMR (125 MHz, $CDCl_3$) δ (ppm) 173.1, 166.1, 133.8, 130.2, 129.1, 128.7, 60.8; IR (KBr, cm^{-1}) 2952(br), 1720, 1601, 1452, 1435, 905, 721, 708; UV/Vis (CH_3CN/H_2O), λ_{max} (ε $Lmol^{-1}cm^{-1}$) 273 (976), 229 (11400); MS (ESI (-)) *m*/*z* calcd for $(C_9H_8O_4 - H)^+$ 179.0344, found 179.0347.

Quinoline-5,8-dione (2.47)

The general method of Barret and Dudon[75] was applied. Iodobenzenediacetate [$PhI(OAc)_2$] (446 mg, 1.52 mmol) was dissolved in CH_3CN (2 mL) and water (1 mL) at 0 °C. 8-Hydroxyquinoline (**2.34**, 100 mg, 0.69 mmol), which was dissolved in CH_3CN (2 mL) and water (1 mL), was added dropwise at 0 °C. The reaction mixture was stirred for 3 h at 0 °C. The resulting yellowish orange color aqueous solution was extracted with EtOAc (8 mL x 5). The combined organic layers were washed with brine and water, and dried over anhydrous $MgSO_4$. The solvent was evaporated to afford quinoline-5,8-dione (**2.47**) as a yellowish orange solid (104 mg, 0.66 mmol, 95% yield): mp 95-107 °C (dec); ^{1}H NMR ($CDCl_3$) δ ppm 9.09-9.07 (1H, dd, *J* = 4.7 Hz, 1.7 Hz), 8.46-8.44 (1H, dd, *J* = 7.9 Hz, 1.7 Hz), 7.74-7.71 (1H, q, *J* = 4.7 Hz), 7.19-7.17 (1H, d, *J* = 10.4 Hz), 7.10-7.07 (1H, d, *J* = 10.4 Hz); ^{13}C NMR (100 MHz, $CDCl_3$) δ (ppm) 184.7, 183.4, 155, 147.6, 139.3, 138.2, 134.8, 129.3, 128.09; IR (KBr, cm^{-1}) 3431(br), 2962, 1670, 1580, 1385, 802; UV/Vis (CH_3CN/H_2O), λ_{max} (ε $Lmol^{-1}cm^{-1}$) 238 (45600); MS (ESI (+)) *m/z* calcd for $(C_9H_5NO_2 + H)^+$ 160.0398, found 160.0396

2-(8-Benzyloxy)quinolin-5-yl)-2-oxoethyl benzoate (2.39)

The target molecule was synthesized according to the general method used by Iwakuma et al.[72] with some modifications. 2-(8-Hydroxyquinolin-5-yl)-2-oxoethyl benzoate (**2.37**, 200 mg, 0.65 mmol) was dissolved in DMF (10 mL). K_2CO_3 (225 mg, 1.63 mmol) was added and the reaction mixture was stirred for 30 min. Benzyl bromide (78 μL, 1.63 mmol) was slowly added dropwise. The reaction mixture was stirred for 12 h and concentrated, and water (10 mL) was added. The aqueous mixture was extracted with EtOAc (10 mL x 4), washed with brine and water, dried over anhydrous $MgSO_4$. The solvent was evaporated, and the residue was purified by flash chromatography with EtOAc/hexane (1:1) to afford 2-(8-

benzyloxy)quinolin-5-yl)-2-oxoethyl benzoate (**2.39**) as a yellowish brown solid (260 mg, 0.65 mmol, 100% yield): mp 120-126 °C (dec); ^{1}H NMR ($CDCl_3$) δ ppm 9.43-9.41 (1H, dd, *J* = 8.8 Hz, 1.5 Hz), 9.04-9.03 (1H, dd, *J* = 4.0 Hz, 1.5 Hz), 8.16-8.13 (2H, m), 8.03 (1H, d, *J* = 8.3 Hz), 7.63-7.57 (2H, m), 7.53-7.46 (4H, m), 7.41-7.31 (3H, m), 7.05 (1H, d, *J* = 8.4 Hz), 5.55 (4H, s); ^{13}C NMR (100 MHz, $CDCl_3$) δ (ppm) 193, 166.4, 158.7, 150, 136, 135.3, 135.3, 133.6, 131.2, 130.2, 129.6, 129, 128.7, 128.4, 128.3, 127.3, 124, 123.5, 108.1, 71.3, 67.2; IR (KBr, cm^{-1}) 3433 (br), 2924, 2853, 1720, 1676, 1601, 825, 758; UV/Vis (CH_3CN/H_2O), λ_{max} (ε $Lmol^{-1}cm^{-1}$) 319 (8010), 238 (24000), 210 (10200); MS(ESI (+)) m/z calcd for $(C_{25}H_{19}NO_4 + H)^+$ 398.1392, found 398.1392; *m/z* calcd for $(C_{25}H_{19}NO_4 + Na)^+$ 420.1212, found 420.1213.

1-(8-(Benzyloxy)quinolin-5-yl)ethanone (2.41)

The general procedure of Iwakuma et al.[72] was utilized. 5-Acetyl-8-hydroxyquinoline (**2.35**, 100 mg, 0.53 mmol) was dissolved in DMF (5 mL). K_2CO_3 (185 mg, 1.34 mmol) was added and the reaction mixture was stirred for 30 min. Benzyl bromide (64 μL, 0.53 mmol) was slowly added dropwise. The reaction mixture was stirred for 24 h and concentrated, and water (5 mL) was added. The aqueous mixture was extracted with EtOAc (8 mL x 4), washed with brine and water, dried over anhydrous $MgSO_4$. The solvent was evaporated, and the residue was purified by flash chromatography with EtOAc/hexane (1:1) to afford 1-(8-(benzyloxy)quinolin-5-yl)ethanone (**2.41**) as a yellowish brown solid (300 mg, 1.08 mmol, 100% yield): mp 124-127 °C (dec); ^{1}H NMR ($CDCl_3$) δ ppm 9.44-9.41 (1H, dd, *J* = 8.8 Hz, 1.5 Hz), 8.96-8.95 (1H, dd, *J* = 3.8 Hz, 1.4 Hz), 7.96 (1H, d, *J* = 8.3 Hz), 7.53-7.49 (1H, q, *J* = 4.1 Hz), 7.47 (1H, d, *J* = 7.3 Hz), 6.94 (1H, d, *J* = 8.3 Hz), 5.47 (2H, s), 2.62 (3H, s); ^{13}C NMR (125 MHz, $CDCl_3$) δ (ppm) 199.3, 158, 149.6, 140.1, 136.2, 135.8, 132.5, 129, 128.3,

128.1, 127.7, 126.4, 123.7, 71.4, 29.1; IR (KBr, cm^{-1}) 3430 (br), 1653, 1560, 1502; UV/Vis (CH_3CN), λ_{max} (ε $Lmol^{-1}cm^{-1}$) 315 (6950), 240 (20100), 208 (14500); MS(ESI (+)) *m*/*z* calcd for $(C_{18}H_{15}NO_2 + H)^+$ 278.1181, found 278.1177.

2-(8-Benzyloxy)quinolin-5-yl)-2,2-dimethoxyethanol (2.42)

The target compound was synthesized according to the general method of Recuero et al.[73] To a solution of KOH (248 mg, 4.43 mmol) in MeOH (4 mL), a solution of 1-(8-(benzyloxy)quinolin-5-yl)ethanone (**2.35**, 154 mg, 0.55) in MeOH (4 mL) was slowly added at 0 °C followed by iodobenzenediacetate (244 mg, 0.83 mmol) in small portions over one minute. The mixture was allowed to come to room temperature and stirred for 24 h. The reaction mixture was concentrated, suspended in EtOAc and extracted with water (10 mL x 2). The aqueous layer was extracted with EtOAc (5 mL x 5) and the combined organic layers were washed with brine and water, and dried over anhydrous $MgSO_4$. The solvent was evaporated, and the residue was purified by flash chromatography with EtOAc/hexane (1:1) to afford 2-(8-benzyloxy)quinolin-5-yl)-2,2-dimethoxyethanol (**2.42**) as a yellowish brown solid (168 mg, 0.50 mmol, 90% yield): mp 168-176 °C (dec); ^{1}H NMR ($CDCl_3$) δ ppm 8.92-8.90 (dd, 1H, 4.1 Hz, 1.1 Hz), 8.86-8.84 (1H, dd, 8.8 Hz, 1.6 Hz), 7.81 (1H, d, J = 8.3 Hz), 7.53 (2H, d, J = 7.2 Hz), 7.45-7.42 (1H, q, J = 4.1 Hz), 7.40-7.31 (3H, m), 6.98 (1H, d, J = 8.4 Hz), 5.42 (2H, s), 3.95 (2H, s), 3.27 (6H, s); ^{13}C NMR (125 MHz, $CDCl_3$) δ (ppm) 154.6, 148.7, 140.4, 136.8, 133.5, 129, 128.8, 128.1, 127.5, 126.9, 125.9, 121.6, 108.7, 102.7, 70.8, 64, 49; IR (KBr, cm^{-1}) 3412(br), 3313, 2934, 1508, 1458, 1385, 825; UV/Vis (CH_3CN), λ_{max} (ε $Lmol^{-1}cm^{-1}$) 311 (4450), 240 (25000), 202 (32200); MS (ESI (+)) *m*/*z* calcd for $(C_{20}H_{21}NO_4 + H)^+$ 340.1549, found 340.1539; calcd for $(C_{20}H_{21}NO_4 + Na)^+$ 362.1369, found 362.1383 .

1-(8-Benzyloxy)quinolin-5-yl)-2-hydroxyethanone (2.43)

2-(8-Benzyloxy)quinolin-5-yl)-2,2-dimethoxyethanol (**2.42**, 168 mg, 0.49 mmol) was dissolved in 50% CH_3COOH (10 mL). 10% HCl (4 mL) was added. The resulting mixture was stirred 12 h. The reaction mixture was made basic with solid $NaHCO_3$. The aqueous layer was extracted with EtOAc (10 mL x 5). The combined organic layers were washed with brine and water, and dried over anhydrous $MgSO_4$. The solvent was evaporated, and the residue was purified by flash chromatography with EtOAc/hexane (1:1) to afford 1-(8-benzyloxy)quinolin-5-yl)-2-hydroxyethanone (**2.43**) as a yellowish brown solid (142 mg, 0.48 mmol, 98% yield): mp 53-55 °C; ^{1}H NMR ($CDCl_3$) δ ppm 9.57 (1H, d, *J* = 8.6 Hz), 9.06 (1H, d, J = 4.1 Hz), 7.92 (1H, d, *J* = 8.2 Hz), 7.62 (1H, q, *J* = 5.9 Hz), 7.50 (1H, d, *J* = 7.3 Hz), 7.39-7.29 (3H, m), 7.03 (1H, d, *J* = 8.2 Hz), 5.53 (2H, s), 4.86 (2H, s); ^{13}C NMR (125 MHz, $CDCl_3$) δ (ppm) 198.5, 159.3, 150.1, 140.4, 135.9, 135.1, 131.6, 129.1, 128.3, 128.2, 127.3, 124.4, 122.3, 108.2, 71.4, 65.8; IR (KBr, cm^{-1}) 3431 (br), 3277, 2924, 1670, 1601, 1564, 1506, 1385, 1315, 794; UV/Vis (CH_3CN), λ_{max} (ε $Lmol^{-1}cm^{-1}$) 322 (6230), 240 (17100); MS (ESI (+)) *m*/*z* calcd for $(C_{18}H_{15}NO_3 + H)^+$ 294.1130, found 294.1130; calcd for $(C_{18}H_{15}NO_3 + Na)^+$ 316.0950, found 316.0952.

2-(8-(Benzyloxy)quinolin-5-yl)-2-oxoethyl diethyl phosphate (2.44)

The general method of Ma et al.[66] was followed. Under an Ar atmosphere, 1-(8-benzyloxy)quinolin-5-yl)-2-hydroxyethanone (**2.43**, 159 mg, 0.54 mmol) was dissolved in pyridine (5 mL). Diethyl chlorophosphate (166 μL, 1.15 mmol) was slowly added dropwise at -5 °C. Reaction mixture was allowed to come to room temperature and stirred for 24 h. EtOAc (10 mL) and water (10 mL) were added to the reaction mixture. The EtOAc layer was separated. The aqueous layer was extracted with EtOAc (10 mL x 3) and the combined

organic layers were washed with brine and water, and dried over anhydrous $MgSO_4$. The solvent was evaporated, and the residue was purified by flash chromatography with the gradient solvent system of 100% hexane, EtOAc/hexane (1:1), EtOAc/hexane (2:1), EtOAc/hexane (3:1), 100% EtOAc, and 10% MeOH in EtOAc to afford 2-(8-(benzyloxy)quinolin-5-yl)-2-oxoethyl diethyl phosphate (**2.44**) as a yellowish brown solid (70 mg, 0.16 mmol, 30% yield): mp 98-101 °C; ^{1}H NMR ($CDCl_3$) δ ppm 9.37 (1H, d, J = 8.7 Hz), 9.01 (1H, d, J = 3.2 Hz), 7.88 (1H, d, J = 8.3 Hz), 7.58-7.55 (1H, q, J = 3.7 Hz), 7.48 (2H, d, J = 7.5 Hz), 7.37-7.29 (3H, m), 6.99 (1H, d, J = 8.3), 5.50 (2H, s), 5.24 (2H, d, J = 10.2), 4.22-4.15 (4H, m), 1.35-1.31 (6H, m); ^{31}P NMR ($CDCl_3$) δ ppm -0.13; ^{13}C NMR (100 MHz, $CDCl_3$) δ (ppm) 193.1, 158.7, 150, 140.4, 135.9, 134.9, 131.2, 129, 128.4, 128.2, 127.2, 124, 123.1, 107.9, 71.2, 69.2, 64.5, 16.3-16.2; IR (KBr, cm^{-1}) 3416(br), 2984, 1686, 1599, 1560, 1502; UV/Vis (CH_3CN/H_2O), λ_{max} (ε $Lmol^{-1}cm^{-1}$) 321 (8370), 240 (20100), 208 (13400); MS (ESI (+)) *m/z* calcd for $(C_{22}H_{24}NO_6P + H)^+$ 430.1419, found 430.1414.

Bis-[2-(8-hydroxyquinolin-5-yl)-2-oxoethyl benzoate] zinc(II) dihydrate (2.40)

The target zinc chelated compound was generated according to the method of Sharma et al.[55] Under an Ar atmosphere, 2-(8-hydroxyquinolin-5-yl)-2-oxoethyl benzoate (**2.37**, 62 mg, 0.20 mmol) was dissolved in THF (10 mL). Diethylzinc (180 µL, 0.101 mmol) was added via syringe. A yellow solution with green fluorescence was visible immediately. The reaction mixture was stirred at room temperature for 48 h. The solvent was evaporated, and the yellow residue was recrystallized from hot acetone with the addition of hexanes until the cloud point was reached to generate bis-[2-(8-hydroxyquinolin-5-yl)-2-oxoethyl benzoate] zinc(II) dihydrate (**2.40**) as a yellow solid (60 mg, 0.08 mmol, 83% yield), mp 303-310 °C (dec): ^{1}H NMR (DMSO) δ ppm 9.74 (1H, d, J = 8.8 Hz), 8.63 (1H, d, J = 3.1 Hz), 8.32 (1H,

d, J = 8.8 Hz), 8.07-8.05 (2H, m), 7.75-7.70 (2H, m), 7.60-7.56 (2H, m), 6.74 (1H, d, J = 8.6 Hz), 5.70 (2H, s), 3.34 (H_2O, s); ^{13}C NMR (100 MHz, DMSO) δ (ppm) 189.8, 169.3, 165.5, 145.2, 139.6, 137.4, 136.82, 133.4, 129.6, 129.3, 129.1, 128.8, 124.4, 111, 110.9, 66.9; IR (KBr, cm^{-1}) 3436(br), 3101, 2943, 1718, 1691, 1385, 1288. UV/Vis (DMSO), λ_{max} (ε $Lmol^{-1}cm^{-1}$) 399 (15200), 300 (18700), 262 (32900); MS (ESI (+)) *m/z* calcd for $(C_{36}H_{28}N_2O_{10}Zn + H)^+$ 713.1113, found 713.1106.

Photochemistry

General methods:

Photolyses were performed in a Rayonet RPR-100 photochemical reactor (Southern New England Ultraviolet Company, Branford, CT) fitted with a merry-go-round apparatus and with 16 x 350 nm (RPR 3500 Å) or 16 x 300 nm (RPR 3000 Å) lamps. The Rayonet reactor was turned on to warm up the lamps for 15 minutes prior to irradiation of the sample. Samples were irradiated in NMR tubes or Pyrex test tubes at 40 – 45 °C in the Rayonet reactor in the presence or absence of oxygen. The tubes were placed in a RPR merry-go-round apparatus and a counter was started at the onset of exposure to record the time of irradiation. Exposure times were controlled by manual removal of the sample from the reactor or alternately by turning the lamps on or off. The light output for the determination of quantum efficiencies was measured by using the potassium ferrioxalate method.[99] Photolysis samples were analyzed using ^1H NMR and RP-HPLC methods. Dimethylformamide (DMF, 2 μL, 2.58 x 10^{-2} mmol) was used as an internal standard in ^1H NMR analyses. HPLC analyses were performed with a C18 Econosphere 250 x 4.6 mm analytical column (Altech Associates, Inc., Deerfield, IL) connected to a Rainin dual pump system. The solvent system

for the separation was 70% CH_3CN and 30% H_2O with 0.1% H_3PO_4. The detection wavelength was 238 nm and flow rate was 1.0 mL/min. Each sample was run three times.

Photolysis of 2-(8-hydroxyquinolin-5-yl)-2-oxoethyl benzoate (2.37)

An NMR tube was charged with 2-(8-hydroxyquinolin-5-yl)-2-oxoethyl benzoate (3.0 mg, 0.01 mmol) dissolved in CD_3CN (900 μL), D_2O (100 μL), and DMF (2 μL, 2.58 x 10^{-2} mmol) and the contents mixed thoroughly. The resulted sample was photolyzed without degassing at 300 or 350 nm with 16 x 3000 Å or 16 x 3500 Å lamps and ^1H NMR spectra (16 scans) were collected after 0, 30, 60, 90, and 120 min of photolysis. The depletion of 2-(8-hydroxyquinolin-5-yl)-2-oxoethyl benzoate (and the appearance of released 2-(benzoyloxy)acetic acid (**2.46**) were quantified from the NMR integrations of the methylene signals at δ 5.63 and 4.78 ppm, respectively. The results are shown in Table 2.3.

Photolysis of 2-(8-benzyloxy)quinolin-5-yl)-2-oxoethyl benzoate (2.39)

An NMR tube was charged with 2-(8-benzyloxy)quinolin-5-yl)-2-oxoethyl benzoate (4.0 mg, 0.01 mmol) dissolved in CD_3CN (900 μL), D_2O (100 μL), and DMF (2 μL, 2.58 x 10^{-2} mmol) and the contents mixed thoroughly. The sample was photolyzed without degassing at 300 or 350 nm with 16 x 3000 Å or 16 x 3500 Å lamps and ^1H NMR spectra (16 scans) were collected after 0, 30, 60, 90, and 120 min of photolysis. The depletion of 2-(8-benzyloxy)quinolin-5-yl)-2-oxoethyl benzoate and the appearance of released 2-(benzoyloxy)acetic acid (**2.46**) were quantified from the integrations of the methylene signals at δ 5.63 and 4.78 ppm, respectively. The results are shown in Table 2.3.

Photolysis of 2-(8-(benzyloxy)quinolin-5-yl)-2-oxoethyl diethyl phosphate (2.44)

An NMR tube was charged with 2-(8-(benzyloxy)quinolin-5-yl)-2-oxoethyl diethyl phosphate (5.0 mg, 0.01 mmol) dissolved in CD_3CN (900 μL), D_2O (100 μL), and DMF (2 μL, 2.58 x 10^{-2} mmol). The sample was photolyzed at 300 or 350 nm without degassing with 16 x 3000 Å or 16 x 3500 Å lamps and ^1H NMR spectra (16 scans) were collected after 0, 30, 60, 90, 120 min of photolysis. The depletion of 2-(8-(benzyloxy)quinolin-5-yl)-2-oxoethyl diethyl phosphate (**2.44**) and the appearance of released diethyl phosphate were quantified from the integrations of the methylene signals at δ 5.29-5.31 ppm and 3.86-3.92 ppm, respectively.

Photolysis of 2.37, 2.39, 2.40, and 2.44 under degas conditions

The above mentioned general procedures were repeated in degassed conditions. In these experiments, photolysis samples were purged with argon for 30 min before running the photolysis. The results are shown in Table 2.3.

Photolysis of 2-(8-hydroxyquinolin-5-yl)-2-oxoethyl benzoate (2.37); Quantum Efficiency Determination by RP-HPLC

A biphenyl stock solution (internal standard) was prepared by dissolving biphenyl (160 mg, 1.04 mmol) in HPLC grade CH_3CN (90 mL) in a 100 mL volumetric flask and diluted to the mark with HPLC grade H_2O (10 mL). A quartz tube was charged with 2-(8-hydroxyquinolin-5-yl)-2-oxoethyl benzoate (10 mg, 0.03 mmol) could was dissolved in HPLC grade CH_3CN (1.8 mL) and H_2O (0.2 mL). Biphenyl (2.0 mL from the stock solution, 3.2 mg, 0.02 mmol) was added to the quartz tube as an internal standard and the contents were mixed thoroughly. The sample was irradiated at 350 nm with 16 x 3500 Å lamps and sample aliquots (50 μL) were collected after 0, 20, 30, 40, and 50 min of photolysis. Each sample aliquot was diluted

with 150 μL of HPLC grade CH_3CN/H_2O, 9:1, and analyzed by RP-HPLC. The depletion of the starting material was quantified using average peak areas from three injections of each aliquot corresponding to the average peak areas of the internal standard. A scatter plot was created by using mmol of 2-(8-hydroxyquinolin-5-yl)-2-oxoethyl benzoate (**2.37**) vs, irradiation time. The slope (*m*) of the best fit line from the linear regression analysis was determined. The light output (*L*) of the 16 x 3500 Å lamps in the photoreactor was determined using the potassium ferrioxalate method[99] in units of millieinsteins per minute. The quantum yield (Φ) in milliinsteins (mE)/mM for the disappearance of 2-(8-hydroxyquinolin-5-yl)-2-oxoethyl benzoate was then calculated as follows.

$$\Phi = |m| / L$$

Where *m* is the slope of the plot and L is the light output from lamps which were used in the actinometry. Results are shown in Table 2.3.

Photolysis of 2-(8-hydroxyquinolin-5-yl)-2-oxoethyl benzoate (2.37): Photoproduct analysis by HPLC

A quartz tube was charged with 2-(8-hydroxyquinolin-5-yl)-2-oxoethyl benzoate (40 mg, 0.12 mmol) which was dissolved in HPLC grade CH_3CN (3.6 mL) and H_2O (0.4 mL). The sample was irradiated at 350 nm with 16 x 3500 Å lamps and sample aliquots (50 μL) were collected after 0, 30, 60, 90, and 120 min of photolysis. Each sample aliquot was diluted with 450 μL of HPLC grade CH_3CN/H_2O, 9:1, and was analyzed by RP-HPLC. After 120 min, the photolysis sample became yellowish orange in color. This sample was concentrated and dissolved in EtOAc (30 mL). The organic layer was extracted with saturated $NaHCO_3$ (20 mL x 3). The organic layer was concentrated to produce a yellow solid. This residue was chromatographed on silica gel (hexane/EtOAc, 1:1) to separate the compounds. All attempts

to isolate products from the column were unsuccessful. The combined aqueous layers ($NaHCO_3$ aliquots) were acidified with 10% HCl solution. The aqueous phase was extracted with EtOAc (25 mL x 3) and the organic phase was washed with brine and water, and dried over anhydrous $MgSO_4$. The solvent was evaporated, and the yellow residue purified by flash chromatography with EtOAc/hexane (1:1) to afford a white solid which was characterized by NMR and MS spectroscopy: ^{1}H NMR (500 MHz, $CDCl_3$) δ ppm 8.12-8.09 (2H, m), 7.63-7.59 (1H, m), 7.50-7.46 (2H, m), 4.92 (2H, s); ^{13}C NMR (125 MHz, $CDCl_3$) δ (ppm) 173.1, 166.1, 133.8, 130.2, 129.1, 128.7, 60.8; MS (ESI (-)) *m/z* calcd for $(C_9H_8O_4 - H)^+$ 179.0344, found 179.0347. The resulting acid **2.46** was dissolved in CH_3CN/H_2O, 9:1, and analyzed by RP-HPLC using the same conditions described above. This compound gave the same retention time as one of the photoproducts. Co-injection with the photolysis mixture produced a peak with the same retention time as the synthetic derivative. The ^{1}H NMR spectrum of this compound in $CDCl_3$ gave a characteristic methylene singlet at 4.92 ppm. The analysis of photoproducts by ^{1}H NMR of 2-(8-hydroxyquinolin-5-yl)-2-oxoethyl benzoate **2.37** gave the same peak. TLC analysis with EtOAc of the photolyzed sample also indicated the presence of this new compound. The generation of 2-(benzoyloxy)acetic acid upon the photolysis of 2-(8-hydroxyquinolin-5-yl)-2-oxoethyl benzoate **2.39** with air, was confirmed by NMR and mass spectroscopy. Hence, the other major photoproduct which contributes to the developing orange color in the course of the photolysis is quinoline-5,8-dione (**2.47**). This photoproduct was synthesized separately as described above and dissolved in CH_3CN/H_2O, 9:1, and analyzed by HPLC using the same conditions described above. It gave a very sharp peak which has the same retention time with one of the photoproducts. Co-injection with the photolysis sample confirmed the generation of quinoline-5,8-dione (**2.47**)

as one of the photoproducts from the reaction. The same experiment was repeated with 2-(8-benzyloxy)quinolin-5-yl)-2-oxoethyl benzoate (**2.39**).

Photolysis of 2-(8-hydroxyquinolin-5-yl)-2-oxoethyl benzoate (2.37): Photoproduct Analysis by ^{1}H NMR

An NMR tube was charged with 2-(8-hydroxyquinolin-5-yl)-2-oxoethyl benzoate (**2.37**, 10 mg, 0.03 mmol) and dissolved in CD_3CN (900 μL) and D_2O (100 μL). The contents were mixed thoroughly. The resulted sample was photolyzed with air at 300 or 350 nm with 16 x 3000 Å or 16 x 3500 Å lamps and ^{1}H NMR spectra (16 scans) were collected after 60 min of photolysis. The depletion of 2-(8-hydroxyquinolin-5-yl)-2-oxoethyl benzoate (**2.37**) and the appearance of released 2-(benzoyloxy)acetic acid (**2.46**) were characterized from the NMR signals (methylene hydrogens) at δ 5.63 and 4.78 ppm, respectively. The photolysis sample was divided into two fractions (500 μL each). One fraction was spiked with an authentic sample of 2-(benzoyloxy)acetic acid (**2.46**) which was synthesized as described in the Experimental section. A dramatic increase in the intensity of the methylene peak at 4.78 ppm confirmed the formation of 2-(benzoyloxy)acetic acid (**2.46**) during the photolysis. The other major photoproduct, the one which explains the color change in the photolysis solution, should be quinoline-5,8-dione (**2.47**). This photoproduct was synthesized separately as described above and used to spike the photolyzed sample which was analyzed by ^{1}H NMR. A dramatic increase of the intensity of two characteristic new peaks (at 7.20 and 7.22 ppm) in the NMR spectrum that belonged to the two olefinic hydrogens of quinoline-5,8-dione (**2.47**) confirmed the formation of this quinoline.

Photolysis of 2-(8-benzyloxy)quinolin-5-yl)-2-oxoethyl benzoate (2.39): Photoproduct Analysis by ^{1}H NMR

The same experiment was repeated with 2-(8-benzyloxy)quinolin-5-yl)-2-oxoethyl benzoate (**2.39**).

Photolysis of bis-[2-(8-hydroxyquinolin-5-yl)-2-oxoethyl benzoate] zinc(II) dihydrate (2.40)

An NMR tube was charged with bis-[2-(8-hydroxyquinolin-5-yl)-2-oxoethyl benzoate] zinc(II) dihydrate (4.0 mg, 0.01 mmol) dissolved in CD_3CN (900 μL), D_2O (100 μL), and DMF (2 μL, 2.58 x 10^{-2} mmol). The sample was photolyzed without degassing at 300 or 350 nm with 16 x 3000 Å or 16 x 3500 Å lamps and ^{1}H NMR spectra (16 scans) were collected after 0, 30, 60, 90, 120 min and 5 h of photolysis. The depletion of bis-[2-(8-hydroxyquinolin-5-yl)-2-oxoethyl benzoate] zinc(II) dihydrate and the appearance of released 2-(benzoyloxy)acetic acid (**2.46**) were quantified from the integrations of the signals at δ 5.63 and 4.78 ppm, respectively. The results are shown in Table 2.3.

Photolysis of 2-(8-(benzyloxy)quinolin-5-yl)-2-oxoethyl diethyl phosphate (2.44): Photoproduct Analysis by ^{1}H NMR

An NMR tube was charged with 2-(8-(benzyloxy)quinolin-5-yl)-2-oxoethyl diethyl phosphate (10 mg, 0.02 mmol) which was dissolved in CD_3CN (900 μL) and D_2O (100 μL). The contents were mixed thoroughly and the resulting sample was photolyzed with air or under Ar purged conditions at 300 or 350 nm with 16 x 3000 Å or 16 or 3500 Å lamps. The ^{1}H NMR spectra (16 scans) were collected after 60 min of photolysis and used to calculate the percent conversion. The depletion of 2-(8-(benzyloxy)quinolin-5-yl)-2-oxoethyl diethyl phosphate and the appearance of released diethyl phosphoric acid were determined from the

NMR signals (methylene hydrogen for the phosphate ester **2.44** and methylene hydrogens of diethyl phosphoric acid) at δ 5.29-5.31 ppm and 3.87-3.90 ppm, respectively. The photolysis sample was spiked with the authentic sample of diethyl phosphoric acid which was synthesized separately from commercially available diethyl chlorophosphate.[76] A dramatic increase in the intensities of the new methylene peak at 3.87-3.90 ppm and the new methyl peak at 1.16-1.22 ppm confirmed the formation of diethyl phosphoric acid.

Control Experiments with the 2-(8-hydroxyquinolin-5-yl)-2-oxoethyl benzoate series 2.37 and 2.39; Dark Reaction

An NMR tube was charged with 2-(8-hydroxyquinolin-5-yl)-2-oxoethyl benzoate **(2.37**, 5.0 mg, 0.02 mmol) dissolved in CD_3CN (900 μL) and D_2O (100 μL). The contents were mixed thoroughly and warmed in a water bath at 40 °C in the dark for 2 h. ^1H NMR spectra were recorded before and after heating. There was no significant change before and after the heating. The sample was kept another 48 h in the dark and the ^1H NMR spectrum was recorded. No significant difference was observed.

Control Experiments with 2-(8-(benzyloxy)quinolin-5-yl)-2-oxoethyl diethyl phosphate (2.44); Dark Reaction

An NMR tube was charged with 2-(8-(benzyloxy)quinolin-5-yl)-2-oxoethyl diethyl phosphate (10.0 mg, 0.02 mmol) and dissolved in CD_3CN (900 μL) and D_2O (100 μL). The contents were mixed thoroughly and warmed in a water bath at 40 °C in the dark for 2 h. ^1H NMR spectra were recorded before and after the heating. There was no significant change after the heating. The sample was kept another 48 h in the dark and the ^1H NMR spectrum was recorded. No significant difference was observed.

References:

1. Dore, T. M. In *Dynamic Studies in Biology: Phototriggers, photoswitches and caged Biomolecules*: Givens, R. S. Goeldner, M., Eds.; Wiley-VCH: Weinheim, Germany, **2005**.
2. Pelliccioli, A. P.; Wirz, J. *Photochem, Photobiol. Sci*. **2002**, *1*, 441-458.
3. Protti, S.; Fagnoni, M. *Chem. Commun*. **2008**, 3611-3622.
4. Givens, R. S.; Conard, P. G., II; Yosef, A. L.; Lee, J, -I. In *CRC Handbook of* Organic Photochemistry and Photobiology; 2nd Ed.; CRC press, New York, **2004**.
5. Ni, J.; Auston, D. A.; Frelich, D. A.; Muralidharan, S.; Sobie, E. A.; Kao, J. P. Y. *J. Am. Chem. Soc*. **2007**, *129*, 5316-5317.
6. Stensrud, K.; Noh, J.; Kandler, K.; Wirz, J.; Heger, D.; Givens, R. S. *J. Org. Chem.* **2009**, *74*, 5219-5227.
7. Parkesh, R.; Vasudevan, S. R.; Berry, A.; Galione, A.; Dowden, J.; Churchill, G. C. *Org. Biomol. Chem*. **2007**, *5*, 441-443.
8. Furuta, T.; Torigai, H.; Sugimoto, M.; Iwamura, M. *J. Org. Chem*. **1995**, *60*, 3953-3956.
9. Bendig, J.; Helm, S.; Hagen, V. *J. Fluoresc*. **1997**, *7*, 357-361.
10. Willenbucher, R. F.; Xie, Y. N.; Eysselein, V. E.; Snape, W. J., Jr. *Am. J. Physio*. **1992**, *262*, G159-G164.
11. Ostap, E. M.; Thomas, D. D.; *Biophysical J.* **1991**, *59*, 1235-1241.
12. Tepe, J. J.; Williams, R. M.; *J. Am. Chem. Soc.* **1999**, *121*, 2951-2955.
13. Hegen, V.; Bendig, J.; Frings, S.; Eckardt, T. Helm, S. *Angewandte Chemie Int. Ed. Engl.* **2001**, *40*, 1046-1048.
14. Eckardt, T.; Hagen, V.; Schade, B.; Schmidt, R.; Schweitzer, C.; Bendig, J. *J. Org. Chem.* **2002**, *67*, 703-710.
15. Givens, R. S., Park, C.-H. *Tetrahedron Lett.* **1996**, *35*, 6259-6266.
16. Park, C.-H. Givens, R. S. *J. Am. Chem. Soc*. **1997**, *119*, 2453-2463.
17. Sheehan, J. C.; Umezawa, K. *J. Org. Chem*. **1973**, *38*, 3771-3774.
18. Lester, H. A.; Nerbonne, J. M. *Ann. Rev. Biophys. Bioeng.* **1982**, *11*, 151-175.
19. Geibel, S.; Barth, A.; Amslinger, S.; Jung, A. H.; Burzik, C.; Clarke, R. J.; Givens, R. S.; Fendler, K. *Biophys. J.* **2000**, *79*, 1346-1357.
20. Park, C. –H.; Givens, R. S. *J. Am. Chem. Soc*. **1997**, *119*, 2453-2463.
21. Du, X.; Frei, H.; Kim, S.–H. *J. Biol. Chem*. **2000**, *275*, 8492-8500.
22. Cornard, P. G. II.; Givens, R. S.; Weber, J. F. W.; Kandler, K.; *Org. Lett*. **2000**, *2*, 1545-1547.
23. Givens, R. S.; Jung, A. H.; Park, C.–H.; Weber, J. F. W.; Bartlet, W. *J. Am. Chem. Soc.* **1997**, *119*, 8369-8370.
24. Givens, R. S.; Weber, J. F. W.; Conrad, P. G.; Orosz, G.; Donahue, S. L.; Thayer, S. A. *J. Am. Chem. Soc*. **2000**, 122, 2687-2697.
25. Sul, J. –Y.; Orosz, G.; Givens, R. S.; Haydon, P. G. *Neuroglia Biol*. **2004**, *1*, 3-11.
26. Zou, K.; Cheley, S.; Givens, R. S.; Bayley, H. *J. Am. Chem. Soc.* **2002**, *124*, 8220-8229.
27. Specht, A.; Loudwig, S.; Peng, L.; Goeldner, M. *Tetrahedron Lett*. **2002**, *43*, 8947-8950.
28. *Greene's Protective Groups in Organic Synthesis*, 4th ed.; Wutts, P. G. M., Greene, T.

M., Eds.; Wiley Interscience-John Wiley and Sons: New York, 2007; pp 980-9832.
29. Protti, S.; Fagnoni, M. *Chem. Commun*. **2008**, 3611-3621.
30. Stensrud, K.; Noh, J.; Kandler, K.; Wirz, J.; Heger, D.; Givens, R. S. *J. Org. Chem*. **2009**, *74*, 5219-5227.
31. Yousef, A. Doctoral dissertation, **2005**, The University of Kansas.
32. Seiler, P.; Wirz, J. *Tetrahedron Lett*. **1971**, 1683-1686.
33. Seiler, P.; Wirz, J.; *Helv. Chimica Acta*. **1972**, *55*, 2693-2712.
34. Lukeman, M.; Veale, D.; Wan, P.; Munasinghe, V. R. N.; Corrie, J. E. T. *Can. J. Chem*. **2004**, *82*, 240-253.
35. Nekipelova, T. D.; Kuzmin, V. A. *High Energy Chem*. **2005**, *39*, 392-396.
36. Nekipelova, T. *Photochem. Photobiol. Sci.* **2002**, *1*, 204-207.
37. Malkin, Ya. N.; Pirogov, N. O.; Kuzmin, V. A.; *J. Photochem*. **1984**, *26*, 193-196.
38. Chandra, A. K.; Turro, N. J.; Lyons, A. L., Jr.; Stone, P. *J. Am. Chem. Soc*. **1978**, *100*, 4964-4966.
39. Turro, N. J. *Modern Molecular Photochemistry*; Benjamin/Cummings Publishing Co., Inc.: Menlo Park, **1978**.
40. Klan, P.; Wirz, J. *Photochemistry of Organic Compounds From Concepts to Practice*; Wiley**, 2009**.
41. Soroka, K.; Vithanage, R. S.; Phillips, D. A.; Walker, B.; Dasgupta, P. K. *Anal. Chem*. **1987**, *59*, 629-636.
42. Hopkins, T. A.; Meerholz, K.; Shaheen, S.; Anderson, M. L.; Schmidt, A.; Kippelen, B.; Padias, A. B.; Hall, H. K. Jr.; Peyghambarian, N.; Armstrong, N.R. *Chem. Mater*. **1996**, *8,* 344-351.
43. Zhu, Y.; Pavlos, C. M.; Toscano, J. P.; Dore, T. M.; *J. Am. Chem. Soc*. **2006**, *126*, 4267-4276.
44. Suzuki, A. Z.; Watanabe, T.; Kawamoto, M.; Nishiyama, K.; Yamashita, H.; Ishii, M.; Iwamura, M.; Furuta, T. *Org. Lett*. **2003**, *5*, 4867-4870.
45. Lu, M.; Fedoryak, O. D.; Moister, B. R.; Dore, T. M. *Org. Lett*. **2003**, *5*, 2119-2122.
46. Furuta, T.; Takeuchi, H.; Isozaki, M.; Takahashi, Y.; Kanehara, M.; Sugimoto, M.; Watanabe, T.; Noguchi, K.; Dore, T. M.; Kurahashi, T.; Iwamura, M.; Tsien, R. Y. *Chem. Bio. Chem* **2004**, *5*, 1119-1128.
47. Lin, W.; Lawrence, D. S.; *J. Org. Chem*. **2002**, *67*, 2723-2726.
48. Furuta, T.; Wang, S. S. H.; Dantzker, J. L.; Dore, T. M.; Bybee, W. J.; Callaway, E. M.; Denk, W.; Tsien, R. Y. *Proc. Natl. Acad. Sci*. U.S.A. **1999**, *96*, 1193-1200.
49. Ando, H.; Furuta, T.; Tsien, R. Y.; Okamoto, H. *Nat. Genet*. **2001**, *28*, 317-325.
50. Bardez, E.; Fedorov, A.; Berberan-Santos, M. N.; Martinho, J. M. G. *J. Phys. Chem. A* **1999,** *103*, 4131-4136.
51. Khalil, Z.; Yanni, A. S.; Abdel-Hafez, A. A.; Khalaf, A. A. *J. Indian Chem. Soc.* **1990**, *67*, 821-823.
52. Khalil, Z. H.; Yanni, A. S.; Abdel-Hafez, A. A.; Khalaf, A. A. *J. Indian Chem. Soc.* **1987**, *64*, 1987, 42-45.
53. Warner, V. D.; Musto, J. D.; Sane, J. N. *J. Med. Chem*. **1977**, *20*, 92-96.
54. Yamamoto, Y.; Iwamura, M.; Suzuki, H.; Yoshimura, N. *Proceedings of Symposium on Solvent Extraction*, **1992**, 93-98.
55. Sharma, R.C.; Nagar, R. *Croat. Chem. Acta*, **1988**, *61*, 849-855.
56. Yamamoto, Y.; Shibahara, K.; Takei, S.; *Bull. Chem. Soc. Jpn*. **1980**, *53*, 809-810.

1996, *8,* 344-351.
57. Yamamoto, Y.; Shibahara, K.; Takei, S.; *Bull. Chem. Soc. Jpn*. **1980**, *53*, 809-810. **1996**, *8,* 344-351.
58. Matsumura, K. *J. Am. Chem. Soc*., **1930**, *52*, 4433-4436.
59. Bauer, D. P.; Macomber, R. S. *J. Org. Chem.* **1975**, *40*, 1990-1992.
60. Pasaribu J. B.; Williams, L. R. *Aust. J. Chem*. **1973**, *26*, 1327-1331.
61. Ikemoto, N.; Liu, J.; Brands, K. M. J.; McNamara, J. M.; Reider, P. J. *Tetrahedron,* **2003**, *59*, 1317-1325.
62. Levene, P. A. *Organic Syntheses*, **1930**, *10*, 88-89.
63. Rather, J. B.; Reid, R. E. *J. Am. Chem. Soc*. **1955**, 18-20.
64. Giddens, A. C.; Boshoff, H. I. M.; Franzblau, S. G.; Barry, C. E.; Copp, Brent, R. *Tetrahedron Lett.* **2005**, *46*(43), 7355-7357.
65. Macaev, F.; Rusu, G.; Pogrebnoi, S.; Gudima, A.; Stingaci, E.; Vlad, L.; Shvets, N.; Kandemirli, F.; Dimoglo, A.; Reynolds, R. *Bioorg. Med. Chem*. **2005**, *13*, 4842-4850.
66. Ma, C.; Kwok, W. M.; Chan, W. S.; Zuo, P.; Kan, J. T. W.; Toy, P. H.; Phillips, D. L., *J. Am. Chem Soc*., **2005**, *127*, 1463-1472.
67. Uggeri, F.; Giordano, C.; Brambilla, A. *J. Org. Chem*. **1986**, *51*, 97-99.
68. Sonda, S.; Katayama, K.; Kawahara, T.; Sato, N.; Asano, K. *Bioorg. Med. Chem*. **2004**, *12*, 2737-2747.
69. Babad, E.; Carruthers, N. I.; Jaret, R. S.; Steinman, M. *Synthesis*, **1988**, *12*, 966-968.
70. Henne, A. L. *Org. React*. **1944**, *2*, 49-93.
71. Buu-Hoi, N. P.; Lavit, D. J. *J. Chem. Soc.* **1955**, 18-20.
72. Iwakuma, T.; Tsunashima, A.; Ikezawa, K.; Takaiti, O. *Eur. Pat. Appl*. **1985**, *55*
73. Recuero, V.; de Gonzalo, G.; Brieva, R.; Gotor, V. *Eur. J. Org. Chem*. **2006**, *18*, 4224-4230.
74. Shieh, C.J.; Kuo, Y.H. *Heterocycles*, **1986**, *24*, 1271-1274.
75. Barret, R.; Daudon, M. *Tetrahedron Lett*., **1990**, *31*, 4871-4872.
76. Schole, J.; Schole, C.; Eikemeyer, J. *Tetrahedron*, **1994**, *50*, 1125-1128.
77. Cossy, J.; Belotti, D. *Tetrahedron Lett*. **2001**, *42*, 4329-4331.
78. Hurley, J. K.; Sinai, N.; Linschitz, H. *Photochem. Photobiol*. **1983**, *38*, 9-12.
79. Tanielian, C.; Wolff, C. *J. Phys. Chem*. **1995**, *99*, 9825-9830.
80. Lown, J. W. *Chem. Soc. Rev*. **1993**, *22,* 165-176.
81. Hansen, M.; Hurley, L. *J. Am. Chem. Soc*. **1995**, *117*, 2421-2429.
82. Nicolaou, K. C.; Dai, W. –M.; Hong, Y. P.; Tsay, S. –C.; Baldrige, K. K.; Siegel, J. S. *J. Am. Chem. Soc*. **1993**, *115*, 7944-7953.
83. Avendaño, C.; Pérez, J. M.; Blanco, M, M.; Fuente, J. Á.; Manzanaro, S.; Vicent, M. J.; Martin, M. J.; Salvador-Tormo, N.; Menéndez, J. C. *Bioorg. Med. Chem. Lett.* **2004**, *14*, 3929-3932.
84. Pérez, J. M.; Avendano, C.; Menendez, J. C. *Tetrahedron Lett*. **1998**, *38*, 4217-4220.
85. Todter, C.; Lackner, H. *Liebigs Ann. Chem*. **1996**, 1385-1394.
86. Kitahara, Y.; Tamura, F.; Kubo, A. *Chem. Pharm. Bull*. **1994**, *42*, 1363-1364.
87. Doyle, T. W.; Balitz, D. M.; Grulich, R. E.; Nettleton, D. E.; Gould, S. J.; Tann, C. H.; Moews, A. E. *Tetrahedron Lett.* **1981**, *22*, 4595-4598.
88. Herlt, A. J.; Rickards, R. W.; Wu, J, -P. *J. Antibiot*. **1985***, 38*, 516-518.
89. Bardez, E.; Devol, I.; Larrey, B.; Valeur, B. *J. Phys. Chem. B* **1997**, *101*, 7786-7793.

90. Song, K. C.; Kim, J. S.; Park, S. M.; Chung, K. C.; Ahn, S.; Chang, S. K. *Org. Lett.* **2006**, *8*, 3413-3416.
91. Goldman, M.; Wehry, E. L. *Anal. Chem*. **1970**, *42*, 1178-1185.
92. Zhang, H.; Wang, Q. –L.; Jiang, Y. –B. *Tetrahedron Lett*. **2007**, *48*, 3959-3962.
93. Bronson, R. T.; Montalti, M.; Prodi, L.; Zaccheroni, N.; Lamb, R. D.; Dalley, N. K.; Izatt, R. M.; Bradshaw, J. S.; Savage, P. B. *Tetrahedron*, **2004**, *60*, 11139-11144.
94. Seitz, W. R. In *CRC Critical Reviews in Analytical Chemistry*; CRC Press: Boca Raaton, FL, **1980**; Vol. 8, pp 367-404.
95. Bailey, D. N.; Hercules, D. M.; Eck, T. D. *Anal. Chem*. **1967**, *39*, 877-880.
96. Döpp, D.; Memarian, H, R. *J. Photochem. Photobiol., A: Chemistry* **1990**, *53*, 59-67.
97. Conard, P. G. II.; Givens, R. S.; Hellrung, B.; Rajesh, C. S.; Ramseier, M. *J. Am. Chem. Soc*. **2000**, *122*, 9346-9347.
98. Finkelstein, H. *Ber. Dtsh. Chem. Ges*. **1910**, *43*, 1528.
99. Hatchard, C. G.; Parker, C. A. *Proc. R. Soc. London A* **1956**, *A220*, 518.